A seismic refraction survey of the earth's crust beneath the lesser antilles

Boynton, Colin Harford

A SEISMIC REFRACTION SURVEY OF THE EARTH'S CRUST BENEATH THE LESSER ANTILLES

by

Colin Harford Boynton

A thesis submitted for the degree of

Doctor of Philosophy

in the

University of Durham

Graduate Society

October 1974

Abstract

Seismic refraction data from the Lesser Antilles Seismic Project of April 1972 are analysed to delineate the crustal layers beneath the Lesser Antilles Island Arc, Grenada Trough, Tobago Trough and Barbados Ridge.

First arrival travel times from 23 of the LASP recording stations are analysed by the classical reversed-profile, modified 'plus-minus' and time-term methods of interpretation.

Two crustal layers of velocities about 6.2km s^{-1} and 7.0km s^{-1} are found beneath the Lesser Antilles ridge. It is suggested that the upper layer is of largely andesitic composition and that the lower layer represents the old oceanic crust which has been intruded with basic magma from the upper mantle beneath the arc. The presence of two crustal layers is common to most island arcs. Shear-wave velocities and Poisson's ratio for the upper crust beneath the arc are estimated, and these suggest that no large magma chambers are present above about 5km.

The crust of the Tobago Trough is shown to consist of a layer of velocity 7.0km s^{-1}, overlain by a thick pile of sediments and ? metamorphics. This structure shows closer affinities to 'Atlantic' crust than to 'Caribbean' crust. The results from the Grenada Trough are shown to be consistent with previous interpretations of the crustal structure.

These results indicate that there may have been an earlier period of subduction at a site some distance west of the present Lesser Antilles subduction zone. This may be related to the possible formation of the Aves Ridge as an active island arc in late Cretaceous - early Tertiary times.

ACKNOWLEDGEMENTS

My thanks are due to Professor M.H.P. Bott and Professor G.M. Brown for providing the facilities of the Department of Geological Sciences and to the Natural Environment Research Council for a research studentship.

I am grateful to Professor M.H.P. Bott for his supervision and helpful criticism of this work.

I would also like to thank all those who participated in LASP, particularly : the officers and crew of HMS HECLA, Dr J. Tomblin and his colleagues at the Seismic Research Unit (Trinidad), M J. Dorel and his colleagues at the Institut de Physique du Globe (Paris), Dr G. Peter, the officers and crew of the NOAA vessel DISCOVERER, Dr M.A. Khan, Dr. R.E. Long, Dr J. Sunderland, Dr P. Kearey, Dr G.K. Westbrook, Mr D. Asbery and Mr G. Ruth.

I have benefited from stimulating discussions with Dr P. Kearey, Dr G.K. Westbrook, Dr K.J.A. Wills, Mr L.R.A. Arnold and many other colleagues in Durham.

My thanks go to Mrs R.L. Reed for typing this manuscript accurately and efficiently.

Contents

Chapter 1

INTRODUCTION TO THE EASTERN CARIBBEAN

1.1 Introduction

The Department of Geological Sciences, University of Durham, in conjunction with the Hydrographic Department of the Ministry of Defence (Navy), conducted two geophysical surveys in the Eastern Caribbean in 1971 and 1972. These surveys were planned as part of the United Kingdom contribution to CICAR (Cooperative Investigation of the Caribbean and Adjacent Regions). Both surveys were conducted from HMS HECLA, an ocean class survey vessel of the Royal Navy. In 1971 continuous bathymetric, magnetic and gravity surveys and several seismic reflection profiles were run east and west of the Lesser Antilles between latitudes 12°54'N and 13°54'N and longitudes 57°W and 65°W. The first part of the 1972 survey consisted of a large scale seismic refraction project, the Lesser Antilles Seismic Project (LASP), during which three lines of shots were fired from HMS HECLA. Seismic receiving stations were situated on many of the islands and a hydrophone station was operated from the NOAA research vessel DISCOVERER. Following LASP, bathymetric, gravity and magnetic surveys were made over the Aves Ridge north of the 1971 area (Fig. 1.1).

Interpretation of the gravity, magnetic and seismic reflection results from east of the Lesser Antilles has been made by Westbrook (1973; Westbrook et al., 1973) and those from west of the Lesser Antilles, by Kearey (1973, 1974).

This thesis describes the interpretation of the seismic refraction results from LASP.

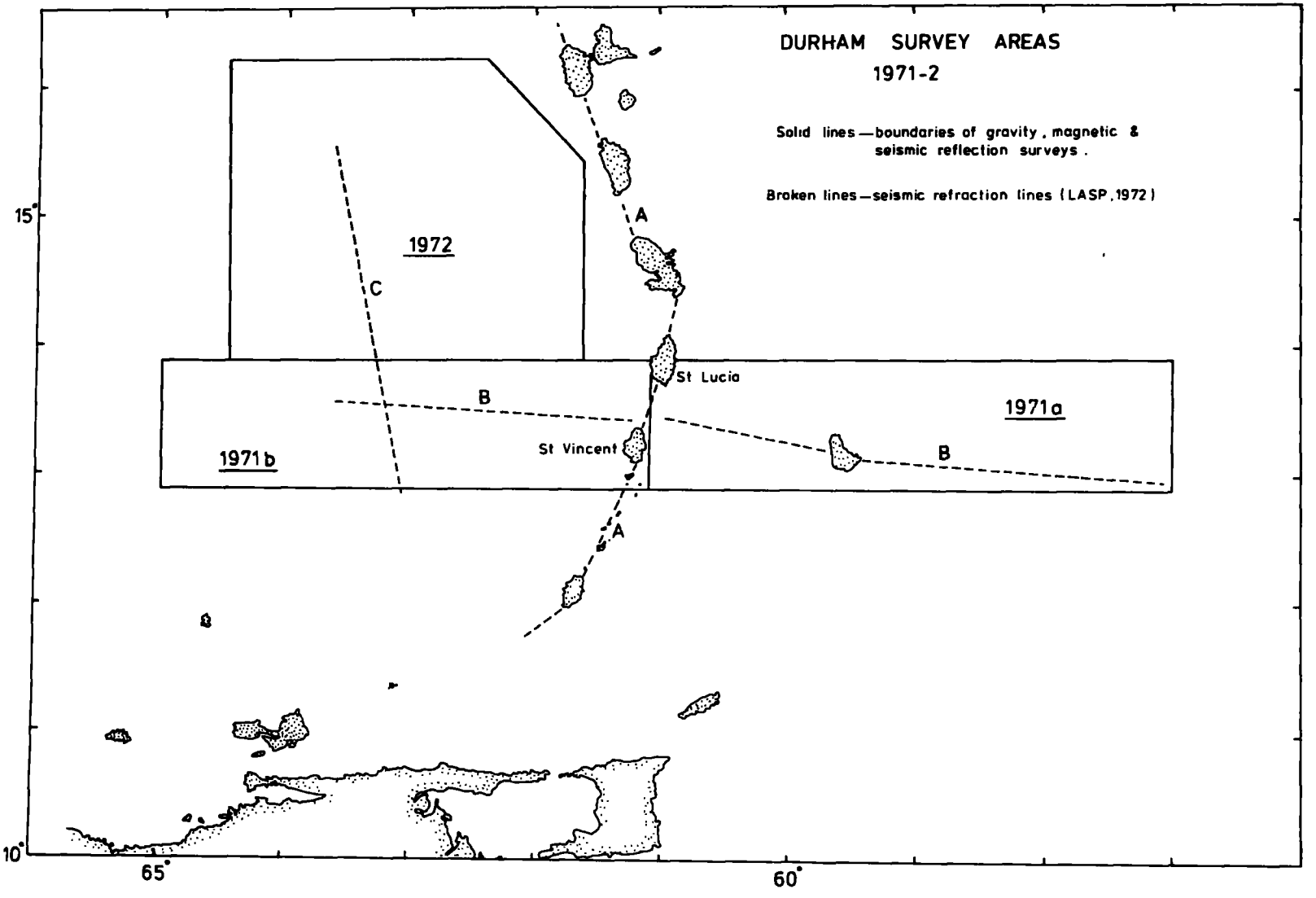
DURHAM SURVEY AREAS
1971-2
Solid lines—boundaries of gravity, magnetic & seismic reflection surveys.
Broken lines—seismic refraction lines (LASP, 1972)
1972
1971a
1971b
A
B
C
St Lucia
St Vincent
15°
10°
65°
60°

Fig. 1.1

1.2 Tectonic Setting

Within the concept of the 'new global tectonics' (Isacks et al., 1968) the Caribbean area can be considered a small, oceanic 'plate'. The Caribbean plate is bounded to the north, east and south by the Americas plate which underlies the Gulf of Mexico, western Atlantic Ocean and South America. The Cocos and Nazca plates adjoin the Caribbean plate to the west and southwest (Fig. 1.2).

The margins of the Caribbean plate are defined by tectonically active belts. The northern margin is defined by a series of predominantly sinistral strike-slip faults extending from the Motagua fault of south Guatemala, through the Cayman Trough to the Puerto Rico Trench. However, the connection between the Puerto Rico trench and Cayman Trough has not yet been proved. The eastern and western Caribbean margins are zones of active underthrusting (Fig. 1.2). In the east the Atlantic plate is being subducted westwards below the Caribbean plate (Chase and Bunce, 1969) giving rise to calc-alkaline volcanism in the Lesser Antilles. In the west the Cocos plate underthrusts the Caribbean plate in a north-easterly direction at the Middle America Trench, and this causes the volcanic and seismic activity of Central America (Sykes and Ewing, 1965). Many authors (e.g. Freeland and Dietz, 1971) consider that the Caribbean plate is, at present, effectively locked on to the South American continent at its southern margin. If this is true, a series of east-west striking sinistral transform faults must exist to the east of the Lesser Antilles subduction zone to allow for the differential lateral movements between North and South America, and for the underthrusting beneath the Lesser Antilles (Ball et al., 1969). The alternative view is that there is

Fig. 1.2 Tectonic units of the Caribbean region

Sources of information : Bracey and Vogt (1970)

Campbell (1968)

Holcombe et al. (1973)

Kearey (1974)

Molnar and Sykes (1969)

Sykes and Ewing (1965)

Tomblin (1971)

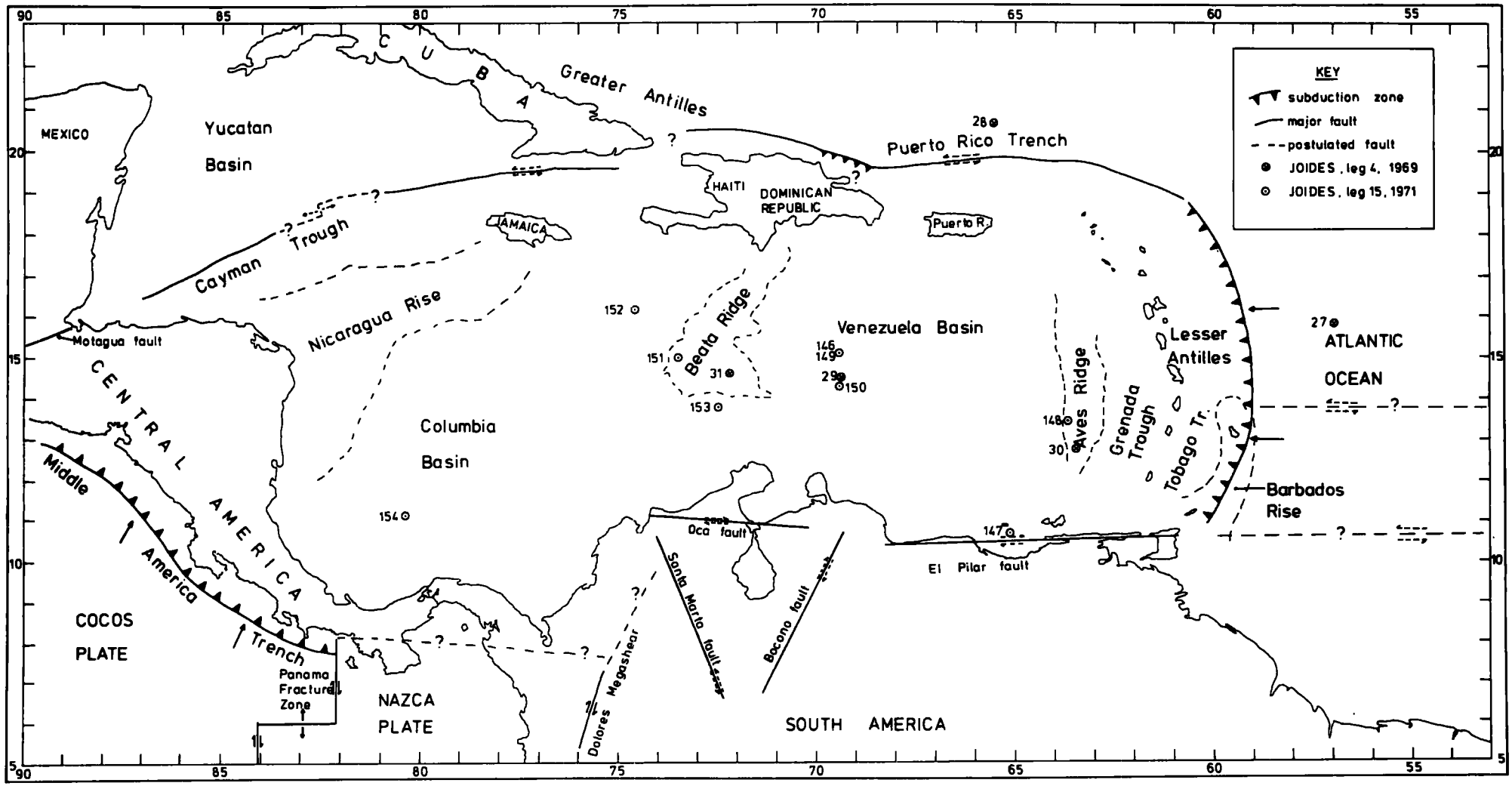
KEY
subduction zone
major fault
postulated fault
JOIDES, leg 4, 1969
JOIDES, leg 15, 1971
MEXICO
Yucatan Basin
CUBA
Greater Antilles
Puerto Rico Trench
HAITI
DOMINICAN REPUBLIC
Puerto R.
JAMAICA
Cayman Trough
Nicaragua Rise
Motagua fault
CENTRAL AMERICA
Middle America Trench
Beata Ridge
Venezuela Basin
Columbia Basin
Aves Ridge
Grenada Trough
Tobago Tr.
Lesser Antilles
ATLANTIC OCEAN
Barbados Rise
Oca fault
El Pilar fault
Santa Maria fault
Bocono fault
Dolores Megashear
Panama Fracture Zone
COCOS PLATE
NAZCA PLATE
SOUTH AMERICA
28
27
152
151
153
154
146
149
31
29
150
148
30
147

dextral strike-slip movement along a series of faults at the southern margin of the Caribbean. Both mechanisms may have been operative at different times.

1.3 Geological Description of the Eastern Caribbean

The eastern Caribbean between the Venezuela Basin and the Atlantic ocean consists of a series of roughly north-south striking topographic features (Figs. 1.2 and 1.3). These are, from west to east, the Aves Ridge (or Aves Swell), Grenada Trough, Lesser Antilles island arc, Tobago Trough and Barbados Ridge. The structure of these features, as defined by previous seismic, gravity and magnetic studies will be discussed in section 1.4. Brief physiographic and geological descriptions are given here. The eastern Caribbean is bordered by the Greater Antilles to the north and by the South American continent to the south.

The Greater Antilles contain geosynclinal deposits of ? late Jurassic to Eocene age which may overlie Palaeozoic metamorphic and igneous rocks (Khudoley and Meyerhoff, 1971). Volcanic rocks range in age from Cretaceous to mid-Eocene. Since the Eocene only non-geosynclinal sediments have been deposited. The Greater Antillean islands show evidence of much vertical uplift since the late Miocene. The geology of the Greater Antilles has been described by MacGillavry (1970) and Weyl (1966).

The age and nature of the Puerto Rico Trench is uncertain. The trench was probably the site of underthrusting of the American plate beneath the Caribbean plate in Mesozoic to early Tertiary times. Most authors consider the trench to have been the site of sinistral strike-slip motion, continuous with the Cayman Trough, since the

Eocene (Malfait and Dinkelman, 1972). However earthquake mechanism studies (Molnar and Sykes, 1969) indicate that present movements are essentially dip-slip to the west and southwest along low angle fault planes. To the northeast of Hispaniola there is an area of distinct WSW dip-slip mechanisms (Bracey and Vogt, 1970; Molnar and Sykes, 1971). The trench may not have developed its present abyssal form until after the Miocene (Monroe, 1968).

A belt of negative gravity anomalies, continuous with that found east of the Lesser Antilles, is associated with the Puerto Rico trench. However, there is no structural continuity between the Greater and Lesser Antilles.

In northern South America the Venezuelan Coast Range of the Araya Peninsula, North Trinidad and Tobago consists of a sequence of late Mesozoic to early Tertiary metamorphic rocks. A strong east-west structural trend is observed and the metamorphics are of a high temperature - high pressure type, their grade increasing from south to north (Maresch, 1974). Eclogitic and amphibolitic rocks have been reported from the island of Margarita (Maresch, 1973). South of the coastal ranges lie Cretaceous and Tertiary sediments which show folding and thrusting to the south (Barr and Saunders, 1968). The El Pilar fault zone marks the southern margin of the Coast Ranges. Metz (1968) has proposed a maximum of 15km dextral strike-slip displacement along the El Pilar fault since the early Tertiary. The Oca, Bocono and Santa Marta faults are a system of transcurrent fractures in northwest Venezuela and north Colombia. All show evidence of significant strike slip movement, but an overall east-west dextral displacement of more than about 100km is unlikely (Rod, 1956; Campbell, 1968; Dewey, 1972; Tschanz et al., 1974). There appears,

therefore, to be insufficient movement along this fault system to account for all the differential motion between the Caribbean and Americas plates. Sykes and Ewing (1965), from a study of earthquake epicentres in the Caribbean region, show a gap of seismicity in central north Venezuela. This may be related to the short observation period but does support the view of Freeland and Dietz (1971), and others, that the Caribbean plate is locked to the South American continent at present.

The Venezuela Basin is the largest of the Caribbean basins. It is mainly between 4 and 6km deep. Seismic refraction studies (Officer et al., 1959) show three main sediment layers with velocities of 1.9, 2.7 and 3.9km s^{-1} and a total thickness of about 2km. These overlie two crustal layers with velocities 6.0 - 6.2km s^{-1} and 7.2 - 7.4km s^{-1}. The average crustal thickness in the basin is 9 - 10km. The structure and stratigraphy of the sedimentary sequence within the basin have been investigated by reflection profiles (J. Ewing et al., 1971a; Edgar et al., 1971) and JOIDES drilling (Bader et al., 1970; Edgar, Saunders et al., 1973). A typical sedimentary section is :

younger turbidites (weak reflector)	1.7 - 1.9km s^{-1}
upper Carib Beds (reflector A")	1.9
lower Carib Beds (reflector B")	2.2 - 3.0
? local sediments (vague reflections)	3.2 - 4.2

These layers and reflectors persist throughout the Venezuelan Basin and have also been identified beneath the turbidites

of the northern Colombia Basin, on the flanks of the Beata Ridge and on parts of the Nicaragua Rise (Fig. 1.2). The younger turbidites are of Quaternary age and overlie Upper Eocene to Pleistocene chalks, oozes, marls and clays with ash bands (upper Carib Beds). Reflector A" has been identified as a series of thin Eocene chert beds. The acoustically transparent Carib Beds represent a period of pelagic siliceous sedimentation. Reflector B" has been tentatively correlated with Coniacian to early Campanian basalts at five JOIDES sites in the Caribbean (sites 146, 150, 151, 152 and 153; see Fig. 1.2). At most sites the basalt probably represents shallow intrusive sills and, therefore, not true basement. This is confirmed by the observation of weak sub-B" reflectors at a few localities (Eaton and Driver, 1969). There is still much discussion concerning the nature of reflector B".

The Aves Ridge is a linear bathymetric high striking north-south, which forms the eastern margin of the Venezuelan Basin between the Venezuelan continental margin and at least 16°N. In the south the ridge is mainly below 1km (Fig. 1.3) but in the north it culminates in a small island, Aves Island. Only sediments are exposed on the island but the presence of igneous or metamorphic rocks at shallow depths has been proposed by Gallovich and Aguilera (1970) from a seismic refraction survey. Several seamounts and guyots occur along the ridge.

Dredging on the crest of the Aves ridge (Hurley, 1965) yielded basaltic rocks, which suggested that the ridge is, at least in part, volcanic. Results from several dredge sites on the southern Aves Ridge were described by Fox et al. (1971). They found limestones, marls and cherts of middle Eocene to Recent age. At two of the more southerly sites a large quantity of granodiorite was found. Another dredge contained dolerite, porphyritic basalt and metamorphosed basalt.

Fig. 1.3 Bathymetric map of the eastern Caribbean (after Kearey et al., 1974)

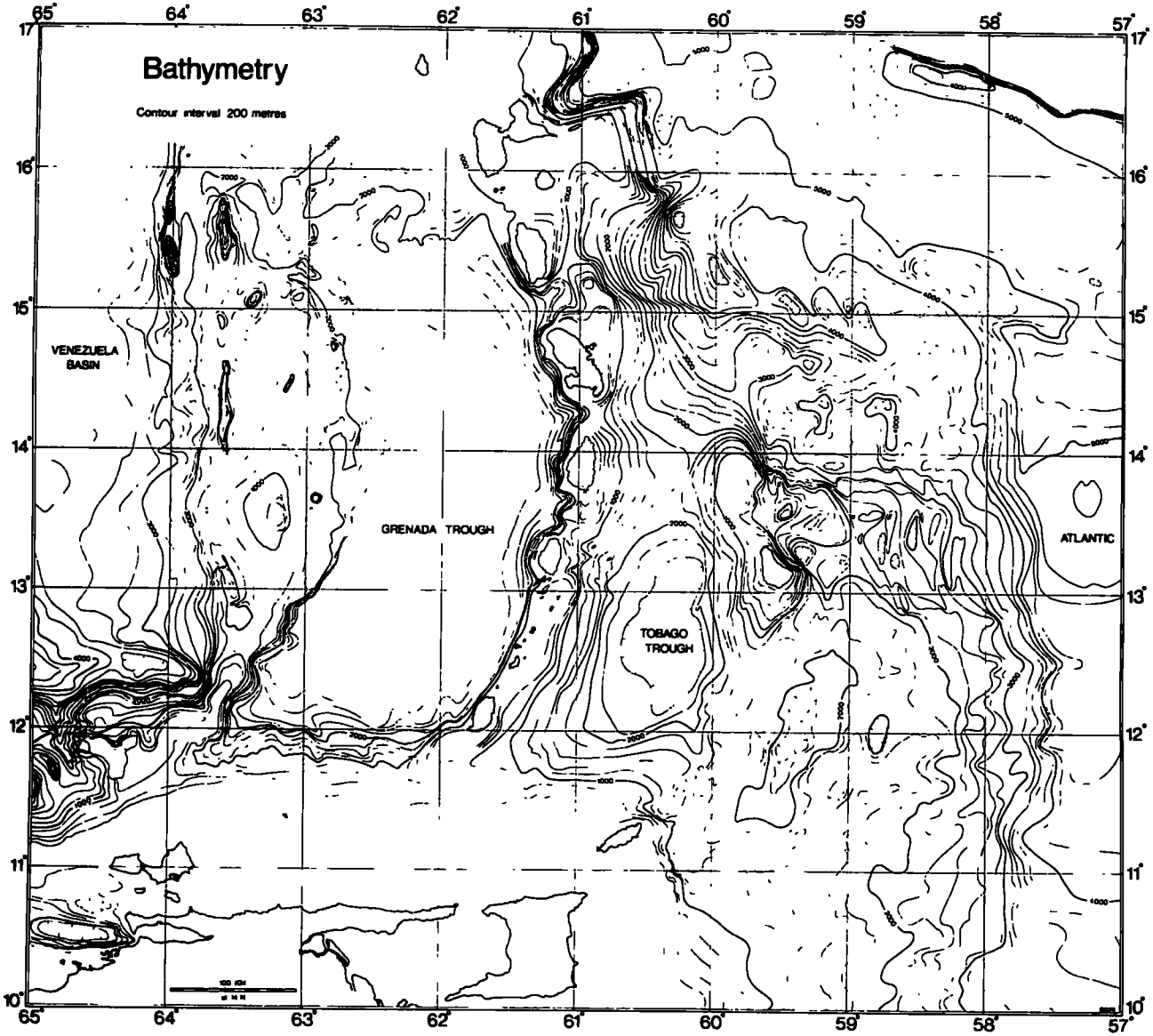
Bathymetry
Contour interval 200 metres
VENEZUELA BASIN
GRENADA TROUGH
TOBAGO TROUGH
ATLANTIC
65°
64°
63°
62°
61°
60°
59°
58°
57°
17°
16°
15°
14°
13°
12°
11°
10°

K-Ar dating of the igneous samples yielded ages between mid-Cretaceous and Palaeocene. On the basis of the good correspondence between the seismic velocities measured from the granitic samples and those of the upper crustal layer (6.0 - 6.4km s^{-1}) recorded in refraction profiles over the Aves Ridge, Fox et al. (1971) proposed that the ridge might be underlain by granitic rocks of late Mesozoic age. However, later dredging in the same locality failed to find granitic rocks (Nagle, 1971). Nagle found metavolcanic greenschists, basalts and volcanosediments. Sites near to Aves Island yielded volcanic conglomerates containing rounded pebbles, breccias, andesites, basalts, dacites, tuffs and limestones. Glassy flows, brecciated rocks and bombs have been recovered from several seamounts on the Aves ridge (Marlowe, 1968).

Two JOIDES sites are located on the Aves Ridge. These are site 30, leg IV (Bader et al., 1970) and site 148, leg XV (Edgar, Saunders et al., 1973) (for location see Fig. 1.4). Hole 30 penetrated 430m of Tertiary sediments. Late to early Pleistocene calcareous clays and more indurated early Pleistocene - late Pliocene silty clays were sampled in the first 270m. Late Miocene siltstones and middle and later early-Miocene foraminiferal oozes were recovered between 366 and 430m. The boundary between the Pliocene clays and Miocene sediments at c350m is correlated with a reflector at 0.4 s subbottom on a seismic reflection profile.

Hole 148 is located 50km northwest of hole 30 on the crest of a ridge on the western margin of the Aves ridge. 250m of calcareous clays of early Pliocene to late Pleistocene age were penetrated before reaching a basal layer of volcanic sands and clays which were drilled to a depth of 22m. The lower unit contains reworked Cretaceous and early Tertiary fossils and has a weathered cap suggesting the existence

Fig. 1.4 Simplified geological map of the Lesser Antilles (modified from Martin-Kaye, 1969)

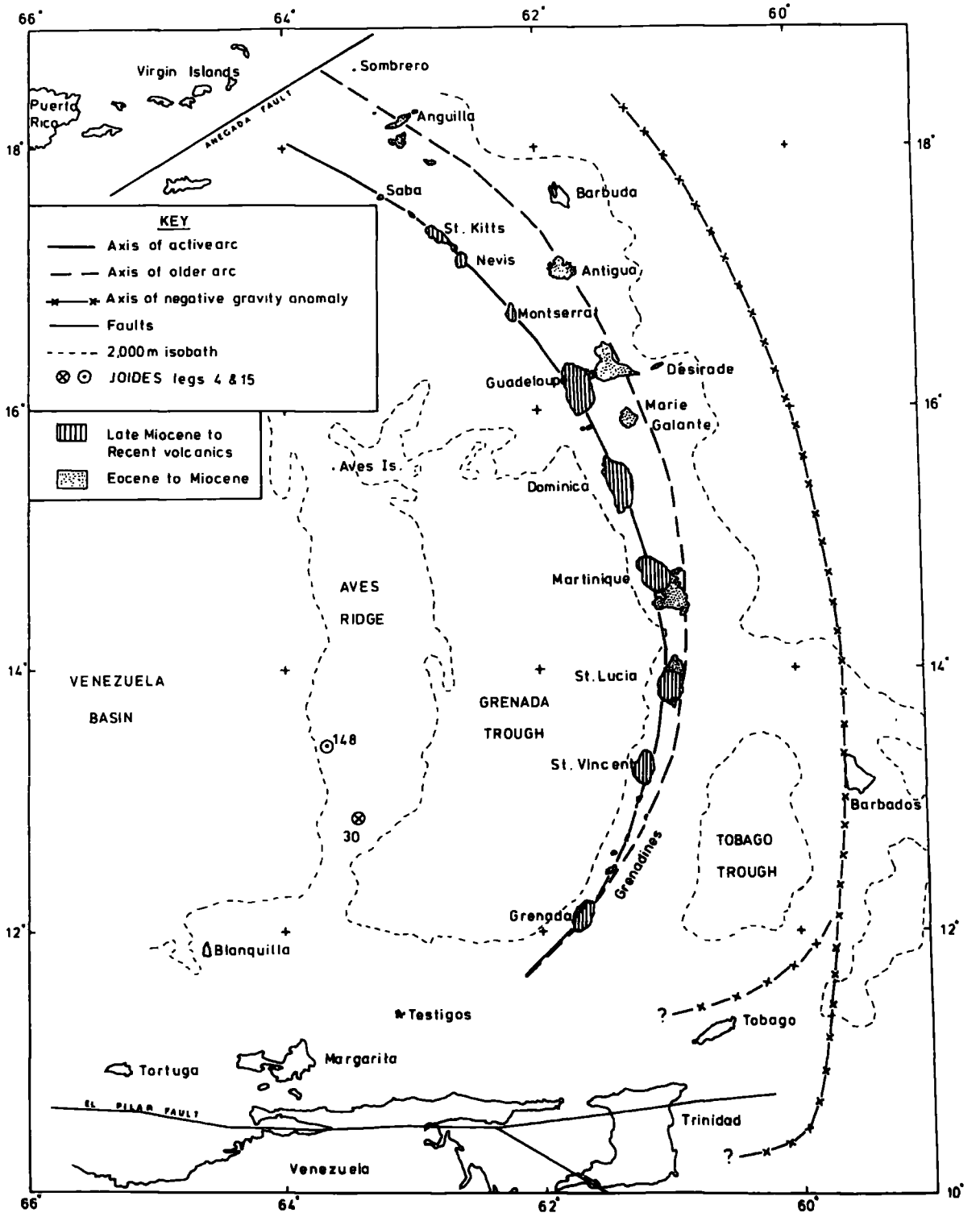
66°
64°
62°
60°
18°
16°
14°
12°
10°
Virgin Islands
Puerto Rico
ANEGADA FAULT
. Sombrero
Anguilla
Saba
Barbuda
St. Kitts
Nevis
Antigua
Montserrat
Guadeloupe
Désirade
Marie Galante
. Aves Is.
Dominica
Martinique
St. Lucia
St. Vincent
Grenadines
Grenada
Barbados
AVES RIDGE
VENEZUELA BASIN
GRENADA TROUGH
TOBAGO TROUGH
148
30
Blanquilla
Testigos
Tobago
Tortuga
Margarita
EL PILAR FAULT
Trinidad
Venezuela
KEY
Axis of active arc
Axis of older arc
Axis of negative gravity anomaly
Faults
2,000m isobath
JOIDES legs 4 & 15
Late Miocene to Recent volcanics
Eocene to Miocene

of a submarine or subaerial unconformity between the two layers. The length of the hiatus marked by the unconformity is uncertain. The change in lithology at 250m is correlated with a seismic reflector at 0.25 - 0.3 s subbottom. The results suggest a period of relatively deep water deposition adjacent to an emergent volcanic island followed by a brief period in shallow water or above sea level, and a later period of deeper pelagic sedimentation. Volcanic ash horizons are noted in both JOIDES holes. At site 148 six periods of volcanic activity in the Lesser Antilles are represented by ash layers in the Plio-Pleistocene section.

The Grenada Trough occupies the area bounded by the Aves and Lesser Antilles ridges which is crescent-shaped and convex eastward. In the broader southern part the floor of the Grenada Trough has a remarkably flat topography, the depth remaining just less than 3km over a wide area. The smoothness of the sea floor suggests a thick sediment cover. The trough bottom becomes more rugged north of about 14^{o}N and, as the trough narrows, it is difficult to differentiate between it and the Aves Ridge on bathymetric grounds alone.

The double arc of the Lesser Antilles consists of an outer eastern arc extending from Sombrero to Grenada and an inner arc starting at Saba and converging with the outer arc such that the arcs are more or less coincident south of Martinique (Fig. 1.4). The Lesser Antilles have been the site of calc-alkaline volcanism since Eocene times. Initially the volcanism occurred along the outer arc, but had ceased by the Miocene.Volcanism restarted in late Miocene - Pliocene times along the inner arc and continues today. Radiometric dates on younger volcanics from the islands of Montserrat through to Saba are no older than 7.2 my (Briden et al., 1974). The older islands from Marie Galante to Sombrero are often known as the 'Limestone Caribbees' as

the older volcanics are much eroded and largely covered with limestones and marls of mainly Miocene - Oligocene age. Further south the younger volcanics and interspersed sediments overlie the folded volcanics and sediments of the earlier episode. Excepting Désirade (see below) the oldest rocks found in the arc are of Eocene age (e.g. Tufton Hall formation on Grenada and the Hillsborough Rectory limestone on Carriacou). Evidence for three periods of earth movements is found from the Lesser Antilles (Martin-Kaye, 1969). Early Tertiary movements folded the Eocene rocks along roughly east-west axes. Andean (or Antillean) movements of Upper Miocene - Pliocene times caused folding associated with considerable volcanic and intrusive activity. Thirdly, Pleistocene to Recent uplift has affected all the Lesser Antilles. Martin-Kaye (1969) showed that Pleistocene marine limestones have been lifted above sea level to heights between 200ft (Grenada) and 1150ft (St Kitts).

Arculus (1973; Arculus and Curran, 1972) proposed that the geochemical associations of the volcanic suites in the Lesser Antilles are best explained as originating by partial melting of an upper mantle peridotite and subsequent differentiation within the crust. He does not consider partial melting of subducted oceanic lithosphere to be a significant petrogenic process here, although volatiles rising from the subducted plate are likely to play an important role in localising the area of magma genesis.

On the island of Désirade (off the east coast of Guadeloupe) the basement complex consists of massive flows and pillow-lavas of spilitic-keratophyric affinities, interbedded and overlying cherts and subjacent trondhjemitic rocks (Mattinson et al., 1973). Gabbroic rock, as dredged off Désirade, could underlie this complex. Isotopic age dating (Fink et al., 1971) shows ages of 98.6 my to 43.4 my for spilites and keratophyres and an age of 145-150 my for the trondhjemite. However,

J. Briden (unpublished data) has found no ages older than 80 my in this complex. Whichever is the correct age, this complex certainly contains rocks older than any found elsewhere in the Lesser Antilles. Mattinson et al. (1973) recognise this complex as an ophiolite assemblage and it seems probable that these rocks are an uplifted portion of the oceanic sea floor. As such, this complex may prove to be the key to the understanding of the early development of the eastern Caribbean. This will be discussed further in Chapter 8.

The Tobago Trough lies between the volcanic ridge of the Lesser Antilles and the sedimentary Barbados ridge (Fig. 1.3). In its central part, the basin reaches a depth of 2,500 m. To the south the trough terminates against the continental slope of South America and to the north it is truncated by a bathymetric rise extending eastward from St Lucia to the Barbados Ridge.

The Barbados Ridge extends north from just northeast of Tobago to about 14^{o}N. Barbados is the only emergent portion of the ridge, the ridge dipping away gently to the north and south of the island. The geology of Barbados has been described by many authors, of whom Senn (1940) and Saunders (1968) provide the basic stratigraphy, which can be divided into the following broad formations :

Coral Rock formation	-	? Pliocene - Recent
Conset Marl	-	Upper Miocene
Bissex Hill formation	-	Miocene
Oceanic formation	-	Upper Eocene - early Miocene
- unconformity -		
Joes River formation	-	Upper Eocene
- unconformity -		
Scotland formation	-	Middle & Lower Eocene

The reef limestones of the young Coral Rock formation cover much of the island but the older rocks are exposed in inliers. Sandstones and shales of the Lower Scotland formation indicate a deep water environment, while the conglomerates, grits, sands and silts of the Upper Scotland formation indicate shallower deposition. Senn (1940) suggested that these sediments were derived from the north coast of South America. These rocks are intensely deformed. Multiple folds and overturned beds with a pronounced northeast-southwest strike trend are common. In boreholes, many overturned and repeated sequences are observed to a depth of 4.5km (Baadsgaard,1960).

Lying unconformably on the older beds is the Oceanic Formation which comprises radiolarian sediments in the lower parts and foraminiferal marls at the top. The benthonic species suggest deposition at a depth of 1000 to 1500 m (Beckmann, 1953) and Baadsgaard (1960) considered that the great thickness of the formation (at least 1500 m) would rule out deposition at such abyssal depths as had been invoked by Senn (1940).

Two local formations, the Bissex Hill formation and the Conset Marl, overlie the Oceanics. These consist of Miocene foraminiferal marls and limestones.

The Coral Rock is up to 100 m thick and was formed as a series of fringing reefs about an emergent island, largely during the Pleistocene. The presence of submerged barrier reefs at depths of 25 m and 80 m off the west coast of Barbados probably reflects pauses in the post-Pleistocene eustatic rise in sea level (Macintyre, 1967).

Samples of flysch rocks similar to those of the Scotland formation have been dredged from the ridge crest 35km north of Barbados (Hurley, 1965). To the south of the island, Hurley found manganese nodules embedded in a lithified limestone which may be from the Oceanic or Bissex Hill formations.

1.4 Previous Geophysical Studies in the Eastern Caribbean

1.4.1 Seismic Refraction

During the 1940s and 1950s many ship-to-ship refraction profiles were run in the Caribbean region by various American oceanographic institutions. The location of the profiles relevant to the Durham survey area are shown in Fig. 1.5. Most of the profiles were reversed so that true velocities could be determined. The methods of measurement and interpretation used for these profiles were similar to those described by M. Ewing et al. (1937, 1939, 1950) and Katz and Ewing (1956). High drift rates of the ships during the shooting and recording of the profiles were encountered throughout the area (Edgar et al., 1971) and this introduced apparent discontinuities between adjacent profiles and also some interpretational difficulties.

Officer et al. (1957) and J. Ewing et al. (1957) interpreted some of their results as indicating a low-velocity mantle (7.2 - 7.7km s^{-1}) beneath a normal oceanic crustal layer with a velocity of 6.6km s^{-1}. A later reinterpretation of the results (Officer et al., 1959) recognised two crustal layers (6.1 and 7.3km s^{-1}) beneath sediments and overlying a normal mantle velocity of 8.1km s^{-1}. The results from a subsequent cruise support the later interpretation (Edgar et al., 1971). The two layers are referred to as the upper and lower crustal layers. The existence of two crustal layers within the Caribbean crust is anomalous. Normal ocean basins consist of sediments (layer 1) overlying a 4-6km s^{-1} layer (layer 2) above a 6.4 - 7.0km s^{-1} layer (layer 3) (Bott, 1971). The correlation of

Fig. 1.5 Previous seismic refraction surveys in the eastern Caribbean

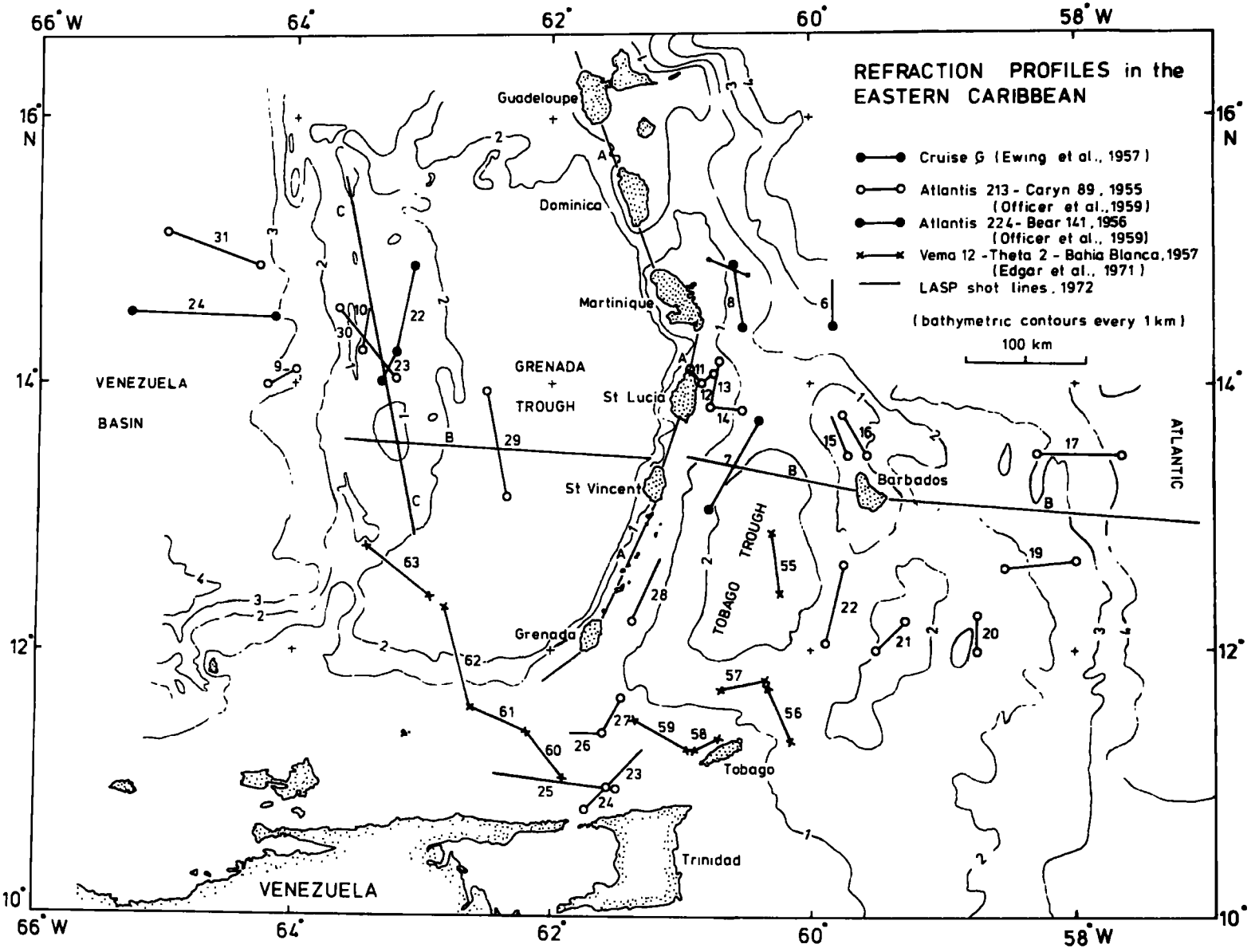
REFRACTION PROFILES in the EASTERN CARIBBEAN
Cruise G (Ewing et al., 1957)
Atlantis 213 - Caryn 89, 1955 (Officer et al., 1959)
Atlantis 224 - Bear 141, 1956 (Officer et al., 1959)
Vema 12 - Theta 2 - Bahia Blanca, 1957 (Edgar et al., 1971)
LASP shot lines, 1972
(bathymetric contours every 1 km)
100 km
66° W
64°
62°
60°
58° W
16° N
14°
12°
10°
Guadeloupe
Dominica
Martinique
St Lucia
St Vincent
Grenada
Barbados
Tobago
Trinidad
VENEZUELA
VENEZUELA BASIN
GRENADA TROUGH
TOBAGO TROUGH
ATLANTIC

the two Caribbean crustal layers with the normal oceanic layers is uncertain.

A summary of the crustal structure as determined from profiles across the eastern Caribbean from the Venezuelan Basin to the Atlantic ocean is shown in Fig. 1.6. Mantle velocities were not recorded under the Aves Ridge, Tobago Trough, Lesser Antilles arc, Grenada Trough or Barbados Ridge. Crustal velocities of 6.2 and 7.4km s^{-1} were observed beneath the Grenada Trough (profile 29, 1955) which are similar to those recorded beneath the Venezuelan Basin. The possibility that the 7.4km s^{-1} layer beneath the Grenada Trough represents an anomalously low-velocity upper mantle is not ruled out by these early results.

The highest velocity observed beneath the Lesser Antilles was 6.4 and the highest beneath the Aves Ridge was 6.7km s^{-1}. The crustal structure found beneath the Tobago Trough (Fig. 1.5, profile 7, cruise G) was similar to that found beneath the Atlantic slope of the Barbados ridge (profiles 17 and 19, 1955) in that a 6.8km s^{-1} velocity occurred directly beneath a 4.0km s^{-1} layer. Thus the crustal structure beneath the Tobago Trough is not a typical Caribbean crustal structure. This point will be discussed later. The highest velocities recorded beneath the Barbados Ridge are 4.9km s^{-1} (profile 22, 1955) and 5.3km s^{-1} (profile 21, 1955) at depths of about 4.5 and 8km below the seabed, respectively. The travel time graph of profile 22 suggests that the crustal layer is considerably deeper than the 4.9km s^{-1} layer.

A considerable variation of layer velocities was found from these refraction profiles. The following rough guide was used by J. Ewing et al. (1957) to relate the velocities obtained to rock types :

Fig. 1.6 Summary of crustal structures across the eastern Caribbean (after Officer et al., 1959)

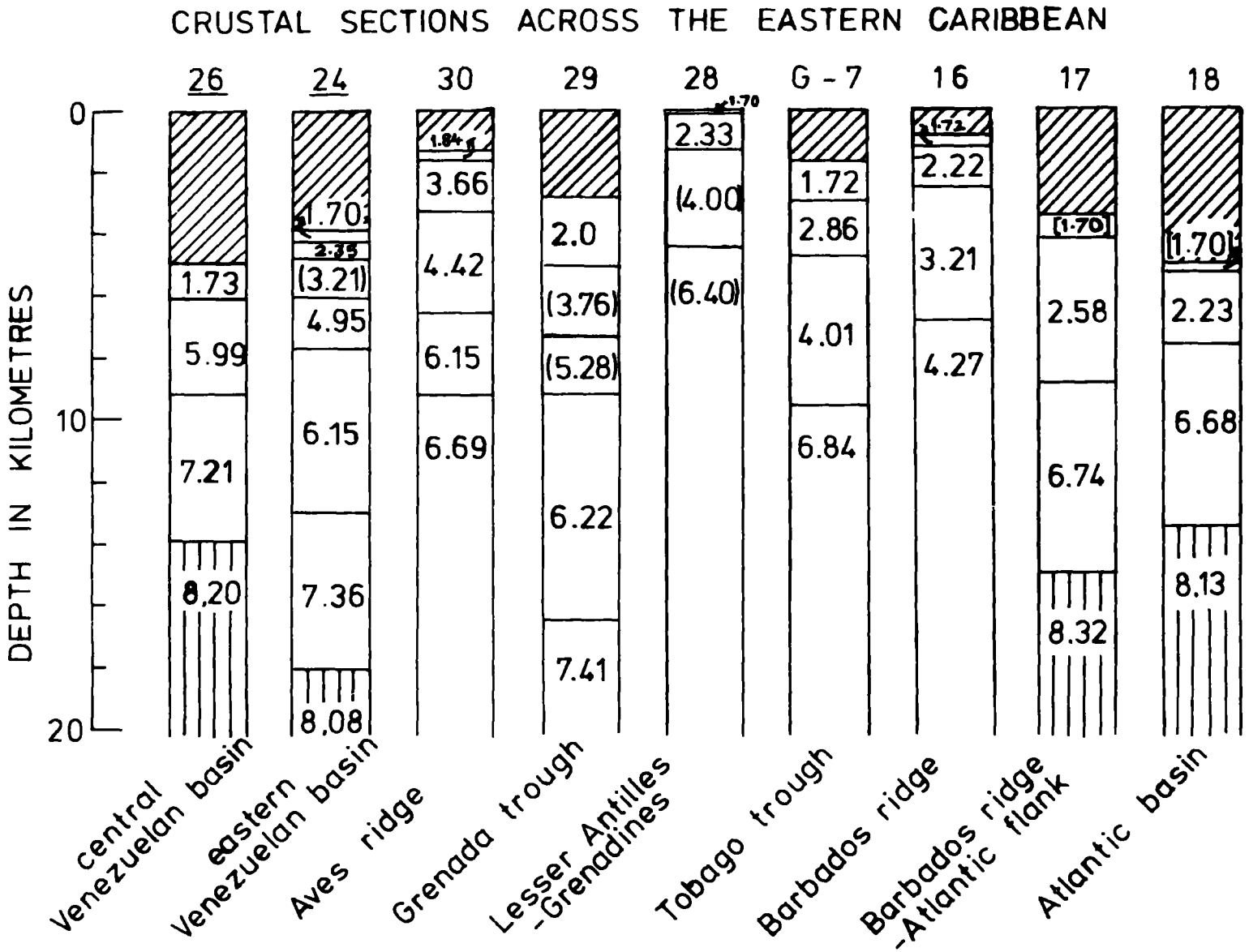
CRUSTAL SECTIONS ACROSS THE EASTERN CARIBBEAN
26
24
30
29
28
G - 7
16
17
18
DEPTH IN KILOMETRES
0
10
20
1.73
5.99
7.21
8.20
1.70
2.35
(3.21)
4.95
6.15
7.36
8.08
1.84
3.66
4.42
6.15
6.69
2.0
(3.76)
(5.28)
6.22
7.41
1.70
2.33
(4.00)
(6.40)
1.72
2.86
4.01
6.84
1.72
2.22
3.21
4.27
[1.70]
2.58
6.74
8.32
[1.70]
2.23
6.68
8.13
central Venezuelan basin
eastern Venezuelan basin
Aves ridge
Grenada trough
Lesser Antilles -Grenadines
Tobago trough
Barbados ridge
Barbados ridge -Atlantic flank
Atlantic basin

	Rock type(s)	Velocity range
A	Unconsolidated sediment	1.6 - 2.0km s^{-1}
B	Partially lithified sediment	2.0 - 3.0
C	Lithified sediments, volcanic rocks, metamorphic rocks	3.2 - 3.8
D	Volcanic or metamorphic	3.8 - 4.5
E	Metamorphic or igneous	4.5 - 5.5
F	Crustal velocities	5.8 - 7.5
G	Mantle velocities	7.8+

The results of these earlier refraction profiles have been found very useful as a control in the interpretation of gravity and magnetic measurements in this region (Kearey, 1973; Westbrook, 1973). The detailed upper crustal structure determined by previous surveys has been found useful in this work as, on the whole, the LASP network did not allow definition of the sediment layers. Where relevant, the results of individual profiles are given in more detail in later chapters.

Arrivals from LASP shot line B at the hydrophone station H1 (station 9 in Fig. 2.1) east of Barbados have been interpreted by Westbrook (1973). Although the velocities observed at this station were unreversed, comparison with the nearby profiles of Officer et al. (1959) suggested that the refractor dips were small. An apparent Moho velocity of 7.79km s^{-1} was observed which corresponds to a true velocity of 8.02km s^{-1} if there is a 1^{o} dip of the Moho towards the west. These results indicate the following structure beneath the station H1 :

	velocity ($km\ s^{-1}$)	thickness (km)	depth (km)
water	1.5	4.46 = depth below lowest hydrophone	
sediment (assumed)	1.7	0.38	4.46
refractor 1	2.45	3.68	4.84
refractor 2	6.73	6.57	8.52
refractor 3	8.02		15.09

The absence of a first-arrival velocity of about $5km\ s^{-1}$ (oceanic layer 2) is probably due to the 'masking' of refracted arrivals from this layer by the thick sediment layer. Introducing a layer of average layer 2 velocity and thickness increases the depth to the 6.73 and $8.02km\ s^{-1}$ refractors by only a small amount.

1.4.2 Seismic Reflection

Many seismic reflection profiles have been run in the eastern Caribbean in recent years. The location of many of these profiles, together with their sources, are shown in Fig. 1.7.

To the west of the Lesser Antilles, Kearey (1973, 1974) has found two strong reflectors which, he considers, correlate with the reflectors A" and B". The Aves Ridge was found to consist of two flanking basement ridges enclosing a central sediment filled trough. Reflectors within this sedimentary trough were similar to those in the Venezuela Basin and Grenada Trough and suggest post-depositional uplift of the Aves Ridge. Apparent truncation of the Grenada Trough by the southern Aves Ridge supports such an uplift.

Fig. 1.7 Location of seismic reflection profiles in the eastern Caribbean

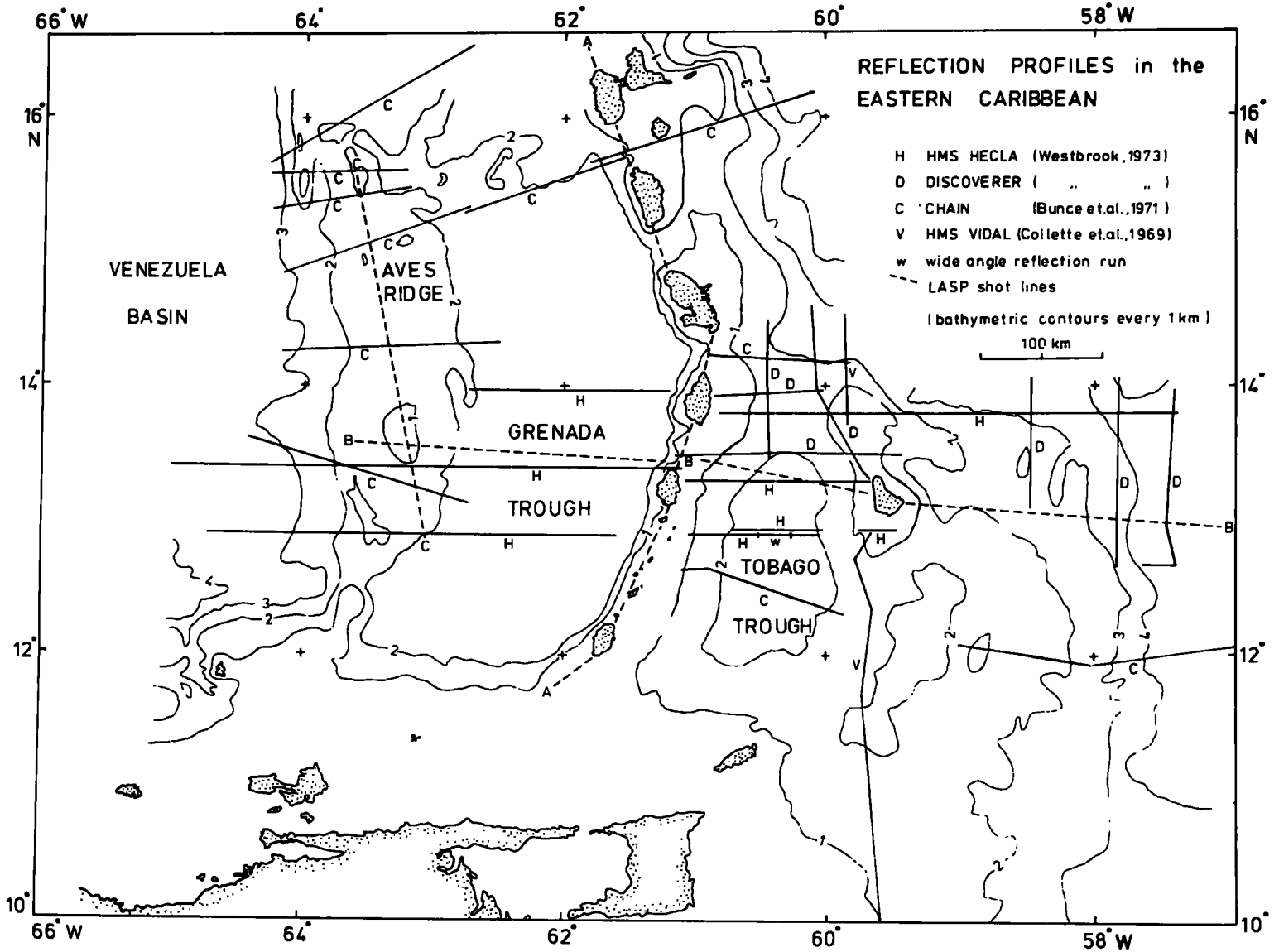
REFLECTION PROFILES in the EASTERN CARIBBEAN
H HMS HECLA (Westbrook, 1973)
D DISCOVERER (" ")
C CHAIN (Bunce et.al., 1971)
V HMS VIDAL (Collette et.al., 1969)
w wide angle reflection run
LASP shot lines
(bathymetric contours every 1 km)
100 km
VENEZUELA BASIN
AVES RIDGE
GRENADA TROUGH
TOBAGO TROUGH
66° W
64°
62°
60°
58° W
16° N
14°
12°
10°

The sediment structure within the Grenada Trough suggests a southerly source, perhaps from the Orinoco river. Volcanic ashes from the Lesser Antilles would be a further likely contributor. The seismic velocities of sediment layers defined by reflection lines in this region have not been measured by wide-angle reflection surveys, but can be inferred from refraction profiles (Officer et al., 1959) and JOIDES logging (Aves Ridge). Bunce et al. (1971) found 1.0 - 1.5km of sediment within troughs on the Aves Ridge and at least 1.5km of material with velocity 2.5km s^{-1} and under in the Grenada Trough. Reflection profiles across the Lesser Antilles (Bunce et al., 1971) show that very little sediment overlies the crest of the volcanic arc, while a thin sediment cover exists over the outer 'limestone' arc. None of the persistent reflections of the Grenada Trough can be correlated across the Lesser Antilles arc.

In the Tobago Trough a sequence of regularly bedded reflecting horizons are observed (Westbrook, 1973). The following generalised description of the sedimentary sequence in the centre of the trough, taken from Westbrook (1973), was obtained by combining refraction results with results from wide-angle and vertical incidence reflection profiles.

layer	velocity (km s^{-1})	thickness (km)
A	1.55	0.4
B	1.9	0.5
C	2.2 - 2.6	0.8
D	2.9 - 3.4	2.0 - 3.0
E	3.8 - 4.3	2.0 - 5.0

It should be noted that isochronous layers defined by reflection profiles show different velocities at different locations,

depending mainly on the depth of burial. An increase of velocity with depth is likely for layers A - C at least. These layers are thought to be turbidites and lie unconformably upon layer D. In the western part of the trough the upper layers overlap the basement rise of the volcanic arc and contain erosional and volcanic products from the arc. The sediments at the east side of the trough are deformed by the uplift of the western flank of the Barbados Ridge. The lower layers may be faulted at this boundary but layers A to C are only warped. On the western flank of the Barbados Ridge, undisturbed sediments overlie disturbed sediments (Westbrook et al, 1973). Below the irregular bathymetry of the eastern flank of the ridge a series of discontinuous reflectors dip westwards at about 5^{o} to 10^{o}. The disturbed sediments beneath the Barbados Ridge (?layer D) may represent the Scotland and Oceanic formations of Barbados. Disturbance of the sediments beneath the ridge is thought to be due to the westward movement of the Atlantic plate beneath them. East of the base of the Atlantic slope of the Barbados Ridge the sediments are not disturbed and three reflecting horizons are prominent. The lowest of these, at a depth of 2.24km below the seabed, may represent the top of oceanic layer 2 (Westbrook, 1973).

1.4.3 Gravity and Magnetics

East of the Lesser Antilles a belt of negative free air gravity anomalies runs southward next to the Barbados Ridge before curving inland to the east of Trinidad (Fig. 1.4). The axis of a positive gravity anomaly coincides with the volcanic arc. A Bouguer anomaly map of the eastern Caribbean is shown in Fig. 1.8.

Fig. 1.8 Bouguer gravity anomaly map of the eastern Caribbean (after Kearey et al., 1974)

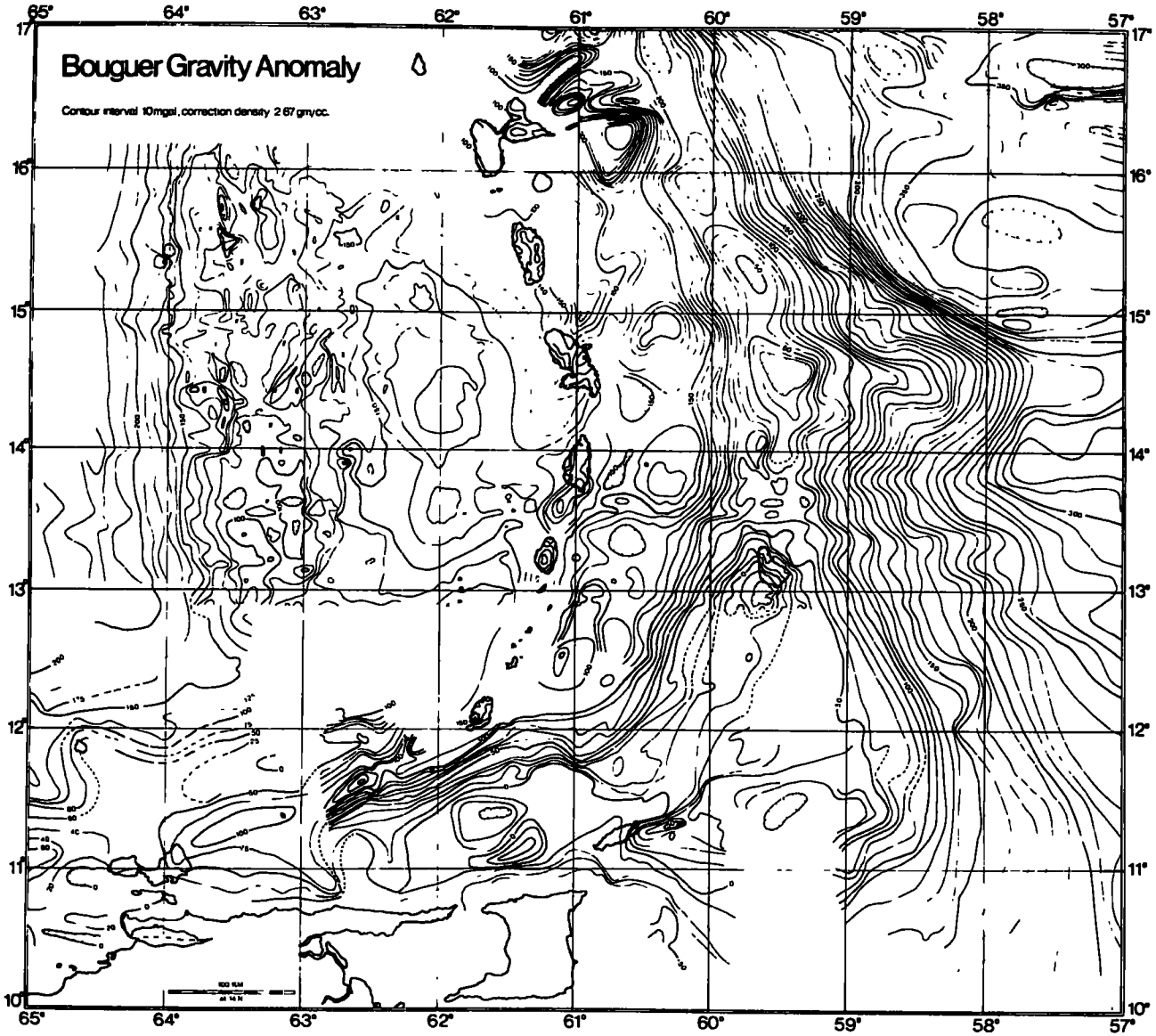
Bouguer Gravity Anomaly
Contour interval 10mgal, correction density 2.67 gm/cc.
65°
64°
63°
62°
61°
60°
59°
58°
57°
17°
16°
15°
14°
13°
12°
11°
10°

Kearey (1974) has shown that the Aves Ridge is underlain by a mass deficiency which may be interpreted in terms of a thickened crust with consequent depression of the Moho and lower crustal layer. From the positive Bouguer anomaly of the Grenada Trough he infers a relatively shallow Moho. Kearey has calculated isostatic anomaly values which are predominantly negative over the Aves Ridge and Grenada Trough and positive over the Lesser Antilles. The short period gravity anomalies of the Aves Ridge and Grenada Trough reflect variations in the depth to the sediment - basement interface.

For the region from the Lesser Antilles through to the Atlantic east of Barbados, Westbrook (1973) has computed crustal models which best satisfy the seismic and gravity observations, by a non-linear optimization method. His models indicate a crustal thickness of 30 - 35km beneath the Lesser Antilles, thinning to about 20km beneath the centre of the Tobago Trough before increasing to about 25km beneath the Barbados Ridge. A thickness of about 20km of sediments and metamorphics is considered to underlie the Barbados Ridge (Westbrook et al, 1973). A gravity high associated with a topographic ridge running east of St Lucia can be explained by a basement ridge with or without a depression of the underlying Moho (Westbrook, 1973).

1.4.4 Seismicity and Earthquake Studies

The seismicity of the eastern Caribbean has been described by Sykes and Ewing (1965), Molnar and Sykes (1969) and Tomblin (1971). Focal mechanism studies (Molnar and Sykes, 1969; and Tomblin, pers. comm. in Westbrook, 1973) show that there are two major fault motions

involved along the eastern Caribbean margin. Some are thrust faults presumably associated with underthrusting and others are vertical or strike-slip motions along vertical fault planes with an easterly strike which may be due to reactivation of old transform faults during the subduction of Atlantic lithosphere. At the junction of the Lesser Antilles and the South American continent, the mechanisms are dextral strike-slip with easterly strike and essentially vertical movements on east-west faults, the latter being related to hinge faults (Molnar and Sykes, 1969).

The focal depths of earthquakes along the Lesser Antilles define a seismic or Benioff zone dipping 40 - 45° to the west and reaching depths of 200km to the west of the island arc. Focal depths of earthquakes beneath the volcanic arc are mainly in the region of 120 to 150km. Westbrook (1973) calculated the frequency distribution of earthquakes with depth for the period 1904 - 1970 and found peaks at 33 - 45km and 150km depth. Dorel et al. (1971a) also noted a secondary peak at 140 - 150km focal depth for events during the period 1952 - 1969. These results depart slightly from the smoother exponential decrease with depth found in other subduction zones (Isacks et al., 1968). Westbrook also presented curves of the distribution of earthquake energy with depth, but these were influenced too much by a few large magnitude events to be of much significance.

Brune (1968) used empirical relationships between seismic moment as a function of earthquake magnitude, and slip rate as a function of moment, to calculate a rate of underthrusting. The rate calculated by this method is, if anything, an underestimate. Westbrook (1973) and Molnar and Sykes (1969) applied Brune's method to the Lesser Antilles arc and both obtained a value of 0.5cm yr^{-1}. Molnar and Sykes also obtained estimates of 2.0 and 2.2cm yr^{-1} by other methods.

The relative delays of arrivals from regional earthquakes at seismic stations along the Lesser Antilles have been discussed by Barr and Robson (1963) and they show that the relative delays between stations along the volcanic arc and Trinidad are small, but that delays at Barbados relative to Trinidad and the arc stations are large, with a mean value of 2.94 s. The delays between Barbados and the arc stations have been recalculated by Tomblin and Aspinall (Aspinall, personal communication, 1973). Their value is about 2.0 s. Such a large delay requires thick low velocity layers below Barbados. Dorel et al. (1971b) have shown that travel time residuals for earthquakes in the distance range 25 - 90° at the seismic observatories along the Lesser Antilles vary with azimuth of the arrival. The amplitude of this variation is 2.4 s for Guadeloupe (SCG), 2.1 s for Trinidad (TRN) and 1.7 s for Martinique (FDF), the arrivals coming in earliest at an azimuth of 190° for Guadeloupe and Martinique and at an azimuth of 320° for Trinidad. The variations at Martinique and Guadeloupe were interpreted as being due to the varying thickness of the subducted Atlantic lithosphere 'seen' by the arrivals from different directions. An arrival from the north or south will have passed through more of the downgoing plate than an arrival from the east and arrivals from the west will not have passed through the plate at all.

1.4.5 Heat Flow

Heat flow measurements in the eastern Caribbean and adjacent Atlantic ocean (Von Herzen et al., 1970) suggest a moderately high heat flow (2.0 HFU) on the Lesser Antillean platform and a moderately low heat flow (0.7 - 1.0 HFU) over the eastern Tobago Trough and

Barbados Ridge. Epp et al. (1970) show that the average heat flow in the Venezuelan Basin is similar to that found in other ocean basins and that the average value in the Grenada Trough is slightly higher.

Chapter 2

THE LESSER ANTILLES SEISMIC PROJECT

2.1 Objectives

In the Eastern Caribbean region the crustal thickness is known with reasonable confidence only beneath the Venezuelan Basin in the west and beneath the more normal Atlantic ocean to the east. Knowledge of the crustal structure of the main units between these two regions is based on gravity interpretations and is therefore uncertain.

The objective of L.A.S.P., therefore, was to determine crustal thickness and structure and the P-velocity in the uppermost mantle for the main structural units across the Lesser Antilles arc.

This information would provide more control on the gravity interpretation and allow an explanation of other observations such as variation in seismic delay time.

2.2 Planning Considerations

The presence of the Windward Islands, Barbados and Aves Island made possible a seismic refraction project based on the optimum method of shooting at sea and recording on land. 300lb depth charges provided an adequate and efficient source for crustal structure projects in British waters (Bott et al., 1970). For these projects the optimum detonation depth was found to be about 100m. Some 300lb shots fired near Aves Island during a Lamont cruise in 1956 gave rise to clear records at a seismological station in Dominica. The use of 300lb charges during L.A.S.P. was, therefore, considered adequate.

It was desirable to set up as many recording sites as possible along the chain of volcanic islands. With a shot spacing of under 10km along line A, detailed determination of both crustal structure and crustal thickness would be anticipated. As line A followed the axis of a single structural feature and its associated positive gravity anomaly a relatively straightforward interpretation would be expected.

The stations along the arc, together with additional stations on Barbados and hydrophone stations east and west of the arc, would provide a network of recording sites which would lend itself to a time-term approach to interpreting the results from line B. This line of shots crosses the major structure from the undisturbed Atlantic region in the east to the Aves ridge to the west. Line B was planned to pass somewhat north of St Vincent so that recording stations at the extremities of the island arc might expect to receive P_n arrivals from the whole line.

Line C was planned to investigate the deep structure of the anomalous Aves Ridge. The line follows the ridge southwards from Aves Island. The provision of a recording station at both ends of the line of shots would allow a reversed profile interpretation of the results. Any arrivals from shots along line C at stations along the Lesser Antilles arc would provide more information concerning the deep structure of the Aves ridge, Grenada Trough and Lesser Antilles arc.

2.3 Layout of Shots and Seismic Stations

Fig. 2.1 shows the location of the recording sites and shots. Exact locations of the sites are given in Appendix A.

Fig. 2.1 Location of LASP shots and recording stations

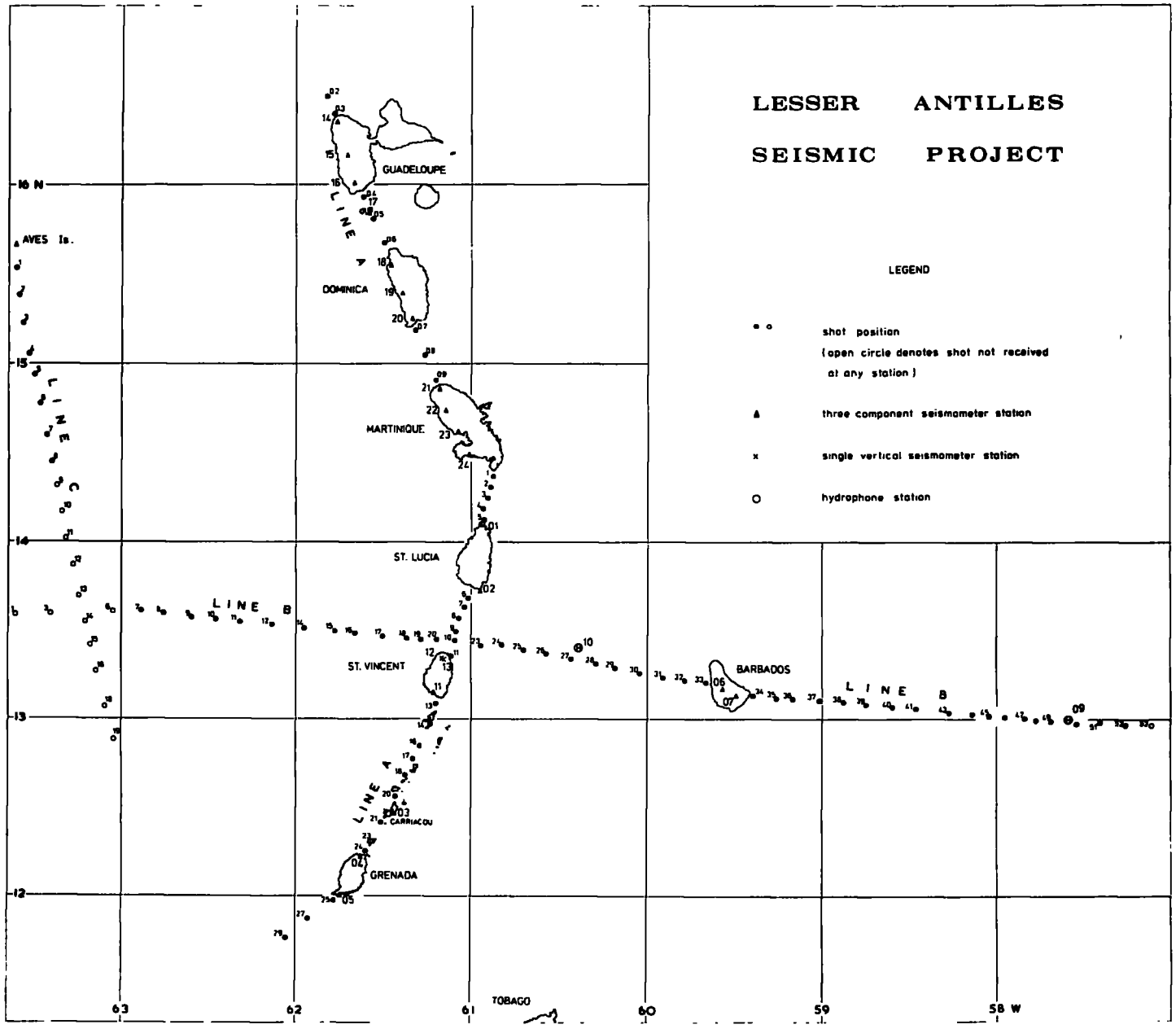
LESSER ANTILLES
SEISMIC PROJECT
LEGEND
shot position
(open circle denotes shot not received at any station)
three component seismometer station
single vertical seismometer station
hydrophone station
GUADELOUPE
DOMINICA
MARTINIQUE
ST. LUCIA
ST. VINCENT
BARBADOS
GRENADA
TOBAGO
AVES Is.
LINE A
LINE B
LINE C
16 N
15
14
13
12
63
62
61
60
59
58 W

Twenty-four temporary or semi-permanent recording stations operated in the region during L.A.S.P. Nineteen of these stations were deployed along the volcanic arc thus : Grenada (2), Carriacou, St Vincent (3), St Lucia (2), Martinique (4), Dominica (3), les Saintes and Guadeloupe (3). Two further land stations were set up on Barbados, one of which was transferred to Aves Island for the second half of the project. A hydrophone station, operated from the N.O.A.A. Ocean Survey Ship DISCOVERER, occupied two positions east and west of Barbados during the firing of portions of line B to the east of St Vincent. It was not possible to arrange for a hydrophone station to be set up either at the western end of line B or at the southern end of line C. A description of the station instrumentations is given in section 2.5.

The numbering of the shot sites in Fig. 2.1 corresponds to the numbering on the initial project plans and will be adhered to throughout this thesis to avoid confusion. Numbers missing from the sequence indicate either a shot site abandoned during the later stages of planning or a misfire.

Thirty one charges were successfully fired along line A. The shots were spread over 600km, so that the average shot spacing was about 20km. This reflects the gaps in the line due to the land areas. Between the islands the average shot spacing was less than 10km.

Line B consisted of three segments. To the east of Barbados nineteen charges were spread over a range of 250km. Here the shot spacing was reduced in the region which corresponded to the expected critical distance for Moho refractions at the hydrophone station, L.A.S.P. 9. Between Barbados and the Lesser Antilles arc eleven charges were fired over 150km. Sixteen charges were exploded to the west of the Lesser Antilles arc along a 260km span. The average

shot spacing along line B was 15.1km. Line C comprised eighteen shots on a line extending 316km S 10° E of Aves Island. The northern end of line C is approximately 230km west of Dominica and its southern end is about 180km WSW of Carriacou.

Shot firing occupied eight nights during the period 13 April to 23 April 1972.

2.4 Shot Firing

2.4.1 Equipment and procedure

On board HMS Hecla the Naval personnel were responsible for navigation and the shot firing routine. Personnel from the Department of Geological Sciences, Durham University, were responsible for broadcasting information concerning the shot firing programme to the receiving stations and for recording the 'shot instants', i.e. the exact time of each explosion.

Broadcasts from HMS Hecla during shot firing adhered rigidly to the following routine :

Time (minutes)	Transmission
T - 10	Voice announcement in French : "Ten minutes to shot drop number X"
T - 5	Voice announcement in English : "Five minutes to shot drop number X"
T - 2	Serial coded clock signal transmitted giving time of day in hours, minutes and seconds
T	Voice announcement in English and French : "Shot number X fired (or misfired)" Followed by the time of the next shot

The seismic source used during L.A.S.P. consisted of single Mk 7* 300lbs depth charges set for detonation at 350'. The charge firing routine ran smoothly and there were only two misfires in a total of 97 charges dropped. One shot, B15, detonated prematurely and caused slight damage in the engine room. Otherwise the 43-56 seconds between charge drop and charge detonation was sufficient for the ship to reach a safe distance (0.30 - 0.37km). In water shallower than 130 metres the charges detonated late because the lower ambient pressure at detonation caused an increase in the time required to operate the pressure dependent time delay mechanism. This allowed the ship to travel further away from the shot before detonation, compensating for the greater vibration of the ship caused by the longer reverberations expected in shallower water.

2.4.2 Shot positions

The final shot positions are shown in Fig. 2.1 and are tabulated in appendix A.

The position of the ship when each shot was dropped overboard was estimated by 'dead reckoning' using either the ship's electromagnetic or taut wire 'logs' and occasional Satellite Navigator 'fixes'. Close in to the islands, when the ship was within radar and visual range of land, it was possible to obtain more accurate positions using radar ranges onto headlands or visual bearings of recognisable landmarks. Where radar fixes were possible, the estimated positions should be accurate to within 0.4km.

Away from land the shot positioning was subject to systematic and cumulative errors due to the inaccuracy of the dead reckoning methods.

The original estimates of the positions of shots on the east and west extremities of line B and the south end of line C may be out by up to 2.5km from the true positions. Two methods of providing a correction to the estimated positions have been used.

Firstly, along the eastern part of line B (shots 23-53) it was possible to calculate the range of the shots from DISCOVERER by measuring the direct water wave travel time to the hydrophone. As the two positions of DISCOVERER were well determined by Satellite Navigator, a much tighter control on the longitude of these shot-positions was possible (Westbrook, 1973). Using this method corrections were applied to the estimated positions of shots B37-B48. The maximum correction was 1.1 minutes of longitude, about 2km. It was found unnecessary to adjust the positions of shots B23-B33.

The other method of correcting the estimated shot positions was to compare the P.D.R. record along the shot lines with detailed, well-controlled bathymetric surveys made by Hecla during 1971-72. This was done for shots along line C by the naval personnel from HMS HECLA. The corrections for shots near to Aves Island were large because the detailed bathymetric survey of the Aves ridge, made after L.A.S.P. in 1972, showed that the charted position of Aves Island was in error by about 3km. Corrections to the estimated positions of shots B20-1 were calculated by the present writer using the method indicated above. It is believed that the final positions quoted in appendix A for shots away from land are accurate to within 1.0km.

It was unfortunate that the accurate Decca Lambda navigation system used during the 1971-72 gravity, magnetic and bathymetric surveys was not set up until after the completion of L.A.S.P. Ship positions using this system are reckoned to be accurate to within 0.2km over the whole survey area (Kearey, 1973).

2.4.3 Shot instants

Aboard HECLA, the output of a hull-mounted geophone, located well below the water line, was recorded simultaneously with the output of a digital clock on both paper and magnetic tape recorders. The clock was checked for error relative to G.M.T. by simultaneously recording the output of the clock and W.W.V. time signals at least every 4 hours.

For each shot, the time of first movement on the hull-mounted geophone was measured to within 0.01s. A correction was then applied for the time taken for the shock wave to travel from the explosion to the ship. The distance from the shot drop position to the ship was determined to the nearest 20m using the ship's distance 'log'. The depth of the shot was calculated in the manner described below. The shot instants of all the shots are given in appendix A. Their accuracy is reckoned to be better than $\pm$ .03s (J. Sunderland, personal communication).

2.4.4 Water depths and detonation depths

The precision depth recorder (P.D.R.) was operated during all the shot firing periods. The water depth at the time of each charge drop was measured off the P.D.R. trace and logged. Corrections were made to these values using the tables of Matthews (1939). The calculated water depths are given in appendix A.

The depth of each shot was initially estimated from the measured time between the charge hitting the water and firing and the known rate of sinking of Mk 7* charges. However, as these estimated depths were greater than the preset 350', it was likely that, either

the sinking rate quoted by the Navy was low, or the pressure dependent time delay mechanism was poorly calibrated, or both.

For a few of the shots it was possible to identify two 'second arrivals' on the geophone records. These were the reflection from the sea-bed and an arrival that had been reflected from both the water surface and the sea-bed. Measurement of the times between arrivals gave accurate values for the detonation depths of these shots. These were then used to determine a more reliable estimate of the charge sinking rate. This rate was then applied to the remaining shots to produce a more accurate detonation depth. The calculated sinking rate was 2.75 ($\pm$ .12) m s^{-1}. The calculated detonation depths are given in appendix A. The histogram in Fig. 2.2 shows the distribution of detonation depths. The mean detonation depth is about 130 $\pm$ 10 m.

2.5 The Seismic Stations

2.5.1 The Durham stations

The five temporary seismic stations provided by Durham University were installed on Grenada (2), Carriacou (Grenadines), and St Lucia (2). All these stations were identical, using three-component sets of Willmore Mk I seismometers together with a seismic recording package designed and built at Durham University, Department of Geological Sciences. The design of the seismic recorder is described by Long (1974).

This equipment records three channels of seismic signal in F.M. mode on eight-track quarter-inch magnetic tape, alongside radio, encoded time and a 100Hz reference frequency, A three channel amplifier, clock and tape recorder are provided, all conveniently housed in a single case.

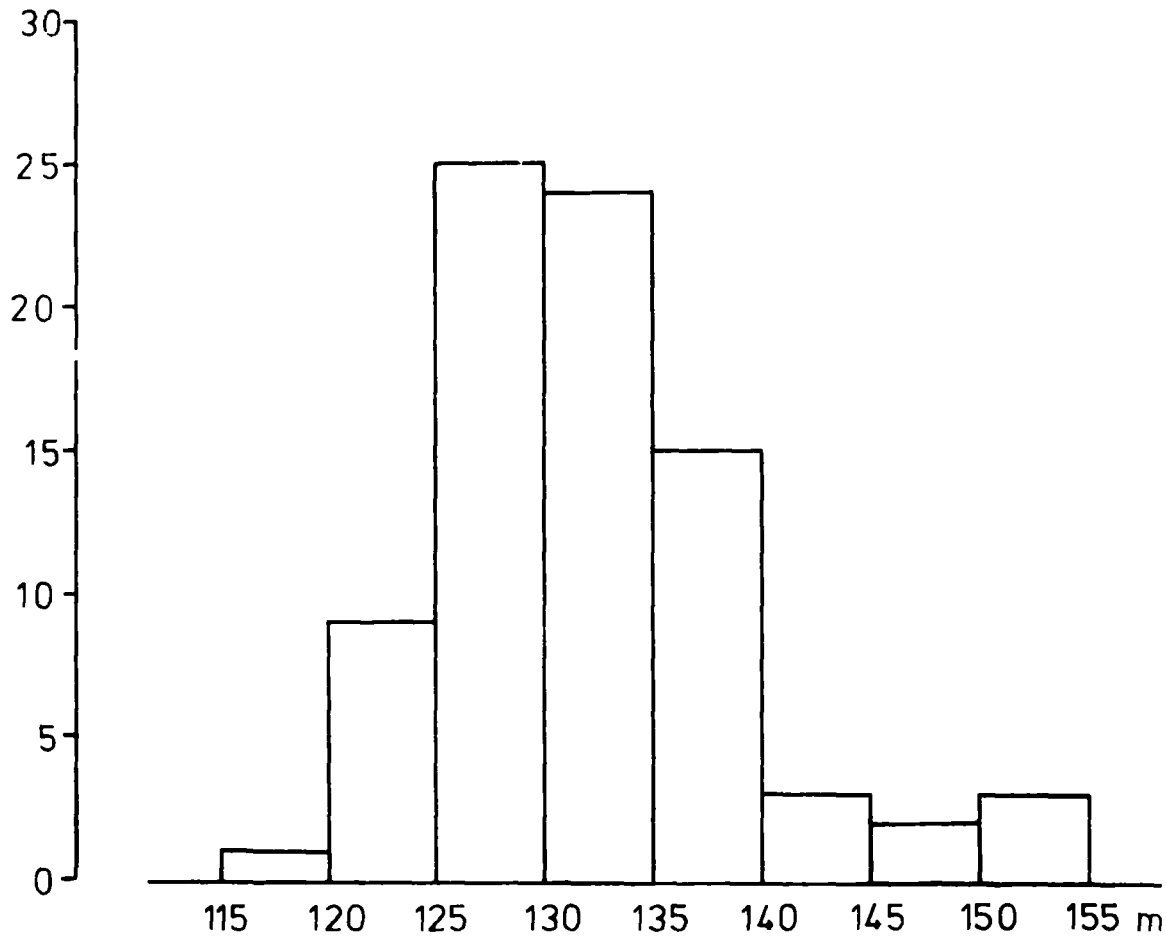

Fig. 2.2 Distribution of calculated detonation depths

The seismic amplifiers have a dynamic range of 20 log $\frac{6\times10^7}{\text{gain}}$ db where the gain is collectively adjustable in ten stages of x2. The actual voltage gain is 100 x 2^n, n = o,9.

The frequency response of the seismic amplifier varies with the gain setting. Over the following ranges the gain is constant to within $\pm$ 5% :

n = 0,3	range	0.5 to 100 Hz
n = 4,7	range	0.5 to 15 Hz
n = 8,9	range	0.5 to 12 Hz

The frequency response of the complete recording system is controlled, at the low frequency end, by the natural period of the seismometers and, at the high frequency end, by the tape speed used. The response in the mid-frequency ranges depends on the seismometer damping.

The magnetic tape drive is geared to give tape speeds of 0.1 inch per second (normal) or 0.05 inch per second (slow). The order of recording across the tape is :

Track 1	Seismic I
2	- not used
3	Seismic II
4	- not used
5	Seismic III
6	100 Hz reference signal
7	Radio
8	Clock

The two unused channels reduce cross-talk between the three seismic channels.

Field Operation :

Factors considered when choosing sites for the stations were :

(a) nearness to solid rock basement

(b) proximity to trees

(c) proximity to coast

(d) proximity to sheer cliff or other seismic 'obstacle'

(e) shelter from wind

(f) remoteness from cultural noises

(g) security of equipment

(h) ease of access for servicing equipment

It was, of course, impossible to satisfy the ideal requirements of all these factors when choosing a site. The sites chosen were ones which were as satisfactory as any that could be found within the general area in which they were to be located. Each of the sites had disadvantages : LASP 1 was sited on unconsolidated material. LASP 2 was near to a steep cliff and suffered from wind noise, as did LASP 3 and LASP 4. LASP 5 was situated very close to the beach.

Notes on the layout of the seismometers at the five Durham stations are given in appendix B.

One hundred metre lengths of twin core screened cable were used as land lines for the seismometers. Care was taken to separate the lines as far as possible between the seismometer pits and the recording apparatus to cut down pick-up on the lines. The input circuit to the seismic amplifiers is shown in Fig. 2.3. The 1.5kΩ resistance is used to balance the resistance of the seismometer coil as the amplifier was designed for use with 3kΩ centre tapped coil

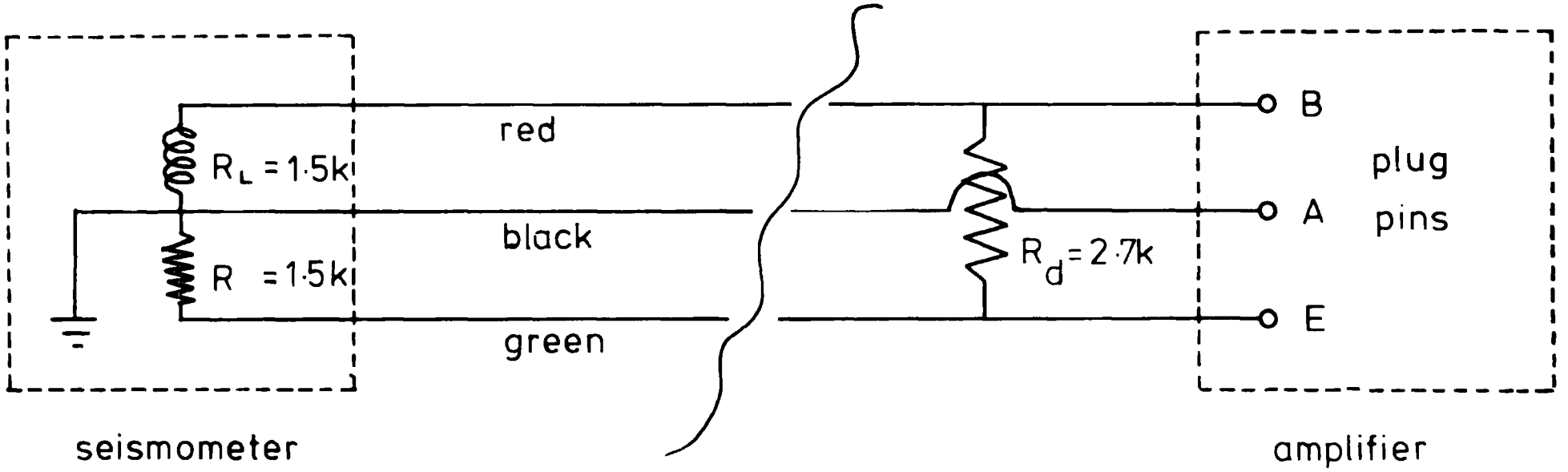

Fig. 2.3 Seismometer input circuit .

seismometers. The 2.7kΩ resistance was added across the input bridge, on the horizontal seismometers only, to provide optimum damping.

The tape recorders were run at the normal speed of 0.1 inch per second. The tape used was Scotch doubleplay (2400 feet, 7" spool), so that each tape provided more than 3 days continuous recording. All the stations recorded continuously during the periods in which shots were fired, except that LASP 5 missed shots C14-19 as the tape ran out overnight. LASP 5 was also shut down for repairs on 18 April. Otherwise, the stations recorded continuously for the whole duration of L.A.S.P.

The gain on the amplifiers was left on setting 9 (about 51,200) unless the noise level became greater than 0.5 x saturation, in which case it was set to 8. At most of the stations the gain was further reduced for the period when shots were being fired close by.

At the two St Lucia stations there was some trouble caused by dirt accumulating on the spooling brake pads on the tape transport. This had the effect of making the brakes bind on the spools, producing increased tension in the tape and a less constant drive speed. The effect of this, after demodulation, was to produce an anomalous noise on the records which varied in intensity. The period of this variation was about the period of one revolution of the spool on the tape transport. This effect was particularly noticeable on records from LASP 1 for the last half of the shots.

Goolay LF radio receivers were provided in anticipation of good reception of the 60 Hz transmissions of the WWV standard time station. It was found that it was impossible to receive these signals in the Windward Islands. This was due either to weak signal strength or inadequacy of the Goolay aerials.

Also provided were high quality commercial short wave/medium wave receivers with in-built whip aerials. These were to be used to receive the broadcasts from HMS HECLA on 3.65 MHz, and to act as an alternative source of time checks to the Goolay receivers. WWV time signals are transmitted on 10 MHz, 5 MHz, 2.5 MHz and other frequencies on the short waveband.

At all the Durham stations reception of WWV transmissions was very poor and for almost the entire duration of the project the signal strength was too weak for adequate recording. A satisfactory method of tying in the station clocks with the shooting ship clock would have been to record the broadcasts from HMS HECLA during the firing of each shot. These broadcasts included transmission of the modulated output of the ship's digital clock which was regularly checked with the WWV timing signals. However, broadcasts from HECLA were only received at the Durham stations when the ship was within close range (under 100km) so this method would have been of limited use.

As a last resort the radio receivers were tuned in to various radio stations which broadcast G.M.T. time 'pips' on the hour at intervals of a few hours during the day. At four of the Durham stations such 'pips' were adequately, if somewhat irregularly, recorded from broadcasts by Radios Barbados and Grenada and the BBC Overseas Service on 15.1 MHz. At LASP 3 (Carriacou), although the G.M.T. 'pips' were heard distinctly, they were not recorded due to an oversight by the operator. However, by comparing the audio monitor from the clock with the radio output, the operator was able to estimate the clock error to within 0.1 to 0.2 s. The error was calculated in this manner at least once every day. Luckily, the clock drift was apparently very low at this station (about 0.2 s per day) and was quite linear.

It is thought that the timing at this station is accurate to within 0.2 s. There is no evidence from the deduced travel times at this station to indicate a systematic clock error.

Of the other four stations, LASP 1 and LASP 4 showed a very low clock drift of less than 0.01 s per hour. The drift at LASP 2 was about 0.28 s per hour and that at LASP 5 approximately 0.62 s per hour. In all cases the drift was almost linear. It is supposed that the clock 'drift' was almost entirely due to the crystal oscillators being slightly 'out of tune'. This was to be expected as there had been no time, before the commencement of LASP, to rigorously check the tuning of the clock crystals.

The high clock drift at LASP 2 and LASP 5, together with the large gaps between time-checks overnight, means that the timing accuracy for these stations is probably no better than 0.1 sec for the majority of the shots.

2.5.2 The French stations

The Institut de Physique du Globe, Paris, deployed eleven temporary recording stations on the islands of Guadeloupe (3), Les Saintes (1), Dominica (3), and Martinique (4). The instrumentation for all these stations was uniform.

Three component sets of Mark Product seismometers with a natural frequency of 2 Hz were used. The outputs of the seismometers were fed into a Lennhartz 7031/Z amplifier-modulator. A radio receiver and clock were included in the equipment. The three seismic signals and the radio and timing signals were each frequency modulated at a different centre frequency, thus :

Seismic	(Z	860 Hz centre frequency
	(L	2200 Hz
	(T	4400 Hz
Radio/Time		9200 Hz
Reference Signal		6400 Hz

The modulated signals were then summed and the summed signal recorded on an Uher two-track recorder using 2cm magnetic tape. A recording speed of 9.5 cm s^{-1} was used throughout. Each tape gave 2 x 1 hour recording time.

The frequency response curve for the French recording systems (Fig. 2.4) shows a bandwidth of 2.5 to 100 Hz. The low frequency cut-off is fairly steep, the magnification at 1 Hz being only one fifth of the peak response.

It was not possible to record continuously at the French stations because of the fast recording speed. Where possible, the stations recorded for periods of about fifteen minutes, five minutes before to ten minutes after each expected shot detonation time. Thus these stations were reliant upon receiving the broadcasts from HECLA to ascertain the planned shot times.

An efficient communications system was set up linking the stations so that all of the stations were able to record most of the shots. Accurate time checks were made using the 10 MHz WWV transmissions or the time 'pips' on Radio Guadeloupe.

The elevations of the French stations (appendix A) range from 17m to 646m. Their distance from the coast was quite variable, LASP 17 (les Saintes) being the station most susceptible to noise due to wave motion. Otherwise, the background noise differs

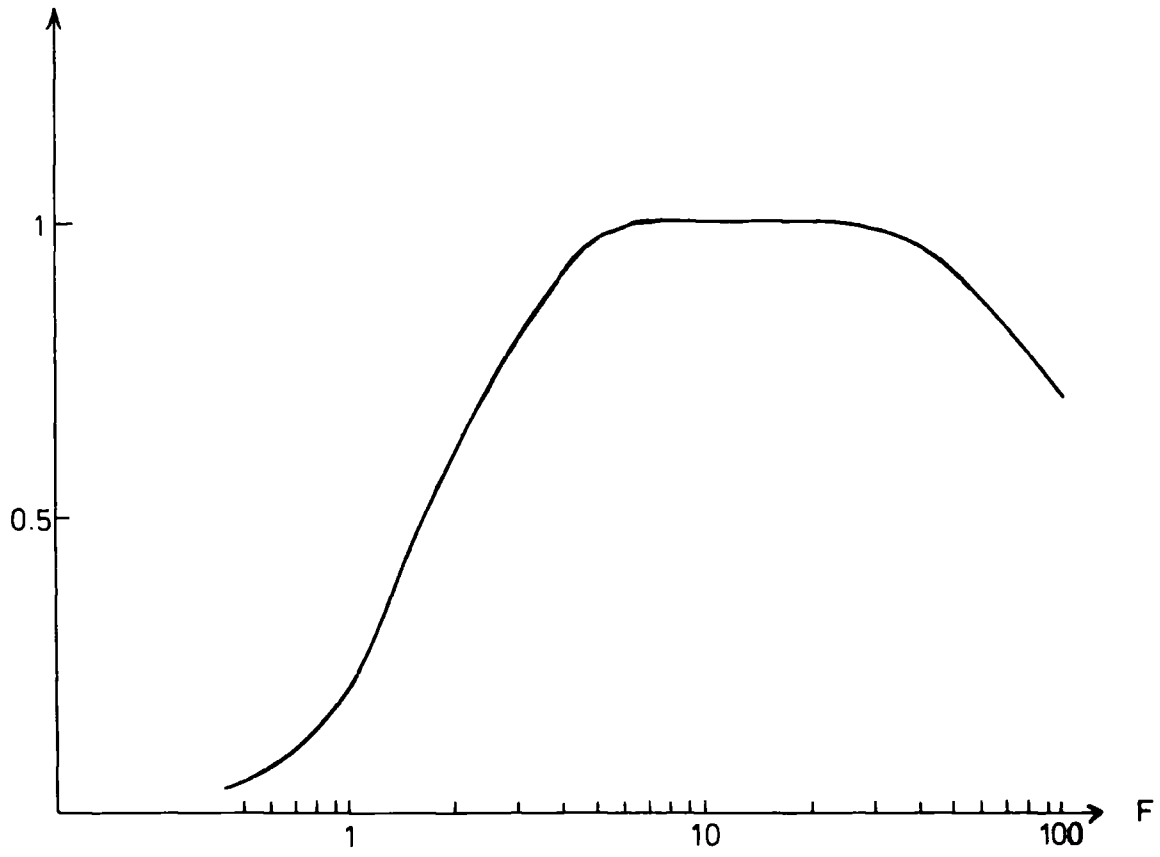

Fig. 2.4 · Frequency response curve for the French recording stations.

considerably, in both amplitude and frequency content from station to station (J. Dorel, personal communication). The stations LASP 16, LASP 20 and LASP 21 showed a high level of noise, the dominant frequencies being 0.5 Hz and 5 to 8 Hz.

Apart from the eleven temporary stations there were also two permanent seismic installations of the Institut de Physique du Globe operating during LASP. These consist of a network of four stations based at the Observatoire St Claude in Guadeloupe and three stations operated from the Observatoire Morne des Cadets in Martinique.

2.5.3 The U.W.I. stations

During LASP the University of the West Indies, Seismic Research Unit (Trinidad) operated a network of three stations on the island of St Vincent. These were semi-permanent stations remaining from the network of seismic stations set up at the time of the Soufriere volcanic crisis in late 1971.(Tomblin et al., 1972).

At Camden Park (LASP 11) there was a three component set of Willmore Mk II seismometers. Each seismometer drove a Racal-Thermionic T8100 Seismic Amplifier-modulator into a Racal-Thermionic T8100 1" magnetic tape recorder. The other two stations (LASP 12 and LASP 13) were situated on Soufriere mountain in north St Vincent. Each consisted of one vertical Mk II Willmore seismometer driving a Teledyne TM 251 Amplifier-modulator into a Motorola FM radio link. At the foot of Soufriere an FM receiver collected the signals and passed them by landline, telephone line and drop-line to Camden Park. Here they were demodulated by a Teledyne TR401 discriminator and passed through a U.W.I. interface into the modulator section of a Racal-Thermionic

amplifier-modulator and then recorded on the same tape as the Camden Park instruments. Also recorded on the tape were radio time signals (WWV), time code and a wow and flutter compensation signal.

The St Vincent network of stations recorded continuously during L.A.S.P. There was a fault in the Camden Park equipment which caused the recordings of the vertical and north-south seismometers to be useless.

The recording of the east-west seismometer was rather poor, but usable. The other two seismometers gave good records despite the windy conditions on Soufriere, which gave a high level of noise at both sites. This was fortunate as these two stations occupied a critical position in the project, being the nearest to the intersection of shot lines A and B.

The magnifications were about 12,000 for all stations.

2.5.4 The Leicester stations

Personnel from the Geology Department, University of Leicester, under the direction of Dr M. A. Khan, operated two seismic recording stations in the survey area. The station at St Phillips, Barbados (LASP 7) consisted of a three-component S.I.E. Seismic system. All recording at this station was done with a 3.5 Hz LC filter in the system. This was observed to have a detrimental effect on the recordings of the seismic arrivals from the more distant shots. Magnification was about 16,000 for most of the shots. WWV signals and the output of a second-marker generator were recorded alongside the geophone signals to provide accurate timing.

The other station consisted of a Mars system with a three-component geophone set. This was located at Cole's Cave, Barbados (LASP 6) for the first half of the project. This site was rather noisy and prone to vandalism. This station was transferred to Aves Island for the second half of the project. A combination of the loose sediment cover, the close proximity of the sea and lack of shelter from the wind caused the Aves site to be extremely noisy. Reception of WWV was poor on the island and for most of the shots the broadcasts from the shooting ship were recorded as an alternative means of timing. Magnifications on the Mars equipment varied from 290 to 9,320.

The Leicester stations did not record continuously and, like the French stations, they relied on the HECLA broadcasts to ascertain the times of the shots. At the Barbados stations several shots were missed through poor radio reception and tapes running out.

2.5.5 The hydrophone stations

A description of the hydrophone system used on DISCOVERER is given by Westbrook (1973). The technique is similar to that described by Shor (1963). The outputs of two Clevite hydrophones, suspended at depths of 30m and 60m in the water, were recorded on magnetic tape together with the output from a digital clock. A fourth track was used to record WWV signals, broadcasts from the shooting ship and identification, by voice, of the shot number and time.

DISCOVERER was at site LASP 9 during the firing of shots B53 to B37 and moved to LASP 10 to receive shots B36-B23.

2.6 Record Processing

The tapes from the five Durham stations and from the three U.W.I. stations were processed by the writer using the facilities in the data processing laboratory of the Department of Geological Sciences, Durham University.

Processed records for the three Leicester stations were supplied by Dr M. A. Khan. First arrival times from the recordings made at the French stations were made available to the writer (J. Dorel, personal communication) as also, were the first arrival times at the hydrophone stations (G. K. Westbrook, personal communication).

The data processing laboratory contains replay facilities for FM recordings on ¼", ½" and 1" tapes. Each track signal is demodulated and 'wow' and 'flutter' is compensated for by subtracting the recorded reference signal from each track. All the signals can be monitored on a multi-trace oscilloscope and played out directly onto paper through a jet-pen recorder. Three Krohn-Hite filters are available for analogue frequency filtering of up to three seismic tracks simultaneously.

Initially the tapes were searched for time checks, i.e. periods when the station clock output was recorded alongside a radio time signal (W.W.V. or G.M.T. 'pips'). These time checks were used to establish a clock drift curve for each station. The expected time of seismic arrivals from the shots was then calculated for each station relative to its clock 'time'. This allowed the shot recordings to be replayed separately without having to replay the whole tape.

On the records the signal-noise ratio for the first arrivals was often very poor for all but the nearest shots. For the more distant shots it was less than unity. To help in identifying the first arrival

the three seismic channels were passed through bandpass filters to remove most of the noise. The optimum bandpass for this purpose was found to be 2 Hz to 8 Hz. Once identified, the arrivals were 'picked' off the unfiltered traces as the filtering process changes the phase of the signal by an amount related to the signal frequency and the pass band of the filter.

As an aid to 'picking' first and later arrivals from a line of shots, the records were laid out side by side with the shot instants aligned and the separation of the records proportional to the shot separation. It was then possible to trace a particular phase through a series of shots. Using this technique, the distance at which a new phase appears as the first arrival could be easily seen.

Polarization filtering

Using optimum bandpass filtering first arrivals were discernable at all stations from shots up to 150km to 200km distant. Beyond this distance the energy in the first arrival was so low that the signal could not be 'drawn' out of the noise by normal filtering. It was necessary to use a technique that gave a better signal enhancement than optimum bandpass filtering.

For the three-component stations this was possible using a polarization filter similar to that developed by Shimshoni and Smith (1964). The method depends on the fact that P-wave signals are rectilinearly polarized whereas most of the noise and other arrivals, such as shear waves and surface waves, are elliptically polarized. The filter forms the time-averaged cross product of the vertical and radial components of ground motion,

$$M_j = \sum_{i=-n}^{+n} H_{i+j} \sim V_{i+j}$$

This gives a measure of the rectilinearity and the total signal power along the record. The time interval for the integration, $(2n + 1), \Delta t$, is critical.

The integration window used is a compromise as the noise suppression is greater for longer integration times as is the uncertainty in picking the arrival. An integration time of 0.4 s was found to give the best results. The filter also outputs two other functions, which give a more familiar form of display. These are :

$$V \times |M| \quad , \quad V \times |M|^{\frac{1}{2}}$$

This filter was programmed for a CTL Modular One computer which is linked to the data processing equipment at Durham. The bandpass filtered seismic channels were electronically digitised at 100 samples per second (tape time) using the recorded reference frequency as a time-base for digitising. The digitised signals were then passed through the filter which was programmed to operate continuously. The signals output by the filter were played-out alongside the unfiltered seismic traces on the jet pen recorder. The delay due to filtering through the Modular One computer was calculated by programming the computer to read in the digitised clock channel and to output it simultaneously with the filter outputs. The delay is :

$$(2n + 1).\ \Delta t/2 \ + \ \text{system delay}$$

The system delay is very small compared to the integration delay.

The filter was effective in improving the signal-noise ratio. However, it was found that where arrivals were not discernable

Fig. 2.5 Two examples of the application of bandpass and polarization filtering to LASP records

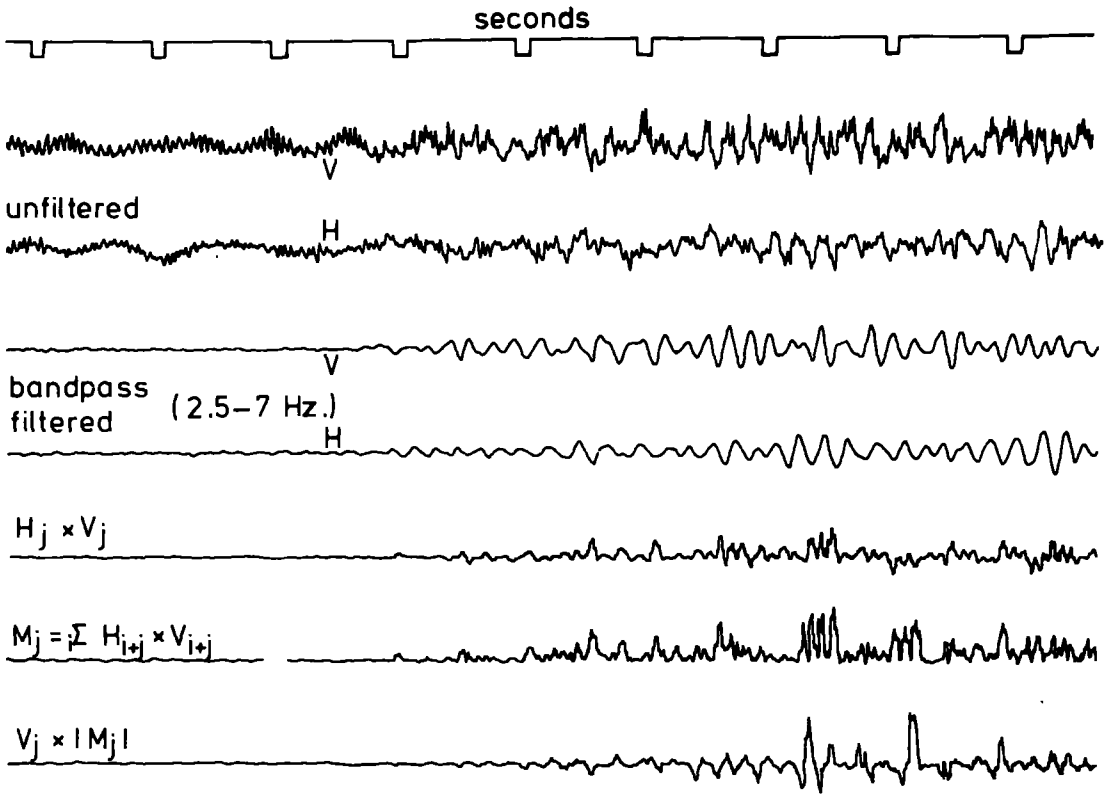

CARRIACOU . SHOT A6 . Δ = 140.2 km.

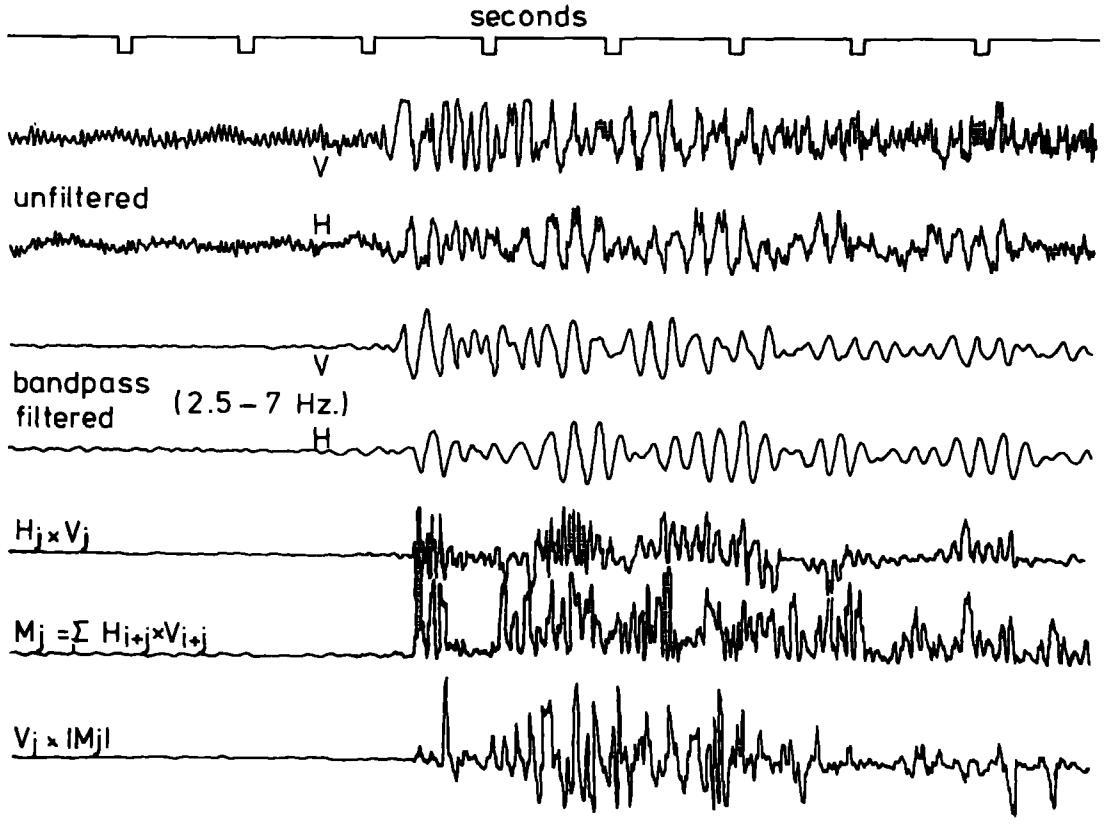

CARRIACOU . SHOT A11 . Δ = 103.3 km.

from the original seismogram, or after bandpass filtering, they were usually not observed after polarization filtering either. The filter was useful in confirming the presence of some doubtful arrivals and indicated the presence of some others from distant shots. Examples of recordings which have been processed using the polarization filter are shown in Fig. 2.5.

2.7 First Arrival Travel Times

The measured first arrival travel time was the time difference between the shot instant time and the time of the first motion of the seismometer at the receiving station.

Two corrections were applied to the raw travel times. These were a datum correction and a correction to compensate for sea bottom topography.

The datum correction gives the travel time which would be observed if both shot and receiver were on the same datum. For this study, the datum used was sea level. The correction is, to a good approximation :

$$\Delta t_d = \frac{\text{Height of station}}{V_s} - \frac{\text{shot detonation depth}}{V_w}$$

where, V_s is the mean velocity between the station and the datum level and V_w is the near-surface water velocity. This correction is small as the two terms often almost cancel one another. Its value never exceeds 0.2 s. The datum correction is subtracted from the travel times.

The second correction is applied together with the datum correction. It is a very important correction in regions where there is extreme variation in sea-bottom topography, e.g. across the flanks of the Grenada and Tobago troughs. The correction effectively 'fills' the sea with sediment of velocity equivalent to the mean sediment velocity above the basement. The correction is a function of the water depth beneath the shot, the mean water velocity, the sediment velocity and the velocity of the refractor in which the arrival is critically refracted (as this controls the angle of the ray-path through the water). The correction used was :

* see below

$$t_s = \frac{D_s}{\bar{V}_w \left(1 - \frac{\bar{V}_w^2}{V_z^2}\right)^{\frac{1}{2}}} - \frac{D_s}{\bar{V}_s \left(1 - \frac{\bar{V}_s^2}{V_z^2}\right)^{\frac{1}{2}}}$$

where $\bar{V}_w$ is the mean velocity in water.

$\bar{V}_s$ is the mean velocity of the sediments

V_z is an estimate of the refractor velocity

D_s is the water depth at the shot site.

The total correction exceeds one second for some shot-station paths.

Both corrections were applied to the travel times before calculating the apparent refractor velocity from the time-distance graphs (see section 2.9). However, for the subsequent time-term analysis of the first arrival data only the datum correction was applied as the effect of the water depth could be removed from each time-term after the calculation of the least squares velocity.

* NOTE : This expression for the 'seabed topography correction ' is incorrect. It should be :

$$D_s/\bar{V}_w \cdot (1 - \bar{V}_w^2/V_z^2)^{1/2} - D_s/\bar{V}_s \cdot (1 - \bar{V}_s^2/V_z^2)^{1/2}$$

The above (incorrect) expression has been used throughout this thesis . Therefore the corrected travel times used in the calculation of all the apparent velocities and in the reversed-profile and plus-minus interpretations are in error by a small amount. However , this error does not effect the time-term solutions because this correction was not appliad there .

2.8 Shot-Station Ranges

The distance between each shot and each station was determined from their geographic locations (appendix A) using the program DISTAZ. This program is described and listed in Appendix C of Westbrook (1973). The ranges calculated using this program are thought to be accurate within $\pm$ 10 metres, which is small compared to the possible error in location of the shots. The program DISTAZ also calculates the true azimuth of each shot from the receiving stations.

2.9 Apparent Refractor Velocities

For each station the corrected first arrival travel times, t, from lines of shots were plotted against the shot-station separation, Δ. If the earth's crust is assumed to be a series of plane, homogenous layers, then the inverse slope of each straight line segment of the $t - \Delta$ plot will give the apparent velocity of the layer in which the first arrival is critically refracted. (The apparent velocity equals the actual refractor velocity only when all the layers down to the refractor are horizontal.) From the $t - \Delta$ plots, groups of arrivals which lay on approximately straight lines were picked out by 'eye'. A simple linear regression was performed on the appropriate t, Δ values to determine the equation of the best fitting straight line. From this was determined the apparent velocity of the refractor and the intercept on the time axis, t_i. The use of the apparent velocities and time intercepts is described in Chapter 3.

2.10 Presentation of Data

First arrival data is presented in reduced travel time versus distance graphs. Here the ordinate is $t - \Delta/6.0$ so that arrivals with an apparent velocity of 6.0 km s^{-1} will plot parallel to the distance axis.

Some stacked records are included. These show tracings of the actual seismograms mounted in a reduced travel-time against distance grid. Where possible the scale used is such that 5 seconds on the reduced time axis equals 40kms on the distance axis. This is in keeping with the scale used by other workers (Fuchs and Landisman, 1966; Holder and Bott, 1971). The advantage of this form of presentation is that it allows second arrival phases to be followed across the records and gives a comparison of the amplitude and shape of the arrivals over the whole profile.

Chapter 3

THE TIME-TERM METHOD

3.1 Introduction

The L.A.S.P. project was planned to provide an adequate network of shots and receiving stations to allow time-term analysis to be used to define refractor velocities and thicknesses within the Earth's crust. Before time-term analysis could be attempted it was necessary to ensure that all the data to be used in each analysis related to the same refractor. Therefore, a preliminary interpretation of the first arrival data was made by means of the classical 'reversed profile' method and a modified 'plus-minus' method.

Both these methods require the shots and receiving stations to be approximately in a line and that the shots be 'observed' in both directions along the line. The reversed profile method assumes that the refractors have uniform velocity and dip and are plane surfaces. The apparent velocities and intercept times observed in both directions are used to determine the 'true' refractor velocity, the apparent dip in the direction of the shot line and the refractor depth beneath each end of the line. The theory of the method is described briefly in Appendix C.

The other method used was adapted, by the present writer, from the 'plus-minus' method of interpreting refraction data which was formulated by Hagedoorn (1959). The advantage of this method is that it shows where there are lateral variations in refractor velocity (which would invalidate the reversed profile interpretation) and also allows a

small degree of irregularity in the refractor topography. The method is described in Appendix D. The modification is necessary as the travel time from one end of the profile to the other (used in calculating the plus time and, therefore, the depths) is not directly measurable as there are no shots occupying the station sites.

3.2 The Least-squares Solution

The time-term method in seismic refraction studies was formulated by Scheidegger and Willmore (1957) and developed by Willmore and Bancroft (1960). The method has been used successfully in the interpretation of large-scale refraction experiments over a number of years. These experiments include the Lake Superior Experiment of 1963 (Berry and West 1966), the Continental Margin Refraction Experiment in 1969 (Bamford 1970, 1971) and the South-West England Seismic Project of 1966 (Holder and Bott 1971).

Given a crust consisting of uniform velocity layers, the travel time for a refracted wave arrival travelling from shot i to station j is given by :

$$t_{ij} = a_i + a_j + \frac{X_{ij}}{V} \qquad (1)$$

where X_{ij} is the shot-station separation.

V is the velocity within the layer in which the wave is critically refracted.

$a_i (a_j)$ is the time-term or time delay associated with the overburden at the shot (station) end of the ray-path.

If there are n stations receiving from m shots, then up to n x m travel-times, t_{ij}, may exist. The number of unknowns in all the equations (1) is n + m + 1. The number of observations is likely to exceed the number of unknowns by a large amount. A constant, α, may be added to the shot time-term and subtracted from the station time-term while still satisfying equation (1). A unique solution is therefore impossible to obtain unless either, the value of one time-term is already known or, one station and one shot occupy the same site.

If, $p_{ij} = 1$ when t_{ij} exists as data

$= 0$ when t_{ij} is absent

and ℓ is the number of sites that are both shots and stations, such that,

$k = n + m - \ell$ is the total number of sites,

Then the normal equations for the i^{th} station and j^{th} shot are :

$$m_i(a_i - \alpha) = \sum_{j=1}^{k} P_{ij}(t_{ij} - X_{ij}/V) - \sum_{j=1}^{k} (a_j + \alpha)\, p_{ij} \qquad (2)$$

$$n_j(a_j + \alpha) = \sum_{i=1}^{k} p_{ij}(t_{ij} - X_{ij}/V) - \sum_{i=1}^{k} p_{ij}(a_i - \alpha) \qquad (3)$$

where m_i is the number of shots received by the i^{th} station

n_j is the number of stations observing the j^{th} shot.

α is the arbitrary constant.

for convenience, let $\alpha = 0$.

The observed travel time T_{ij}, differs from the calculated travel time by an amount δ_{ij} known as the residual travel time, i.e. $T_{ij} = t_{ij} + \delta_{ij}$.

A solution of the normal equations for the time-terms is achieved by minimising the sum of the squared residual travel times, I, with respect to the time-terms.

$$I = \sum_{i=1}^{k} \sum_{j=1}^{k} p_{ij}(T_{ij} - t_{ij})^2 \qquad (4)$$

The minimising condition is $\partial I / \partial K = 0 \; ; K = 1,k$

and for the i^{th} term we obtain

$$\sum_{i=1}^{k} \sum_{j=1}^{k} a_j p_{ij} + \sum_{i=1}^{k} a_i \sum_{j=1}^{k} p_{ij} = \sum_{i=1}^{k} \sum_{j=1}^{k} p_{ij}\left(T_{ij} - \frac{X_{ij}}{V}\right) \qquad (5)$$

this being one of k normal equations represented in matrix form by

$$\left[A_{ij}\right] . \left[a_j\right] = \left[\sum_{j=1}^{k} \left\{ p_{ij}\left(T_{ij} - \frac{X_{ij}}{V}\right) + p_{ij}\left(T_{ji} - \frac{X_{ji}}{V}\right) \right\} \right] \qquad (6)$$

where $A_{ij} = p_{ij} + p_{ji}$

$$A_{ii} = \sum_{j=1}^{k} \left(p_{ij} + p_{ji}\right)$$

Now multiply both sides of equation (6) by the inverse matrix of $\left[A_{ij}\right]$

$$\left[a_j\right] = \left[A_{ij}\right]^{-1} . \left[\sum_{j=1}^{k} \left(T_{ij}p_{ij} + T_{ji}p_{ji}\right) - \sum_{j=1}^{k} \frac{X_{ij}}{V}\left(p_{ij} + p_{ji}\right) \right] \qquad (7)$$

which is of the form

$$a_j = e_j - f_j / V \qquad (8)$$

where $\left[e_j\right] = \left[A_{ij}\right]^{-1} . \left[\sum_{j=1}^{k} \left(T_{ij}p_{ij} + T_{ji}p_{ji}\right) \right]$

$$\left[f_j\right] = \left[A_{ij}\right]^{-1} . \left[\sum_{j=1}^{k} X_{ij}\left(p_{ij} + p_{ji}\right) \right]$$

Now, if sufficient redundancy remains in the data, the equation of condition $\partial I / \partial (1/V) = 0$ will provide an estimate of V, the refractor velocity.

from equation (1) substituting from (8) gives :

$$t_{ij} = e_i - \frac{f_i}{V} + e_j - \frac{f_j}{V} + \frac{X_{ij}}{V} \qquad (9)$$

and applying the minimization condition yields :

$$V = \frac{\sum_{i=1}^{k} \sum_{j=1}^{k} p_{ij}(X_{ij} - f_i - f_j)^2}{\sum_{i=1}^{k} \sum_{j=1}^{k} p_{ij}(X_{ij} - f_i - f_j)(T_{ij} - e_i - e_j)} \qquad (10)$$

$$\text{or} \quad V = \frac{\sum_{i=1}^{k} \sum_{j=1}^{k} p_{ij} d_{ij}^2}{\sum_{i=1}^{k} \sum_{j=1}^{k} p_{ij} C_{ij} d_{ij}} \qquad (11)$$

where $C_{ij} = T_{ij} - e_i - e_j$

$d_{ij} = X_{ij} - f_i - f_j$

The usual way of deriving the velocity and the time-terms from the normal equations is by inversion of the matrix $[A_{ij}]$ and calculation of the matrices $[e_j]$, $[f_j]$, $[c_{ij}]$ and $[d_{ij}]$. This method was used by Berry and West (1966), Holder (1969) and Bamford (1970). If the matrix $[A_{ij}]$ is singular, then inversion is impossible. This is the case when no site is occupied by both a shot and a station. In the L.A.S.P. network no shot site was sufficiently close to a station site for their appropriate time-terms to be considered as equal. It was preferred to allocate a value to one time-term from geological considerations, thus allowing a value of α to be determined subsequent to the solution.

3.2.1 Use of an iterative method of solution

To allow for the lack of coincident shot and station locations the author wrote a computer program which solved the time-term equations by the iterative method described by Mereu (1966).

Given a network of m shots and n stations the (m+n) normal equations (2,3) which are derived from the observational equations are divided into two groups and placed in the form :

$$\begin{aligned} m_i\, a_i + \sum_{j=1}^{n} p_{ij} b_j &= T_i - \frac{D_i}{V} \\ n_j\, b_j + \sum_{i=1}^{m} p_{ij} a_i &= T_j - \frac{D_j}{V} \end{aligned} \qquad (12)$$

$$i = 1, \ldots\ldots, m \qquad j = 1, \ldots\ldots, n$$

where
$$m_i = \sum_{j=1}^{n} p_{ij} \qquad n_j = \sum_{i=1}^{m} p_{ij}$$

$$\begin{aligned} T_i &= \sum_{j=1}^{n} p_{ij} X_{ij} & T_j &= \sum_{i=1}^{m} p_{ij} t_{ij} \\ D_i &= \sum_{j=1}^{n} p_{ij} X_{ij} & D_j &= \sum_{i=1}^{m} p_{ij} X_{ij} \end{aligned} \qquad (13)$$

(p_{ij}, m_i, n_j have the same meanings as in equations (2), (3) above.)

Equations (12) in their present form cannot be solved conveniently by an iterative method as the refractor velocity, V, is also an unknown. To overcome this difficulty two new sets of equations that do not contain V are defined :

SET 1	SET 2
$m_i x_i + \sum_{j=1}^{n} p_{ij} y_j = T_i$;	$m_i u_i + \sum_{j=1}^{n} p_{ij} w_j = -D_i$
$n_j y_j + \sum_{i=1}^{m} p_{ij} x_i = T_j$;	$n_j w_j + \sum_{i=1}^{m} p_{ij} u_i = -D_j$

(14)

The time-terms are related to the unknowns x_i, y_j, u_i and w_j thus :

$$a_i = x_i + u_i/V$$

$$b_j = y_j + w_j/V \qquad (15)$$

this can be proved as follows :

let C, X, T and D denote matrices and λ (= $^1/V$) a scalar.

We must solve $C.X = T - \lambda .D$

let X_1 and X_2 be solutions to $C.X_1 = T$

and $C.X_2 = -D$. Then :

$$X_1 = C^{-1}.T \text{ and } X_2 = -C^{-1}.D$$

$$\therefore \quad X = C^{-1} (T - \lambda.D)$$

$$X = X_1 + \lambda.X_2 \qquad \text{Q.E.D.}$$

In order to apply the Gauss-Seidel method of iteration, equations (14), set 1 are placed in the form :

$$x_i = \left[T_i - \sum_{j=1}^{n} p_{ij} y_j \right] \Big/ m_i$$

$$y_j = \left[T_j - \sum_{i=1}^{m} p_{ij} x_i \right] \Big/ n_j \qquad (16)$$

The iteration is started by setting all the y_j equal to zero and solving for x_i giving new estimates of y_j which are used to solve for x_i, etc. Equations (14), set 2 are arranged in a similar manner and solved in the same way. The computations are speeded up by solving both sets independently in the same iterative loop of the computer program. The solution is considered to have converged when all the values of x, y, u, w change by an amount less than 0.01 between two successive iterations. Convergence is found to occur

after a few iterations for well-connected sets of data. Convergence takes place without having to fix the value of one of the time-terms. The calculated time-terms are later adjusted by a constant α.

After equations (14) have been solved, the velocity V is calculated by minimising the sum of the squared residuals, as before.

$$V = - \frac{\sum_{i=1}^{m} \sum_{j=1}^{n} d_{ij}^{2}}{\sum_{i=1}^{m} \sum_{j=1}^{n} C_{ij} d_{ij}} \qquad (17)$$

where $C_{ij} = p_{ij} (x_i + y_j - t_{ij})$

$$d_{ij} = p_{ij} (u_i + w_j + X_{ij})$$

A listing of the program TIMES is given in Appendix E.

3.3 Statistics of the Time Term Method

The statistical treatment of the simple time-term approach to give estimates of the standard deviations on the velocity and time-term solutions is discussed by Scheidegger and Willmore (1957), Berry and West (1966) and Bamford (1971). The calculations depend on whether it is assumed that the measurements from the whole network come from the same distribution, or it is assumed that measurements from each site are from the same distribution. Bamford prefers the latter assumption as 'the quality of data at one site is at least as important as the manner in which it is related to the remainder'. Both approaches assume that the errors are in some sense normally distributed and are exact only when all possible observations exist as data.

The error calculations used here are those of Berry and West (1966).

The fit of the time-term model to the observational data is indicated by the standard deviation of the solution,

$$\sigma = \left[\frac{\sum_{i=1}^{k} \sum_{j=1}^{k} \delta_{ij}^{2} p_{ij}}{\left(\sum_{i=1}^{k} \sum_{j=1}^{k} p_{ij} \right) - N} \right]^{\frac{1}{2}} \qquad (18)$$

where $N = k + 1$ is the number of unknowns.

$\delta_{ij} = T_{ij} - t_{ij}$ as above.

A measure of the quality of the data contributing to the time-term a_ℓ is provided by the standard deviation of its data,

$$\overline{\sigma} = \left[\frac{\sum_{i=1}^{k} \left(\delta_{i\ell}^{2} p_{i\ell} + \delta_{\ell i}^{2} p_{\ell i} \right)}{\sum_{i=1}^{k} (p_{i\ell} + p_{\ell i}) - 1} \right]^{\frac{1}{2}} \qquad (19)$$

The standard error of the time-term a_ℓ is given by,

$$\sigma_\ell = \frac{\overline{\sigma}_\ell}{\left[\sum_{i=1}^{k} (p_{i\ell} + p_{\ell i}) \right]^{\frac{1}{2}}} \qquad (20)$$

The sharpness of the minimum of I (and therefore of σ) is controlled more by the site distribution, as reflected in $\sum_i \sum_j p_{ij} \delta_{ij}^2$, than by the degree to which the calculated velocity approaches the true velocity.

3.4 Inversion of Time-Terms to Depth

If the P-velocity above the refractor, V(Z), is constant or varies only with vertical depth, Z , and at Z =h the velocity increases sharply to V(h), then :

$$t_{ij} = \frac{X_{ij}}{V(h)} + 2\int_{o}^{h} \frac{\left(V(h)^2 - V(Z)^2 \right)^{\frac{1}{2}}}{V(h).V(Z)} \, dZ \qquad (21)$$

In this ideal case the time-terms would be equal and related to depth Z by

$$a_i = \int_{o}^{h} \frac{\left(V(h)^2 - V(Z)^2 \right)^{\frac{1}{2}}}{V(h).V(Z)} \, dZ \qquad (22)$$

Sufficient (but not necessary) conditions for the valid use of this equation to convert time-terms to depth are :

(1) The velocity of the refracting horizon is very nearly constant (to within 1%)

(2) The curvature of the refractor is slight (i.e. $h\delta\theta/X_{ij} \lessapprox 1^{o}$ where $\delta\theta$ is the difference in algebraic dip of the refractor under the shot and recording site).

(3) The regional dip of the refractor is not too large (less than about 10^{o}).

If the above parameters are such that the conditions imposed are stretched to their limit, or surpassed, then the time-terms and depths calculated from the time-term analysis can be considered as first approximations to their true values. Further

approximations can be achieved by applying corrections to both the travel times, T_{ij}, and the distances, X_{ij}, and reanalysing the data. The corrections are calculated from the previous approximation and the values should converge to their true values fairly rapidly. The correction to the distances X_{ij} arises because this parameter, although defined in equation (1) as the shot-station separation, is rigorously defined as the distance between the points at which the perpendiculars to the refracting interface beneath the shot and the station cut the interface (X^1 in Fig. 3.1).

The correction to the travel times is given by Willmore and Bancroft (1960) as :

$$\Delta t_k = a_k . C_k$$

where a_k is the approximate time term

$$\text{and } C_k = \left[(1 - r^2 . \sin^2 \theta_{2k}) / (1 - r^2) \right]^{\frac{1}{2}} - 1 \qquad (23)$$

$r = V_o/V$ (for the case where $V(Z) = V_o$, constant)

θ_{2k} = refraction angle appropriate to the site k (θ_{2a} or θ_{2b} in Fig. 3.1)

Both shot and station time-terms contribute a correction to T_{ij}.

In most cases the corrections to X_{ij} have more effect than the corrections to T_{ij}. When calculating X^1 it must be remembered that the interface is, strictly, a surface in three-dimensions. Where data is limited it is difficult to define the calculated surface accurately. For most structures it is a good approximation to consider the surface as varying in two-dimensions only (in the vertical plane containing the shot and station). This approximation holds well for a line of shots where the receiving stations are also in line (e.g. Line A of L.A.S.P.).

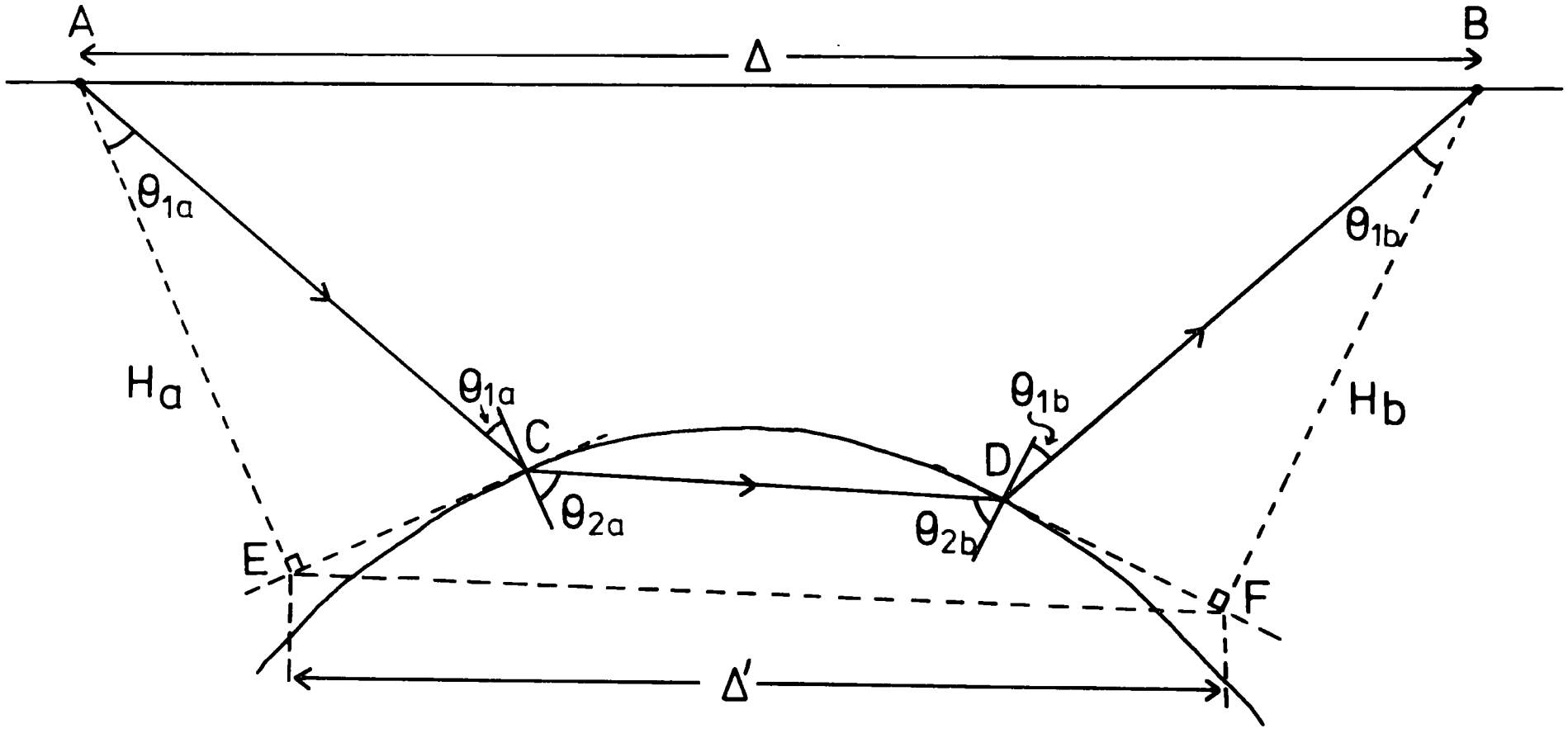

Fig. 3.1 Ray-path notation for discussion of iterative time-term interpretation.

If the velocity in the upper layer, $(V(Z)$, is constant and equal to V_o, then equation (22) reduces to

$$a_i = Z_i \quad (1). \left[\frac{1}{V_o^2} - \frac{1}{V_h^2} \right]^{\frac{1}{2}}$$

where $Z_i(1)$ is the vertical thickness of the upper layer beneath site i.

$$\text{i.e. } Z_i(1) = a_i \left[\frac{1}{V_o^2} - \frac{1}{V_h^2} \right]^{-\frac{1}{2}}$$

This relation can be extended for use with more than one refractor (Ocola, 1972).

If $Z_i(L)$ is the vertical thickness of the L^{th} refractor directly under the i^{th} site, V_L is the velocity of the L^{th} refractor and the velocities, time-terms, and thicknesses up to the k-2 refractor are known, then the thickness of the (k-1) refractor is :

$$Z_i(k-1) = \left\{ a_i(k) - \sum_{L=1}^{k-2} Z_i(L) \left[\frac{1}{V_L^2} - \frac{1}{V_k^2} \right]^{\frac{1}{2}} \right\} \left\{ \frac{1}{V_{k-1}^2} - \frac{1}{V_k^2} \right\}^{-\frac{1}{2}}$$

This relation is exact only if all the refractors are plane and horizontal but will give a good approximation to the layer thicknesses if the aforementioned conditions are satisfied.

In general, it must be stressed that the time-term method of interpreting seismic refraction data is only an approximate method. If the structures under investigation satisfy the conditions outlined above, then the results of applying the method are likely to be fairly accurate.

Computer programs were written in Fortran IV to invert the time-terms to depth for a two refractor model (DEP2) and an n - (<10) refractor model (DEPN). Listings of these programs are given in Appendix E.

CHAPTER 4

INTERPRETATION OF FIRST ARRIVAL DATA FROM LINE A

4.1 Introduction

The time-distance plots for the first arrivals at stations along the arc (Figs. 4.1, 4.2, 4.3 and 4.4) show a fairly uniform pattern. Except for shots closer than about 7km, the travel times for ranges up to 90km indicate a velocity of about 6.1km s^{-1}. Beyond 90km range many of the time-distance plots show a change in gradient indicating a higher velocity. This higher velocity is, on the whole, poorly defined, there being only a small number of arrivals defining it at each station. Where the higher velocity segments are best defined the apparent velocity is about 7km s^{-1}. For convenience, the arrivals from the 6.1km s^{-1} layer are called 'Pg' arrivals, and those from the ?7km s^{-1} layer, 'P^*' arrivals. However, no correlation between the layers corresponding to Pg and P^* under the Lesser Antilles arc and the layers so defined in other parts of the world is suggested.

There is a large scatter of the travel times of the Pg arrivals (Figs. 4.1, 4.2 and 4.3) indicating that either the sediment-basement interface is irregular, or the velocity distribution in the overlying low-velocity layers varies along the profile, or that the Pg velocity varies laterally. The scatter of the points for the higher velocity segments of the time-distance plots is more pronounced, so that the apparent velocities are less well defined. This probably results from the presence of locally steep dips on this lower interface. The apparent Pg velocities are listed in Table 4.1(a). Many of these

Table 4.1 Least squares fit of straight lines to travel time data from line A

(a) Pg segments :

Station	Direction	Velocity ($km\ s^{-1}$)	Time Intercept (s)	No. of Observations
14 Guadeloupe	S	5.98 ± 0.24	1.37 ± 0.42	3
15 ,,	S	6.06 ± 0.31	1.65 ± 0.41	3
16 ,,	S	6.28 ± 0.11	1.86 ± 0.23	5
17 ,,	N	5.85 ± 0.15	1.19 ± 0.24	3
	S	6.38 ± 0.10	2.00 ± 0.38	4
18 ,,	N	6.17 ± 0.10	1.61 ± 0.18	5
19 ,,	N	6.27 ± 0.07	1.51 ± 0.19	3
	S	6.22 ± 0.13	1.76 ± 0.38	6
20	S	6.01 ± 0.08	1.10 ± 0.23	4
21 Martinique	S	5.42 ± 0.25	-0.35 ± 0.60	3
22 ,,	S	6.13 ± 0.08	1.17 ± 0.21	9
23 ,,	N	5.72 ± 0.90	1.16 ± 1.48	3
	S	5.55 ± 0.51	0.74 ± 0.69	3
1 St Lucia	N	6.04 ± 0.09	1.38 ± 0.06	3
	S	6.11 ± 0.09	0.71 ± 0.19	6
2 ,,	N	4.08 ± 0.20	-3.30 ± 0.72	5
	S	6.35 ± 0.42	1.32 ± 0.30	5
13 St Vincent	N	6.21 ± 0.21	1.42 ± 0.19	4
	S	6.43 ± 0.27	1.60 ± 0.36	5
12 ,,	N	6.39 ± 0.22	1.53 ± 0.17	5
	S	6.65 ± 0.30	1.88 ± 0.36	5
11 ,,	N	5.92 ± 0.15	1.04 ± 0.20	5
	S	6.49 ± 0.08	1.65 ± 0.11	8
3 Carriacou	N	5.86 ± 0.07	0.64 ± 0.09	6
	S	6.03 ± 0.07	1.34 ± 0.14	5
4 Grenada	N	5.85 ± 0.09	0.06 ± 0.22	5
	S	5.60 ± 0.27	0.66 ± 0.45	3
5 ,,	N near	6.52 ± 0.18	2.00 ± 0.18	3
	N far	6.02 ± 0.04	0.43 ± 0.13	6
	S	5.41 ± 0.14	0.80 ± 0.14	3

(b) P^{*} segments :

14 Guadeloupe	S	6.83 ± 0.15	2.92 ± 0.75	4
15 ,,	S	7.33 ± 0.13	4.97 ± 0.46	4
18 Dominica	S	6.80 ± 0.07	2.85 ± 0.30	8
22 Martinique	N	6.68 ± 0.10	2.13 ± 0.35	5
2 St Lucia	S	7.19 ± 0.14	2.97 ± 0.29	6
11 St Vincent	N	7.63 ± 0.21	5.25 ± 0.45	4
3 Carriacou	N near	6.86 ± 0.12	2.12 ± 0.32	5
	N far	7.28 ± 0.23	3.57 ± 0.86	3
4 Grenada	N	7.00 ± 0.52	3.41 ± 1.70	5

were determined from only three or four observations so that the gradients and intercepts of the least squares fit straight lines are not well controlled. The weighted mean apparent Pg velocity is 6.09 ± 0.02km s^{-1}. The higher apparent velocities are given in Table 4.1(b).

4.2 Apparent Velocities

Reduced travel time-distance graphs for the Grenada and Carriacou stations are shown in Fig. 4.1. Apparent velocities observed at the Grenada stations from shots 25 to 29 are lower than the average Pg velocity observed along the arc. If the basement velocity is near to the average, then there must be a thickening of the sediments and/or volcanic debris to the south of Grenada. This would be expected as previous workers have postulated a basinal feature between Grenada and Trinidad (Ewing et al. 1957) which is interpreted by some as a south-westward extension of the Tobago trough (Lattimore et al. 1971).

The south Grenada station observed apparent velocities of 6.52km s^{-1} then 6.02km s^{-1} from shots to the north. Only three close shots define the higher velocity and it is probable that the velocity is unreliable and that the arrivals are Pg arrivals. The three arrivals show high reduced travel times (1.4 s to 1.7 s). The reduced travel times for the more distant arrivals are about 0.4 s. This pattern is also seen on the Grenada north plot. Here, however, shots 24 and 23 may be too close to have penetrated to basement. The difference in reduced travel times suggests that the basement is at a much shallower depth beneath the northern

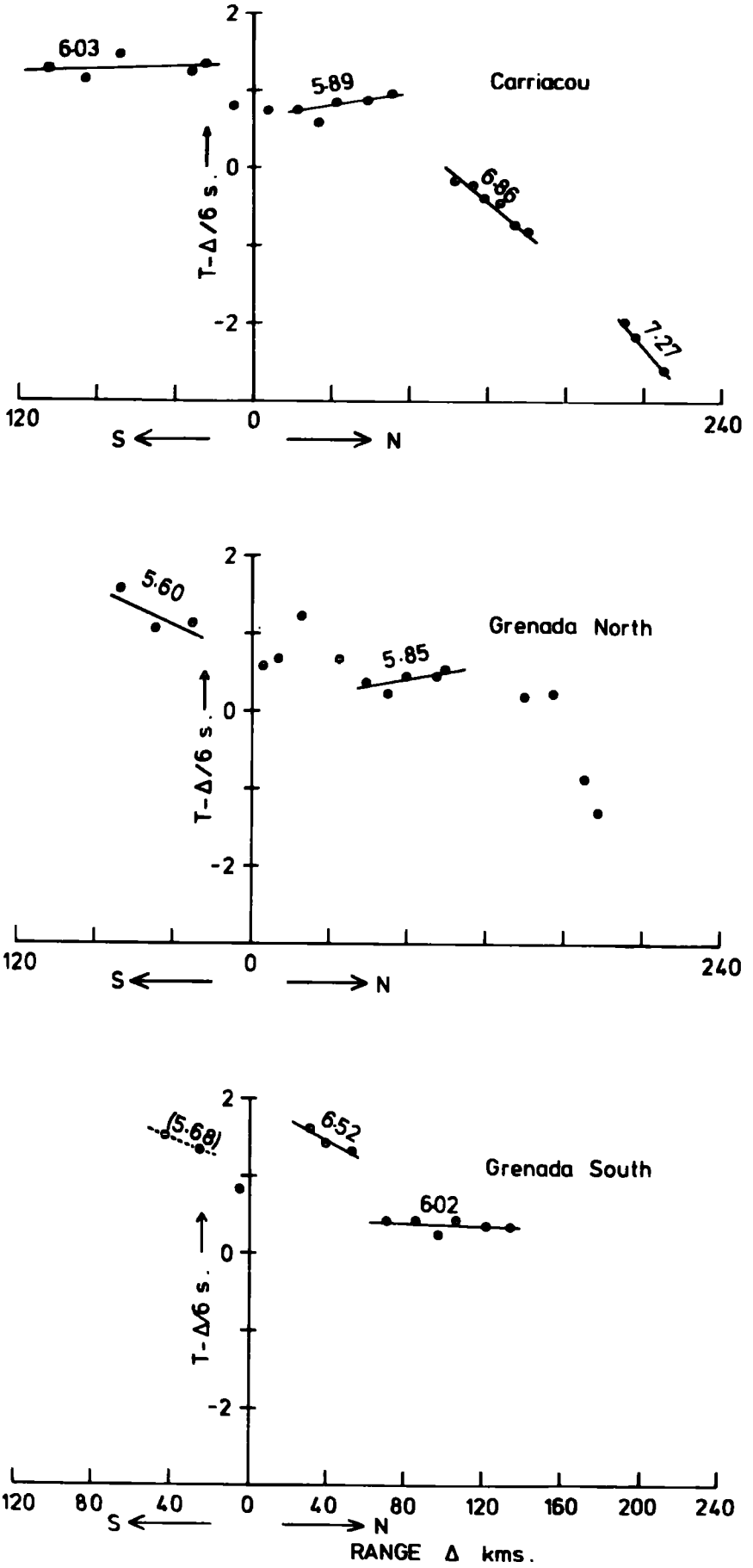

Reduced travel time graphs — Line A shots 1 - 29

Fig. 4.1

Grenadines than it is beneath the region between Grenada and Carriacou. This was the explanation given by Officer et al. (1959) for the 0.6 s offset they observed in the 6.4km s^{-1} segment of the travel time graph for their profile 28. Profile 28 (see Fig1.5) was located on the eastern side of the Grenadines running parallel to the ridge, and the observed offset occurred just opposite Carriacou. Further evidence of a distinct step in the basement in this region comes from the arrivals at the Carriacou station (Fig. 4.1). Near arrivals from the north have an apparent velocity of 5.9km s^{-1} and a time intercept of 0.6 s. Arrivals from the south show an apparent velocity of 6.0km s^{-1} and a time intercept of 1.3 s.

More distant arrivals at the north Grenada and Carriacou stations show higher apparent velocities which are thought to represent P^{*} refractions.

Arrivals at the three St Vincent stations (Fig. 4.2) from shots 13 to 23 show apparent velocities of 6.4 to 6.7km s^{-1} which are higher than the average Pg velocity observed. If it is assumed that these arrivals are Pg arrivals, a 2^{o} - 4^{o} dip of the refractor to the north is indicated for the region between Carriacou and St Vincent. The first arrivals from shots 1 to 5 at St Vincent are indistinct. The records at Camden Park (LASP 11) indicate an apparent velocity of 7.6km s^{-1} for these shots, at distances between 115 and 140km. Arrivals at the two stations on Soufriere (12 and 13) from these shots are very poor. A few have been picked, but not with any certainty.

Fig. 4.3 shows the reduced travel time graphs for first arrivals at the two St Lucia stations. St Lucia North received Pg first arrivals out to at least 120km range to the south. However,

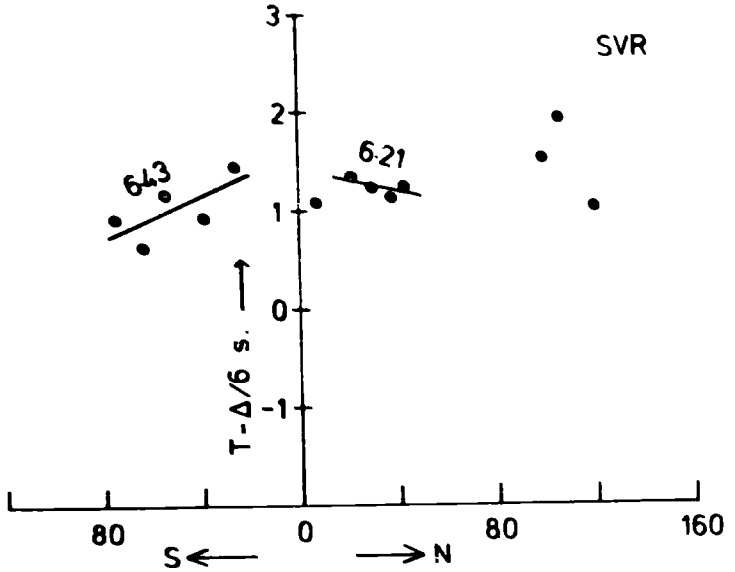

Fig. 4.2

ST. VINCENT STATIONS

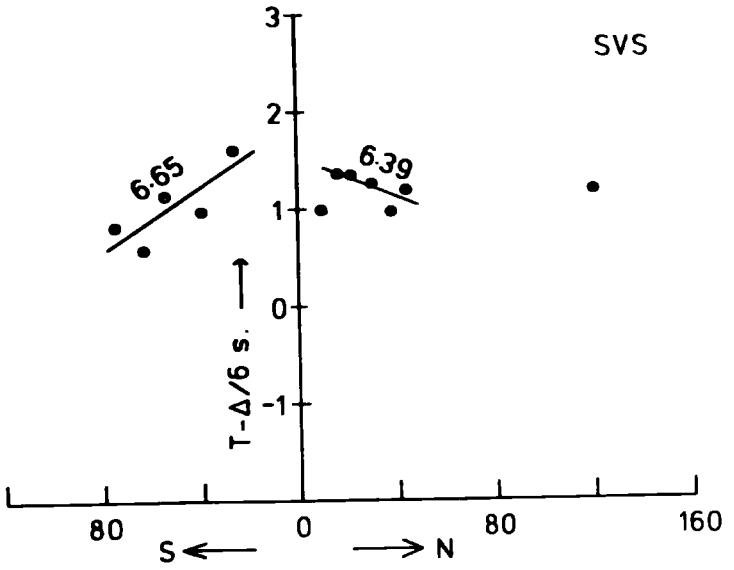

reduced travel time graphs
line A shots 1 - 23

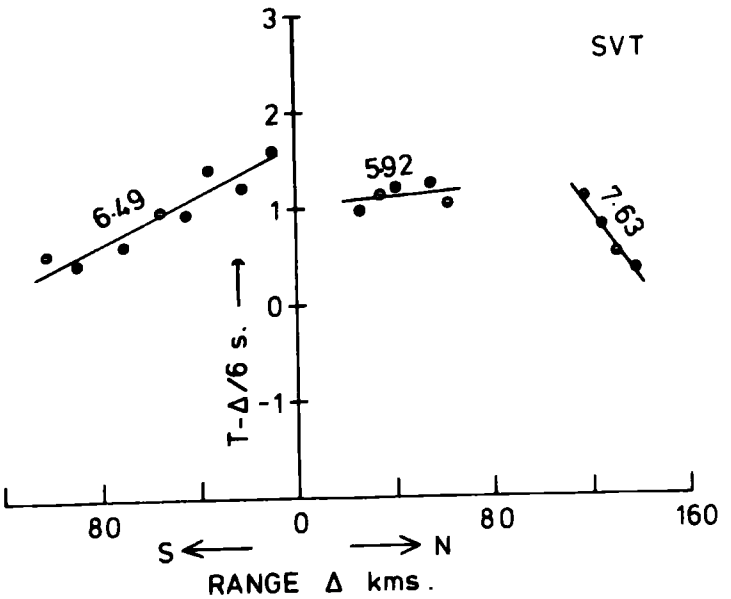

the arrivals at the St Lucia South station from the south show a different pattern. Here shots 6 to 11 indicate an apparent velocity of about 6.3km s^{-1}, although the high scatter of points leads to a large uncertainty in this value. First arrivals from shots 13 to 20 show a velocity of 7.2km s^{-1} over the distance range 74 to 138km. It may be that the first two or three points on the lines defining this velocity are, in fact, Pg arrivals continuing the trend of arrivals from shots 6 to 11. The more distant shots must define a higher velocity refractor at depth.

Arrivals from the north at St Lucia show a confusing pattern (Fig. 4.3). At the north station shots 1, 2 and 3 give an apparent velocity of 6.0km s^{-1} with a time intercept of 1.4 s whilst the nearer shots, 4 and 5, indicate a velocity of about 4km s^{-1} and a time intercept near zero. Shots 1 to 5 give arrivals with an apparent velocity of 4.1km s^{-1} at the St Lucia South station. These are in the distance range 46-76km and the time intercept is -3.3 s. These arrivals at the south station can be interpreted as being caused by waves travelling in a near-surface layer with velocity about 4km s^{-1} and passing into a region of higher velocity under St Lucia before reaching the station. The northern part of St Lucia is underlain by tuffs and agglomerates with local limestone lenses, whilst the remainder of the island is composed of harder volcanic rocks such as hornblende-dacites and andesite porphyries (Martin-Kaye, 1969). The geological evidence is thus consistent with a lateral change in velocity as proposed above. If the velocity discontinuity occurs below the northern tip of the island, then a velocity of about 6km s^{-1} is required under the rest of the island to give the observed travel times.

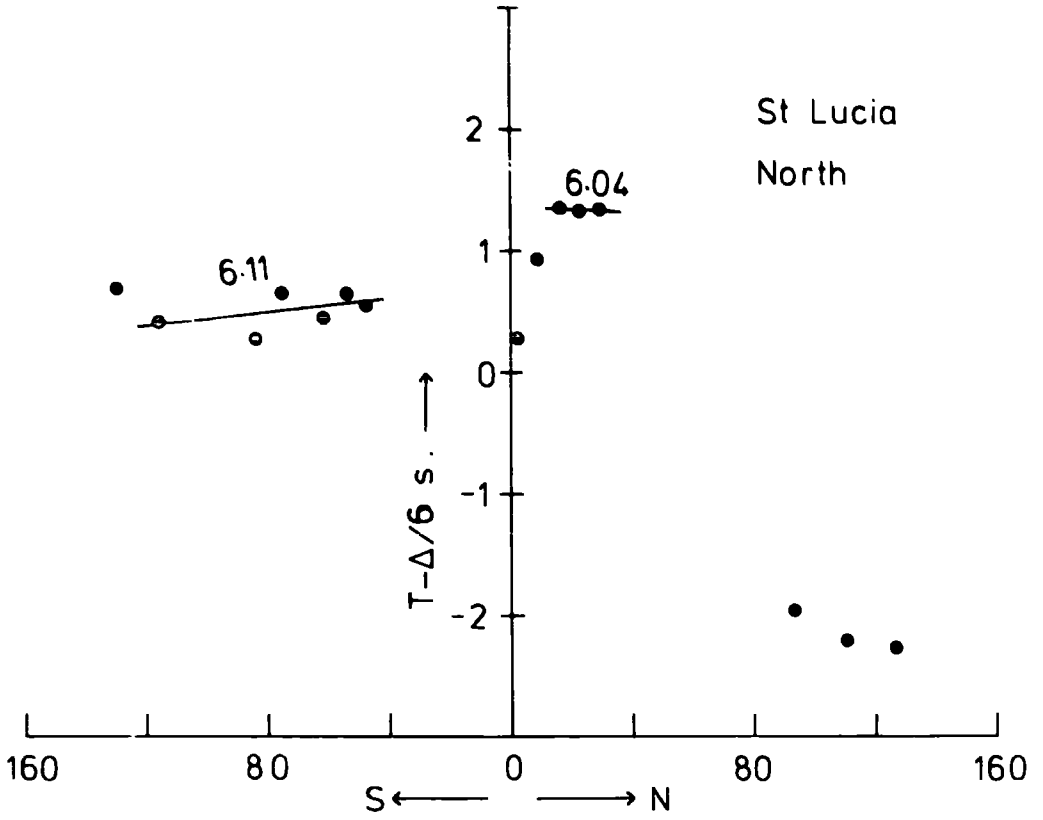

Reduced travel time graphs Line A shots 0·7–20

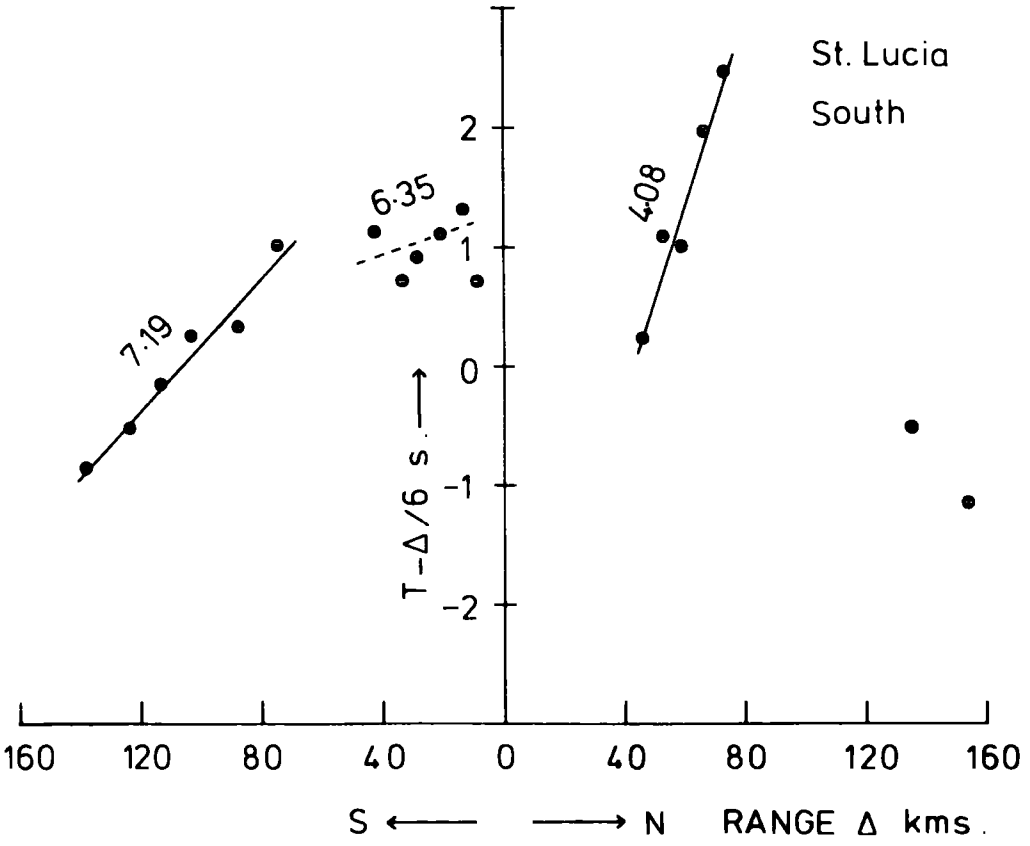

Fig. 4.3

Moving the discontinuity to the south would require a higher velocity (e.g. 8km s^{-1} if it lies 30km north of the south station). A velocity greater than 6km s^{-1} is unlikely for near-surface volcanic rocks so the velocity discontinuity, at the depth sampled by these arrivals, cannot be further south than the north end of the island.

If a 'normal' 6km s^{-1} basement underlies the 4km s^{-1} material beneath the shots, then head-waves produced by refraction at the basement would be expected to arrive before the 'direct' wave, for at least the more distant shots, unless the basement was deeper than about 10km. A higher velocity first arrival was not seen on the records and, if present, it must have been of very low energy.

The above explanation would also explain the travel times for the arrivals from shots 4 and 5 at the St Lucia North station. However, the higher velocity arrivals observed from shots 1, 2 and 3 are not consistent with the model proposed above. These would appear to be caused by refraction in a higher velocity layer beneath the shots. The nature of the arrivals at the south station preclude the possibility of this layer being the true basement. It could be a thin igneous sill or lava flow in which head waves were generated which were received as first arrivals at the north station.

Weak arrivals from shots 0.7, 0.8 and 0.9 were 'picked' from the records at the two St Lucia stations. However, the 'first-arrivals' are not consistent when plotted. At the north station they indicate a velocity of about 6.5km s^{-1} with a time intercept of -1 s. Arrivals from a deep high velocity layer would give a time intercept more positive than the Pg time intercept. At the south station the two picked first arrivals, at ranges of 135 and 153km, indicate a velocity greater than 7km s^{-1} with a large positive

Fig. 4.4 Summary of first arrival travel time data from the French stations (Dorel, personal communication)

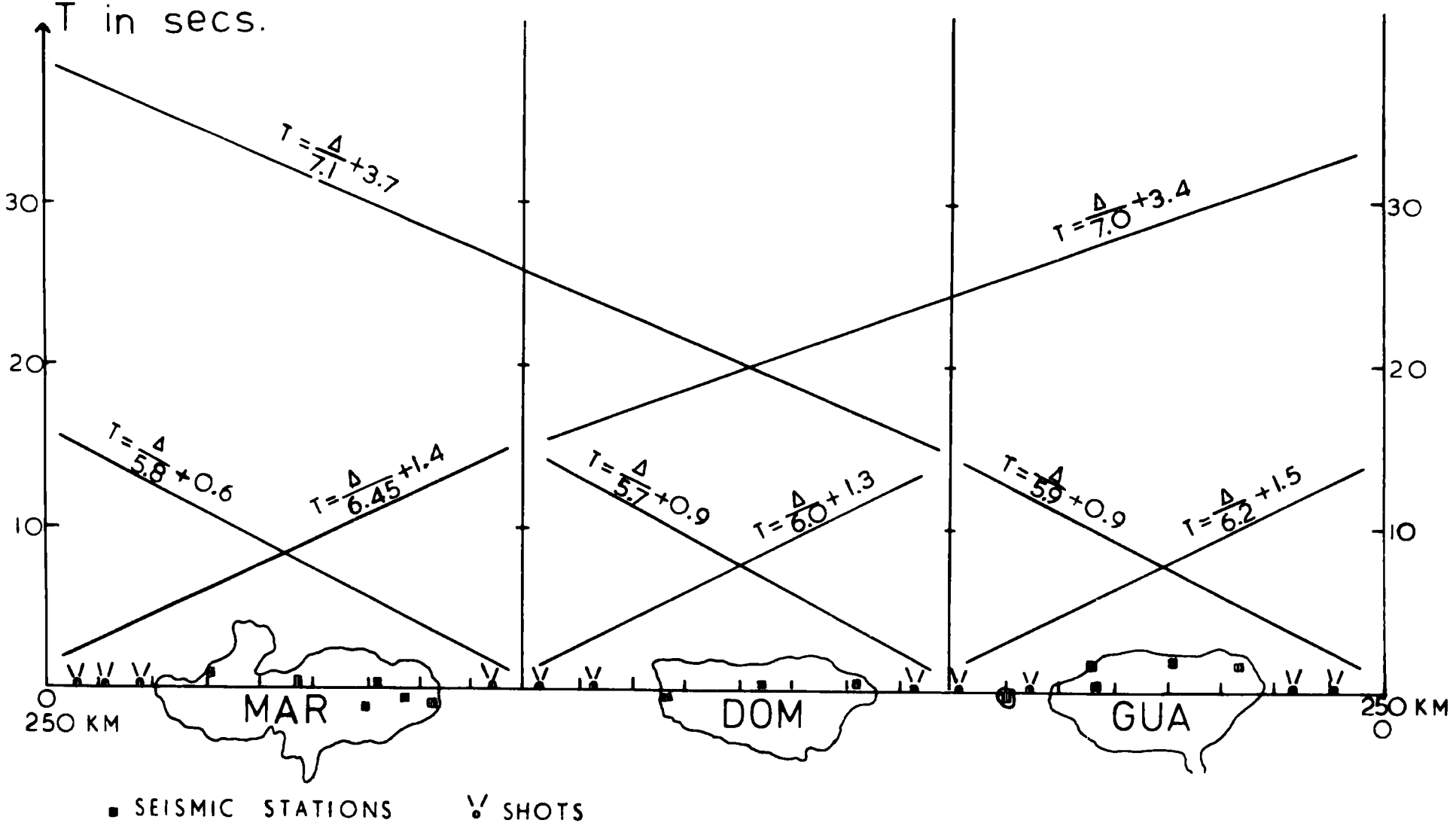
T in secs.
30
20
10
$T = \frac{\Delta}{7.1} + 3.7$
$T = \frac{\Delta}{7.0} + 3.4$
$T = \frac{\Delta}{5.8} + 0.6$
$T = \frac{\Delta}{6.45} + 1.4$
$T = \frac{\Delta}{5.7} + 0.9$
$T = \frac{\Delta}{6.0} + 1.3$
$T = \frac{\Delta}{5.9} + 0.9$
$T = \frac{\Delta}{6.2} + 1.5$
0
250 KM
MAR
DOM
GUA
250 KM
SEISMIC STATIONS
SHOTS

time intercept. These arrivals are consistent with refraction in a deep high velocity layer but, with the lack of more information from this region, a reliable apparent velocity could not be calculated.

Along the northern part of line A the shots were further apart and the stations were more numerous and closer together. This allowed the French workers (J. Dorel, personal communication) to trace the first arrivals from one shot along a line of stations, rather than trace the arrivals at one station from a line of shots as was found easier for the southern part of the profile. A summary of the results from the French stations is given in Fig. 4.4. Shot A2 was recorded well by ten stations at distances between 24 and 242km to the north. Apparent velocities of 6.45 and 7.0km s^{-1} were measured with a crossover distance of about 90km. In the opposite direction arrivals from shots 0.2 and 0.3 showed apparent velocities of 5.9 and 7.1km s^{-1} with the crossover distance being about 90km again. Reversed determinations of the Pg velocity were provided by arrivals from shots 0.7 and 0.9 and shots 0.4, 0.5 and 0.6 to the north and south.

First arrivals were observed at some of the French stations from shots 1 to 11. The first arrivals from beyond about 100km indicated apparent velocities of 6.7 to 7.3km s^{-1}. This adds to the evidence for the existence of a higher velocity layer at depth.

The maximum range at which first arrivals were detected along line A is about 250km. Out to this range there are no first arrivals showing apparent velocities indicative of the Moho.

4.3 Interpretation of the Pg data

4.3.1 Reversed profiles

Estimates of the true Pg velocity and the dip of the basement

were calculated for pairs of stations along the arc, using the reversed profile technique (Table 4.2). For these calculations, an average overburden velocity of 3.5km s^{-1} was assumed. The 'overburden' has been shown to consist of two or three layers by previous workers (see Fig. 1.6 , and Section 4.3.3 for a discussion of the relevant profiles). However, the previous profiles are not coincident with the LASP shot sites and it is considered sufficient, for this preliminary interpretation, to use the average overburden velocity indicated by these earlier profiles. The average of the calculated Pg velocities is 6.13km s^{-1} and the dips are all less than 3^{o}.

4.3.2 Plus-minus interpretation

The scatter of points on most of the first arrival Pg segments suggests that the basement interface is not planar and that lateral variations in Pg velocity may be present. Thus the calculated apparent velocities and dips are average values. The pattern of shots and stations along line A suggested using a version of the plus-minus method of Hagedoorn (1959) to investigate the lateral variations of the Pg velocity and the variations in depth to the interface. This method has been described in Section 3.1.

Pairs of stations were chosen where both received Pg arrivals from at least three of the intervening shots. The difference in travel times from each shot to each of the stations are the 'minus' times. These were plotted as ordinates against Y-2X as abscissae (see Appendix D). The number of points on each 'minus' graph varied from 3 to 7. It was impossible, therefore, to define in detail any lateral variations in Pg velocity between the two stations. The

Table 4.2 Estimates of Pg velocity by reversed profile method

Stations	Reversed velocity ($km\ s^{-1}$)	Refractor dip (+ve to north)
Guadeloupe-Dominica		
14 - 17	5.91	0.5
14 - 18	6.07	-0.6
14 - 19	6.12	-0.9
15 - 18	6.11	-0.4
15 - 19	6.16	-0.7
16 - 18	6.22	0.3
16 - 19	6.28	0.0
17 - 18	6.27	0.6
17 - 19	6.32	0.3
Dominica - Martinique		
19 - 23	5.96	1.7
20 - 23	5.86	1.1
Shot-shot reverses		
0.2, 0.3 - 0.4, 0.5, 0.6	6.05	-1.0
0.4, 0.5, 0.6 - 0.7, 0.9	5.85	-1.1
0.7, 0.9 - A2	6.10	-2.1
St Lucia - St Vincent		
1 - 11	6.01	0.6
1 - 12	6.25	-0.9
1 - 13	6.16	-0.3
2 - 11	6.13	1.4
2 - 12	6.17	1.1
2 - 13	6.28	0.4
St Vincent - Carriacou		
13 - 3	6.37	0.1
12 - 3	6.22	2.5
11 - 3	6.16	2.0
Carriacou - Grenada		
3 - 4	5.94	0.6
3 - 5 (near shots)	6.26	-1.5
3 - 5 (far shots)	6.03	0.0

coordinates of each point on the 'minus' graph were used to calculate a least squares straight line. The gradient of this line is an estimate of the average Pg velocity along the shot profile. The standard error of the regression line can perhaps be used as an indication of whether there is lateral inhomogeneity in the refractor. However, the number of observations will also affect the error. The velocities calculated for each pair of stations are listed in Table 4.3 together with an indication of the standard deviation. These show a considerable variation which cannot be correlated with a simple lateral variation. The arithmetic mean of the velocities is 6.15 ± 0.08km s^{-1} but a value of 5.89 ± 0.08km s^{-1} was obtained from a weighted mean analysis. Fig. 4.5 shows a typical 'minus' graph for one pair of stations (Martinique OBM and St Vincent SVR).

To investigate further the lateral variations in Pg velocity the 'minus' times at pairs of adjacent sites were used to obtain an estimate of the refractor velocity in the immediate neighbourhood of the sites. Several estimates were obtained from each pair of adjacent station (shot) sites by considering the travel times to all the enclosing shot (station) pairs within the range of Pg first arrivals. The range of the velocity estimates at each pair of sites is shown in Fig. 4.6 together with the mean value at each site. It can be seen that there is a considerable variation in the estimated velocity for each site and no distinct trend of lateral variation can be discerned. For instance, one might expect to find high refractor velocities under the islands and lower velocities in between, but this is not found to be the rule. However, there do appear to be distinct areas of high velocity in the regions of Carriacou and shots A7 - A10 and areas of low velocity about shot sites A0.5 - A0.6 and A0.7 - A0.8.

Fig. 4.5 Typical 'minus' graph : - Line A

(see also Appendix D)

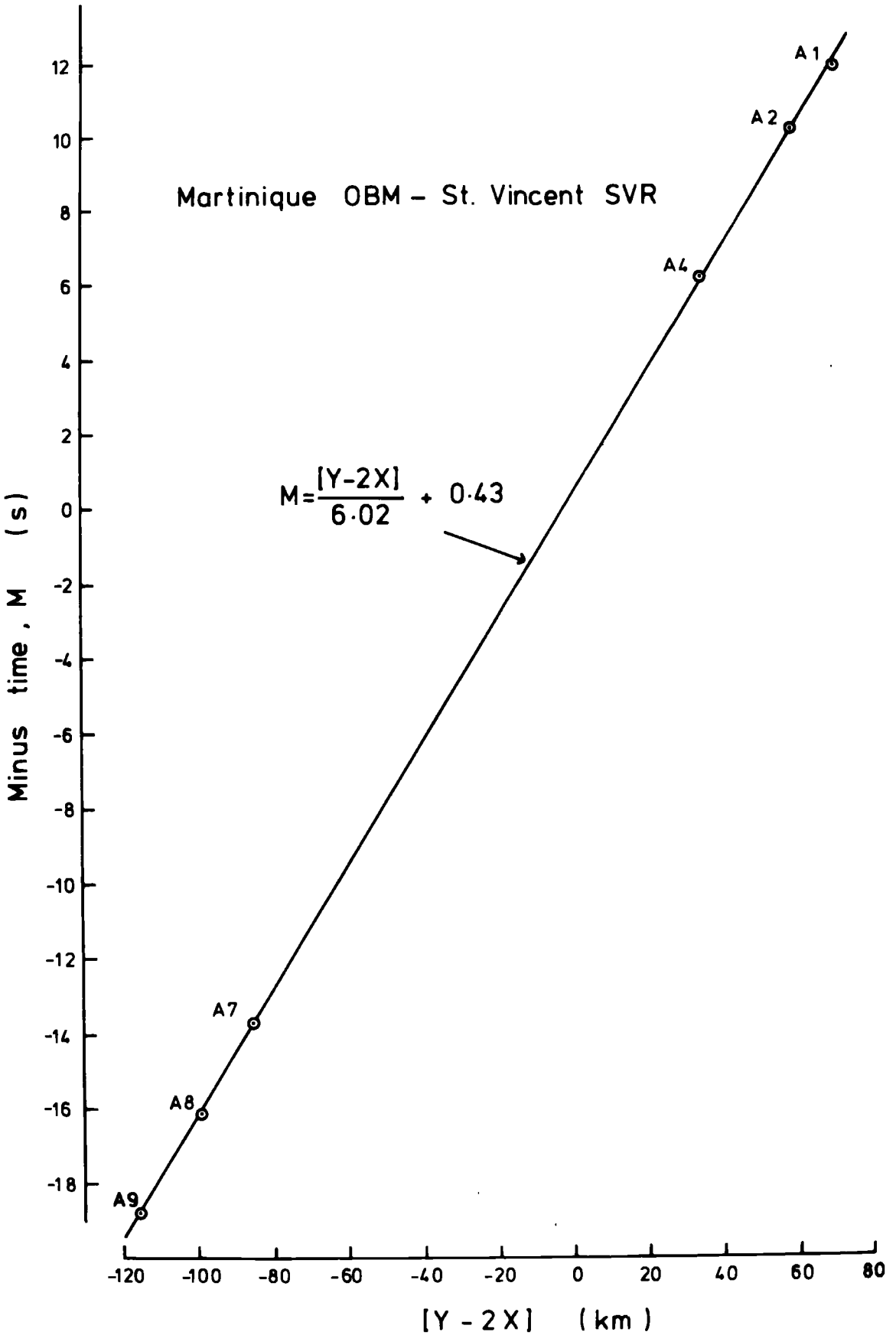
Martinique OBM – St. Vincent SVR
$M=\frac{[Y-2X]}{6\cdot02}+0\cdot43$
A1
A2
A4
A7
A8
A9
Minus time, M (s)
12
10
8
6
4
2
0
-2
-4
-6
-8
-10
-12
-14
-16
-18
-120
-100
-80
-60
-40
-20
0
20
40
60
80
[Y - 2X] (km)

Fig. 4.6 Variation of P_g velocity along line A.

The vertical bars indicate the range of velocities estimated from each shot or station pair. The mean value for each pair is marked with a cross and the number of velocity estimates is indicated alongside.

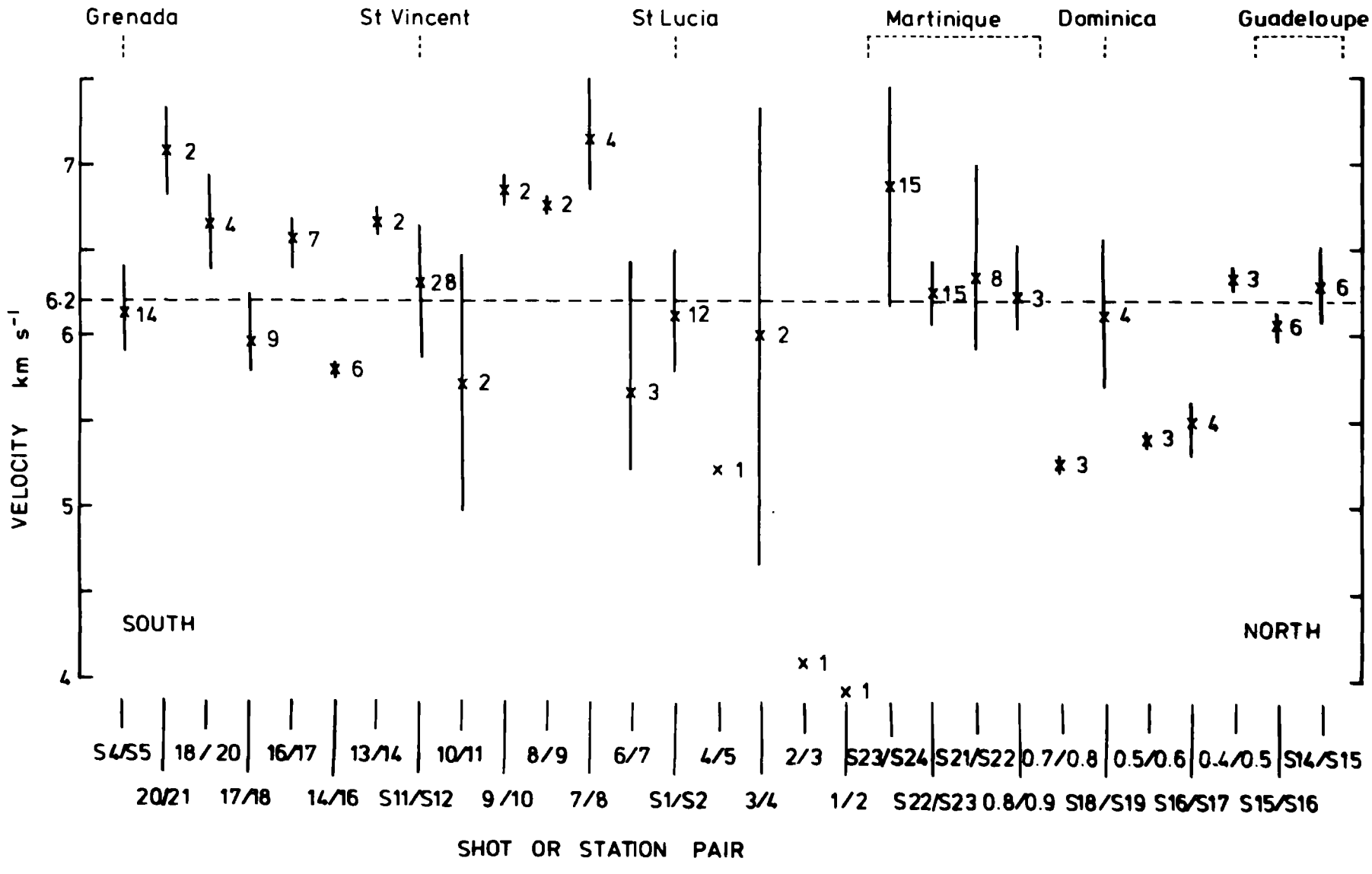
Grenada
St Vincent
St Lucia
Martinique
Dominica
Guadeloupe
VELOCITY km s⁻¹
7
6·2
6
5
4
SOUTH
NORTH
2
4
7
2
28
2
2
2
4
14
9
6
3
12
2
1
15
15
8
3
4
3
6
3
4
6
1
1
S4/S5
18/20
16/17
13/14
10/11
8/9
6/7
4/5
2/3
S23/S24
S21/S22
0.7/0.8
0.5/0.6
0.4/0.5
S14/S15
20/21
17/18
14/16
S11/S12
9/10
7/8
S1/S2
3/4
1/2
S22/S23
0.8/0.9
S18/S19
S16/S17
S15/S16
SHOT OR STATION PAIR

Table 4.3 Estimates of Pg velocities from 'minus' graphs

Stations	No. of minus times	Avr. velocity from minus graph	Intercept on minus time axis
14 18	3	5.81 ± 0.23km s^{-1}	0.26 S
14 22	5	6.53 ± 0.03	-0.52
14 24	4	6.55 ± 0.05	-0.33
15 18	3	5.85 ± 0.26	0.01
15 22	5	6.48 ± 0.05	-0.56
15 24	4	6.51 ± 0.04	-0.42
16 18	3	5.75 ± 0.28	-0.17
16 22	5	6.42 ± 0.06	-0.56
16 24	4	6.44 ± 0.04	-0.43
17 22	4	6.19 ± 0.08	-0.54
17 24	3	6,23 ± 0.01	-0.50
19 22	3	5.63 ± 0.22	-0.51
19 23	3	5.69 ± 0.22	-0.50
19 24	3	5.82 ± 0.37	-0.95
22 2	3	4.88 ± 0.40	0.48
22 12	6	6.04 ± 0.02	0.45
22 13	6	6.02 ± 0.02	0.43
24 2	4	5.36 ± 0.39	-1.14
24 12	5	6.28 ± 0.05	0.61
24 13	5	6.27 ± 0.07	0.53
1 12	4	6.13 ± 0.22	0.57
1 13	3	6.12 ± 0.43	0.56
1 11	3	6.05 ± 0.07	0.56
2 12	4	6.94 ± 0.11	0.30
2 13	3	6.83 ± 0.01	0.23
2 11	4	6.00 ± 0.28	0.12
11 3	4	6.10 ± 0.10	0.40
11 4	6	6.49 ± 0.11	0.25
11 5	7	6.50 ± 0.08	0.07
12 3	5	6.19 ± 0.08	0.27
12 4	6	6.30 ± 0.08	0.34
12 5	6	6.29 ± 0.07	0.22
13 3	5	6.10 ± 0.08	0.22
13 4	5	6.12 ± 0.09	0.48
13 5	5	6.21 ± 0.10	0.30

There are several likely factors which may contribute to the variation of the velocity estimates at each site. Firstly, the error in each measured travel time, which is of the order of 0.1 s, will be increased when the differences are calculated and will produce a fractional error of up to 3% in each velocity estimate. Secondly, it must be remembered that the use of minus times will only give an approximation to the refractor velocity which is exact only in the case of a flat horizontal refractor separating two homogeneous layers.The accuracy of this approximation is reduced by the presence of an uneven refractor and by lateral or vertical variations in the overburden velocity. Unfortunately, there is very little information available on the velocity structure of the overburden in the vicinity of the shot and station sites. It is therefore impossible to determine the extent to which these factors apply here. It is also probable that a few of the travel times used are not due to true 'refractions'. This has been shown (Section 4.2) to be true for some of the travel times from shots A1 to A5.

"Plus' times were calculated for the same station pairs used to construct the 'minus' graphs. The depth to the interface was calculated for each shot site from its 'plus' time and the velocity calculated from the 'minus' graph, assuming a mean overburden velocity of 3.5km s^{-1} throughout. The distance between one station and its nearest shot (dx), used in estimating t_{12} (see Appendix D), was under 15km for most of the profiles but was inevitably larger for a few others. Some of the values of t_{12} used may be poor estimates. However, for individual profiles the relative values of the 'plus' times for each shot should be accurate because the same value of t_{12} is used in the 'plus' time calculation for each shot.

Average 'plus' times and depths to the basement were calculated after removing values obtained from the more dubious profiles. These are listed in Table 4.4. Most of the average depths are between 0.7km and 4km. There are two areas where the structure appears to be more severe. The first is in the region of shot 0.8 (between Martinique and Dominica) where the calculated depth exceeds 7km. It was noted that travel times from shot 0.8 gave large positive residuals on the time-distance graphs described earlier. Figure 4.6 shows that this shot is above a region of low Pg velocity. This would lead one to expect a lower 'plus' time so there must be a deeper basement here. The second area of anomalous structure was around shots 2, 3 and 4 (between St Lucia and Martinique) where the basement depth appears to exceed 10km below shot 3. In section 4.3.2 it was suggested that some of the arrivals from shots A1 to A5 were not refracted arrivals. This would invalidate the plus-minus analysis in this region. In either area, errors in the seabed topography corrections applied to the travel times could contribute to the larger plus-times, but only to a small degree.

The intercept on the 'minus' time axis of the 'minus' graphs gives an estimate of the difference between the delay times to the refractor beneath the two stations. The value of this intercept for each pair of stations is included in Table 4.3. Ignoring the values associated with poorly fitted least squares lines, we see that the delay time differences between the stations range from about zero to 0.6 s. These delay time variations suggest large variations in upper crustal structure along the island arc ridge.

Table 4.4 Pg 'plus' times and depth estimates from line A

Shot	Average 'plus' time (s)	Average depth (km)
A0.4	0.94	3.87
A0.5	0.76	3.11
A0.6	0.91	3.80
A0.7	0.54	2.37
A0.8	1.70	7.08
A0.9	0.84	3.44
A1	1.35	5.81
A2	1.81	7.71
A3	2.46	10.36
A4	1.52	6.47
A7	0.41	1.72
A8	0.59	2.46
A9	0.55	2.36
A10	0.49	2.06
A14	0.58	2.41
A16	0.60	2.47
A17	0.24	0.98
A18	0.31	1.24
A20	0.18	0.75
A21	0.43	1.77
A23	0.61	2.53

In summary, the application of the plus-minus method to the first arrival data from line A indicates that :

(i) there is a degree of lateral variation in the Pg velocity along line A

(ii) the basement is at depths between 0.7 and 4km beneath the shot sites, except for the two regions discussed above, and is on average deeper under the northern part of the line

(iii) there is considerable variation in basement structure beneath the islands.

4.3.3 Pg time-term solution

All the first arrival travel times identified as 'Pg' by the preliminary analysis were combined into one data set, set A, to determine a least-squares Pg velocity and Pg time-terms by the time-term method. The least-squares velocity calculated from the time-term solution was 6.20 ± 0.16km s^{-1}. This value is not significantly different from those obtained from the reversed profile and plus-minus interpretations. Table 4.5 lists the site time-terms from this solution. The criterion used to determine the arbitrary constant α in this solution was a compromise between assuming the time-terms for shot 0.7 and station 17 to be equal and assuming equality of the time-terms of shot 20 and station 3. These assumptions are justified as the shot-station separation of these pairs is small and they are located in regions where the basement topography appears to be gentle. A histogram of the travel time residuals for this solution is shown in Fig. 4.7. Most of the residuals are smaller than 0.2 s.

Fig. 4.7 Histogram of travel time residuals for P_g time-term solution A

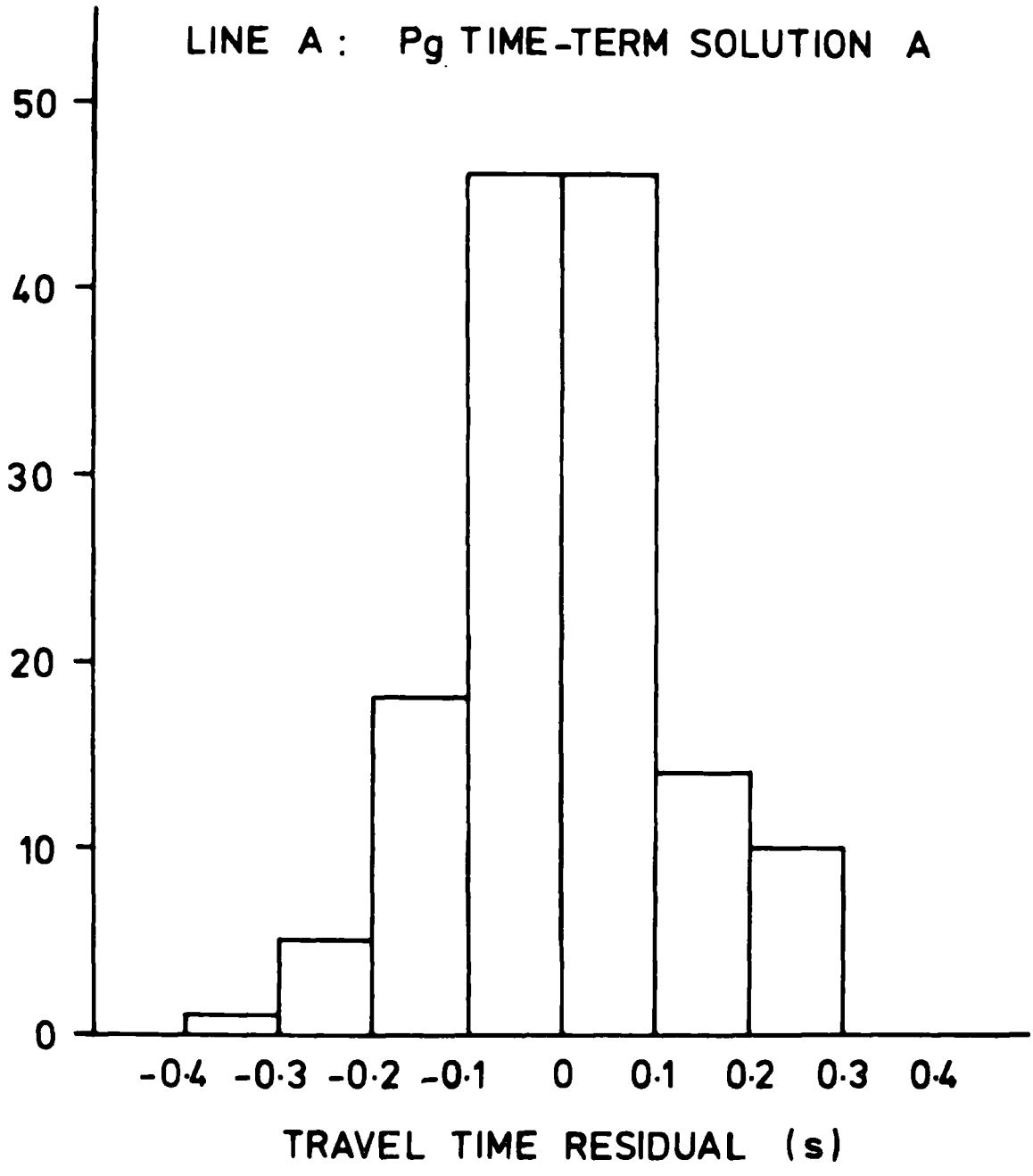
LINE A : Pg TIME-TERM SOLUTION A
50
40
30
20
10
0
-0·4 -0·3 -0·2 -0·1 0 0·1 0·2 0·3 0·4
TRAVEL TIME RESIDUAL (s)

Table 4.5. Pg time-term solution from data set A

least-squares velocity = 6.20 ± 0.16km s^{-1}

Site	Pg time-term	Site	Pg time-term
A0.2	1.17 ± 0.06 (4)	station 2	0.43 ± 0.05 (11)
A0.3	0.46 ± 0.08 (3)	A6	0.91 ± 0.02 (4)
station 14	0.77 ± 0.02 (4)	A7	1.11 ± 0.09 (5)
station 15	0.76 ± 0.05 (5)	A8	0.89 ± 0.04 (4)
station 16	0.81 ± 0.04 (5)	A10	1.29 ± 0.10 (4)
A0.4	1.08 ± 0.03 (5)	A9	0.92 ± 0.02 (4)
station 17	0.96 ± 0.15 (3)	A11	0.82 ± 0.16 (3)
A0.5	0.88 ± 0.02 (4)	station 13	0.69 ± 0.02 (17)
A0.6	1.43 ± 0.10 (4)	station 12	0.69 ± 0.03 (16)
station 18	0.94 ± 0.03 (4)	station 11	0.71 ± 0.03 (15)
station 19	0.80 ± 0.15 (3)	A13	1.12 ± 0.04 (4)
A0.7	1.22 ± 0.11 (5)	A14	0.58 ± 0.08 (5)
A0.8	2.70 ± 0.08 (4)	A17	0.37 ± 0.05 (5)
A0.9	1.10 ± 0.05 (4)	A18	0.54 ± 0.03 (6)
station 21	0.45 ± 0.05 (3)	A20	0.47 ± 0.11 (3)
station 22	0.26 ± 0.04 (8)	station 3	0.42 ± 0.05 (9)
station 23	0.55 ± 0.04 (8)	A21	1.18 ± 0.05 (2)
station 24	0.63 ± 0.05 (7)	A23	1.15 ± 0.10 (2)
A1	0.83 ± 0.03 (3)	A24	1.20 ± 0.20 (2)
A2	1.55 ± 0.06 (4)	station 4	0.25 ± 0.05 (8)
A3	1.76 ± 0.03 (5)	station 5	0.40 ± 0.05 (7)
A4	1.20 ± 0.06 (5)	A25	1.24 ± 0.19 (2)
A5	0.78 ± 0.04 (3)	A27	1.13 ± 0.02 (3)
station 1	0.08 ± 0.06 (9)	A29	1.66 ± 0.17 (2)

N.B. Time-terms are shown with the calculated standard errors and numbers of observations (in brackets)

To check the consistency of the time-term solution, data set A was divided into four sets, B to E, which contained data from shots 0.2 to 0.9, 6 to 11, 13 to 20 and 21 to 29, respectively. Within these smaller sets the data was well connected. Table 4.6 presents the time-term solutions obtained from these four data sets. The least-squares velocities range from 5.99 to 6.15km s^{-1} and are slightly lower than the velocity calculated from set A. Taking into account the slight variation in velocity, the time-terms calculated from sets B to E compare well with those obtained from set A. The assumptions used to determine the constant α were :

Set B : basement depths below shot 0.9 and station 21 and below shot 0.5 and station 17 assumed equal.

Set B : basement depth below shot 6 and station 2 assumed equal.

Set D : basement depth below shot 20 and station 3 assumed equal.

Set E : time-term for station 3 taken as that calculated using set D.

The first-arrival travel times used in all the solutions were corrected to sea level but no correction was applied to compensate for the water depth below each shot. The calculated shot time-terms therefore include the delay time associated with that part of the ray path which is in water. A water 'layer' with P velocity 1.5km s^{-1} was included in the overburden structure when the time-terms were inverted to estimate the depth to basement at each site along the profile.

Inversion of the time-terms to give the depth to the refractor can be performed accurately only if the velocity-depth structure

Table 4.6 Pg time-term solutions from data sets B-E

Set B (A0.2 - A0.9)

$V = 6.14 \pm 0.15 km\ s^{-1}$

site	Pg time-term (s)
A0.2	1.16 ± 0.06 (4)
A0.3	0.49 ± 0.07 (4)
station 14	0.71 ± 0.02 (3)
station 15	0.70 ± 0.07 (4)
station 16	0.77 ± 0.05 (5)
A0.4	0.99 ± 0.07 (4)
station 17	0.82 ± 0.09 (4)
A0.5	0.86 ± 0.02 (4)
A0.6	1.38 ± 0.15 (2)
station 18	0.88 ± 0.02 (5)
station 19	1.11 ± 0.13 (3)
A0.7	1.25 ± 0.01 (5)
A0.8	2.37 ± 0.05 (6)
A0.9	1.12 ± 0.04 (5)
station 21	0.78 (1)
station 22	0.35 ± 0.05 (3)
station 23	0.60 ± 0.04 (3)
station 24	0.26 ± 0.07 (3)

Set C (A1 - A11)

$V = 6.15 \pm 0.17 km\ s^{-1}$

site	Pg time-term (s)
station 1	0.18 ± 0.05 (5)
station 2	0.58 ± 0.10 (5)
A6	0.78 ± 0.03 (4)
A7	0.98 ± 0.08 (5)
A8	0.75 ± 0.03 (4)
A9	0.81 ± 0.05 (4)
A10	1.15 ± 0.10 (4)
A11	0.66 ± 0.12 (3)
station 13	0.71 ± 0.04 (4)
station 12	0.73 ± 0.06 (5)
station 11	0.73 ± 0.05 (5)

Set D (A13 - A20)

$V = 6.14 \pm 0.11 km\ s^{-1}$

site	Pg time-term (s)
station 13	0.46 ± 0.03 (5)
station 12	0.50 ± 0.03 (5)
station 11	0.67 ± 0.02 (5)
A13	1.24 ± 0.07 (3)
A14	0.70 ± 0.06 (4)
A16	0.88 ± 0.03 (4)
A17	0.43 ± 0.03 (4)
A18	0.63 ± 0.03 (4)
A20	0.24 (1)
station 3	$0.24 \pm .05$ (5)

Set E (A21 - A29)

$V = 5.99 \pm 0.17 km\ s^{-1}$

site	Pg time-term (s)
station 3	0.24 ± 0.05 (5)
A21	0.94 ± 0.04 (2)
A23	1.05 ± 0.05 (2)
A24	1.10 ± 0.09 (2)
station 4	0.25 ± 0.03 (5)
A25	1.05 ± 0.17 (2)
A27	0.88 ± 0.03 (3)
A29	1.27 ± 0.09 (3)
station 5	0.43 ± 0.03 (5)

in the overlying layers is known. In most refraction surveys this is determined using arrivals from closely spaced shots near to the receiving stations. In the LASP project, the shot spacing was too wide to give any information on the low velocity layers above the basement. It had been planned to use the results from the nearby profiles of Officer et al. (1959) to provide the layer velocities and thicknesses required. For line A, results from five of these profiles were used. These were profiles 11 and 12 to the north of St Lucia, profile 28 along the Grenadines and profiles 26 and 27 to the south and southeast of Grenada (Fig. 1.5). Table 4.7 shows the velocity depth models derived for each of these profiles, including the total depth to basement, where available.

Two methods were employed to estimate the depth to basement from the Pg time-terms and the previous results. Firstly, the overburden was approximated to a single layer with a P wave velocity equal to the average velocity of the actual layers, as defined from the earlier profiles. These average values are given in Table 4.7 (V_n, etc.). The mean of these average overburden velocities is 3.3km s^{-1}. Using this value at all the sites the Pg time-terms from the analysis of data set A were inverted to overburden thickness following the method described in section 3.4. These thicknesses, Z (1), are listed in Table 4.8.

The alternative method is to extrapolate from the results of the previous profiles to estimate the detailed upper structure at each site. The problem is now the n-layered case discussed in section 3.4 where the velocities are known to the n-1 layer and the thicknesses to the n-2 layer. The least-squares velocity and time-terms provide estimates of the thickness of the n-1 layer (in this case the 4.0 - 4.4km s^{-1} layer). Extrapolation of the structure

Table 4.7 Crustal structure from selected profiles of Officer et al.(1959)

profile 11

Tn	V	Ts
0.08	1.54	0.08
0.05	1.76	0.13
0.96	2.68	0.77
0.41	3.44	0.88
0.62	4.40	2.49
2.12	6.31	4.35

$\overline{Vn}$ = 3.16 $\overline{Vs}$ = 3.61

profile 12

Tw	V	Te
0.09	1.52	0.95
0.11	1.71	0.61
0.67	2.39	0.18
0.85	3.25	1.25
2.56	4.29	1.51
4.28	5.97	4.50

$\overline{Vw}$ = 3.48 $\overline{Ve}$ = 3.04

profile 28

Ts	Vs
0.04	1.51
0.06	1.70*
1.34	(2.33)
3.05	(4.00)
4.49	(6.40)

$\overline{Vs}$ = 3.24

profile 26

Te	Ve
0.16	1.51
	(1.64)
1.26	(2.03)
2.35	(2.57)
	(4.33)

profile 27

Ts	V	Tn
0.16	1.51	0.68
	1.64	
1.26	2.03	1.66
2.35	2.57	1.93
	4.33	

N.B. V = layer velocity (km s^{-1})
T = layer thickness (km)
$\overline{V}$ = average overburden velocity (km s^{-1})

* assumed value
( ) unreversed value

Table 4.8 Depth estimates from Pg time-term solution A

Site	Water depth (km)	Z (1) (km)	Z (2) (km)
A0.2	0.91	2.26 ± 0.22	
A0.3	0.04	1.70 ± 0.30	
station 14		3.00 ± 0.07	
,, 15		2.96 ± 0.19	
,, 16		3.16 ± 0.14	
A0.4	0.26	3.55 ± 0.13	
station 17		3.74 ± 0.57	
A0.5	0.06	3.28 ± 0.07	
A0.6	1.02	3.00 ± 0.39	
station 18		3.66 ± 0.11	
,, 19		3.12 ± 0.58	
A0.7	0.55	3.36 ± 0.42	
A0.8	2.07	5.30 ± 0.32	
A0.9	0.93	1.94 ± 0.19	
station 21		1.75 ± 0.19	
,, 22		1.01 ± 0.16	
,, 23		2.14 ± 0.16	
,, 24		2.46 ± 0.21	
A1	0.20	2.72 ± 0.12	2.63 ± 0.19
A2	0.97	3.60 ± 0.25	4.05 ± 0.39
A3	0.93	4.52 ± 0.13	5.49 ± 0.20
A4	0.24	4.06 ± 0.22	4.74 ± 0.34
A5	0.03	2.97 ± 0.17	2.98 ± 0.27
station 1		0.31 ± 0.21	
,, 2		1.68 ± 0.18	
A6	0.53	2.21 ± 0.07	
A7	1.05	1.67 ± 0.36	
A8	0.46	2.32 ± 0.14	
A9	0.58	2.12 ± 0.09	
A10	1.39	1.52 ± 0.40	
A11	0.40	2.19 ± 0.61	
station 13		2.69 ± 0.09	
,, 12		2.69 ± 0.10	
,, 11		2.77 ± 0.13	
A13	0.45	3.22 ± 0.15	2.83 ± 0.21
A14	0.04	2.17 ± 0.29	2.13 ± 0.39
A16	0.11	2.76 ± 0.19	2.73 ± 0.25
A17	0.04	1.34 ± 0.18	1.36 ± 0.24
A18	0.04	2.00 ± 0.11	2.25 ± 0.15
A20	0.04	1.74 ± 0.43	1.88 ± 0.58
station 3		1.64 ± 0.18	1.87 ± 0.25
A21	0.04	4.51 ± 0.18	4.48 ± 0.24
A23	0.04	4.39 ± 0.38	4.32 ± 0.51
A24	0.04	4.58 ± 0.76	4.58 ± 1.02
station 4		0.97 ± 0.18	
,, 5		1.56 ± 0.18	
A25	0.03	4.77 ± 0.72	3.01 ± 1.12
A27	0.03	4.32 ± 0.06	2.35 ± 0.10
A29	0.42	5.42 ± 0.66	4.04 ± 1.03

observed at one profile over any great distance is invalid as the velocity-depth structure is seen to vary along the arc. From the results of profiles 11 and 12, thicknesses of 0.1, 0.8 and 0.6km were assumed for the 1.7, 2.4 and 3.3km s^{-1} layers beneath shots A1 to A5. The overburden thicknesses calculated from this model (Table 4,8, $z(2)$) are similar to those obtained from the single layer approximation at shots 1, 2 and 5, but are somewhat greater at sites 3 and 4. This discrepancy could be due to an increase in the thickness of the unconsolidated sediments away from the islands.

From profile 28, thicknesses of 0.06 and 1.34km were assumed for the 1.7 and 2.33km s^{-1} layers at sites 24 to 21, but north of Carriacou (20 - 13) the thickness of the 2.33km s^{-1} layer was reduced by 1.0km to allow, partially, for the observed step in the first arrival line. The depths calculated in this way for sites 13 to 24 are all close to the values obtained using the single layer approximation (Table 4.8). The values for sites 21 - 24 compare well with the depth of 4.5km found below the southern end of profile 28.

Profiles 26 and 27 are southeast of shots 25 - 29 (Fig.1.5) but a tentative extrapolation of the structure determined in these profiles was made. Thicknesses of 1.2 and 1.5km for the 1.64 - 2.03 and 2.57km s^{-1} layers yielded basement depths which were 1.4 - 2.0km smaller than the depths calculated by the single layer approximation at sites 25 - 29. This suggests that either the average velocity assumed for the single layer was too large or that the two low velocity layers are thinner under sites 25 to 29. The refraction results of Officer et al. (1959) indicate that the basement is 'downbuckled' between Grenada and Trinidad so it is unlikely that the basement will be at less than 4km beneath sites 25 - 29. The more realistic depths are probably given by the single layer approximation, thus indicating that the 1.64 - 2.03km s^{-1} layer thins towards Grenada.

The upper crustal structure along line A determined using the single layer approximation is shown in Fig. 4.8. There are two areas where the basement topography seems rather extreme. The first is in the region north of St Lucia where the basement appears to slope from a very shallow depth under north St Lucia to a depth of 5.5km below shot 3 over a distance of only 16km. Larger depths were also indicated by the 'plus'-time analysis in this region and their relation to lateral variations in Pg velocity have been discussed (section 4.3.2). The second area is about Grenada where the station time-terms indicate a much shallower basement than do the time-terms from shots on either side. If the overburden beneath the islands has a higher velocity than that seen between the islands, then the depths calculated from the station time-terms would be larger. The presence of much intrusive and volcanic material at or near the surface on the volcanic islands suggests that velocities much higher than 3.3km s^{-1} may be found under parts of the islands. However, the effect of an increased average overburden velocity beneath Grenada and St Lucia would not completely remove the basement anomalies. Also, such a velocity change would be unlikely to be very sharp so the effect would be noticed at the adjacent shot sites also.

These 'anomalies' could also be due to a statistical bias in the time-term solution due to poorly connected data. This is very likely to be the cause of the 'structure' below Grenada as most of the shots received by the Grenada stations are to the north, there being only 5 travel times from shots to the south. It is noted that St Lucia lies at the western end of the East St Lucia ridge, a prominent east-west structural feature described by Westbrook (1973). This may be related to the structure determined by time-term analysis.

Fig. 4.8 Summary of basement structure beneath Line A as determined from P_g time-term solution A.

(error bars on basement depths represent 68% confidence limits)

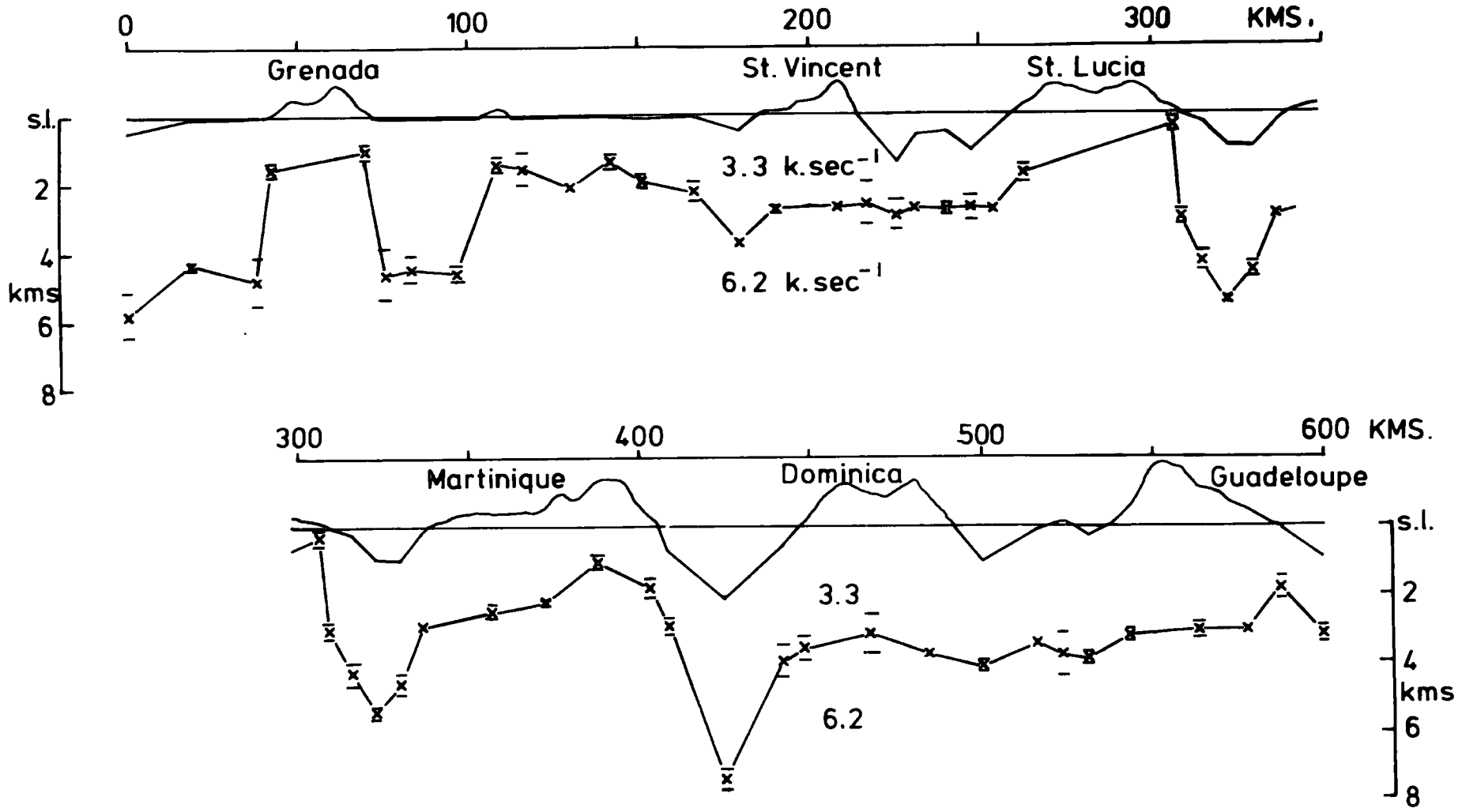

SECTION ALONG LINE A

As the Pg time-term solution indicates a considerable dip on the basement in some areas, an iterative solution was applied, following the method described in section 3.4, to see if an improved solution could be obtained. The application of this technique resulted in a reduction in the severity of the refractor topography in the more anomalous regions without a significant change in the least-squares velocity. However, the standard deviation of the solution increased slightly and showed no sign of converging to a minimum value. It is considered that this iterative procedure did not produce a more reliable interpretation than that obtained in the first approximation.

4.3.4 The composition of the basement

The Pg velocity determined under line A is within the range of velocities shown by many igneous rocks of acid, intermediate and basic compositions. At depths of 2.5 to 5km the rock will be subjected to pressures in the region of 0.6 to 1.3 kbar. Velocity measurements (Birch, 1960, 1961 and others) for granite show average values of 5.88km s^{-1} at 0.5 kbar and 6.14km s^{-1} at 1.0 kbar. The average density of granite, however, is about 2.65gm cm^{-3} and a thick layer of granitic composition beneath the arc cannot be reconciled with the high positive gravity anomaly observed. Determinations of the P velocity in basalts and andesites are available only for low pressures (Press, 1966), but it is probable that velocities of 6km s^{-1} and above will be found at a few kilometres depth. The majority of the volcanic rocks comprising the islands are of andesitic composition and only a small amount of basalt is seen. Also several dioritic intrusions are exposed at the surface (Martin-Kaye, 1969). Whichever

process for the derivation of the andesites is preferred, the source is likely to be in the upper mantle or lower part of the crust. There is therefore no strong geochemical evidence for a layer of basic material high in the crust. Considering the wide occurrence of andesites at the surface, it is proposed that the 6.1 to 6.2km s^{-1} layer consists of material of bulk andesitic composition extruded through the crust during the formation of the island arc and later intruded by rocks of dioritic composition.

4.4 The P^* refractor

The observation of apparent velocities between 6.7 and 7.3km s^{-1} at some stations along line A was discussed in sections 4.1 and 4.2. The observed velocities and time intercepts are shown in Table 4.1(b). Most of these velocities are ill-defined as indicated by the errors of the straight line fit. Two questions need to be answered :

(1) Do these arrivals define a single continuous refractor beneath the arc? And, if this is so

(2) What is the depth of this refractor?

Pairs of stations were selected for which high velocities were recorded at each in the direction of the other. A reversed profile interpretation was then made, allowing for the upper crustal structure determined from the analysis of Pg arrivals. The results of these interpretations are shown in Table 4.9. The range of the calculated velocities is quite large. Within the errors of the

Table 4.9 The P^* refractor : reversed profile interpretation

station A - station B	velocity (km s^{-1})	dip	depth to P^* refractor (km) under A	under B
shot A2 - shot A0.2	7.05	0.8°N	14.0	17.4
22 Martinique - 14 Guadeloupe	6.75	0.3°S	13.8	13.0
22 ,, - 15 ,,	6.98	3.6°N	12.0	23.0
22 ,, - 18 Dominica	6.73	1.7°S	14.0	9.6
3 Carriacou - 2 St Lucia (6.86km s^{-1})	7.01	2.5°N	9.4	15.9
3 Carriacou - 2 St Lucia (7.28km s^{-1})	7.23	0.6°S	16.0	14.5

velocity determination it is not possible to resolve satisfactorily whether these arrivals are from a single continuous refractor, or not. The average depth to this 'refractor' is about 14km. An 'average' upper crustal model along line A, consisting of 3km of 3.5km s^{-1}, above 12km of 6.2km s^{-1}, overlying a 7.0km s^{-1} layer, is consistent with a crossover distance of about 100km between 6.2 and 7.0km s^{-1} first arrival segments.

The first arrival travel times which indicated apparent velocities of about 7km s^{-1} were collected into one data set for time-term analysis. The data set consisted of 61 travel times linking 22 shot sites with 12 station sites. Five of the shot sites were linked with only one station and only six were connected with more than three stations. The resulting solution yielded a least-squares velocity of 6.96 ± 0.25km s^{-1}. The time-terms calculated in the solution varied greatly in value. The shot time-terms covered a range of 1.44 s and the station time-terms a range of 2.09 s. Different criteria were used to estimate the value of the constant and gave widely differing values. The magnitude of the fluctuations in the time-terms was too large to be due to real structures within the crust. Some of the calculated time-terms were smaller than the corresponding Pg time-terms for that site. Possible explanations for the inconsistency of this solution are :

(1) that the arrivals used were not all due to critical refraction in the same layer

(2) that the velocity varies laterally under the refractor

(3) that there was insufficient data to effect a statistically reliable solution.

If some data is removed from the set, the number of observations in the normal equations approach the number of unknowns and the solution becomes less reliable. It is impossible, therefore, to test rigorously how much the first explanation holds. There are also too few observations for a 'minus'time analysis to provide a reliable indication of lateral variations in velocity.

In conclusion, more distant arrivals along line A suggest the existence of a refractor of velocity 6.7 to 7.3km s^{-1} at a depth of 12 - 16km below the Lesser Antilles arc. However, it has not been possible either to determine whether it is continuous along the arc, or to define its shape in detail.

It is possible that the P^{*} refractor represents the top of the oceanic layer 3 of the original oceanic crust which has been downwarped as a result of the growth of the pile of volcanic and intrusive material during the formation of the island arc. If this is so, it would very likely have been intruded by the denser, more basic components of the magma rising from the upper mantle. A velocity of 7km s^{-1} would be reasonable for layer 3 modified in this way. However, the thickness of the oceanic layer is unlikely to have increased much beyond its normal thickness of 6 - 8km. As the top of the 7km s^{-1} layer is at a depth of about 15km, this would imply a depth to the downwarped Moho of about 23km beneath the arc. This is much shallower than the Moho depth suggested by gravity interpretations (Westbrook, 1973; Kearey, 1973) and the arguments given later (section 4.5).

It seems probable, therefore, that there has been a considerable thickness of material of lower crustal density (2.9 - 3.0 gm cm^{-3}) intruded into the crust within and below the old oceanic layer in this region. What is this material? Ultrabasic xenoliths

have been found in extrusive igneous rocks along the arc by several workers (K. Wills, personal communication). Wills considers these xenoliths to have originated from magma chambers not deeper than 20km. Thus 'frozen' magma chambers containing cumulate rocks might exist under the arc at about the depth defined by the P^* refractor. These cumulate rocks are likely to be largely gabbroic in composition. Laboratory determinations of the P velocity of gabbro at varying pressures (Press, 1966) indicate average values between 6.9 and 7.0km s^{-1} at pressures corresponding to the lower part of the crust.

High pressure modifications of diorite and granodiorite would also show velocities in the region of 7km s^{-1}. Such rocks have been suggested as a possible constituent of the lower part of the continental crust (Ringwood and Green, 1966). However, there is no evidence for the existence of such rocks under the island arcs.

4.5 Minimum depth to the Mohorovicic discontinuity

It has already been stated (section 4.2) that no sub-Moho refractions were observed at stations along the arc from shot line A. If it is assumed that there is a discontinuous increase from 7km s^{-1} to 8km s^{-1} at some depth below the P^* refractor, it is possible to estimate a minimum depth to this discontinuity from the maximum distance at which distinct first arrivals are recorded along the profile. The following model is assumed :

layer velocity	layer thickness
3.3km s^{-1}	3km
6.2	15
7.0	?
8.0	

For a profile length of 200km the minimum depth to the Moho is calculated to be 37.6km and for a profile 250km long, the Moho must be at least 44km deep. Arrivals are observed up to 200km along the arc and some of the French stations received distinct arrivals from shots up to 250km away. If the velocity increases with depth below the 6.2km s^{-1} refractor or below the 7km s^{-1} refractor, then the crossover distance at which Moho arrivals would be seen as first arrivals increases and the minimum depth to the Moho is reduced.

Gravity models (Westbrook, 1973) indicate a maximum crustal thickness of 35km beneath the arc. The density-depth structure assumed in these gravity interpretations is consistent with the seismic model proposed here, but Westbrook investigated the effect of varying the depth of the 7km s^{-1} layer. He found that the Moho must be depressed when the 7km s^{-1} layer is brought closer to the surface to retain the fit of the gravity anomaly. The effect of increasing the density with depth within the lower layers would be to increase the crustal thickness required to fit the observed gravity anomaly.

From these considerations it is suggested that the average crustal thickness beneath the Lesser Antilles island arc is about 35km.

4.6 Gravity considerations and summary

In this chapter the interpretation of first arrival data from line A has been presented. A 6.1 - 6.2km s^{-1} layer has been defined in detail along the whole length of the arc. The presence of

a 7km s^{-1} refractor at a depth of 12 - 16km is suggested, but no direct evidence concerning the base of the crust is available. Various considerations (section 4.5) indicate that the Moho, if present as a distinct discontinuity beneath the arc, would lie at a depth of about 35km.

At this point a consideration of the gravity anomaly along the island arc is relevant. A Bouguer gravity profile along the length of line A (Fig. 4.9) was constructed from the Bouguer gravity map shown in Fig. 1.8 and measurements from the Grenadine islands by Masson Smith and Andrew (1965). There are several features of interest in this profile :

South of Grenada the gravity decreases substantially towards the Venezuelan coast indicating the presence of a sedimentary basin or a depression of the Moho, or both. This is the region where the island arc axis swings southwest towards Margarita, off the line of shot line A. Seismic results (Officer et al. 1959; Edgar et al. 1971; this work) have proved a thickening of sediments south of Grenada. A significant thickening of the crust beyond the already considerable proposed thickness beneath the arc is not expected.

The Bouguer anomaly in the southern part of the arc, south of St Lucia, is distinctly higher (more positive) than it is in the northern part of the arc. This could be caused by a somewhat thicker crust in the north, an increase in the depth to the subducted Atlantic lithosphere below the northern part of the arc, or the presence of more low density material in the crust in the north. Certainly, the depths to the 6.1km s^{-1} refractor under the sites in the northern part of line A are slightly greater than those beneath the southern sites. Westbrook (1973), from a study of earthquake focal depths across the arc, found inconclusive evidence that the Benioff zone is deeper below

Fig. 4.9 Bouguer gravity profile : Line A
(taken from Bouguer gravity map, Fig. 1.8;
additional measurements on the Grenadines
are from Masson Smith and Andrew, 1965)

BOUGUER GRAVITY PROFILE — LINE A.

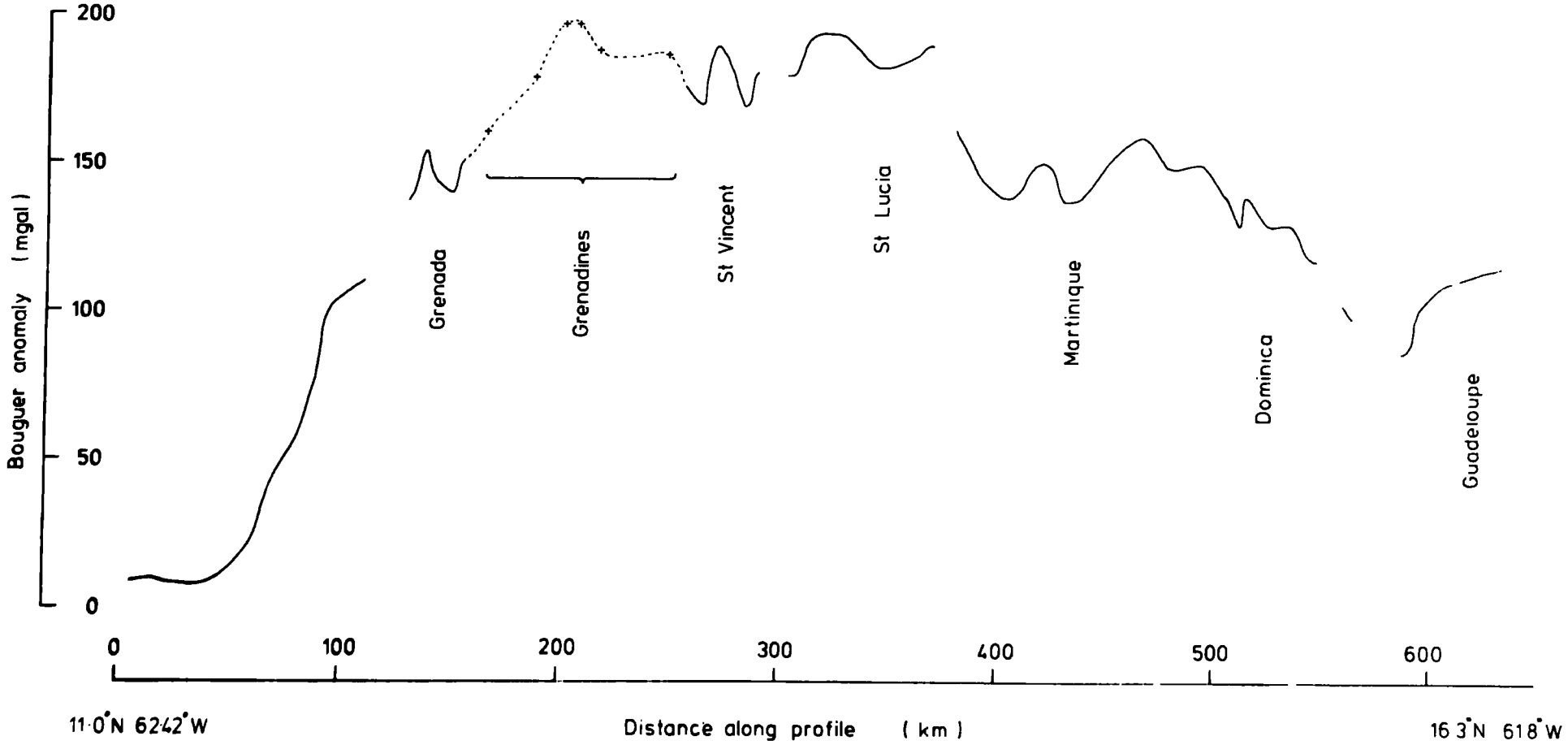

the middle portion of the Lesser Antilles than it is at either end. Geochemical differences between volcanic centres along the arc are consistent with a greater depth to the subducted plate beneath the northern islands (K. Wills, personal communication). There is no direct evidence of either a deeper Benioff Zone or a thicker crust in the region north of St Lucia.

The gravity 'low' between Dominica and Guadeloupe does not appear to be due to variations in the upper crustal structure as the structure determined from the Pg time-term analysis is fairly uniform in this region. This gravity low might therefore indicate a downwarp of the 7km s^{-1} layer or the Moho.

Chapter 5

INTERPRETATION OF FIRST ARRIVAL DATA FROM THE TOBAGO TROUGH

5.1 Introduction

Eleven charges were fired across the northern end of the Tobago Trough from north of St Vincent to Barbados (Fig. 2.1). These were received at many of the stations along the Lesser Antilles arc and also at the two Barbados stations and the hydrophone station (LASP 10) midway between St Vincent and Barbados.

Several refraction and reflection profiles have been run in the Tobago Trough - Barbados Ridge area by previous workers (see section 1.4.1 and Fig. 1.5). Basement velocities of 6.84 and 7.06km s^{-1} at depths of 8.5 and 12.3km were found for profiles G-7 and 55 in the Tobago Trough. The other layers defined by these profiles all had velocities under 4km s^{-1} and are assumed to be sediments and metamorphics. Westbrook (1973), by comparing the upper crustal structure determined from profile G-7 with the results of seismic reflection profiles, deduced the velocity layering below the hydrophone station to be :

velocity (km s^{-1})	Thickness (km)	
1.5	2.1	water
1.7	0.9	unconsolidated sediment
2.5 - 3.0	1.8 - 2.1	partially consolidated to consolidated sediment
4.0	4.2	metamorphics

total depth to basement = 9 - 9.3km

The profiles 15, 16 and 22, described by Officer et al (1959), are located on the Barbados Ridge (Fig. 1.5). Profiles 15 and 16 are short lines northwest of Barbados. 15 was unreversed and the highest apparent velocity observed was 3.4km s^{-1}. 16 was reversed and penetrated to a 4.3km s^{-1} layer at a depth of 5km at the south end. Profile 22 was a longer profile some way south of Barbados and defined a layer of velocity 4.9km s^{-1} at a depth of 4.8km below its northern end. Some way east of the crest of the Barbados Ridge, profile 21 found a layer with velocity 5.3km s^{-1} at a depth of 8 - 10km. The velocities faster than 4km s^{-1} seen under the Barbados Ridge are thought to represent metamorphosed sediments or igneous intrusions. No velocity of 6km s^{-1} or more was observed at any of the profiles on the Barbados Ridge. Westbrook (1973) has computed crustal models across the Tobago Trough and Barbados Ridge which fit the observed gravity at latitude $13^{\circ}04'$N. These suggest a minimum crustal thickness of about 20km beneath the central Tobago Trough, the crust thickening to about 26km beneath the Barbados Ridge.

5.2 Observed Velocity Data

The stacked records for shots B23 - 33 at the St Vincent station SVS are shown in Fig. 5.1. The first arrivals up to about 100km range indicate an apparent velocity of 5.6km s^{-1}. The amplitude of this first arrival phase diminishes rapidly away from the station and can only just be discerned from shot 28. No first arrival phase can be picked from shot 29, but a low amplitude phase is seen on the records for shots 30 - 32. This phase has an apparent velocity of 8.8km s^{-1}. No correlable second arrival phases can be seen except the high amplitude 'T' phase which has an apparent velocity of 1.5km s^{-1}.

Fig. 5.1 Stacked records of shots B23 - 33 at St Vincent SVS

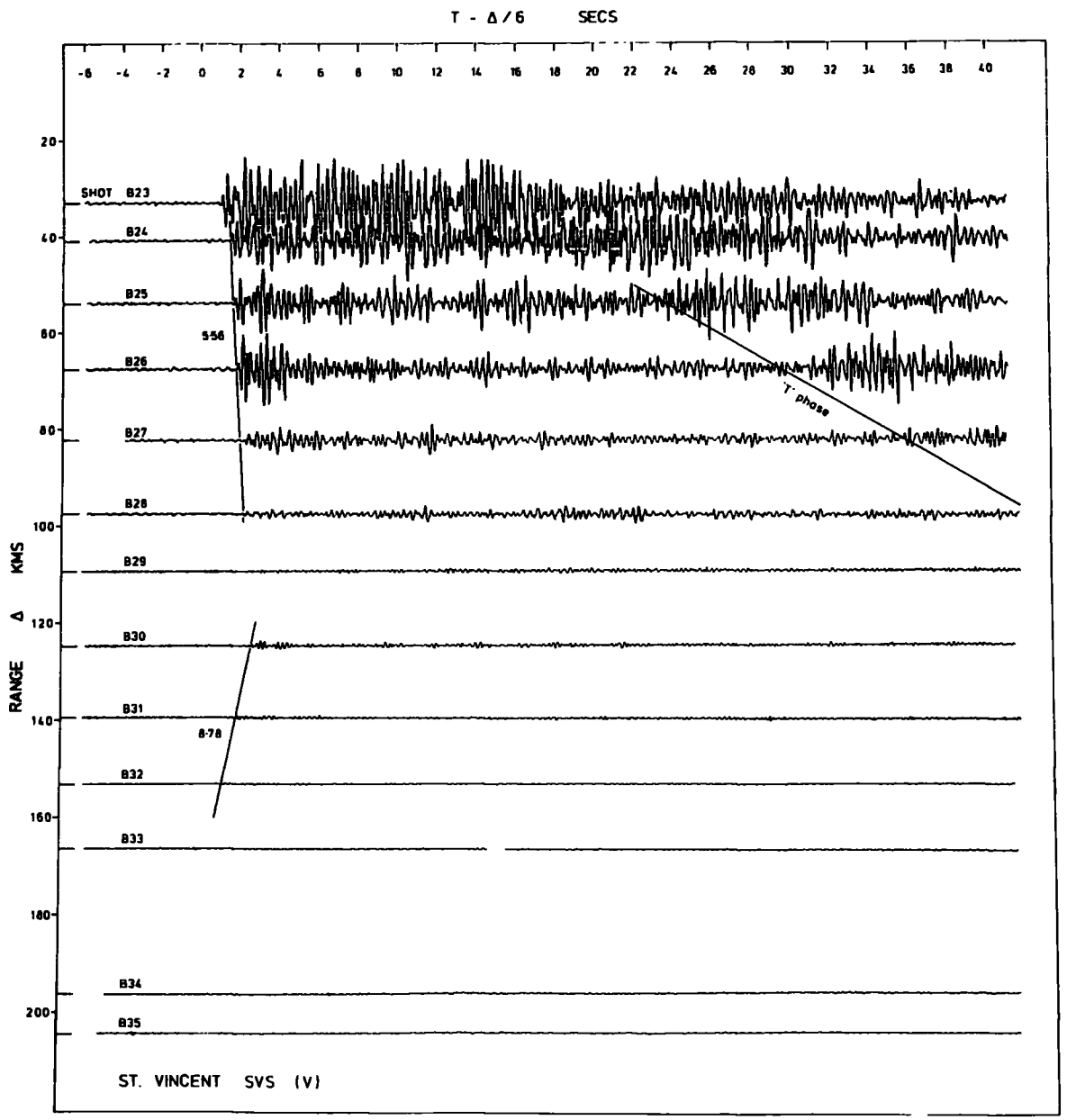
T - Δ / 6 SECS
-6 -4 -2 0 2 4 6 8 10 12 14 16 18 20 22 24 26 28 30 32 34 36 38 40
RANGE Δ KMS
20
40
60
80
100
120
140
160
180
200
SHOT B23
B24
B25
B26
B27
B28
B29
B30
B31
B32
B33
B34
B35
5·56
8·78
T phase
ST. VINCENT SVS (V)

Fig. 5.2 Stacked records of shots B23 - 33 at Carriacou

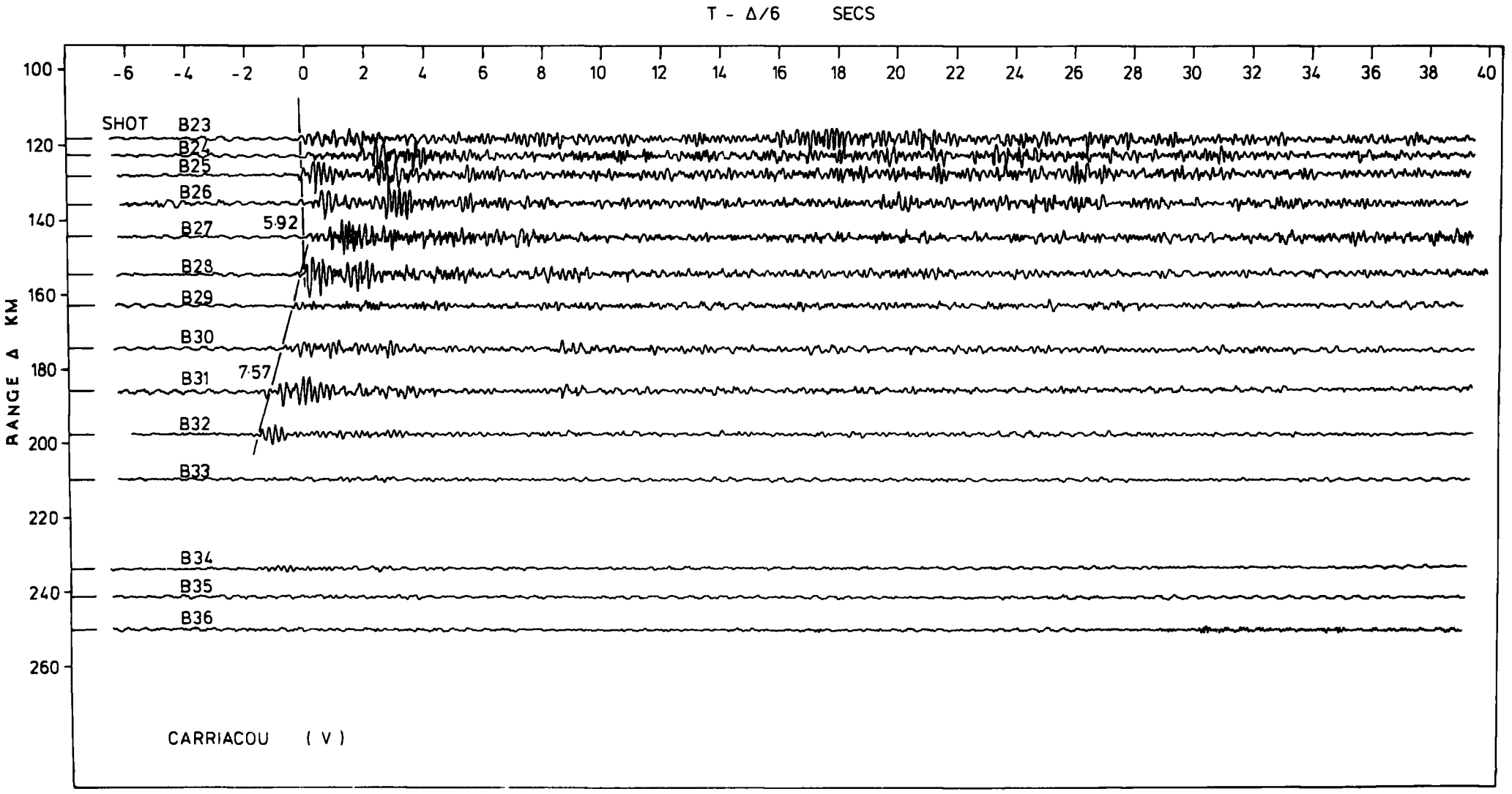
T - Δ/6 SECS
-6 -4 -2 0 2 4 6 8 10 12 14 16 18 20 22 24 26 28 30 32 34 36 38 40
100 120 140 160 180 200 220 240 260
RANGE Δ KM
SHOT
B23
B24
B25
B26
B27
B28
B29
B30
B31
B32
B33
B34
B35
B36
5·92
7·57
CARRIACOU (V)

The stacked records from Carriacou are shown in Fig. 5.2. Once again, two distinct first arrival phases are seen, but, perhaps because the station is a long way off the shot line, the crossover distance between the first arrival phases is about 140km here. It should be noted that no arrivals other than 'T' phase were seen at stations along the arc from any of the shots to the east of Barbados except at station OBM on Martinique (Dorel, personal communication).

The first arrival travel times for four of the arc stations are shown in Fig. 5.3. Each of these graphs shows two distinct segments, the first with an apparent velocity of 5.5 - 5.9km s^{-1} and the second with a velocity of 8.7 - 8.9km s^{-1} (7.6km s^{-1} for Carriacou). The first arrival data from the Barbados stations and the hydrophone station are plotted in Fig. 5.4 with those from St Vincent SVR for comparison. At the hydrophone station, apparent velocities of 7.32km s^{-1} and 5.78km s^{-1} were observed from the west and from the east, respectively. First arrivals at the Barbados stations from shots closer than about 40km indicate velocities of 3.0 - 3.5km s^{-1} with small negative time intercepts. Beyond about 50km a much higher velocity phase becomes the first arrival. Velocities of 9.5 and 9.0km s^{-1} were observed at Cole's Cave and St Phillips, respectively. The St Phillips recordings were of better quality than those at Cole's Cave, so the 9.0km s^{-1} velocity is considered the more reliable. No arrivals were seen at Barbados from shots at more than 100km range. The apparent velocities obtained from the first arrival travel times are summarised in Table 5.1.

5.3 The Basement Structure

In the region between St Vincent and the hydrophone station the first arrivals are refractions from the basement. Application of

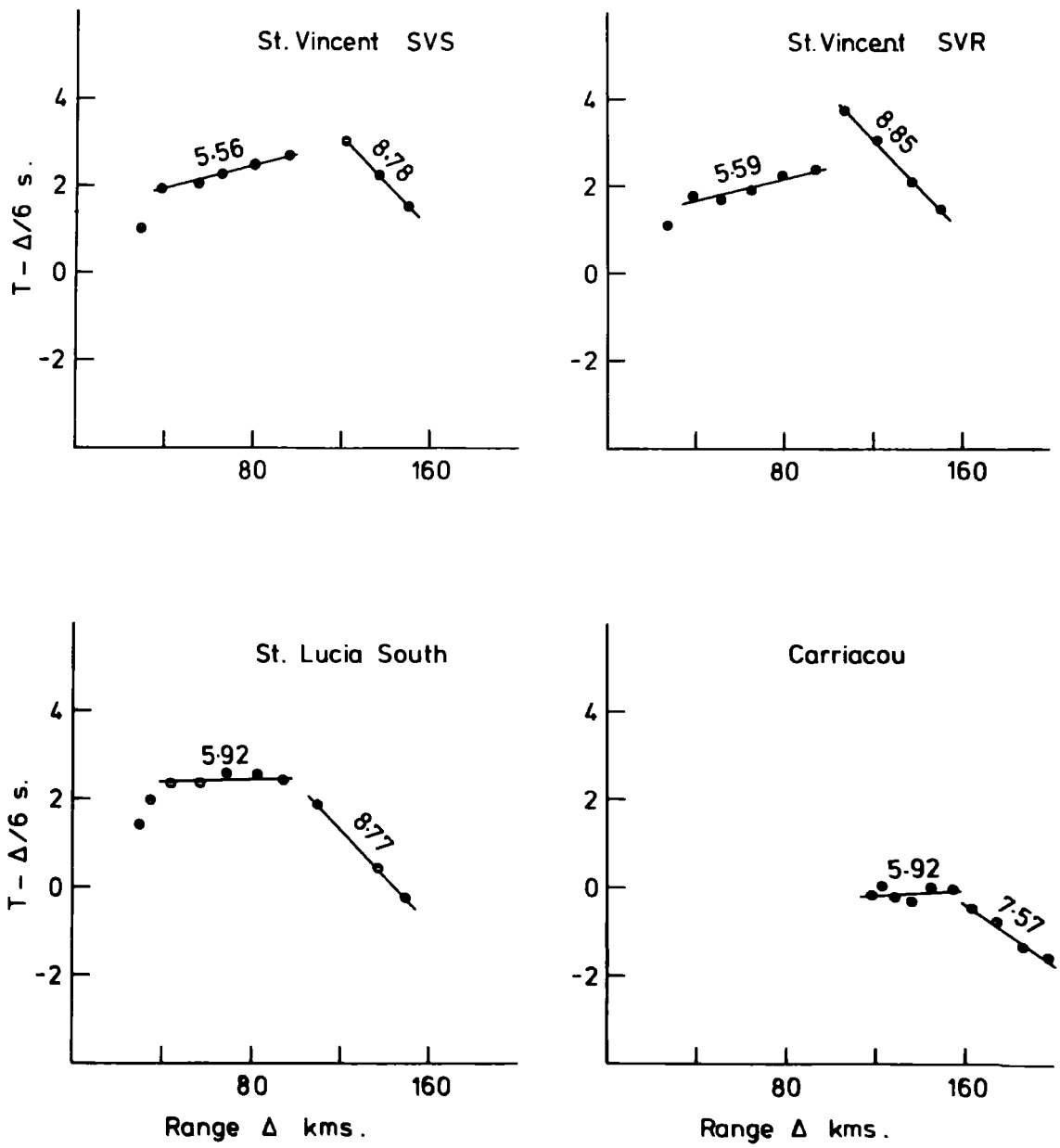

Reduced travel time graphs — Line B (east) shots 23-33

Fig. 5.3

Fig. 5.4 Summary of first arrival travel time data from the Tobago Trough

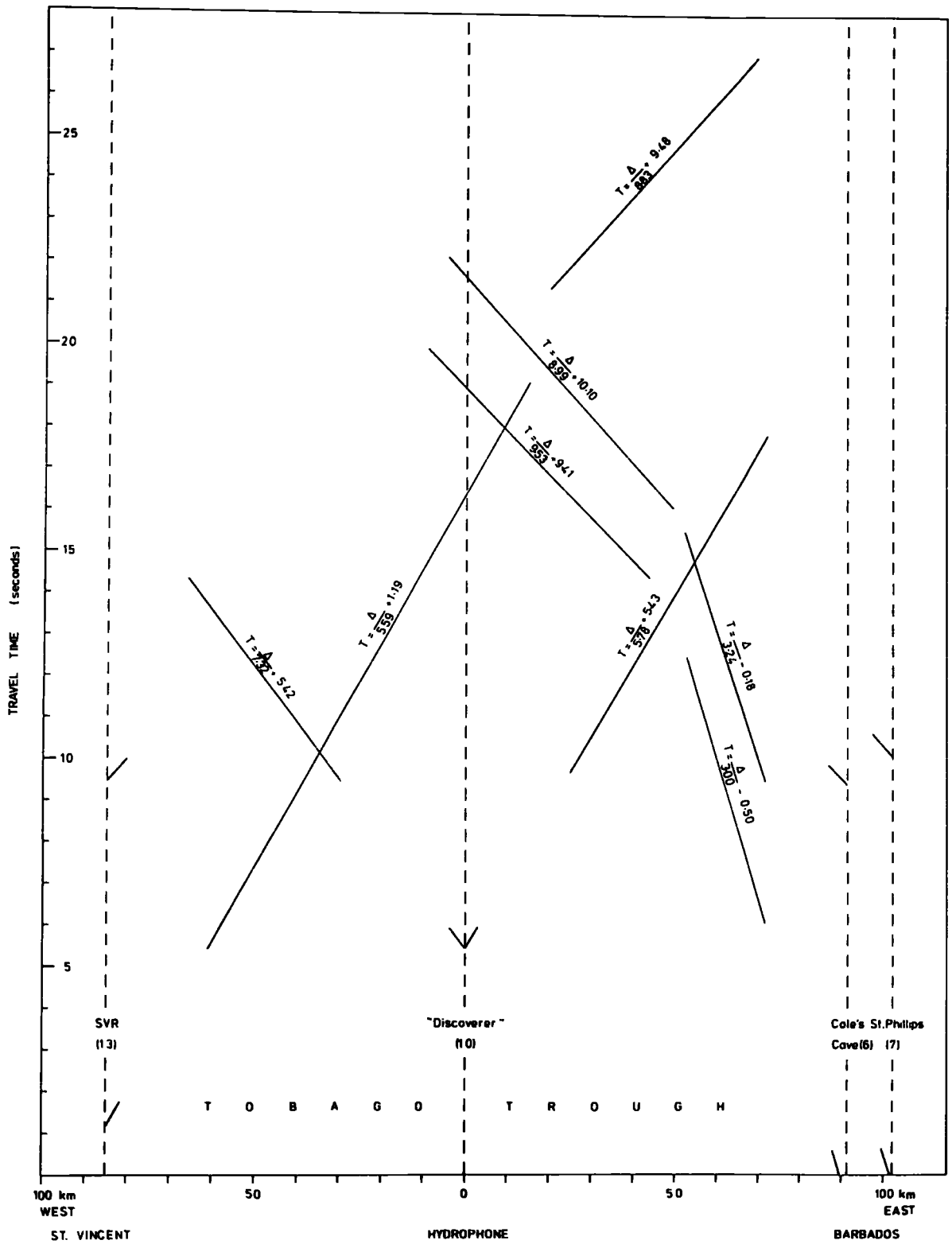
TRAVEL TIME (seconds)
25
20
15
10
5
T = Δ/8.83 + 9.48
T = Δ/8.99 + 10.10
T = Δ/5.53 - 9.41
T = Δ/5.59 + 1.19
T = Δ/4.22 + 5.42
T = Δ/5.78 + 5.43
T = Δ/3.24 - 0.18
T = Δ/3.00 - 0.50
SVR
(13)
"Discoverer"
(10)
Cole's St.Philips
Cave(6) (7)
T O B A G O T R O U G H
100 km
WEST
50
0
50
100 km
EAST
ST. VINCENT
HYDROPHONE
BARBADOS

Table 5.1 Apparent velocities observed from shots B23 - 33

	Station	Shots	Apparent velocity ($km\ s^{-1}$)	Time intercept (s)
2	St Lucia	25-29	5.92 ± 0.08	2.29 ± 0.17
		30-33	8.77 ± 0.06	7.62 ± 0.10
13	SVR	24-28	5.59 ± 0.09	1.19 ± 0.19
		29-32	8.83 ± 0.23	9.48 ± 0.39
12	SVS	24-28	5.56 ± 0.02	1.37 ± 0.04
		30-32	8.78 ± 0.06	9.48 ± 0.11
11	SVT	24-28	5.44 ± 0.03	0.23 ± 0.09
3	Carriacou	23-28	5.92 ± 0.17	-0.41 ± 0.65
		29-32	7.57 ± 0.24	5.18 ± 0.75
10	hydrophone II	23-25	7.32 ± 0.15	5.42 ± 0.13
		29-31	5.78 ± 0.07	5.45 ± 0.10
6	Barbados	27-30	9.53 ± 0.01	9.41 ± 0.01
	(Cole's cave)	31-32	(3.0)	(-0.5)
7	Barbados	28-30	8.99 ± 0.28	10.10 ± 0.27
	(St Phillips)	31-32	(3.2)	(-0.2)
22	Martinique OBM	24-32	7.03 ± 0.29	3.63 ± 1.09
4	Grenada North	23-31	7.76 ± 0.21	6.60 ± 0.63

the reversed profile technique yields a refractor velocity of 6.2 - 6.5km s^{-1} with an apparent dip to the east of 3.8 - 5.7° depending on which apparent velocity is used at the arc end (Table 5.2). The lower velocities observed at Barbados are due to refraction in a sediment layer or layers but, as this section is unreversed, the true velocity cannot be determined. The arrivals giving the higher apparent velocities at Barbados are interpreted as being refracted from the same layer as those giving the 5.8km s^{-1} apparent velocity at the hydrophone station (Fig. 5.4). If this is so, the basement has a velocity of about 7.0km s^{-1} and a dip of 7 - 8° towards the east (Table 5.2).

The possibility that the apparent velocities of 9.0 - 9.5km s^{-1} observed at Barbados are indicative of arrivals from the Moho is ruled out because the distances at which these arrivals are observed as first arrivals are too small to allow critical refraction at the Moho. Also the delay times are too small for a Moho as deep as that suggested by the gravity models of Westbrook (1973).

It must be remembered that the reversed profile technique is only accurate when applied to homogeneous plane layers and when the shots and stations are in a line, so this technique will only give an approximate interpretation. The interpretations using the data from the St Vincent stations SVS and SVR should be the most accurate, as these stations are most in line with the shots. The results of Table 5.2 were calculated assuming that the overburden approximated to a single layer with an average velocity of 3.5km s^{-1}. Shallow refraction studies in this area (section 5.1) suggest that the average overburden velocity is between 3 and 4km s^{-1}. The calculation was repeated for overburden velocities of 3 and 4km s^{-1} and it was found that the dip increased with the assumed overburden velocity, whilst the basement velocity remained about the same.

Table 5.2 Results from reversed profiles across the Tobago Trough

Station A	Station B	refractor velocity (km s^{-1})	refractor dip (to east)	depth below A (km)	depth below B (km)
hydrophone II	St Lucia S.	6.53	3.8^{o}	11.2	4.7
,,	SVR	6.31	5.1^{o}	11.4	2.5
,,	SVS	6.29	5.2^{o}	11.4	2.9
,,	SVT	6.21	5.7^{o}	11.5	0.5
,,	Carriacou	6.53	3.8^{o}	11.2	-0.9
,,	Cole's Cave	7.13	7.9^{o}	10.9	18.9
,,	St Phillips	7.00	7.2^{o}	11.0	20.4

(These results are calculated assuming an average overburden velocity of 3.5km s^{-1})

The results indicate that the basement velocity is higher beneath the eastern part of the Tobago Trough than it is on the flank of the Lesser Antilles ridge. The interpretation of profile 55 (section 5.1; Fig. 1.5) supports this conclusion. A similar high basement velocity (6.84km s^{-1}) was found from profile G-7 (J. Ewing et al., 1957) which crosses the LASP shot line B between shots 26 and 27 - about 18km west of the position of the change in basement velocity indicated by the LASP results. It may be that the 6.0 - 6.3km s^{-1} layer is sufficiently thin, here, for the thick sediment layer to mask first arrivals from this layer on a north-south profile.

The basement is at a depth of approximately 11km beneath the hydrophone position. Extrapolating the 7.0km s^{-1} refractor to the east suggests that it will be at a depth of about 20km below Barbados. The basement may level off under the Barbados Ridge, in which case this estimate will be too large. Earlier profiles (section 5.1) show a 4.9 - 5.3km s^{-1} layer beneath the Barbados Ridge, south of Barbados, which might be expected to extend under Barbados and the eastern part of the Tobago Trough. Refractions from such a layer might only appear as second arrivals at the hydrophone and Barbados stations, but the records at these stations show no arrivals with a velocity of about 5km s^{-1}. Even if a distinct high velocity layer does not exist in the overburden, it is likely that a gradual increase of velocity with depth is present. In either case, the average overburden velocity would be expected to increase towards Barbados, which would require a steeper dip on the basement under the shots nearer to Barbados to fit the observed travel times. A depth of 20km to the basement beneath Barbados would, therefore, appear to be reasonable.

This section of the first arrival data from LASP did not lend itself to interpretation by the modified 'plus-minus' technique (Appendix D). This was due to the lack of pairs of stations with sufficient common arrivals to construct a reliable 'minus' graph. However, each of the three St Vincent stations observed arrivals from shots 23 - 25 in common with the hydrophone station. For these, the 'minus' times indicate that the refractor velocity is slightly lower between shots 23 and 24 than it is between shots 24 and 25. The following velocities were obtained from the average gradient of the 'minus' graphs :

hydrophone II - St Vincent SVR 6.18 ± 0.39km s^{-1} (2.54 s)
hydrophone II - ,, SVS 6.16 ± 0.22km s^{-1} (2.66 s)
hydrophone II - ,, SVT 6.26 ± 0.04km s^{-1} (2.88 s)

The numbers in brackets above are the 'minus' time intercepts which give an estimate of the difference in delay times beneath each station in the pair. The 'plus' times for the shot sites (P) were calculated, and the depth to the basement (Z) estimated, as for line A in Chapter 4 :

	B23		B24		B25	
	P (s)	Z (km)	P (s)	Z (km)	P (s)	Z (km)
hydrophone - SVR	1.22	5.18	1.54	6.54	1.67	7.09
SVS	1.23	5.23	1.48	6.22	1.72	7.32
SVT	1.89	7.99	1.80	7.61	1.95	8.24

The depths calculated using arrivals at SVT are significantly larger than those calculated from the other stations. Station SVT is

much further off the line of the shots than the others, so the velocities determined from this station are expected to be less reliable. The results are in general agreement with the basement structure determined by the reversed profile method.

Although the amount of travel time data was small, a time-term analysis was attempted for the basement arrivals in the regions east and west of the hydrophone position. In the western region the data consisted of 27 travel times connecting six shots and five receivers. The least-squares velocity from the time-term solution is 6.13 ± 0.11 km s^{-1} which compares well with the P_g velocities observed along line A. Two methods were used to estimate the constant α (section 3.2). The first was to give the time-term for the station SVR a value of 0.69 s, which is that calculated in the P_g time-term station for line A (α = 1.03 s). The other assumed that the time-term at the hydrophone site had a value midway between the time-terms at shot sites 27 and 28 (α = 0.36 s). In the former case, the time-terms for the St Lucia station and St Vincent stations SVS and SVT are respectively larger and smaller than the values obtained from the P_g solution for line A data (Table 5.3(a)). The shot time-term at the hydrophone site is considerably larger than those for shots B27 and B28. Using the second assumption, the shot time-terms are larger, while the time-terms at the arc stations are reduced and give negative values at SVT and SVS. The inconsistency between the time-terms for the stations at either end of this profile may be partly caused by the fact that most of the travel times are observed in one direction, only three 'basement' arrivals being received at the hydrophone station. However, simulated data studies show that this should not have a large effect on the time-terms.

Depths to the basement below the shot sites were calculated from both sets of time-terms assuming a constant overburden velocity of 3.5km s^{-1}. These are shown in Table 5.3(a). The depths in the right-hand column are more consistent with the depths obtained from the reversed profile interpretation.

The data for the time-term solution for the basement east of the hydrophone station consisted of ten travel times connecting six shot sites (B27 - 32) with the two Barbados stations and the hydrophone station. The number of unknowns was, therefore, the same as the number of observations, so a reliable solution could not be expected. The velocity determined was 7.4 km s^{-1} but , due to the minimal number of travel time connections , the confidence limits on this value are very poor . The shot time-terms increase in value towards Barbados but, depending on the value assigned to the constant α, the Barbados station time-terms are too low, or the time-term for the hydrophone site is too high. The values shown in Table 5.3(b) are obtained by using a value of 4.04 s for α , such that the time-term for the hydrophone site is consistent with those at shots B27 and B28. The basement depth was estimated from the shot time-terms assuming average overburden velocities of 3.5km s^{-1} and 4.0km s^{-1} (Table 5.3(b)). Respective depths of 10.2 and 11.8km under shot 27, and 22.7 and27.0km under shot 32 were obtained, indicating average dips of 10° and 12°. This solution is considered unreliable. With the paucity of first-arrival data pertaining to the basement in this region, the reversed profile interpretation is considered the more accurate of those discussed.

Table 5.3 (a) Time-term solution : St Vincent - hydrophone II

least-squares velocity = 6.13 ± 0.11 km s^{-1}

Site		no. of observations	time-terms (s) $\alpha = 1.03$	time-terms (s) $\alpha = 0.36$	s.e.	depths to 6.13km/s layer (km) $\alpha = 1.03$ ($V_o = 3.5$km s^{-1})	depths to 6.13km/s layer (km) $\alpha = 0.36$	s.e.
station	2	6	1.04	0.37	0.05	4.4		0.2
,,	11	6	0.36	-0.31	0.03	1.5		0.1
,,	12	6	0.57	-0.10	0.02	2.4		0.1
,,	13	6	0.69	0.02	0.05	2.9		0.2
	B23	5	0.80	1.47	0.04	2.2	5.0	0.2
	B24	5	1.35	2.02	0.05	4.0	6.9	0.2
	B25	5	1.81	2.48	0.05	5.0	7.9	0.2
	B26	4	2.15	2.82	0.03	5.7	8.6	0.1
	B27	4	2.48	3.15	0.02	6.8	9.7	0.1
station	10	3	3.95	3.28	0.07		10.2	0.3
	B28	4	2.73	3.40	0.05	7.6	10.5	0.2

Table 5.3 (b) Time-term solution : hydrophone II - Barbados

Site	no. of observations	time-terms (s) (α = 4.04s)	depth to 7.38km s^{-1} layer (km) V_o = 3.5km s^{-1}	V_o = 4.0km s^{-1}	s.e.
B27	1	3.42	10.2	11.8	0.2
station 10	4	3.72 $\pm$ 0.01	11.3	13.1	0.1
B28	2	4.01 $\pm$ 0.04	12.3	14.3	0.2
B29	2	4.28 $\pm$ 0.01	13.3	15.4	0.1
B30	3	4.68 $\pm$ 0.03	15.3	18.0	0.1
B31	1	5.17	17.8	21.0	0.2
B32	1	6.06	22.7	27.0	0.2
station 6	3	3.81 $\pm$ 0.02			
station 7	3	4.70 $\pm$ 0.02			

Notes : α = arbitrary time-term constant

V_o = assumed average overburden velocity

s.e. = standard error

5.4 The Deep Structure

It has been noted (section 5.2) that shots on the western flanks of the Barbados ridge gave rise to high apparent velocities at the stations on St Lucia, St Vincent and Carriacou. A high apparent velocity was also observed at the Grenada North station from the shots across the Tobago Trough. The distance range of these arrivals is 155 to 220km. The apparent velocity observed at the Grenada station is 7.76 ± 0.21km s^{-1} and the time intercept is 6.60 ± 0.63 S (Fig. 5.5). The first arrival travel time from shot 29 was omitted from the least-squares velocity calculation as this arrival came in about 0.4 s earlier than was expected from the trend of the other arrivals. There is a possibility that this was due to a poor 'pick'. but the arrival appeared distinctive and this travel time is thought to be correct. The significance will be discussed later. Grenada is a long way off the line of shots : the direct path from the station to shot 33 is at an angle of about 40° to the shot line. The 'true' velocity will therefore be higher and it is proposed that these arrivals are due to refraction at the Moho. The seismic observatory on Martinique (OBM) is as far north of shot line B as Grenada is south of the line. Clear first arrivals from shots B23 - 36 were reported from this station (Dorel, personal communication). However, the reduced travel times determined from the line of shots show a considerable scatter (Fig. 5.5). The travel times for shots 24 to 32 inclusive are best fitted by a line with reciprocal gradient 7.03 ± 0.29km s^{-1}. The travel times for shots 33 to 36 cannot be reconciled with any first arrival phase, and if they are genuine arrivals, it seems likely that they are second arrivals. The arrivals from shots 24 - 32 show a significantly

Fig. 5.5 Reduced travel time graphs for arrivals from shots B23 - 33 at Grenada North and Martinique OBM

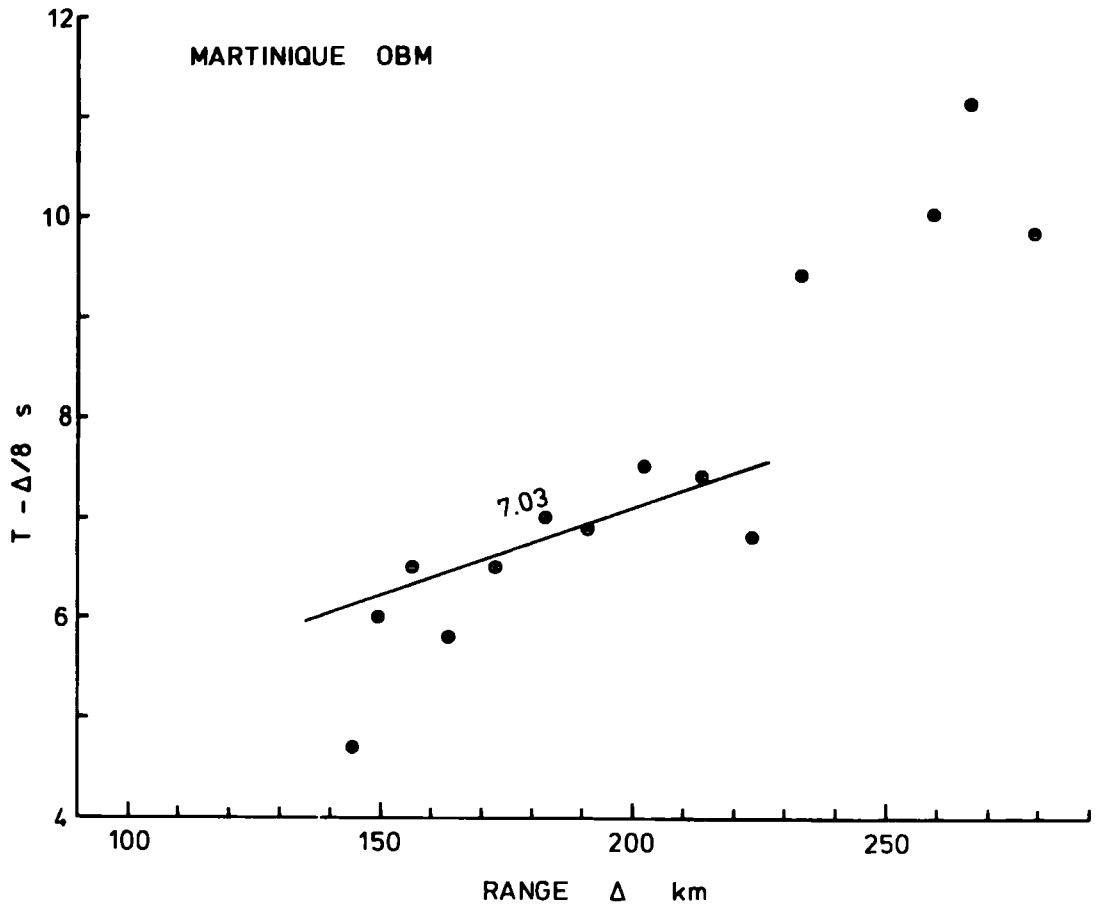

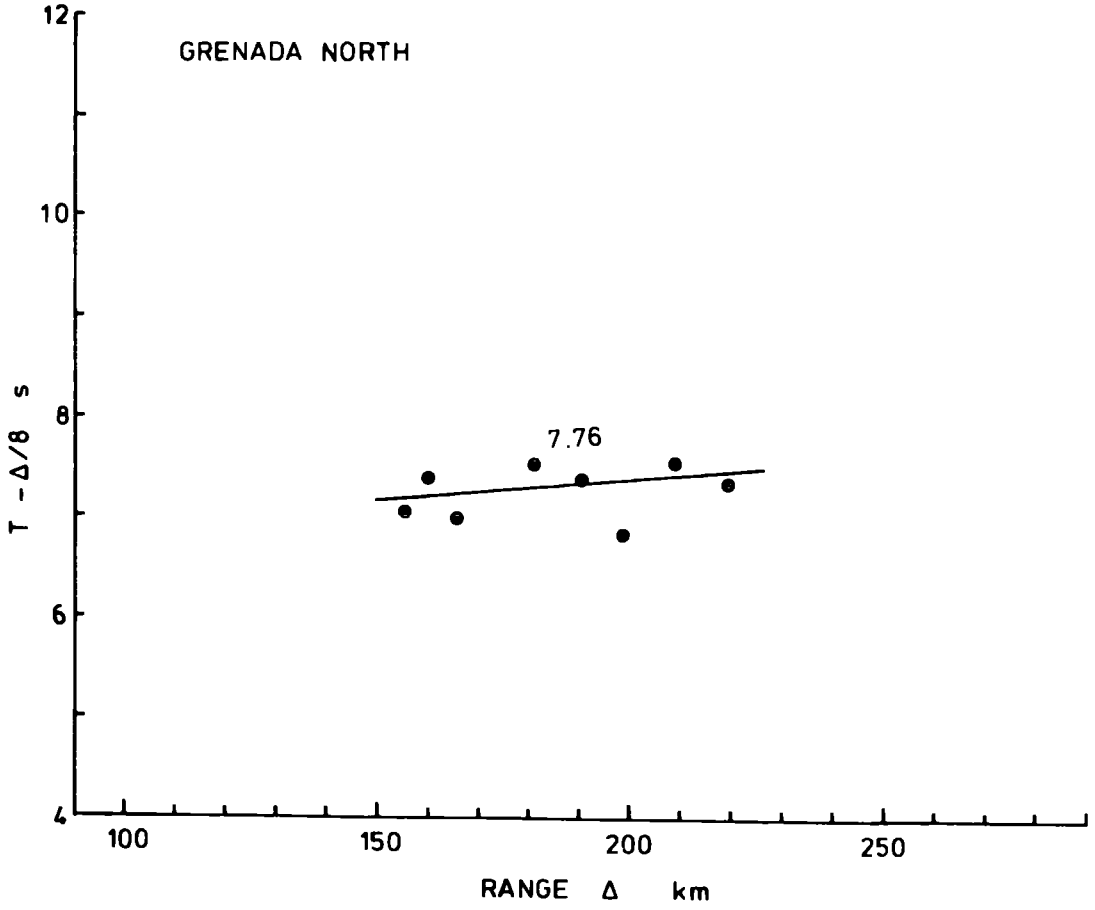

Reduced travel time graphs : shots B 23-36 .

lower apparent velocity and time intercept than those observed at the Grenada station and it is considered likely that they are refractions from the lower crustal layer rather than Moho refractions. None of the other French stations recorded arrivals from this shot line.

The high velocity arrivals at St Lucia South, St Vincent SVS and SVR, Carriacou and Grenada North will now be considered further. If these arrivals are due to critical refraction at the Moho, the waves will have travelled part of the way at the upper mantle velocity. The nearest profiles for which the upper mantle velocity has been determined are in the Atlantic basin east of Barbados (Officer et al., 1959; section 1.4.1). Here the values are between 8.0 and 8.3km s^{-1}. The reduced travel times, $T - \Delta/8$, will give an estimate of the delay due to the passage of the waves through the crust below the shot and the receiving station. The delay beneath the station should be constant for all Moho arrivals provided the shots are at about the same azimuth from the station. Thus, differences in the reduced travel times observed at each station should largely reflect differences in the delay beneath the shot. The reduced travel times are given in Table 5.4. Those for Carriacou and St Lucia are significantly smaller than the corresponding values at the other stations, reflecting the smaller observed time intercepts (Table 5.1). Assuming that the delay time beneath a particular shot does not vary much with azimuth, these smaller reduced travel times can only be explained by a smaller delay time to the Moho beneath these two stations.

Applying the condition that the delay time beneath a shot is approximately the same for all ray paths, it is possible to estimate the relative delay times beneath the stations. To obtain estimates

Table 5.4 Reduced travel times (T- $\Delta/8$) - Tobago Trough

	B29	B30	B31	B32	B33
St Lucia South	-	7.07	-	6.41	6.06
St Vincent SVS	-	8.64	8.36	7.93	-
St Vincent SVR	9.07	8.94	8.46	8.13	-
Carriacou	7.09	7.17	6.94	6.93	-
Grenada North	7.59	8.19	7.76	-	-

of the actual delay beneath each station it is necessary to know the value of the delay below one station. The crustal structure beneath the arc is not well defined, but, using the thickness estimated in Chapter 4, 3.09 s is considered a reasonable value for the delay time for St Vincent SVR. The values obtained are :

	St Lucia	SVS	Carriacou	Grenada
station delay relative to SVR	-0.35	-1.45	-1.76	-0.68
station delay time (taking 3.09 s for SVR)	2.74	1.64	1.33	2.41

Using these station delay times, the average delay time for each shot can be estimated :

shot	B29	B30	B31	B32	B33
average shot delay time	4.76	5.05	4.78	4.79	4.75

These values are too small, the delays for shots 31-33 being smaller than the corresponding basement time-terms (Section 5.3). Also, the estimates of the Moho delay times for the stations vary too much to be acceptable. Thus, a simple crustal model cannot explain all these "Moho arrivals". The crustal structure appears to vary, not only in a direction perpendicular to the island arc, but also in the direction parallel to the visible structural trends. Clearly time-term analysis is unsuitable in this situation.

Direct modelling was seen to be the only means of achieving an interpretation of the deep structure of this region. However, even the simplest models contain too many variables to employ any sort of automatic optimisation procedure for ray-tracing. The author applied a trial-and-error technique to produce a model which best fitted the available data. Initially, the arrivals at St Lucia and St Vincent from shots 29 to 33 are considered. The delay times to the 7.0km s^{-1} layer at shots 29 to 33 increase away from the stations as the overburden thickens beneath the Barbados Ridge. Therefore, to account for the observed decrease in the overall crustal delay away from the stations, the lower crustal layer must thin away from the stations. It is found that with the simplest structure; a layer with an average velocity of 3.5km s^{-1} overlying a 7.0km s^{-1} layer dipping at 7^{o} to the east; a westerly dip on the Moho of about 15^{o} is needed to fit the observed apparent velocities. Introducing a wedge of 5.0km s^{-1} between the 3.5km s^{-1} layer and the 7.0km s^{-1}, with a dip of 1^{o} - 3^{o} to the west on its upper surface, has the effect of reducing the dip required on the Moho.

The model shown in Fig. 5.6 yields an apparent Moho velocity consistent with that observed at SVR from shots 29 - 32. Similar models fit the data from SVS and St Lucia South. However, these models are not consistent with other data. Firstly, the inclusion of a 5km s^{-1} layer in the overburden beneath Barbados requires a larger dip on the basement to account for the observed basement velocities in this region (section 5.3). Furthermore, the observed gravity suggests that the Moho becomes shallower under the centre of the Tobago Trough (Westbrook, 1973), so the Moho should dip to the east, rather than the west, beneath shots 29-33.

Fig. 5.6 Crustal model for the Tobago Trough which is consistent with the travel times observed from shots B29 - 32 at St Vincent SVR

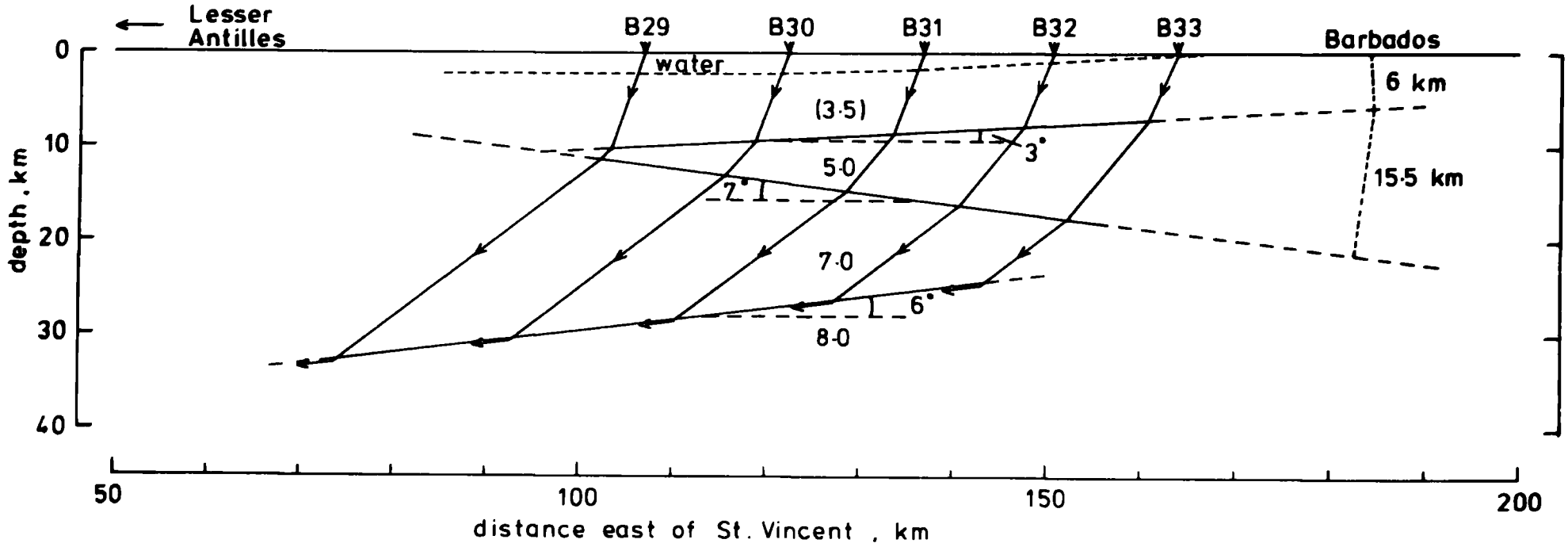
Lesser Antilles
B29
B30
B31
B32
B33
Barbados
water
(3·5)
5·0
7·0
8·0
3°
2°
6°
6 km
15·5 km
depth, km
0
10
20
30
40
50
100
150
200
distance east of St. Vincent , km

The measurement of these high apparent velocities at St Vincent and St Lucia suggests that an anomalously high uppermost mantle velocity may be present beneath the Tobago Trough. Reliable determinations of P_n velocities are sparse in island arc regions, mainly because the crust is thicker and there are greater accumulations of sediments which reduce the effectiveness of ship-to-ship refraction profiles in such regions. Several anomalously high velocities have been reported from the vicinity of island arcs : 8.9km s^{-1} beneath the north flank of the Aleutian Ridge (Shor, 1964); 8.3 - 8.5km s^{-1} below the Havre Trough (behind the Kermadec Ridge) and South Fiji Basin (Shor et al., 1971a); 8.3 - 8.6km s^{-1} on the ocean side of the Puerto Rico trench (Officer et al., 1959). More reliable measurements in normal oceanic regions (e.g. Raitt, 1956) show a maximum value of about 8.7km s^{-1}. A sub-Moho velocity between 8.7 and 9.0km s^{-1} in the Tobago Trough would make it possible to interpret the observed apparent velocities without requiring an unreasonable dip on the Moho. It is a pity that these velocities were not reversed by more distant arrivals at the Barbados stations, so that an estimate of the true velocity could be determined.

The apparent ? P_n velocities observed at Carriacou and the Grenada North station are substantially lower than those observed on St Vincent and St Lucia. If it is assumed that the strike of the 7.0km s^{-1} refractor beneath the Tobago Trough is at right angles to the shot line, and that its true dip is 7.2° (Table 5.2), then the apparent dip in the direction of Carriacou will be about 5.5°. Assuming the structure beneath shots 29 - 32 to consist of the 7.0km s^{-1} layer overlain by a layer of constant average velocity 3.5km s^{-1}, then the 7.6km s^{-1} velocity at Carriacou can be explained by refraction in an

8.0km s^{-1} layer dipping at about 7^{o} to the west. Including a wedge of 5km s^{-1} material, as above, will require a dip on the Moho of about 3.5^{o} to the east. This dip is more consistent with the gravity interpretation (Westbrook, 1973) but, again, there is no evidence for a 5km s^{-1} layer in this region. The depth to the Moho cannot be determined unambiguously as a reliable estimate of the delay beneath Carriacou is not available. The T- $\Delta/8$ values (Table 5.4) appear to be too small to allow a reasonable crustal thickness beneath both shot and station. This appears to rule out the possibility that these arrivals are Moho refractions, but the observed apparent velocity cannot be obtained by refraction in an intra-crustal layer without contradicting the earlier interpretation.

P_n arrivals received at Grenada North from shots 23 - 27 would have passed through a different crustal structure beneath the shots than the arrivals from shots 28 - 31. The basement beneath shots 23 - 27 has been identified as a layer of velocity 6.3km s^{-1} (section 5.3), and is assumed to overlie the 7km s^{-1} layer defined beneath the island arc. Considering this variation in upper crustal structure across the Tobago Trough, it may be misleading to calculate a single apparent velocity for the arrivals at Grenada from shots 23 - 31. The apparent velocities calculated for the two regions are 7.2 ± 0.6km s^{-1} (shots 23 - 28) and 7.8 ± 1.0km s^{-1} (shots 28 - 31). The closer arrivals could be P^{*} arrivals, but the reduced travel times, T- $\Delta/8$, for the arrivals from shots 28 - 31 received at Grenada North are significantly larger than those for the corresponding arrivals at Carriacou, and the interpretation of these as P_n arrivals is more convincing.

Taking the arrivals from shots 23 - 31 at Grenada North to be P_n arrivals, an estimate of the crustal thickness beneath each shot can be made : Subtracting an estimated station delay time of 3.2 s from the reduced travel time, $T - \Delta/8$, will give estimates of the shot delay times and these can be used to find the depth to the Moho, taking into account the effect of the upper crustal structure determined from time-term analysis (section 5.3) and estimating the position of the P^* refractor under the flanks of the island arcs. The Moho depths thus determined for shots 23 - 25 and 27 - 31 are indicated in Fig. 5.7 for comparison with the depths computed by Westbrook (1973) from gravity measurements and the available seismic control. The Moho 'structure' estimated from the delay times should, rigorously, be displaced between 10 and 20km towards the west, along the section, because the critically refracted wave from each shot has travelled this distance towards the station before reaching the Moho. The early arrival from shot 29 causes the estimated crustal thickness to be smaller beneath this shot. The gravity model shows an area of thinner crust below shot 26, but this is too far to the west of shot 29 for there to be a correlation between these two 'structures'.

If the high velocity arrivals received at stations from Grenada to Martinique are P_n arrivals, an interesting pattern is observed : The apparent velocities observed at the stations on St Vincent and St Lucia, which are almost in line with the shot line, are significantly higher than those observed at Grenada, Carriacou and Martinique, the ray paths to these islands being at large angles to the shot line. The high P_n velocity suggested by the arrivals travelling westwards along the shot line is not supported by the

velocities observed to the north and south. Therefore, a marked velocity anisotropy may exist in the upper mantle beneath the Tobago Trough.

Following the original hypothesis of velocity anisotropy (Hess, 1964), workers in the Pacific Ocean have found convincing evidence of velocity anisotropy in the upper mantle (Raitt et al., 1971). They observed azimuthal variations in P_n velocity with an amplitude of up to 8% of the mean velocity, the maximum velocity being observed in a direction normal to the magnetic lineations. The anisotropy is due to the preferred orientation of anisotropic olivine crystals within the upper mantle, caused by some process of flow. This effect might also be expected within the upper mantle in the vicinity of island arcs where magma is rising through the mantle. Thus, some variation in P_n velocity with azimuth beneath the Tobago Trough would not be surprising. However, the implied variation is more than 10% which is significantly more than the maximum variation found by Raitt et al. (1971). The velocities are not determined with sufficient accuracy to go further than to state that they are consistent with a marked degree of anisotropy.

5.5 Discussion

The major results from this chapter are :

(1) The crustal layer beneath the western slopes of the Tobago Trough has a velocity of about 6.3km s^{-1} and dips at about 5^{o} to the east. This layer is correlated with the 6.1 - 6.2km s^{-1} layer determined beneath line A.

(2) Beneath the central Tobago Trough and Barbados Ridge the crustal layer has a velocity of about 7.0km s^{-1} and is at depths of about 11 and 20km beneath the centre of the Tobago Trough and Barbados, respectively. These results are in general agreement with the structure determined from profiles G - 7 and 55 (Fig. 1.5).

(3) The seismic records show no evidence for a layer of velocity about 5km s^{-1} overlying the 7km s^{-1} layer below the Tobago Trough.

(4) A number of weak arrivals recorded at stations along the island arc from the more distant shots indicate apparent velocities between 7.5 and 8.9km s^{-1}, but these have not been positively identified as P_n arrivals. If they are all Moho refractions, a marked velocity anisotropy is indicated.

Figure 5.7 summarises the crustal structure of the Tobago Trough as determined from seismic and gravity work.

The crust beneath the Tobago Trough has been shown to consist of a single layer with a velocity of 7.0km s^{-1} and is, therefore, unlike the two-layered Caribbean crust found beneath the Venezuela Basin and Grenada Trough by Officer et al. (1959). The crust of the Tobago Trough, although considerably thickened, is similar to the Atlantic crust in its broad structure. Thus, from the seismic results, it is suggested that the crust beneath the Tobago Trough may have been part of the Atlantic plate, before the commencement of subduction of the Atlantic plate beneath Barbados. This conclusion, which is supported by other evidence, has important implications regarding the tectonic development of the eastern Caribbean and will be discussed in detail in Chapter 8.

Fig. 5.7 Crustal section across the Tobago Trough

Legend

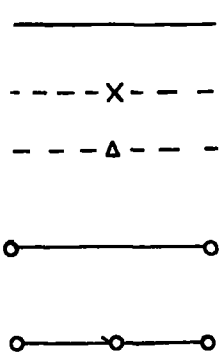

basement from reversed profile interpretation

,, ,, time-term ,,

Moho depths indicated by delay times observed at Grenada North

'Moho' from optimized gravity model (Westbrook, 1973)

inferred position of P* refractor

profiles 22 and G-7 : after Ewing et al. (1957)

profile 55 : after Edgar et al. (1971)

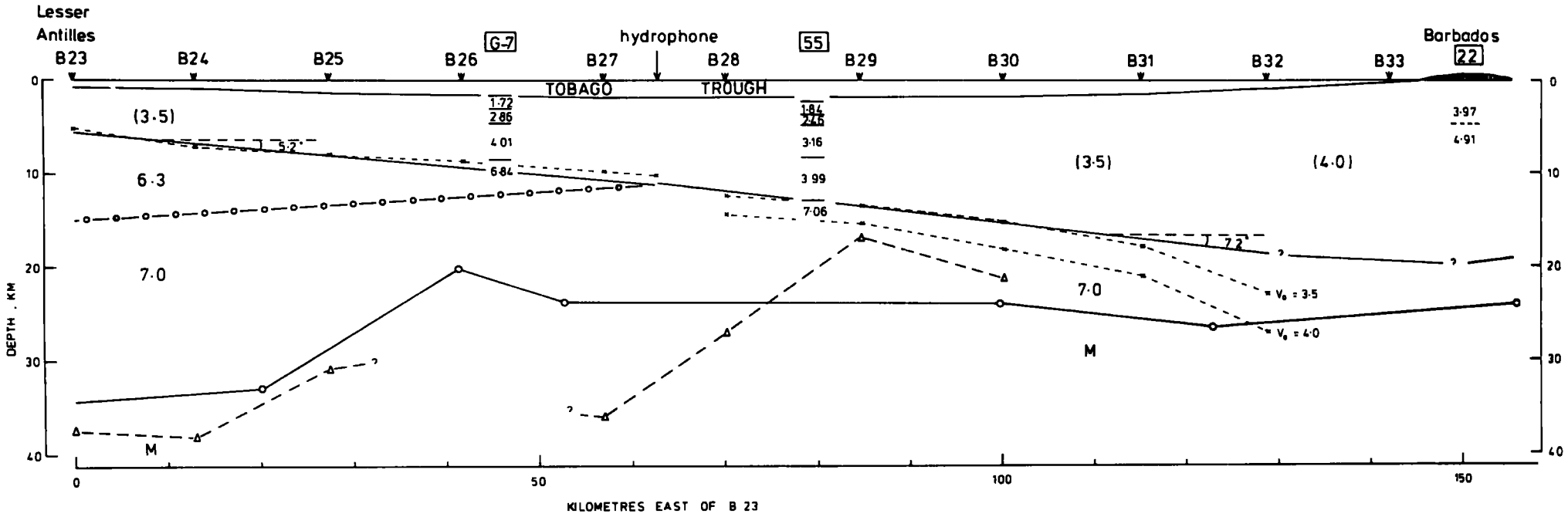
Lesser
Antilles
B23
B24
B25
B26
G-7
B27
hydrophone
B28
55
B29
B30
B31
B32
B33
Barbados
22
TOBAGO
TROUGH
(3·5)
1·72
2·86
4·01
6·84
5·2
6·3
7·0
1·84
2·76
3·16
3·99
7·06
7·2
(3·5)
(4·0)
3·97
4·91
7·0
M
M
V_0 = 3·5
V_0 = 4·0
DEPTH . KM
0
10
20
30
40
50
100
150
KILOMETRES EAST OF B 23

Chapter 6

INTERPRETATION OF FIRST ARRIVAL DATA FROM THE GRENADA TROUGH AND AVES RIDGE

6.1 Introduction

The western part of line B was run almost due west from just north of St Vincent across the Grenada Trough to the Aves Ridge (Fig. 2.1). Line C ran 316km southwards from Aves Island. The results obtained from these two lines were disappointing, mainly because the 300lb charges were found to be too small to allow arrivals from shots along line C and the westernmost shots of line B to be observed at the stations on the Lesser Antilles islands. It had been hoped that distinct arrivals would be recorded up to 300km from the shots, but it was found that no arrivals were received from even the nearest part of line C, at ranges of just under 200km. First arrivals were observed at the Aves Island station (LASP 8) from shots C1 - C8 and at stations from Grenada to Martinique from shots B20 - B7 (Fig. 2.1). These lines were not reversed because of the lack of hydrophone stations in the centre of the Grenada Trough and in the middle and south of line C on the Aves Ridge. The interpretations of the observed arrivals are therefore tentative.

To obtain any definite interpretation of the observed arrivals it was necessary to compare the LASP results with previous refraction studies in the area. Only one refraction profile has been located in the central part of the Grenada Trough prior to LASP; this being profile 29 (Figs. 1.5 and 6.1) described by Officer et al.(1959).

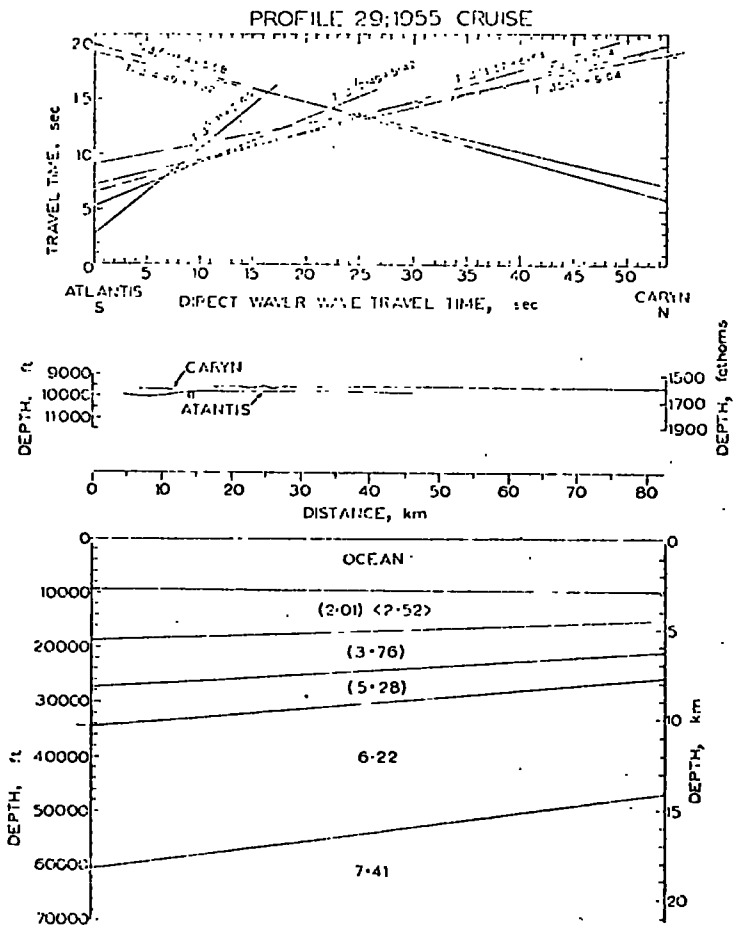

Fig. 6.1 Profile 29 (after Officer et al., 1959)

The highest velocity observed in this profile was 7.4km s^{-1} which Officer correlated with the lower crustal layer of the Venezuela Basin. The 7.4km s^{-1} layer is overlain by a 6.22km s^{-1} layer, the interface being at a depth of 14 - 18km. Edgar et al. (1971) described two refraction profiles across the southern part of the Grenada Trough (profiles 62 and 63, Fig. 1.5). These both showed thick sediment layers and only profile 63 penetrated to the crustal layer; a layer of velocity 6.3km s^{-1} at a depth of 10km beneath the eastern end. A number of profiles were run across the Aves Ridge in 1955-6 and these are discussed in section 6.3 in relation to the arrivals at the Aves Island station.

6.2 Results from Line B (West)

The stacked records from shots B20 - 6 at the St Vincent SVS station are shown in Fig. 6.2. These are typical of the records seen at the three St Vincent stations and the stations on Carriacou and St Lucia South. The first arrivals from shots B20 - 15 are distinct and define two apparent velocities. Shots 14 and 12 show no first arrivals that can be 'drawn' out of the noise by filtering and a weak sequence of later arrivals. Evidence of a high velocity first arrival phase is seen from shots B11 - 8. The cause of the sudden reduction in first arrival amplitudes beyond shot 15 is unknown. Water depths of about 3km underlie shots B17 - 9 so there is no reason why less energy should be transmitted into the substrata beneath shots 14 and 12 than beneath the nearer shots. If a step in one of the crustal layers exists between shots 15 and 14, this would have the effect of diffracting the head waves and causing delays and dispersion

Fig. 6.2 Stacked records of shots B20 - 6 at St Vincent SVS

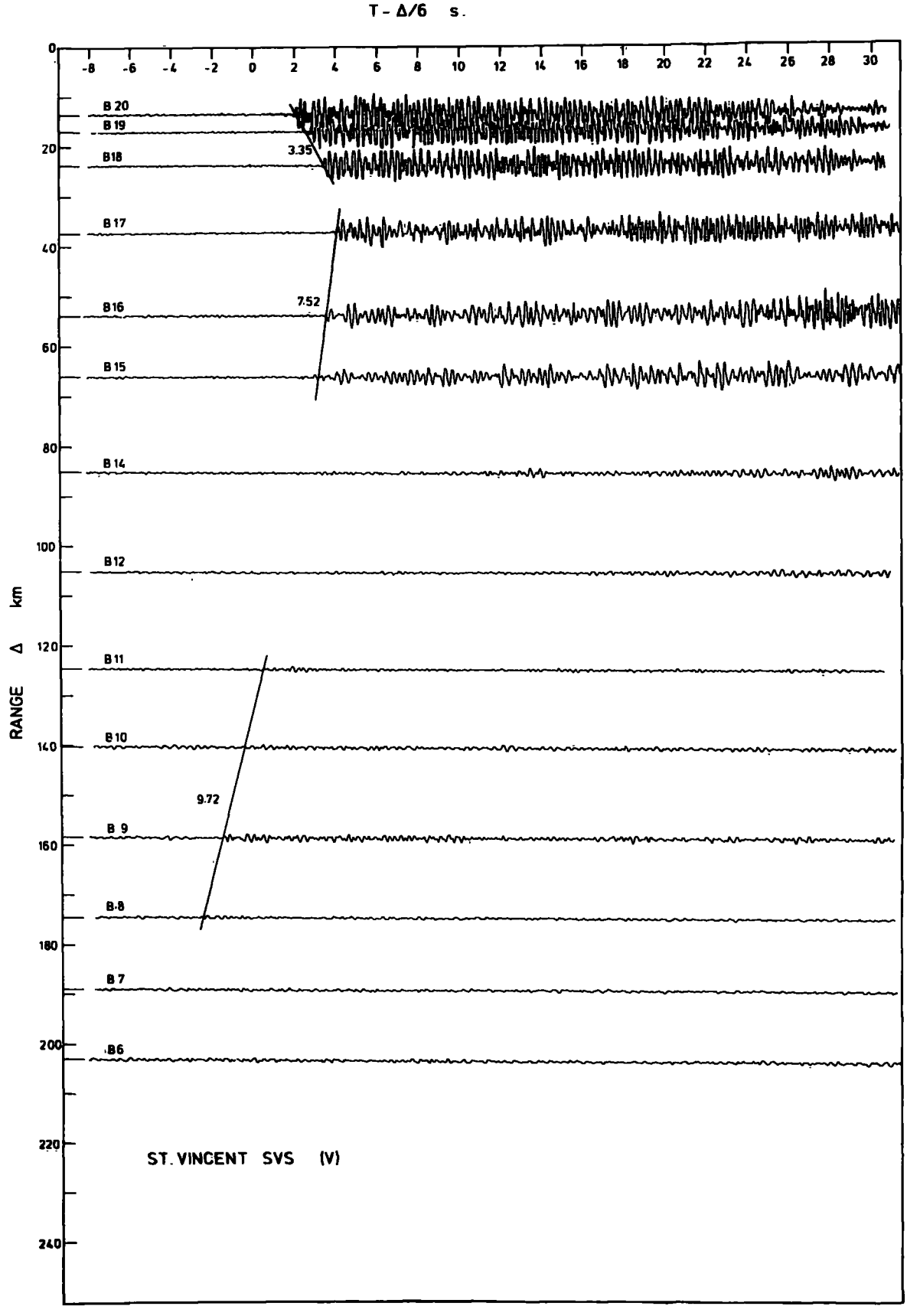
T - Δ/6 s.
-8 -6 -4 -2 0 2 4 6 8 10 12 14 16 18 20 22 24 26 28 30
0
20
40
60
80
100
120
140
160
180
200
220
240
RANGE Δ km
B 20
B 19
B18
B 17
B16
B 15
B 14
B12
B11
B10
B 9
B8
B 7
B6
3.35
7.52
9.72
ST. VINCENT SVS (V)

of energy. This is a likely explanation, but seismic reflection records (Kearey, 1973) show no perturbation of the seabed or sediment layers in this region, which might reflect such a step. Also, the Bouguer gravity anomaly across this region shows no evidence for a feature of this nature (Fig. 1.8). The high velocity phase observed from the more distant shots may represent Moho refractions.

The reduced travel time graphs for the first arrivals from shots 20 - 7 at four of the arc stations are shown in Fig. 6.3 and a summary of the least squares apparent velocities observed at all the arc stations is given in Table 6.1. An impressive feature of all the graphs is the large increase in reduced travel time over the flanks of the Lesser Antilles ridge (shots 20 - 17). This is reflected in the low apparent velocities observed at the north St Vincent stations. These low velocities can be explained as being caused by refraction in a near-horizontal layer of consolidated sediments. However, it is strange that these 'sediment' refractions should remain first arrivals out to 25km range. Also, at SVT (Fig. 6.3), there is an increase in travel time between shots 20 and 19 even though their ranges are almost the same. The ranges of shots 17 - 20 from the three St Vincent stations and St Lucia South are within the typical distance range of P_g first arrivals along line A. It is considered more likely, therefore, that the arrivals from these shots have been refracted in the 6.2km s^{-1} layer, defined from line A, and that this layer dips sharply away from the ridge crest. Kearey (1973) observed a sharp gravity gradient change at the eastern margin of the Grenada Trough which he interpreted in terms of a rapid thinning of the sediments towards the Lesser Antilles. He estimated the basement slope to be 6° at latitude $13^{\circ}24'$ N and 11° at latitude $13^{\circ}34'$ N.

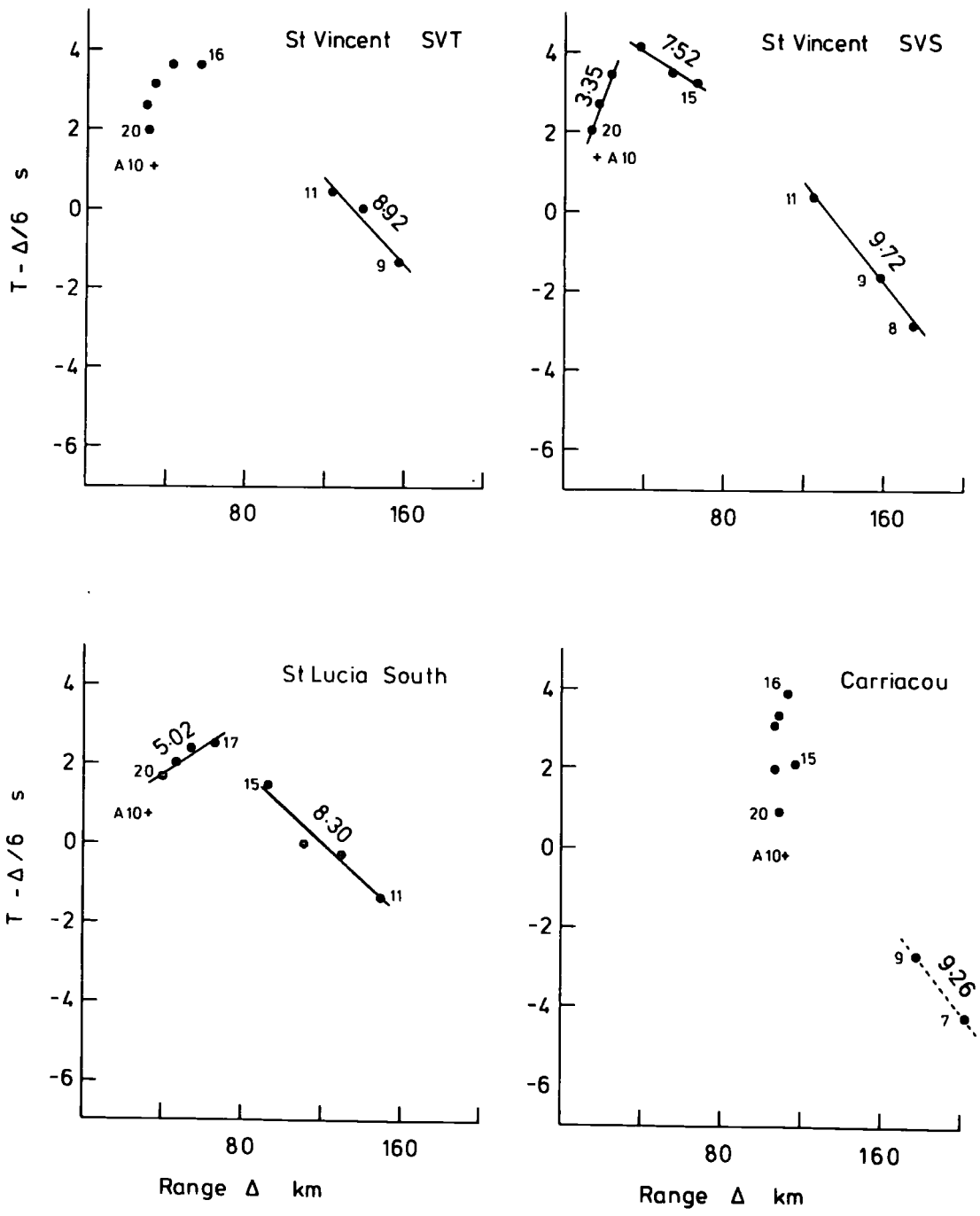

Reduced travel time graphs – Line B (west) shots 1 - 20

Fig. 6.3

Table 6.1 Least squares fit of straight lines to travel-time data from line B (west)

Station	Shots	Velocity	Time Intercept	No. of observations
22 Martinique OBM	12 - 1	7.79 ± 0.07	4.84 ± 0.25	8
2 St Lucia South	20 - 17	5.02 ± 0.19	0.48 ± 0.40	4
	15 - 11	8.30 ± 0.60	5.57 ± 1.06	4
13 St Vincent SVR	20 - 18	3.75 ± 0.19	0.50 ± 0.27	3
	17 - 15	7.60 ± 0.44	5.17 ± 0.43	3
	11, 9	(8.9)	(6.8)	2
12 St Vincent SVS	20 - 18	3.35 ± 0.27	0.35 ± 0.44	3
	17 - 15	7.52 ± 0.40	5.38 ± 0.38	3
	11, 9, 8	9.72 ± 0.32	8.36 ± 0.52	3
11 St Vincent SVT	11 - 9	8.92 ± 0.99	7.34 ± 1.75	3
3 Carriacou	9, 7	(9.3)	(7.7)	2

A simple calculation was made to find the approximate increase in the depth to the 6.2km s^{-1} layer beneath shots 20 - 16, relative to its depth beneath shot A10, which would account for the increased delay times observed at SVT and St Lucia South. The average velocity in the sediments above the 6.2km s^{-1} layer along the Lesser Antilles is about 3.5km s^{-1} (Officer et al., 1959). Assuming this to be the average velocity of the overburden, the increased thicknesses required are :

	B20	B19	B18	B17	B16
St Vincent SVT	3.3	6.1	8.5	10.8	10.9
St Lucia South	4.1	5.8	7.4	8.4	-

From time-term analysis, the depth to the 6.2km s^{-1} refractor beneath shot A10 was found to be 2.9km (Chapter 4). The depth to the 6.22km s^{-1} refractor below the southern end of profile 29 is 10.5km. The difference in these depths, 7.6km, is smaller than the largest of those estimated for shots 20 - 16. Nevertheless, the values are not unreasonable. These results indicate that the dip on the 6.2km s^{-1} refractor, in the direction of the shot line, varies between 10^{o} and 20^{o}. This is considerably steeper than the basement slopes on the eastern flank of the Lesser Antilles ridge. However, this steeper slope is supported by bathymetric, seismic reflection and gravity studies (Kearey, 1973).

The travel times from shots B17 - 20 to the three St Vincent stations and both St Lucia stations were included in the P_g time-term solution A for line A (Chapter 4). The effect of this was to constrain the velocity and station time-terms to those found

from the travel times along line A. The shot time-terms and corresponding overburden thicknesses were :

Shot	A10	B20	B19	B18	B17
No. of observations	4	5	5	2	2
time-terms (s)	1.29 ± 0.10	2.04 ± 0.03	2.69 ± 0.10	3.26 ± 0.13	4.21 ± 0.08
water depth (km)	1.39	1.96	2.28	2.56	2.81
sed.thickness (km)	1.5 ± 0.4	3.0 ± 0.1	4.7 ± 0.4	6.3 ± 0.5	9.3 ± 0.3
depth to basement (km)	2.9	5.0	7.0	8.9	12.1

These results imply a dip of about 11^{o} on the refractor along line B. A time-term solution of the arrivals from shots A10 and B17 - 20, alone, was attempted. The least squares velocity of the solution was 6.09 ± 0.15km s^{-1}. The relative values of the shot time-terms were similar to those of the previous solution but there was more variation in the station time-terms, those for the St Lucia stations being smaller than those for St Vincent. Unfortunately, the shot-station pattern was such that a reliable estimate of the constant α, required to give the shot and station time-terms their correct relative values, could not be made. If the time-term for shot A10 was assumed to be the same as that from the previous solution, the time-terms for shots B20 - 17 were 2.11 ± 0.06, 2.75 ± 0.04, 3.43 ± 0.07 and 4.26 ± 0.09 s, respectively. These values compare well with those from the previous solution.

The arrivals at Carriacou from shots B20 - 15 were emergent and it was difficult to 'pick' the first onset with much confidence. The travel times (Fig. 6.3) indicate larger delays, away from the ridge,

than those seen at the other stations. These shots are at distances of between 106 and 117km from Carriacou, which is about the range of the crossover distance between P_g and P^* first arrivals observed along the arc. Three explanations of these arrivals seem plausible :

(1) They are head waves from the 6.2km s^{-1} refractor and the delay is due to a thickening of the sediment overburden.

(2) They are head waves from the 7.0km s^{-1} refractor and the delay is due to a thickening of the sediment overburden.

(3) As (2), but with a thickening of the 6.2km s^{-1} layer also.

Explanation (3) is rejected because a deepening of the lower crustal layer is not expected beneath the Grenada Trough. The delays are so large that an unreasonably large increase in the thickness of the overburden would be required, using either of explanations (1) and (2). It is concluded that the first onset had not been correctly identified from the Carriacou records.

Apparent velocities of 7.5 - 7.6km s^{-1} for the arrivals from shots 15 - 17 at SVS and SVR are given in Table 6.1. However, from the reduced travel time graph (Fig. 6.3), it is not easy to decide whether the arrival from shot 17 is a continuation of the phase defined by shots 18 - 20, or whether it is related to the higher velocity phase indicated by shots 15 and 16. It seems probable that the arrivals from shots 15, 16 and, perhaps, 17, at SVS and SVR are caused by refraction in the lower crustal layer of the Grenada Trough (i.e. the 7.4km s^{-1} layer defined in profile 29, Fig. 6.1). To prove this hypothesis it is necessary to know the path followed by the waves between shot and station.

It is not known whether the 7.4km s^{-1} refractor beneath the Grenada Trough is continuous with the 7.0km s^{-1} refractor under the Lesser Antilles or where the velocity change occurs. If it is assumed that the refractor is continuous, and that the velocity change occurs fairly sharply at the edge of the Grenada Trough, the reduced travel time $T - \Delta/7.4$ will give an estimate of the sum of the delay times to the refractor at each end of the ray path. Profile 29 (Fig. 6.1) crosses the LASP shot line B between shots 10 and 11 and the depth to the 7.4km s^{-1} layer, here, is about 16.25km. Given the velocity-depth structure shown in Fig. 6.1, the delay to the 7.4km s^{-1} layer is about 3.2 s. The apparent velocities observed at SVS and SVR are greater than 7.4km s^{-1} suggesting a slight dip to the east on the refractor in the region of shots 15 to 17. Thus the depth to the refractor might be greater than 16.25km beneath these shots. A depth of 14km to the 7km s^{-1} refractor below St Vincent is taken as this is the average value calculated in Chapter 4. The delay time to the 7km s^{-1} refractor is therefore estimated to be 1.5 s. The sum of the delays to the 7 - 7.4km s^{-1} refractor beneath profile 29 and St Vincent is, thus, about 4.7 s. This can be compared with the observed reduced travel times :

SVR		SVS	
Shot	$T - \Delta/7.4$	Shot	$T - \Delta/7.4$
15	5.00	15	5.31
16	4.84	16	5.15
17	5.08	17	5.35

The discrepancy between the 'observed' and calculated delay times can be explained by a slight variation in depth to the 7.4km s^{-1} layer beneath shots 15 to 17, an increase in the depth of the 7km s^{-1} layer beneath St Vincent and/or a slower average velocity along the refractor. Thus, refraction in the 7.4km s^{-1} layer can explain these arrivals.

A difference of about 0.3 s is noted between the delay times at the two stations. This is surprising as their P_g time-terms are similar and a large variation in the depth of the P^* refractor is not likely over such a short distance.

The arrivals which define the apparent velocities between 8.3 and 9.7km s^{-1} (Table 6.1) are weak and predominantly emergent and are, therefore, very difficult to 'pick' from the records (Fig. 6.2). This, together with the fact that no more than three shots define the higher velocity at each station, renders the determination of the velocity and time intercept inaccurate. The values obtained differ considerably from station to station and it is impossible to interpret these arrivals in any detail. A few of the arrivals are sufficiently convincing to indicate the presence of a higher velocity refractor, presumably the Moho, beneath the 7.4km s^{-1} refractor in the western Grenada Trough. If these arrivals are Moho refractions, they may indicate anomalously high P_n velocities and a marked degree of anisotropy under the Grenada Trough, as was suggested for the Tobago Trough (Chapter 5).

Dorel (personal communication) has found arrivals at the station OBM on Martinique from all the shots 1 - 20, which are at distances of 140 - 300km. The travel times from shots 12 - 1, inclusive, indicate an apparent velocity of 7.8km s^{-1}. The reduced travel times, $T - \Delta/8$, for the arrivals from the Grenada Trough, range between 4.8 and 5.6 s (Fig. 6.4). The velocity is consistent with these arrivals being Moho refractions, but the reduced travel

Fig. 6.4 Reduced travel time graph for arrivals from shots B20 - 1 and A7 - 11 at Martinique OBM

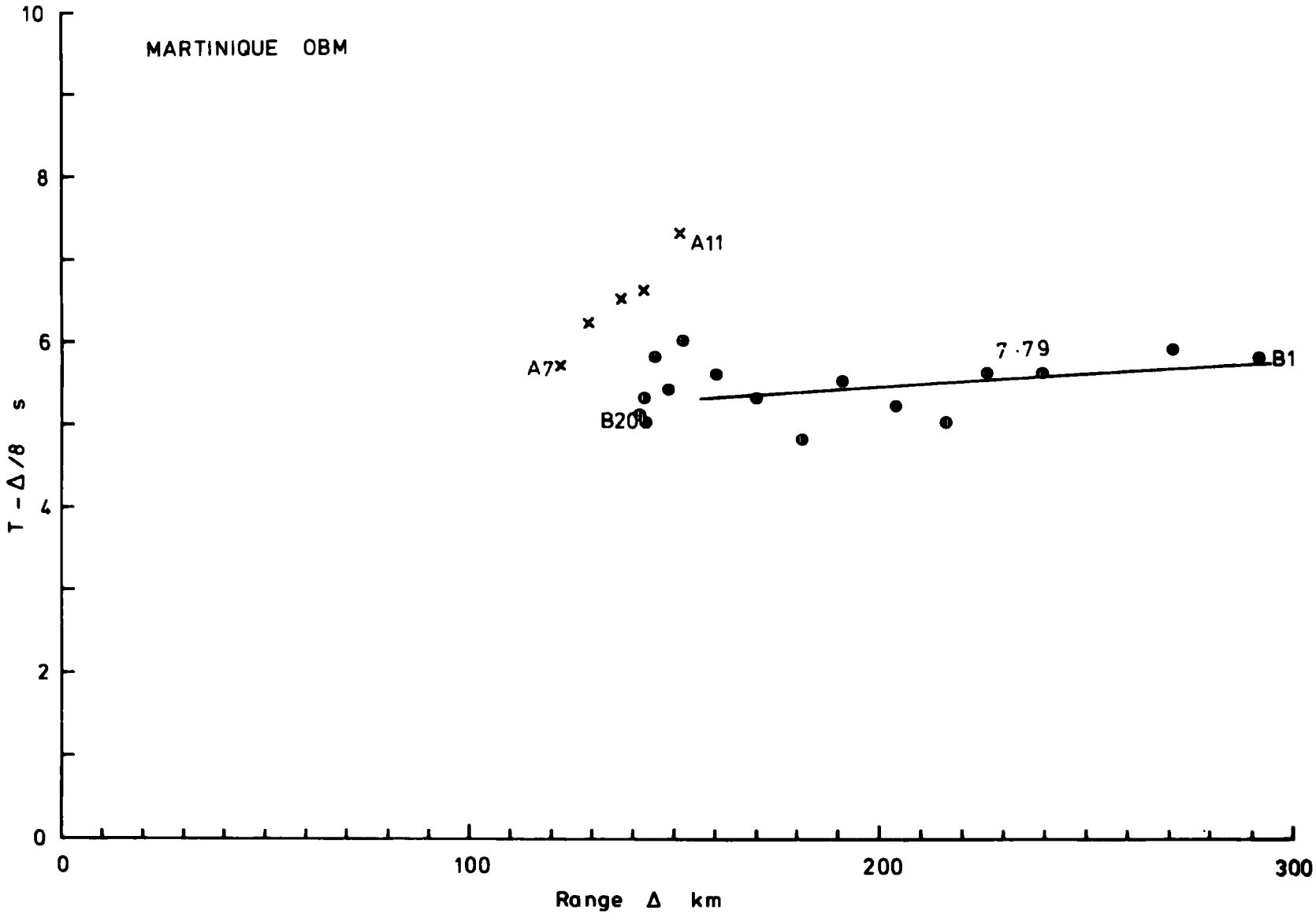
MARTINIQUE OBM
A11
A7
B20
7·79
B1
T - Δ/8 s
Range Δ km
0
2
4
6
8
10
0
100
200
300

time values are rather small. For a P_n velocity of 8.0km s^{-1}, a reasonable estimate of the delay time to the Moho beneath station OBM is 3.1 s (sections 4.5 and 5.4). This would imply a maximum delay time to the Moho beneath the Grenada Trough of 2.5 s, which is less than the delay time due to the 7.4km s^{-1} layer calculated from profile 29 (Fig. 6.1). However, if the P_n velocity is increased, it is found that the reduced travel time, $T - \Delta/V$, increases more than the consequent increase in the crustal delay times. The 'P_n' travel times from shots B10 - 16 to OBM are found to be consistent with the crustal thickness, as determined by gravity interpretations for the Grenada Trough (Kearey, 1973), if an upper mantle velocity of 8.6km s^{-1} is assumed. Similarly, a velocity of 8.7km s^{-1} will allow the arrivals from shots B7 - 1 to be explained in terms of refraction at the Moho below the Aves Ridge. However, for any reasonable P_n velocity, the reduced travel times from shots B17 - 20 (Fig. 6.4) are too small for these arrivals to be Moho refractions, unless the crust beneath the Lesser Antilles is considerably thinner than indicated by the observations along line A (Chapter 4). They are, presumably, waves refracted in the lower crustal layer along the arc.

6.3 Results from Line C

The stacked records from the Aves station (LASP 8) for shots C1 - 8 are shown in Fig. 6.5. It can be seen from the records that the station was very noisy. This was due to the exposed nature of the island and the proximity of the sea. Clear first arrivals can be traced across the first five records only. No second arrivals that are persistent over consecutive records can be seen. The first arrivals

Fig. 6.5 Stacked records of shots C1 - 8 at the Aves Island station

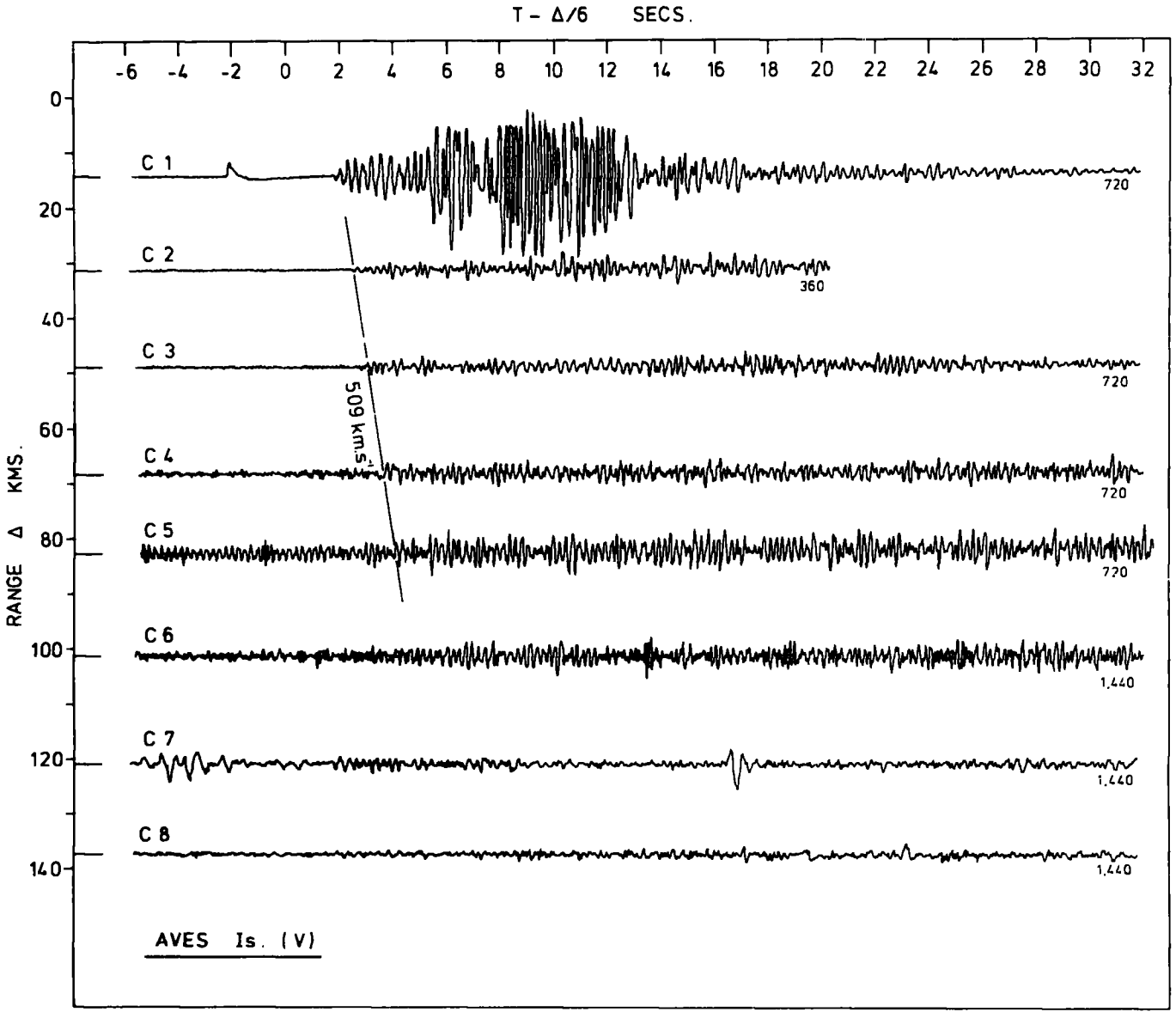
T - Δ/6 SECS.
-6 -4 -2 0 2 4 6 8 10 12 14 16 18 20 22 24 26 28 30 32
RANGE Δ KMS.
0
20
40
60
80
100
120
140
C 1
720
C 2
360
C 3
720
509 kms⁻¹
C 4
720
C 5
720
C 6
1,440
C 7
1,440
C 8
1,440
AVES Is. (V)

from shots C2 - 5 define an apparent velocity of 5.09 $\pm$ 0.02km s^{-1} with a time intercept of 1.68 $\pm$ 0.04 s. The first arrival for shot C1 is probably a refraction from a sediment layer.

In order to determine the significance of the observed apparent velocity it is necessary to consider the results of other seismic refraction work on the Aves Ridge. A small-scale seismic refraction survey was conducted across Aves Island in 1970 (Gallovich and Aguilera, 1970) which defined four layers with velocities of 1.5 - 1.6, 2.3 - 2.5, 2.9 - 3.4 and 4.0 - 4.5km s^{-1}, the depth of the highest velocity layer being about 70m. They concluded that the upper layers represented unconsolidated to consolidated sediments and that the 4.0 - 4.5km s^{-1} layer was composed of basaltic lavas or metamorphics. Four profiles from the Aves Ridge were presented by Officer et al. (1959). These were profiles 10, 22, 23, 30 (Fig. 1.5). Profiles 22 and 30 were reversed and penetrated to the 'basement' while profiles 10 and 23 were shorter lines. The velocity-depth structures determined for profiles 22, 23 and 30 are shown in Fig. 6.6.

The 5.09km s^{-1} velocity observed at the Aves station is closest in value to the unreversed velocity of 4.98km s^{-1} observed on profile 22. However, this layer gave first arrivals only over a restricted distance range of about 15km, whereas the first arrival at the Aves station persists for at least 85km. If the refractor beneath Aves Island has a true velocity of 5.1km s^{-1}, the time intercept gives a depth of about 4.1km to this layer which is within the range of depths of the 4.98km s^{-1} refractor in profile 22.

Alternatively, the observed velocity may be correlated with the velocities of 6.15 and 6.24km s^{-1} observed in profiles 30 and 22, respectively. If the true velocity of the refractor is 6.2km s^{-1}

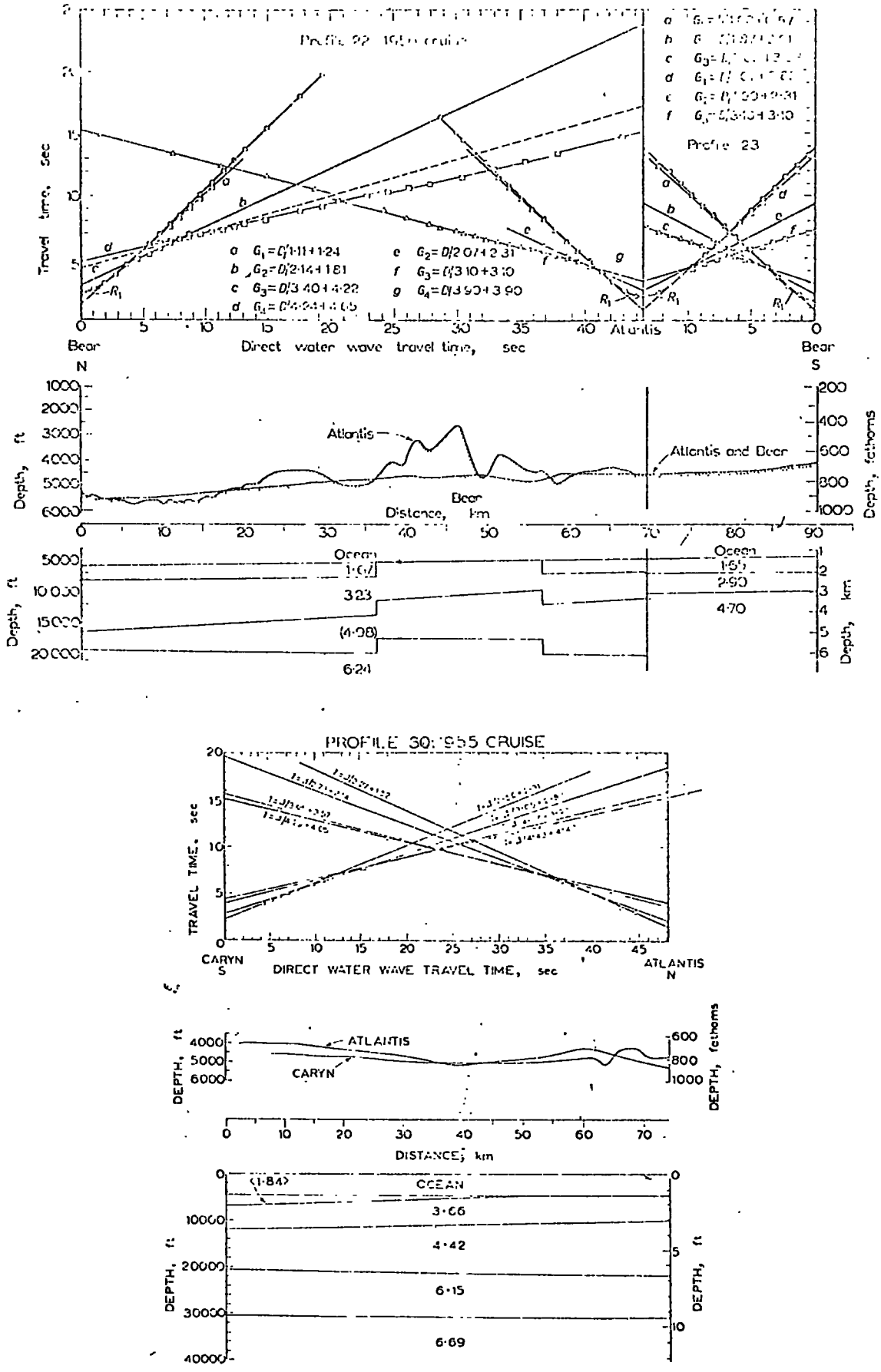

Fig. 6.6 Profiles 22, 23 and 30

(after Officer et al., 1959)

then, for an average overburden velocity of 4km s^{-1}, the refractor will have a dip of about 11^{o} southwards along line C. This dip is severe and implies a considerable depth to the refractor below C5. If the overburden velocity is 3.5km s^{-1} the required dip is about 9^{o}. The time intercept indicates a depth of 4.4 or 3.6km to this '6.2km s^{-1}' refractor beneath Aves Island, assuming an average overburden velocity of 4km s^{-1} or 3.5km s^{-1}. respectively. These depths are significantly smaller than the depths calculated from profiles 22 and 30 to the 6.1 - 6.2km s^{-1} layer (Fig. 6.6). The first interpretation is preferred. The velocity of about 5km s^{-1} may represent metamorphic rocks, basic lavas, or an igneous intrusion.

6.4 Summary

Interpretation of the travel time data from line B (west) and line C has been hampered by the small quantity of the data and its poor quality. However, the following conclusions have been supported from the data :

(1) The 6.2km s^{-1} layer defined beneath the Lesser Antilles Ridge slopes at an angle of 10^{o} - 15^{o} towards the Grenada Trough and is probably continuous with the 6.22km s^{-1} layer found beneath profile 29 (Fig. 6.1).

(2) Arrivals from shots B15 - 17 at two of the St Vincent stations are consistent with refraction in the 7.4km s^{-1} layer defined by profile 29, if this refractor is continuous with the 7.0km s^{-1} refractor found under line A.

Fig. 6.7 Diagrammatic crustal section across the Grenada Trough and Aves Ridge

Legend

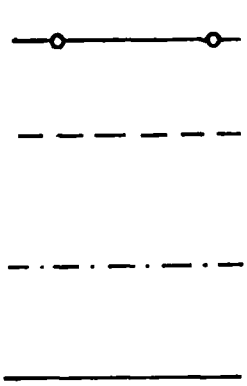

position of 6.2km s^{-1} refractor from time-terms for shots B17 - B20 and A11.

inferred position of 6.2km s^{-1} refractor and 7.0 - 7.4km s^{-1} refractor beneath the Grenada Trough

'basement' ($V < 4$km s^{-1}) used in the interpretation of a gravity profile at 13°24'N by Kearey (1973)

'Moho' computed for 100% isostatic compensation relative to a standard crustal thickness of 35km for the gravity profile at 13°24'N

profiles 24 and 29 : after Officer et al. (1959)

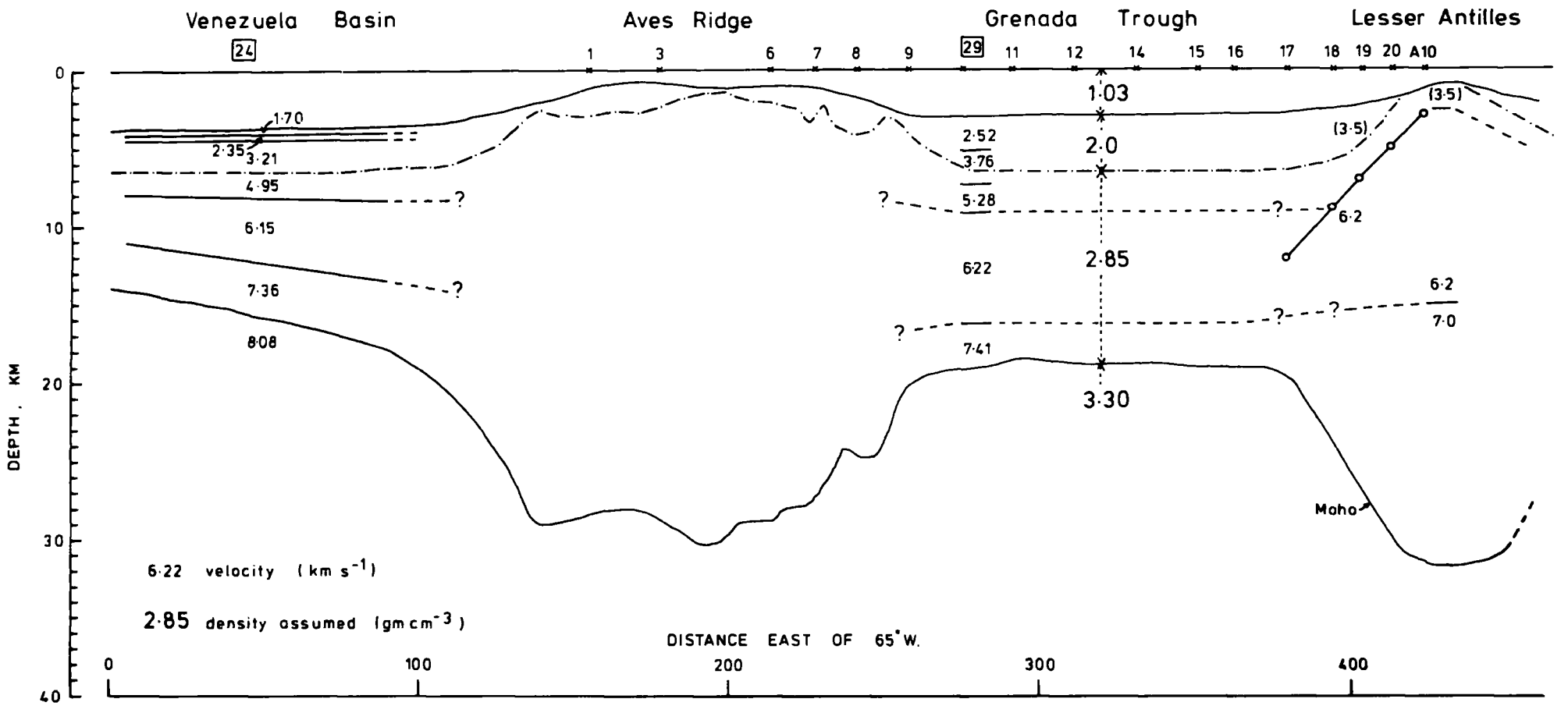
Venezuela Basin
Aves Ridge
Grenada Trough
Lesser Antilles
24
29
1 3 6 7 8 9 11 12 14 15 16 17 18 19 20 A10
1·70
2·35
3·21
4·95
6·15
7·36
8·08
2·52
3·76
5·28
6·22
7·41
1·03
2·0
2·85
3·30
(3·5)
(3·5)
6·2
6·2
7·0
Moho
DEPTH, KM
0
10
20
30
40
6·22 velocity (km s⁻¹)
2·85 density assumed (gm cm⁻³)
DISTANCE EAST OF 65°W.
0
100
200
300
400

(3) A few arrivals from the more distant shots along line B indicate the presence of a higher velocity refractor beneath the 7.4km s^{-1} layer. This supports the conclusion of Officer et al. (1959) that the 7.4km s^{-1} layer is equivalent to the lower crustal layer in the Venezuela Basin and not an anomalously low-velocity upper mantle. Further support for this conclusion is provided by interpretations of gravity measurements in this region (Kearey, 1974).

(4) The travel times of possible Moho refractions from shots B16 - 1 to station OBM (Martinique) are consistent with the crustal thicknesses beneath the Grenada Trough and Aves Ridge as determined from gravity interpretation (Kearey, 1973).

A diagrammatic east-west crustal section across the Grenada Trough and Aves Ridge is shown in Fig. 6.7.

Chapter 7

SHEAR-WAVE VELOCITIES AND POISSON'S RATIO

7.1 S-wave Velocity Measurements

The previous three chapters have been concerned with the interpretation of the first arrival data from LASP. The later arrivals on the records have also been examined. On the whole, there are few distinct second arrivals, other than the 'T' phase observed across the Grenada and Tobago troughs. However, several records from the Durham and U.W.I. stations between Grenada and St Lucia show fairly strong S-wave arrivals from some of the shots along line A (Fig. 2.1). These are mainly from shots south of St Vincent which were detonated on the seabed, but some are also observed for shots north of St Vincent in deeper water.

These second arrivals are identified as S-waves by their travel times, apparent velocities and low frequency (see below). Those from shots detonated above the seabed must travel through the water as P-waves and be converted to S-waves at one of the interfaces along the ray path. Theoretical considerations (Ergin, 1952; Gutenberg, 1944) suggest that the conversion is most likely to occur at the water-seabed interface, provided the seabed is fairly solid, which it is over the Lesser Antilles ridge. For S_g arrivals (corresponding to P_g of Chapter 4) the conversion cannot occur at the basement because the S-wave velocity of the refractor is about the same as, or less than, the P-wave velocity in the overlying layer, so that S head waves cannot be generated.

The possibility that these second arrivals are surface waves is rejected as the computed travel time graphs all show a significantly positive time intercept (see later).

Fig. 7.1 shows the stacked records from St Vincent SVT of shots A13 - 24. The S-phase is clearly present on shots 14 - 20. The predominant frequency in the first arrival is 6 - 8Hz, whilst that in the S-phase is noticeably lower, being 4 - 5Hz. The records shown are those recorded on the east-west orientated horizontal seismometer and show, approximately, the tangential component of particle motion, as the waves are arriving from the south. The other two components were not available for this station.

Figs. 7.2 and 7.3 show the stacked records from Grenada South of shots A29 - 13 for the vertical and north-south (radial) seismometers. These show distinct S-wave arrivals from most of the shots which, for shots 13 - 18, can be correlated from record to record. As predicted by the polarization of P- and S-waves, the S-wave amplitudes are larger on the radial seismometer, whereas the P amplitudes are slightly larger on the vertical seismometer. The difference in frequency between the two phases is less noticeable here than it is in Fig. 7.1. The lower first arrival frequency may be due to attenuation of the higher frequencies by the sediments below the Grenada South station.

Many of the S-wave arrivals were emergent so that their onsets were difficult to recognise. However, 28 reliable travel times were measured at stations from Grenada to St Lucia. Four of these recorded S-waves from three or more adjacent shots and, for these, it was possible to calculate an apparent S-wave velocity. The travel times were reduced to sea level datum, corrected for the water depths (using a correction velocity of 2.08km s^{-1} for the sediment layer) and then reduced to a velocity of 4km s^{-1}. The reduced travel time graphs are shown in Fig. 7.4.

Fig. 7.1 Stacked records of shots A13 - 24 at St Vincent SVT (east - west component)

Figs. 7.2 & 7.3 Stacked records of shots A13 - 29 at Grenada South

7.2 - vertical component

7.3 - north-south component

Fig. 7.4 Reduced travel time graphs for S-wave arrivals at St Vincent, Carriacou and Grenada

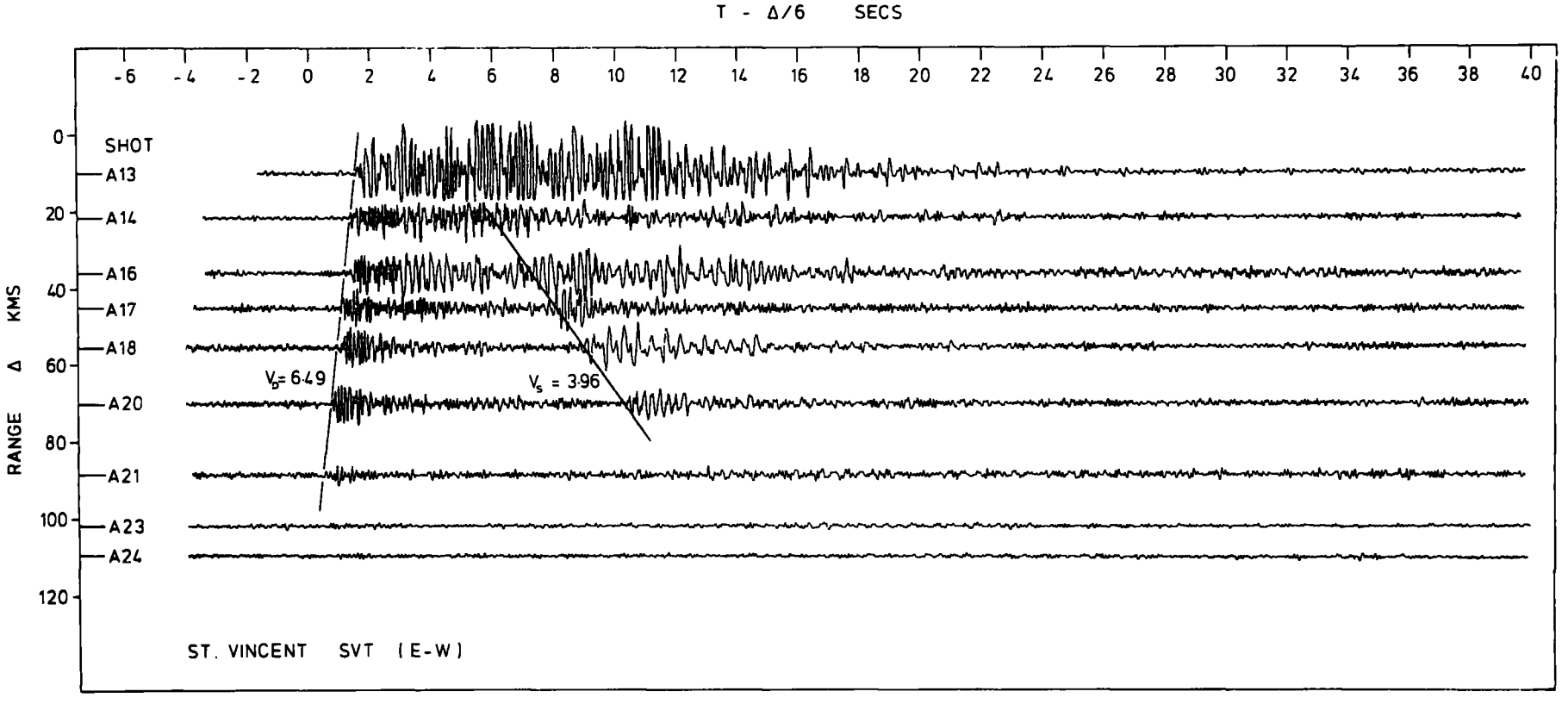
T - Δ/6 SECS
-6
-4
-2
0
2
4
6
8
10
12
14
16
18
20
22
24
26
28
30
32
34
36
38
40
RANGE Δ KMS
0
20
40
60
80
100
120
SHOT
A13
A14
A16
A17
A18
A20
A21
A23
A24
V_p= 6·49
V_s = 3·96
ST. VINCENT SVT (E-W)

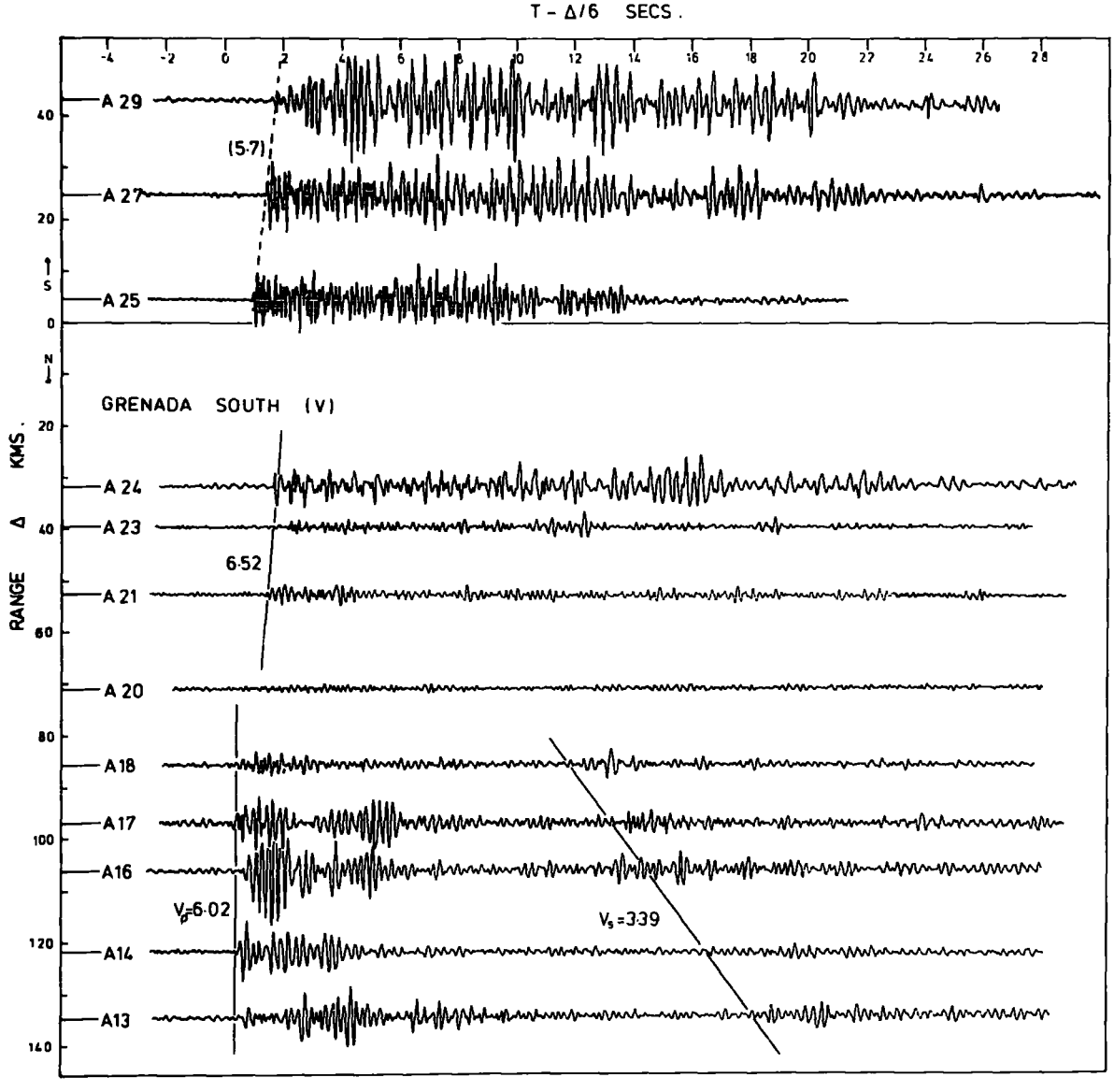
T - Δ/6 SECS.
-4
-2
0
2
4
6
8
10
12
14
16
18
20
22
24
26
28
A 29
(5·7)
A 27
A 25
S
N
GRENADA SOUTH (V)
RANGE Δ KMS.
20
40
60
80
100
120
140
A 24
A 23
6·52
A 21
A 20
A18
A17
A16
V_p=6·02
V_s=3·39
A14
A13

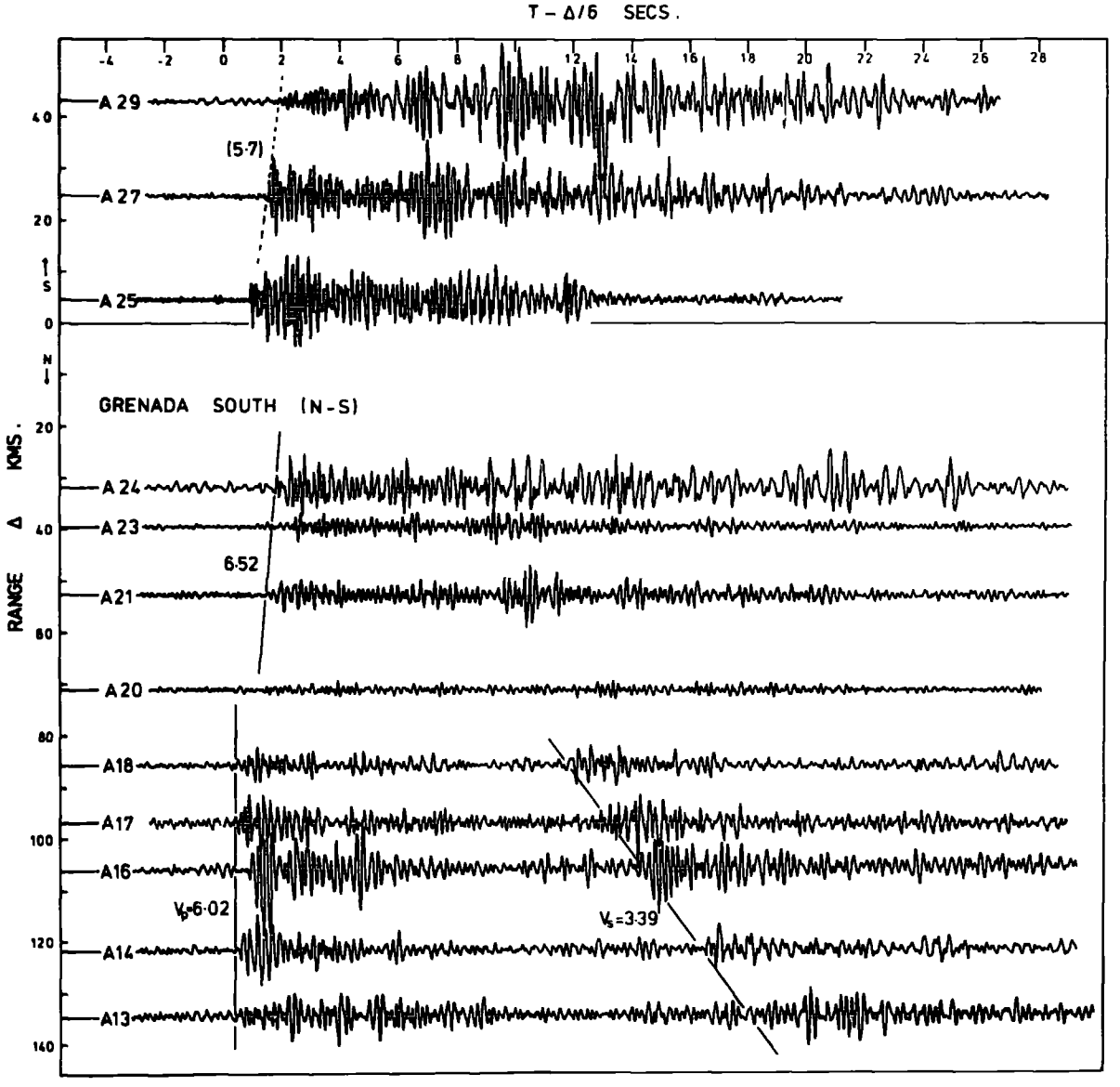
T – Δ/6 SECS.
-4
-2
0
2
4
6
8
12
14
16
18
20
22
24
26
28
A 29
(5·7)
A 27
A 25
S
N
GRENADA SOUTH (N-S)
RANGE Δ KMS.
20
40
0
A 24
A 23
6·52
A21
60
A 20
80
A18
A17
100
A16
V_p=6·02
V_s=3·39
120
A14
A13
140

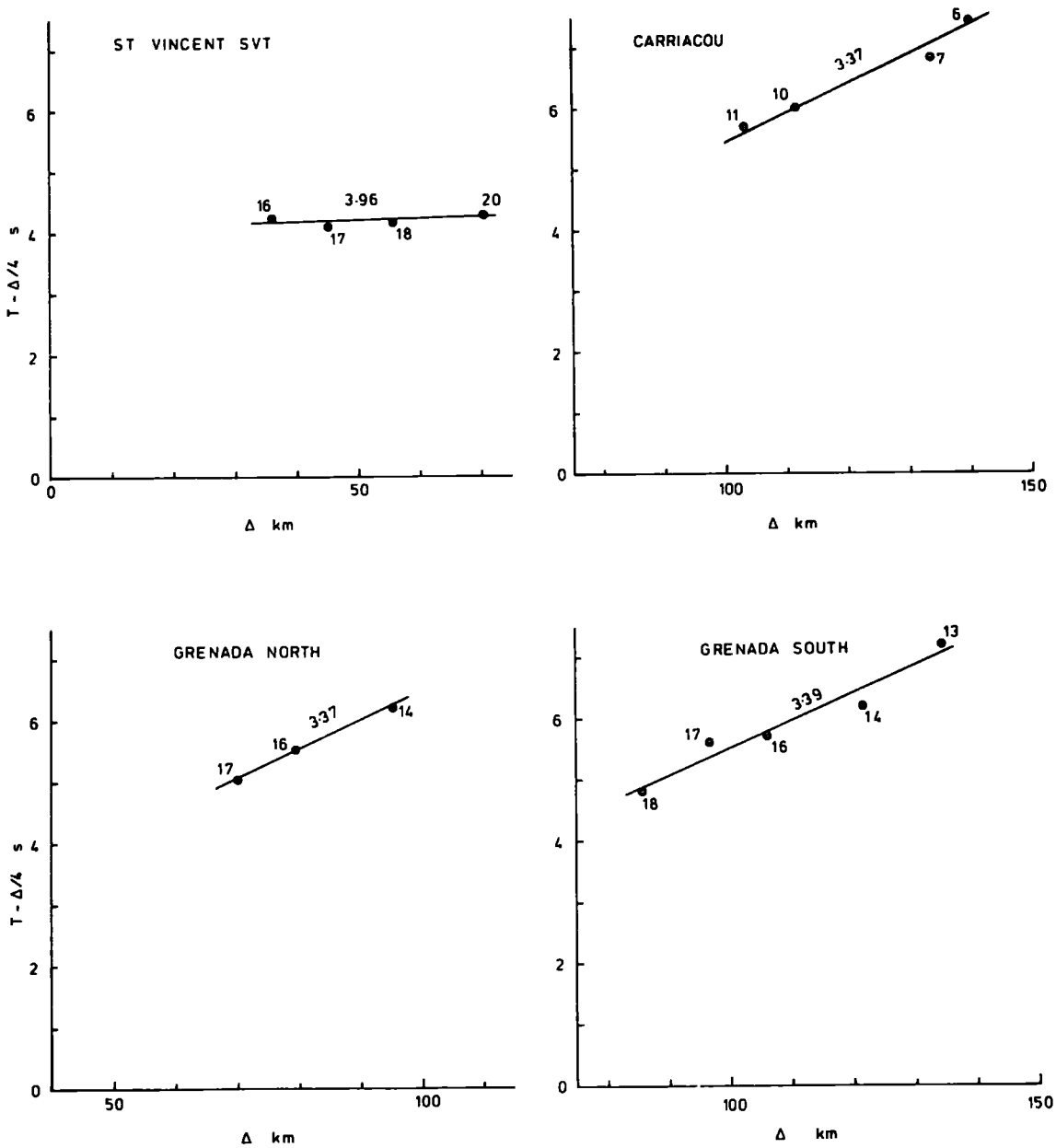
ST VINCENT SVT
3·96
16
17
18
20
T - Δ/4 s
Δ km
CARRIACOU
3·37
6
7
10
11
Δ km
GRENADA NORTH
3·37
14
16
17
T - Δ/4 s
Δ km
GRENADA SOUTH
3·39
13
14
16
17
18
Δ km

It was expected that the first S-wave arrival beyond about 120km would be a refraction from the lower crustal layer (V_p = 7.0km s^{-1}). However, all the travel times measured were consistent with refraction in the upper crustal layer (V_p = 6.2km s^{-1}). The absence of S^* arrivals corresponding to the P^* arrivals (Chapter 4) might reflect the existence of localised magma chambers at depths between 10 and 20km, as postulated by Wills (1974) from a study of plutonic nodules from the Lesser Antilles.

The apparent S-wave velocities, determined by least squares, were :

	velocity (km s^{-1})	time intercepts (s)
St Vincent SVT - shots A16 - 20	3.96 $\pm$ 0.05	4.06
Carriacou - shots A6 - 11	3.37 $\pm$ 0.07	0.73
Grenada North - shots A14 - 17	3.37 $\pm$ 0.03	1.77
Grenada South - shots A13 - 18	3.39 $\pm$ 0.07	1.00

(errors shown are standard errors)

The velocity observed to the south of St Vincent is significantly larger than those observed northwards from Grenada, suggesting a northward dip on the basement beneath shots 13 - 20. A true velocity of 3.64km s^{-1} and a dip of 3.2° are found by reversing these velocities. An alternative method of estimating the true S-wave velocity is to use the basement dips calculated from the first arrival data (Chapter 4). These are all smaller than 3°,

so there is a discrepancy between the true velocity calculated for SVT and those calculated for the other stations. The results of the calculations are :

	apparent velocity (km s^{-1})	dip (positive to N)	corrected velocity (km s^{-1})
St Vincent SVT	3.96	2.0°	3.78
Carriacou	3.37	0.4°	3.40
Grenada North	3.37	0.6°	3.42
Grenada South	3.39	0°	3.39

The velocity measured at SVT seems spurious and it is considered that the best value for the S-wave velocity in the upper crustal layer is 3.4km s^{-1}.

7.2 Estimation of Poisson's Ratio

Poisson's ratio can be defined as the ratio of the lateral contraction to the longitudinal extension of a deforming elastic body (Bullen, 1965, p. 23). It can be expressed in terms of various elastic parameters of the solid and is related to the longitudinal and shear wave velocities, V_p and V_s, by the expression :

$$\text{Poisson's ratio, } \sigma = (V_p^2 - 2.\ V_S^2)/2.\ (V_p^2 - V_S^2)$$

Many solids have elastic constants which approximate to Poisson's relation, such that $V_p = 3^{\frac{1}{2}}.V_S$ and $\sigma = 0.25$ (Bullen, 1965, p. 75).

Two methods were used to estimate values of Poisson's ratio for the crustal material beneath the Lesser Antilles. The first was by straightforward substitution of the calculated P and S velocities into the above expression, thereby obtaining an estimate of Poisson's ratio in the upper crustal layer. The second method uses the average P- and S-wave velocities along a particular ray path, calculated from the P and S travel times, to determine an average value of Poisson's ratio along the ray path.

7.2.1 Poisson's ratio from measured velocities

The corrected S-wave velocities observed at Grenada, Carriacou and St Vincent were combined with the corrected P-wave velocities, observed at the same stations from the same shots, to calculate Poisson's ratio. For Carriacou, the P-wave velocity observed from shots 6 - 11 is considered to be P^*, so a velocity of 6.17km s^{-1} was assumed, this being the average P_g velocity observed in this region. The results from this approach are :

	P velocity (km s^{-1})	S velocity (km s^{-1})	σ
St Vincent SVT	6.16 $\pm$ 0.08	3.78 $\pm$ 0.07	0.20 $\pm$ 0.03
Carriacou	6.17	3.40 $\pm$ 0.07	0.28
Grenada North	5.94 $\pm$ 0.08	3.42 $\pm$ 0.05	0.25 $\pm$ 0.04
Grenada South	6.03 $\pm$ 0.06	3.39 $\pm$ 0.09	0.25 $\pm$ 0.04

The standard errors given above show that a precise measurement of Poisson's ratio depends on accurate determinations of the velocities. Therefore, this method is likely to give inaccurate estimates of Poisson's ratio.

7.2.2 Poisson's ratio from P- and S-wave travel times

Poisson's ratio can be estimated from the P and S travel times provided both waves follow approximately the same path. This is true if the ratio of the P- and S-wave velocities is constant in all the layers the waves pass through.

The average P- and S-wave velocities along the ray path were estimated from the observed travel times by assuming that the length of the ray path approximates to the shot-receiver separation. This approximation is good if the shot-receiver separation is large compared to the depth of penetration of the wave, but may lead to a significant underestimate of the average velocity at short ranges. The estimates of Poisson's ratio calculated from these average velocities are therefore likely to be slightly low.

Estimates of Poisson's ratio were obtained from the 28 pairs of travel times and range from 0.260 to 0.332 with a mean value of 0.290 ± 0.005. After removing the values obtained from travel times for ranges greater than 100km (where the P arrival may be P^*), the mean was recalculated and found to be 0.293 ± 0.006. These values are substantially higher than those obtained using the measured P_g and S_g velocities. No correlation was observed between the values of Poisson's ratio and the shot-station separation, suggesting that insignificant error was introduced by approximating the length of the ray path to the horizontal separation. This determination of Poisson's ratio is considered to be more reliable than that determined in the previous section.

7.3 Discussion

Most rocks do not obey Poisson's relation and have a Poisson's ratio somewhat larger than 0.25. Determinations of Poisson's ratio in the crust beneath North America have been summarised by Suzuki (1965) : Values of 0.26 - 0.27 in the upper crust, increasing to 0.28 - 0.29 in the lower crust, are suggested. Christensen and Fountain (1974) have shown that Poisson's ratio in granulites decreases as the quartz content increases. As the upper crust beneath island arcs is probably more basic than the upper continental crust, the value of 0.29 found here for the Lesser Antilles is probably a reasonable average value.

The volcanic activity along the Lesser Antilles requires the presence of sizeable reservoirs of semi-molten magma within the crust beneath some of the islands. Theoretical considerations (Walsh, 1968 and 1969) show that seismic waves passing through partially melted rock will be subjected to attentuation and differential reductions of P and S velocities, giving larger Poisson's ratios. Furthermore, Anderson and Spetzler (1970) have shown that only a small amount of partial melting is required to produce the high attenuation and low velocities observed in the low-Q zone of the upper mantle. Thus, if S-waves pass through significant amounts of partially melted magma, a large increase in Poisson's ratio and much attenuation are to be expected. As this is not observed for the upper crustal waves considered here, it is concluded that most of the magma chambers along the Lesser Antilles island arc lie at depths of more than 5km. This conclusion is supported by Wills (1974), who suggests, from geochemical considerations, that magma chambers with volumes up to $5km^3$ lie at depths between 10 and 20km beneath the arc.

Chapter 8

LATE MESOZOIC - CAENOZOIC EVOLUTION OF THE EASTERN CARIBBEAN

8.1 Introduction

The major results of the interpretation of the LASP data have been summarised at the end of Chapters 4 - 7 (sections 4.6, 5.5, 6.4 and 7.3). In this chapter these results, and other published evidence, are used to support the idea that the Aves Ridge is an ancient island arc formed during late Cretaceous - earliest Tertiary times, when 'Atlantic' lithosphere was possibly being subducted beneath 'Caribbean' lithosphere at about the present site of the Lesser Antilles ridge. The structure determined for the Lesser Antilles ridge (Chapter 4) is discussed in relation to the development of the island arc and is compared to the structure found beneath other island arcs.

8.2 Evidence for an Earlier Phase of Subduction

The interpretation of the reversed refraction line between Barbados and the western hydrophone station (LASP 10) indicates that a single crustal layer of velocity 7.0km s^{-1} underlies the eastern part of the Tobago Trough (Chapter 5). Two previous refraction lines in the Tobago Trough (J. Ewing et al., 1957; Edgar et al., 1971) defined a layer of similar velocity. None of these refraction lines showed evidence of a layer of velocity between 4.5 and 6.5km s^{-1} above the 7km s^{-1} layer. Thus, the velocity structure of the Tobago

Trough crust is similar to that determined beneath the eastern hydrophone station (LASP 9) situated on the Atlantic slope of the Barbados Ridge, which differs from the typical Atlantic crustal structure only in the increased sediment thickness and the apparent absence of layer 2 (section 1.4.1).

In the Grenada Trough, however, the velocity structure has been found to be similar to that of the Venezuela Basin (Officer et al., 1959). Here there are two crustal layers of velocities 6.0 - 6.3 and 7.1 - 7.4km s^{-1}. Fig. 8.1 summarises the velocity structure determined in these regions.

Considering the similarities in velocity structure, it is suggested that the crust of the Tobago Trough was once part of the Atlantic plate and that the crust of the Grenada Trough originated as part of the Caribbean plate. Support for this conclusion is provided by an east-west trending positive gravity anomaly, associated with the St Lucia East Ridge (Westbrook, 1973), which can be traced across the present subduction zone into the Atlantic Ocean at about latitude $13^{o}45'N$ (see Fig. 1.8). The presence of this feature on both sides of the present subduction zone is difficult to explain unless the subduction zone has cut a formerly continuous linear feature. This would be the case if the crust between the Lesser Antilles and the subduction zone had once been part of the Atlantic plate.

The present boundary between the Caribbean and Atlantic plates is beneath the Barbados Ridge (Sykes and Ewing, 1965; Molnar and Sykes, 1969; Chase and Bunce, 1969; Westbrook et al., 1973). If the Tobago Trough crust was once part of the Atlantic crust, the boundary between the two plates must once have been further west,

Fig. 8.1 Crustal sections across the eastern margin of the Caribbean

Sources : (1) Officer et al. (1959)

(2) this work; Ewing et al. (1957); Edgar et al. (1971)

(M = Moho from gravity interpretation)

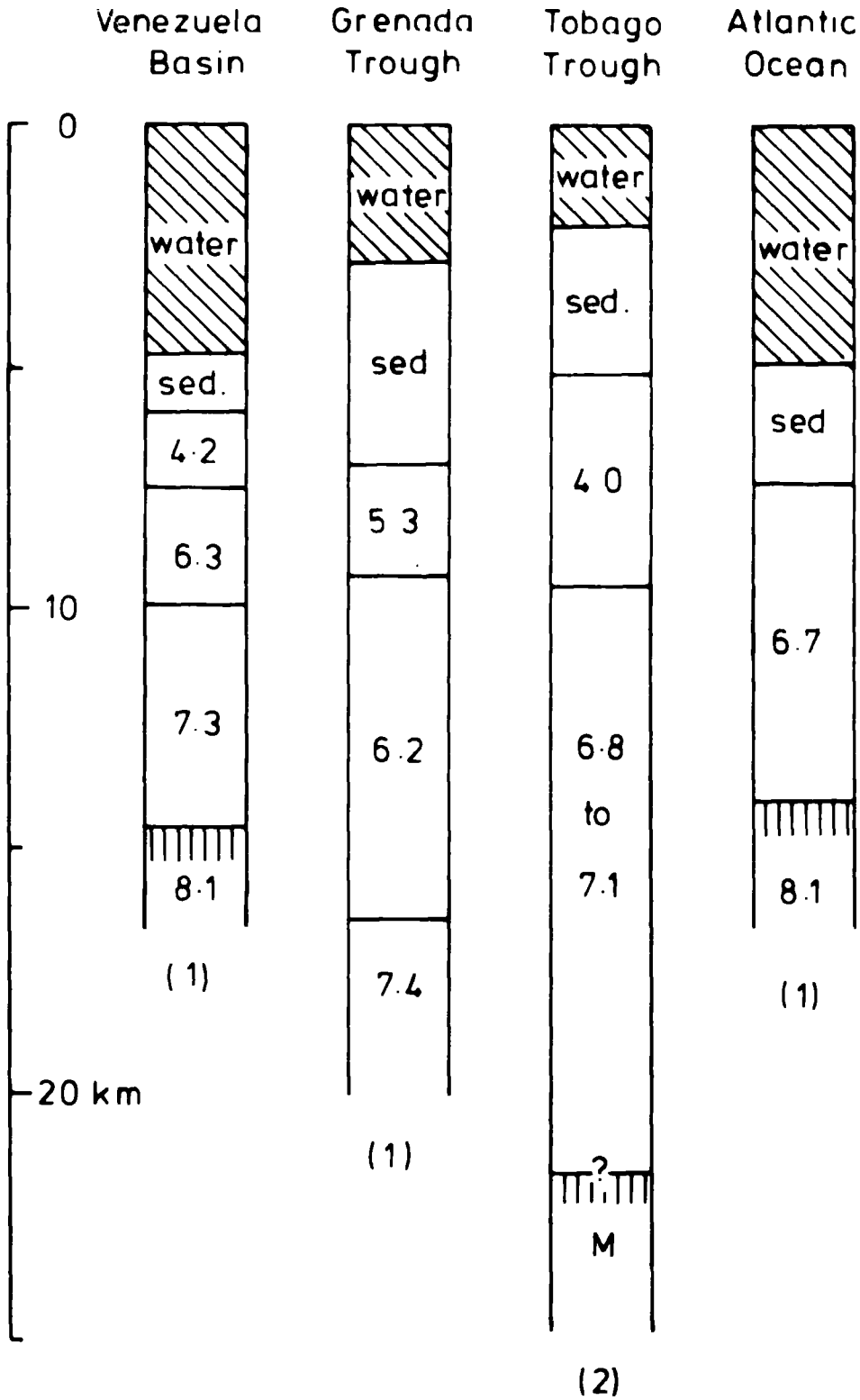
Venezuela Basin
Grenada Trough
Tobago Trough
Atlantic Ocean
0
10
20 km
water
sed.
4·2
6·3
7·3
8·1
(1)
water
sed
5 3
6·2
7·4
(1)
water
sed.
4 0
6·8
to
7·1
?
M
(2)
water
sed
6·7
8·1
(1)

probably at the present site of the Lesser Antilles island arc. The Lesser Antillean islands show evidence of volcanism since the Eocene. This implies that subduction of Atlantic lithosphere beneath the Barbados Ridge commenced about 60 - 65 mybp (earliest Tertiary), because the subducted lithosphere has to reach a depth of about 120km before sufficient volatiles are released to trigger the magma formation. The pre-Tertiary plate boundary may have been either a destructive boundary (subduction zone) or a conservative boundary (transcurrent fault). However, as the Atlantic plate would probably have been moving westwards at about the same rate as it is at present (Le Pichon and Hayes, 1971; Le Pichon and Fox, 1971), and the Caribbean plate was probably moving in a southwesterly direction relative to South America (Maresch, 1974), it is difficult to envisage a conservative boundary between these plates. If there was subduction of one plate beneath the other at this time one would expect to see the remnants of its associated island arc. The Aves Ridge has been identified as a volcanic ridge which was formed during the Upper Cretaceous (Fox et al., 1971). Its position, approximately parallel to and 240km west of the Lesser Antilles, is consistent with it being the island arc associated with the possible subduction of Atlantic lithosphere beneath the Caribbean plate in the region of the Lesser Antilles.

The idea that the Aves Ridge was formed by volcanism associated with subduction of Atlantic lithosphere, at a position some distance west of its present site, has been suggested previously by several authors (Freeland and Dietz, 1971; Malfait and Dinkelman, 1972; Mattinson et al., 1973; Kearey, 1974). Little conclusive evidence has been advanced to prove this idea, so discussion of

alternative theories of the origin of the Aves Ridge and of the deeper implications of the above model is of interest here.

Kearey (1974) has discussed the origin of the Aves Ridge with reference to its crustal structure and the general development of the eastern Caribbean. He dismisses the idea that the Aves Ridge could be an ancient ocean ridge, because these ridges are thought to be composed of normal oceanic material above an upwarped, anomalous upper mantle (Talwani et al., 1965) and, once they have become inactive, they should sink to regain isostatic equilibrium and, therefore, lose their topographic expression. The Aves Ridge bears a superficial resemblance to other aseismic ridges of the Iceland - Faeroe type, but Kearey (1974) considers that there are fundamental differences in structure and composition between the Aves Ridge and these aseismic ridges. Kearey considers the following two theories of the origin of the Aves Ridge to be most plausible :

(1) That it is an ancient island arc formed during a distinct earlier period of subduction.

(2) That it represents an origional portion of the Lesser Antilles separated from the active arc by some form of back-arc spreading.

The latter theory is based on the work of Karig (1970, 1971, 1972) who suggests that the 'inter-arc' basins behind some of the active island arcs of the western Pacific were formed by secondary spreading processes occurring behind the 'frontal' arc. In Karig's terminology, the Aves Ridge would be a 'third' or 'remnant'

arc; the Grenada Trough, an 'inactive basin' with normal heat flow; and the Lesser Antilles island arc, the 'frontal' arc. However, if the Aves Ridge was formed by rifting from the Lesser Antilles island arc, the rocks of both arcs should show a considerable overlap.of ages. The oldest volcanic rocks on the Lesser Antilles are of Eocene age (Martin-Kaye, 1969), while ages of samples dredged from the Aves Ridge range from Upper Cretaceous to earliest Tertiary only. It seems unlikely that older rocks should exist on the Lesser Antilles, completely hidden by the younger rocks. Furthermore, this theory suggests a younger age for the Grenada Trough than for the Caribbean crust to the west of the Aves Ridge. If this is so, it is strange that the same anomalous 'Caribbean' crustal structure should be found in the Grenada Trough as in the Venezuela Basin. These two criticisms would appear not to support the theory that the Grenada Trough developed by some form of back-arc spreading.

The age relations of the volcanic rocks on the Aves Ridge and Lesser Antilles lend support to the idea that the Aves Ridge originated as an island arc. A model of the development of the eastern Caribbean from the Upper Cretaceous to the Present is presented in Fig. 8.2. It is proposed that underthrusting of Atlantic lithosphere beneath the Caribbean plate, at about the present site of the Lesser Antilles, commenced 90 - 100 mybp and that this produced volcanism at the Aves Ridge between 85 and 70 mybp (Fig.8.2a). A readjustment of plate motions then caused the underthrusting to cease about 70 mybp, and a further adjustment 60 - 65 mybp caused subduction to commence at its present site, beneath the Barbados Ridge (Fig. 8.2b). Volcanism started in the Lesser Antilles, along the axis of the 'Limestone Caribbees', about 40 mybp and continued

Fig. 8.2 A model for the late Mesozoic-Caenozoic development of the eastern Caribbean

(see text for discussion)

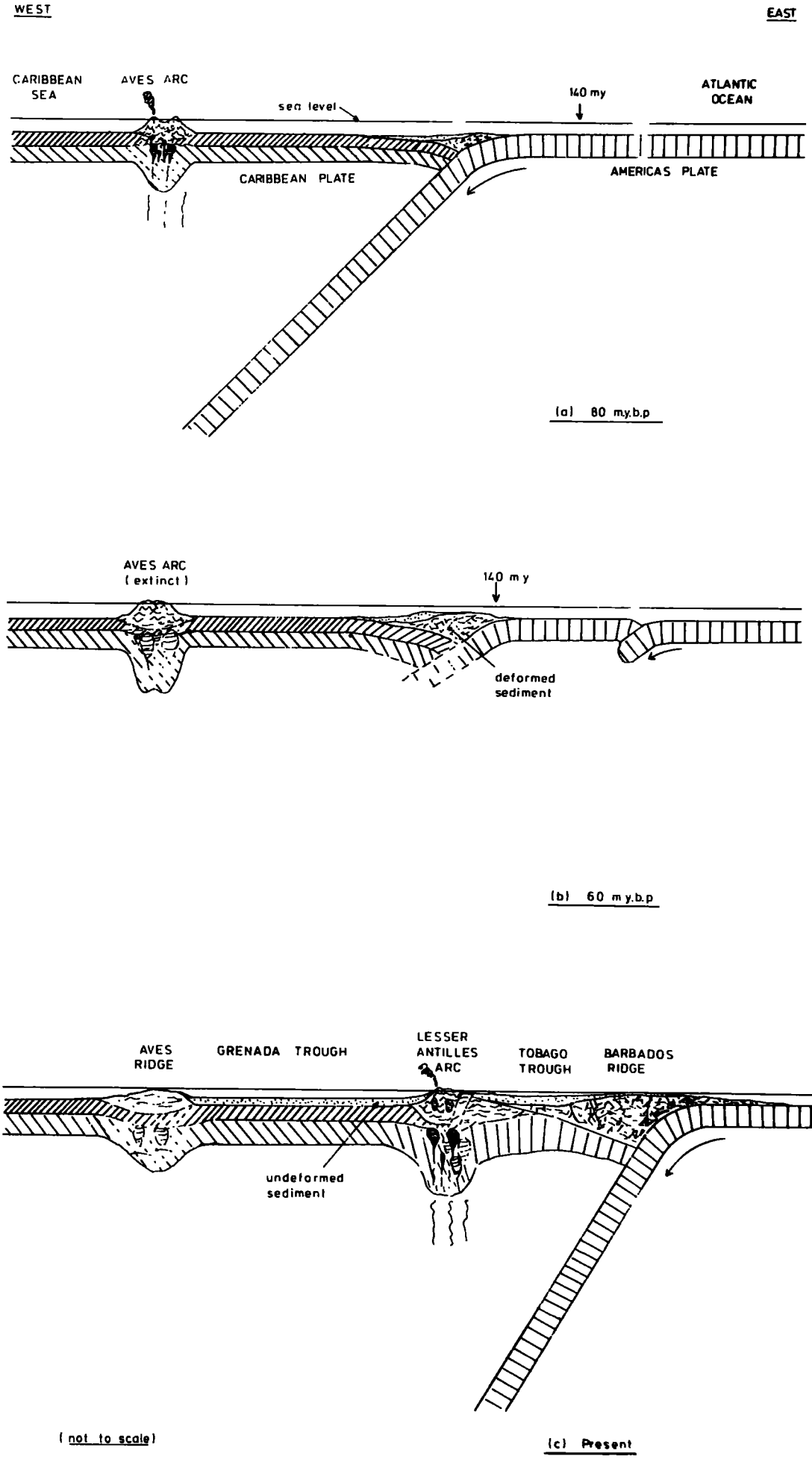
WEST
EAST
CARIBBEAN SEA
AVES ARC
sea level
140 my
ATLANTIC OCEAN
CARIBBEAN PLATE
AMERICAS PLATE
(a) 80 m.y.b.p
AVES ARC
(extinct)
140 m y
deformed sediment
(b) 60 m y.b.p
AVES RIDGE
GRENADA TROUGH
LESSER ANTILLES ARC
TOBAGO TROUGH
BARBADOS RIDGE
undeformed sediment
(not to scale)
(c) Present

until the late Oligocene. A pause or slowing down of the subduction might explain the gap between the two periods of volcanism represented in the Lesser Antilles. A further slight adjustment in the direction of plate motions may explain the slight displacement of the present zone of volcanic activity along the arc, which commenced less than 10 mybp (Fig. 8.2c).

The late Jurassic age determined by Fink et al. (1971) from an ophiolite suite on La Désirade provides a vital constraint on any model of the Mesozoic history of the eastern Caribbean. Mattinson et al. (1973) suggest that this suite of rocks is an uplifted portion of the oceanic crust beneath the eastern flank of the Lesser Antilles. This crust is, at present, part of the Caribbean plate, but the proposed model suggests that it was part of the Atlantic plate prior to the Upper Cretaceous.

Studies of plate motions affecting the Atlantic area (Le Pichon and Fox, 1971; Le Pichon and Hayes, 1971) suggest that the North Atlantic started to open about 180 mybp and that the opening of the South Atlantic did not commence until about 140 my. Thus, if subduction beneath the Aves Ridge continued for 25 - 30 my, it is conceivable that 140 - 150 my old Atlantic crust could exist to the east of the present island arc (at the top of the old subduction zone).

The results of JOIDES drilling (Edgar, Saunders et al, 1973) indicate that the Caribbean crust is of late Cretaceous age (c80my). If this is so, it is unlikely that the igneous complex on Desirade can represent uplifted Caribbean crust. However, several authors (Mattinson et al., 1973; Eaton and Driver, 1969) consider that the reflector B'' is not the true oceanic basement, as was assumed by

Edgar, Saunders et al. (1973). Thus, the Caribbean crust may be older than 80 my and is, perhaps, of late Jurassic age (Mattinson et al., 1973). However, it is believed that the crust beneath the Tobago Trough is most likely to be of Atlantic origin if the dates from Desirade are confirmed as late Jurassic.

A number of problems arise from the proposed model of the development of the eastern Caribbean : The Aves Ridge is about 240km west of the Lesser Antilles, which are 150km west of the present site of underthrusting. If a similar angle of underthrusting is assumed for both subduction zones, the pre-Tertiary ocean trench would have been situated under the eastern part of the present Grenada Trough. Gravity studies (Kearey, 1974) show no evidence of the remains of such a feature. However, if the angle of underthrusting were smaller, the site of subduction would be further away from the island arc. It is possible, therefore, that the pre-Tertiary ocean trench occupied the position of the present island arc. Structures related to the subduction at this site may well have been destroyed or masked by the subsequent development of the Lesser Antilles island arc. Two facts which might support a shallower angle of underthrust are that the Aves Ridge is less convex in plan than the Lesser Antilles ridge and that it has a broader cross-section (Figs. 1.3 and 6.7). Frank (1968) has demonstrated a possible relation between the curvature of island arcs and the angle of underthrust of subducted lithosphere. A less steep subduction zone would give off volatiles over a wider area so a more diffuse zone of magma genesis is expected. This would give rise to a broader belt of volcanic activity at the surface.

A more serious criticism of the proposed model is that there is no evidence of the pile of deformed sediments, equivalent to that of the Barbados Ridge, which would probably have accumulated in the ocean trench during the period of subduction at this site. Evidence of these disturbed sediments should be seen under the newer undeformed sediments in the eastern Grenada Trough. Kearey (1974) found no evidence, from seismic reflection sections, of any deformed sediment in the Grenada Trough. Indeed, if Kearey's identification of the Caribbean reflectors A'' (Eocene) and B'' (? Upper Cretaceous) within the Grenada Trough is correct, a continuous period of quiescent deposition, from Upper Cretaceous times until the present, is implied. If the two prominent reflectors observed in the Grenada Trough were proved to be younger (e.g. if the lower reflector was A''), the older deformed sediments may be buried beneath the thick sequence of undisturbed layers in the eastern Grenada Trough. In this case, their presence might be revealed by seismic refraction studies. Unfortunately, the LASP results in this region (Chapter 6) are too inconclusive to define the crustal structure in any detail.

For the deformed sediments to be 'hidden' below the undisturbed layers in the Grenada Trough, their volume must be fairly small. If the rate of supply of sediments to the trench was as large as that to the present trench, opposite the southern Antilles, and the period of subduction was of the same order as that at the present trench, a considerable pile of sediments would have accumulated in the trench. The huge volume of the sediment pile forming the Barbados Ridge has been related to the proximity of the South American continent (Chase and Bunce, 1969). Detritus from

this land mass has considerably increased the thickness of sediment on the Atlantic plate which underthrusts the Caribbean plate in the region of the Barbados Ridge. Further north the supply of detritus from South America is negligible and the trench contains only a small accumulation of oceanic sediments. In late Cretaceous time the South American land mass would have been in close proximity to the southern portion of the postulated ocean trench. However, several authors have postulated the existence of an active east-west destructive plate margin along the northern margin of the South American land mass at this time. Malfait and Dinkelman (1972) assumed this to be a southward dipping subduction zone, with Caribbean lithosphere underthrusting the continental crust. Maresch (1974) suggested that an 'extinct' island arc had collided with the continental land mass and was being thrust over the continental margin at this time. In either case, it is possible that much of the sediment derived from the northern areas of the South American land mass was channelled into the ocean trench of this southern subduction zone, or the 'flysch foredeep' of Maresch (1974), thereby reducing the supply to the north-trending ocean trench.

It is admitted that it is a great coincidence that evidence of the postulated ocean trench and deformed sediment pile should have been destroyed or masked by the development of the present arc and the deposition of a thick sequence of Tertiary sediments in the Grenada Trough. Nevertheless, it is considered that the proposed model provides the most satisfactory explanation of the differing crustal structure beneath the Grenada and Tobago troughs and of the origin of the Aves Ridge. This model may be modified as new information becomes available (see section 8.5).

8.3 Development of the Lesser Antilles Island Arc

The new global tectonics theory (Isacks et al., 1968) suggests that island arc systems in oceanic regions are formed as a result of subduction of one oceanic plate beneath another. The crustal thickening beneath island arcs is generally assumed to be entirely due to the addition of magma, derived from the mantle or subducted lithosphere, either by extrusion at the surface or by intrusion into the existing crust. However, if the model discussed in section 8.1 holds, then the development of the Lesser Antilles island arc may also be affected by the pre-existing trench structure.

In Chapter 4 it was shown that the crust beneath the Lesser Antilles arc consists of two crustal layers with velocities of about 6.2 and about 7.0km s^{-1}. The tops of these two layers lie at depths of 1 - 8km and 12 - 18km, respectively. The total thickness has been estimated to be about 35km. The lower layer is considered to be the original oceanic crust, thickened by the intrusion of basic magmas from the upper mantle beneath the arc. The upper layer probably consists of the pile of volcanic material extruded through the sea floor during the building up of the island arc since the Eocene (see section 4.3.4). It is probably largely of andesitic composition, but may include significant proportions of basaltic and dacitic material and also some dioritic intrusions. All these materials are represented by surface exposures on the islands (Martin-Kaye, 1969). The results of shear-wave studies (Chapter 7) suggest that magma chambers of significant size are not present in the upper crustal layer.

Fig. 8.3 shows, schematically, successive stages in the development of an island arc.

Fig. 8.3 A model for the development of the Lesser Antilles Island Arc

(see text for discussion)

(a)

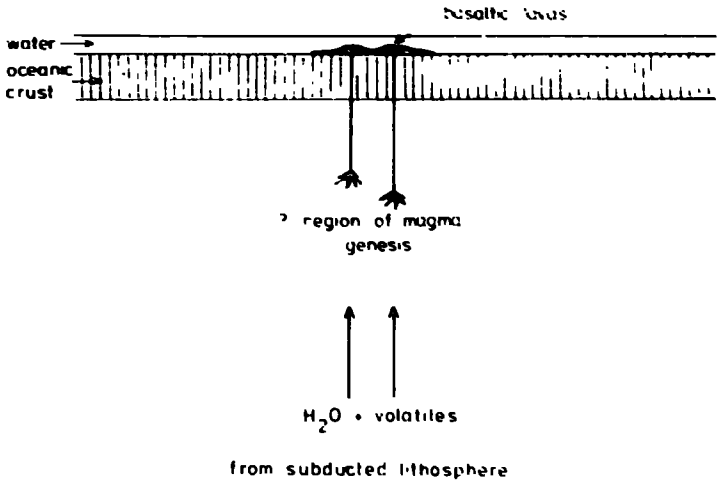
basaltic lavas
water
oceanic crust
? region of magma genesis
H_2O + volatiles
from subducted lithosphere

(b)

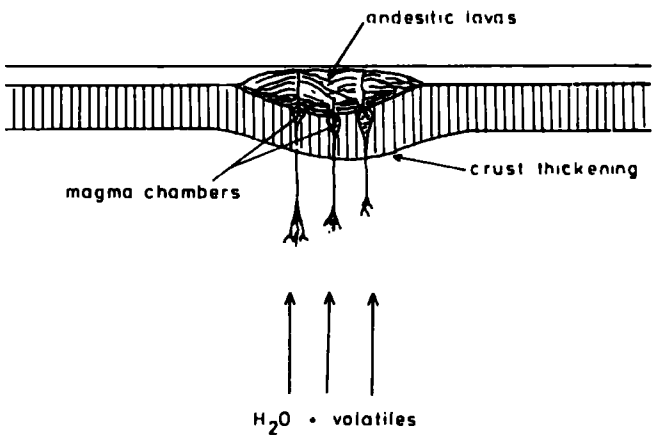
andesitic lavas
crust thickening
magma chambers
H_2O + volatiles

(c)

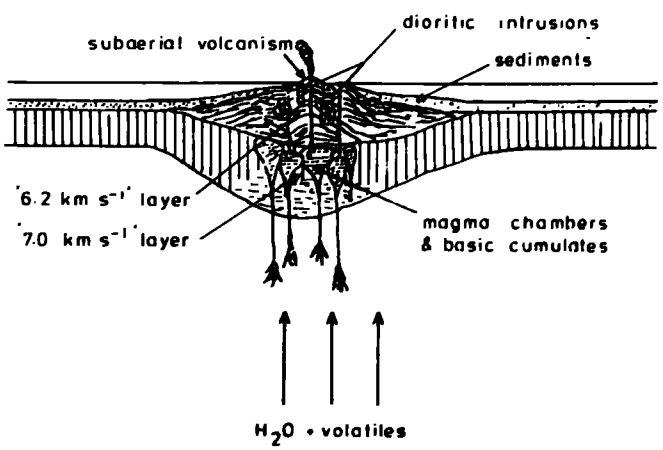
dioritic intrusions
subaerial volcanism
sediments
'6.2 km s^{-1}' layer
'7.0 km s^{-1}' layer
magma chambers & basic cumulates
H_2O + volatiles

For the purpose of this discussion, it is assumed that the parental magma of the calc-alkaline suite observed in the islands is derived by partial melting of an upper mantle peridotite (Arculus and Curran, 1972). A derivation by partial melting of the subducted oceanic plate can explain a change in chemistry of the volcanics with distance from the trench (Hatherton and Dickinson, 1969). However, the occurrence of calc-alkalic and undersaturated lavas at the same locality, as observed in Grenada (Arculus, 1973), suggests that the volcanism is not directly related to the subduction process. Partial melting in the upper mantle is caused by the change in temperature field caused by the subduction of oceanic lithosphere (Toksöz, Minear and Julian, 1971; Griggs, 1972) and the supply of water and other volatiles from the subducted plate.

As the convergence rate of the Caribbean and Atlantic plates is between 0.5 and 1.0cm yr^{-1} (Molnar and Sykes, 1969), there will have been a delay of 10 - 20 my after the commencement of subduction before the subducted lithosphere reached the depths at which volatiles are given off and magma genesis began.

Once magma genesis has begun, the first stage of island arc formation begins (Fig. 8.3a). This consists of the extrusion of primitive lavas on to the ocean floor. These lavas are probably of basaltic composition as they have been derived directly from the upper mantle partial melt. The second stage (Fig. 8.3b) consists of the creation of magma chambers within the old ocean crust, supplied with primitive magma derived from the upper mantle. This causes a thickening of the crust. Andesitic magma is derived from these magma chambers by differentiation, and is extruded through the ocean floor, gradually building up a volcanic ridge. In the final

stage of development (Fig. 8.3c) the volcanic pile has grown above sea level and subaerial volcanism is occurring. Some of the older magma chambers have become inactive and a basic cumulate sequence has 'frozen in'. With the passage of melts from the mantle into the crust, the boundary between the lower crust and mantle has probably become rather diffuse. Dioritic material, derived from the magma chambers within the lower crust, has been intruded into the volcanic pile.

The two distinct periods of volcanism on the Lesser Antilles (Martin-Kaye, 1969) require a slight modification of this scheme. The axis of late Miocene to Recent volcanoes is displaced to the west relative to the axis of the earlier volcanoes. This is distinct where the two arcs diverge to the north, but is still discernable at the southern end of the ridge,where the younger volcanic centres lie slightly to the west of the geometric centre of the ridge. Westbrook (1973) has noted that short-period magnetic anomalies characterise the area of the volcanic ridge east of the islands. He relates these to the existence of multiple intrusions within the volcanic pile associated with the earlier period of volcanic activity.

This scheme for the development of the island arc is similar to that proposed by Kuno (1968) and Mitchell and Reading (1971) for island arcs in general. The model obtained is also consistent with observations by Brown and Schairer (1971) and Wills (1974), on the derivation of plutonic xenoliths found in the Lesser Antilles. It does not support the suggestion of Lewis (1971) that fractionation of the basaltic magmas occurs at three levels in the crust. He proposed that the last stage of fractionation occurs

at very shallow depths in the crust, but the results presented here suggest that the lower crust is the site of most of the magma differentiation.

If an ocean trench and its associated sediment fill occupied the site of the Lesser Antilles before the commencement of subduction beneath the Barbados Ridge, some modification of the above model may be required : Presumably, the sediments would have been buried under the volcanics in the earliest stages of arc development, and were metamorphosed. In this case, it may be that at least part of the andesitic magma was derived by contamination of a fairly primitive magma by these metasediments. This additional material may also explain the large crustal thickness of the Lesser Antilles arc.

8.4 Comparison of Crustal Structure Beneath Island Arcs

Seismic refraction profiles across the crustal regions of island arcs have been reported for only a few arcs and many of these have failed to penetrate to the base of the crust. This reflects the inadequacy of ship-to-ship refraction experiments in areas of large crustal thickness and/or complex structure. The method of shooting at sea and recording on the islands using temporary seismic stations (as in LASP) will probably provide more answers in the future.

Fig. 8.4 summarises the velocity structure determined for some other island arcs, for comparison with the Lesser Antilles structure determined from this work. Most of the sections shown are characterised by two crustal layers of velocities 5.5 - 6.0 and 6.0 - 7.0km s^{-1}. The velocities determined for the Lesser Antilles crust seem to be slightly higher than the average of those in the

Fig. 8.4 Comparison of crustal structure of island arcs

Sources : (1) this work; (2) Officer et al. (1959); (3) Ewing et al. (1971b); (4) Finlayson et al. (1972); (5) Shor et al. (1971a); (6) Murauchi and Yasui (1968); (7) Sugimura and Uyeda (1973); (8) Shor (1964).

(M = Moho from gravity interpretations)

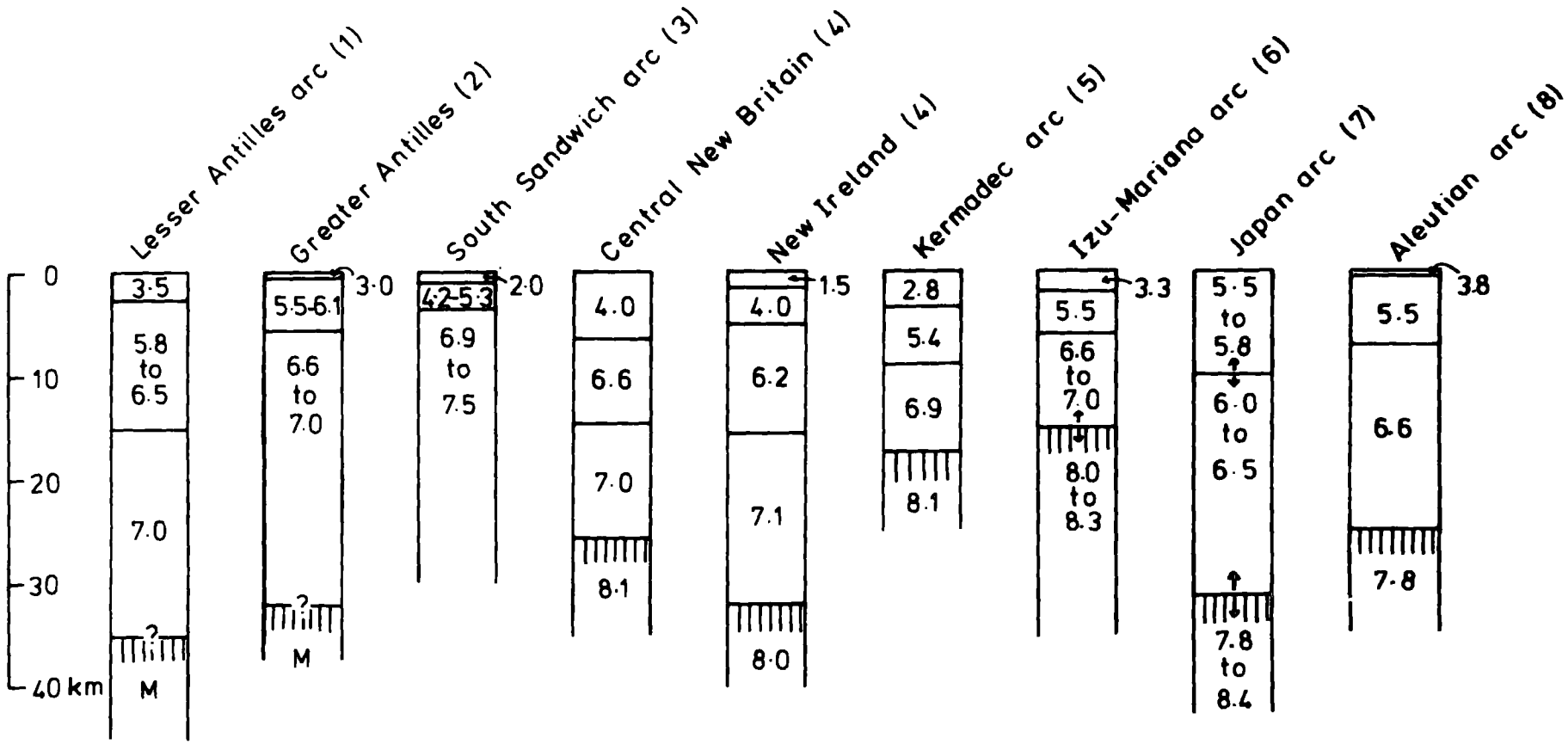
Lesser Antilles arc (1)
Greater Antilles (2)
South Sandwich arc (3)
Central New Britain (4)
New Ireland (4)
Kermadec arc (5)
Izu-Mariana arc (6)
Japan arc (7)
Aleutian arc (8)
0
10
20
30
40 km
3·5
5·8 to 6·5
7·0
?
M
5·5-6·1
3·0
6·6 to 7·0
?
M
4·2-5·3
2·0
6·9 to 7·5
4·0
6·6
7·0
8·1
1·5
4·0
6·2
7·1
8·0
2·8
5·4
6·9
8·1
3·3
5·5
6·6 to 7·0
8·0 to 8·3
5·5 to 5·8
6·0 to 6·5
7·8 to 8·4
3·8
5·5
6·6
7·8

other arcs. This may be related to the thicker crust beneath the Lesser Antilles; the greater load pressures causing the higher velocities. Alternatively, it may reflect the difference in the crustal structure present before the development of the arcs. The main crustal layer in the Caribbean crust has a velocity of 7.2 - 7.5km s^{-1}, while typical layer 3 velocities in the Pacific region are 6.7 - 7.0km s^{-1} (Shor et al., 1971b).

Kuno (1968) suggested that the 3.3 - 5.5km s^{-1} layers recorded under the Izu-Mariana ridges (Murauchi and Yasui, 1968) were composed of basaltic and andesitic lavas and pyroclastic rocks of Oligocene to Pliocene age, which constitute the basement of the Quaternary basaltic and andesitic volcanoes of the Izu islands. The lower crustal layer of this ridge was considered, by Kuno (1968), to consist of the lower crustal layer of the ocean basin intruded by voluminous gabbroic bodies representing the complementary material for the Tertiary and Quaternary volcanic rocks. Kuno showed that the volume relations between the postulated gabbroic rocks and the Caenozoic lavas and pyroclasts agree roughly with calculated proportions of the solid materials subtracted and the magmas produced.

Several refraction profiles across the Kermadec Ridge at the southern end of the Tonga-Kermadec island arc system (Shor et al., 1971a) show an oceanic layer which is irregularly thickened and a thick basement layer which is considered to be volcanic under the ridge. This structure suggests a similar mode of development for this island arc to that proposed for the Lesser Antilles (this work) and the Izu-Mariana arc (Kuno, 1968).

The similarity of the crustal structures determined for the Lesser Antilles and for New Ireland (Finlayson et al., 1972) is quite remarkable (Fig. 8.4). Both New Britain and New Ireland are characterised by two periods of volcanic activity (Bain, 1973), as in the Lesser Antilles arc, but the tectonic history of the Bismarck Archipelago is probably more complex than that of the Lesser Antilles : Earthquake focal mechanism studies (Johnson and Molnar, 1972) suggest that the Solomon Sea 'plate' is, at present, underthrusting New Britain, at the southern edge of the South Bismarck 'plate', in a NNW direction, but that present motion at the plate boundary bordering New Ireland is sinistral strike-slip. The structure of New Ireland and the nearby Pacific islands suggest formation by typical island arc processes, so the present plate motions in this complex area may not have been initiated very long.

Wiebenga (1973) shows that an area of very high positive free air gravity anomalies in the central part of New Britain coincides with an area where apparently shallow Moho depths (15 - 20km) were found from seismic refraction work. He suggests that the mantle 'intrusion' necessary to explain these observations would require the area to be under tension rather than compression. Wiebenga explains the observed seismic zone as being due to a rifted lithospheric slab sinking under its own weight.

It can be seen, therefore, that island arc areas undergoing very different tectonic histories may show similar crustal structures. The crustal structure beneath such active areas may be of limited value in deciphering the tectonic history of that area.

8.5 Suggestions for Further Investigations

The eastern Caribbean has been the subject of many geological and geophysical investigations in recent years. However, even with the immense amount of data now available, it has not been possible to elucidate the detailed history of the area with much confidence. It is considered that additional data is required in two main areas :

(1) Dating of sediments and 'basement' in the Grenada Trough, Tobago Trough and on the Aves Ridge.

(2) Further investigations of crustal structure, particularly crustal thicknesses, beneath the five major structural units of the eastern Caribbean.

The first of these requirements could be fulfilled by future JOIDES drilling sites, or similar ventures organised independently.

A further large-scale seismic refraction experiment could, if planned carefully, give a clearer picture of the crustal structure than the LASP results have. The main shortcomings of the LASP project were the smallness of the shot charges and the poor station coverage in several critical areas (see section 6.1).

It is proposed that the firing of a few large charges (e.g. one ton of explosives each), at suitable sites at the north, centre and south of the Lesser Antilles ridge, would allow the

crustal layering and crustal thickness beneath the arc to be determined in detail. Stations should reoccupy the LASP sites and as many additional sites as is possible. Investigations of the Grenada and Tobago troughs and the Aves Ridge present more of a problem. Ship-to-ship reversed refraction profiles using larger charges than those used previously may produce the desired results, especially in the troughs where the crust is thought to be thinner than beneath the ridges (Chapters 5 and 6). The use of ocean-bottom seismometers may increase the distances from which usable arrivals are received. Land stations should record as many of the seaward shots as possible, to give travel times for the maximum number of raypaths and azimuths.

Such a large-scale refraction project would have to be organised cooperatively at international level. However, as the Lesser Antilles arc is one of only two Pacific-type island arcs found in the Atlantic basin, the results from such a survey would be of much interest.

References

Anderson, D.L. and Spetzler, H., 1970. Partial melting and the low-velocity zone.
Phys. Earth planet. Interiors, 4, 62-64.

Arculus, R.J., 1973. The alkali-basalt-andesite association of Grenada, Lesser Antilles.
Unpublished Ph.D. thesis, University of Durham.

Arculus, R.J. and Curran, E.B., 1972. The genesis of the calc-alkaline rock suite.
Earth planet. Sci. Lett. (Neth.), 15, 255-262.

Baadsgaard, P.H., 1960. Barbados, W.I. : Exploration results 1950-1958.
21st Int. Geol. Congr. Rept. 18, 21-27.

Bader, R.G. et al., 1970. Initial reports of the Deep Sea Drilling Project, 4.
Washington (U.S. Government Printing Office), 753p.

Bain, J.H.C., 1973. A summary of the main structural elements of Papua New Guinea. in, The Western Pacific : Island Arcs, Marginal Seas, Geochemistry;
ed. P.J. Coleman (University of Western Australia Press), 147-162.

Ball, M.M., Harrison, G.C.A. and Supko, P.R., 1969. Atlantic opening and the origin of the Caribbean,
Nature, Lond., 223, 167-168.

Bamford, S.A.D., 1970. An appraisal of the seismic refraction method in crustal studies.
Unpublished Ph.D. thesis, University of Birmingham.

Bamford, S.A.D., 1971. An interpretation of first-arrival data from the Continental Margin Refraction Experiment.
Geophys. J.R. astr. Soc., 24, 213-229.

Barr, K.G. and Robson, G.R., 1963. Seismic delays in the eastern Caribbean.
Geophys. J.R. astr. Soc., 7, 342-349.

Barr, K.W. and Saunders, J.B., 1968. An outline of the geology of Trinidad.
Trans. 6th Caribbean geol. Conf., 1 - 10.

Beckmann, J.P., 1953. Die Foraminiferen der Oceanic Formation (Eocaen - Oligocaen) von Barbados, Kl. Antillen :
Eclog. geol. Helv., 46, 301-412.

Berry, M.J. and West, G.F., 1966. An interpretation of the first arrival data of the Lake Superior experiment by the time-term method.
Bull. seism. Soc. Am., 56, 141-171.

Birch, F., 1960. The velocity of compressional waves in rocks to 10 kbars : Pt. 1.
J. geophys. Res., 65, 1083-1102.

Birch, F., 1961. The velocity of compressional waves in rocks to 10 kbars : Pt. 2.
J. geophys. Res., 66, 2199-2224.

Bott, M.H.P., 1971. The interior of the Earth.
Edward Arnold, London, 316p.

Bott, M.H.P., Holder, A.P., Long, R.E. and Lucas, A.L., 1970. Crustal structure beneath the granites of southwest England. in, Mechanism of igneous intrusion, 93-102, eds. Newall, G. and Rast, N.
Geol. J. Spec. Issue, 2.

Bracey, D.R. and Vogt, P.R., 1970. Plate tectonics in the Hispaniola area. Bull. geol. Soc. Am., 81, 2855-2860.

Briden, J.G., Rex, D.C. and Tomblin, J.F., 1974. Isotopic age dates for the Lesser Antilles.
Abstracts of 7th Caribbean Geol. Conf., 13.

Brown, G.M. and Schairer, J.F., 1971. Chemical and melting relations of some calc-alkaline volcanic rocks.
Mem. geol. Soc. Am., 130, 139-158.

Brune, J.N., 1968. Seismic moment, seismicity and rate of slip along major fault zones.
J. geophys. Res., 73, 777-784.

Bullen, K.E., 1965. An introduction to the theory of seismology. (3rd Edition) Cambridge Univ. Press.

Bunce, E.T., Phillips, J.D., Chase, R.L. and Bowin, C.O., 1971. The Lesser Antilles arc and the eastern margin of the Caribbean Sea. in, The Sea, ed. Maxwell, A.E., 4, part 2, 359-386, Interscience.

Campbell, C.J., 1968. The Santa Marta wrench fault of Columbia and its regional setting. Trans. 4th Caribbean geol. Conf. (1965), 247-261.

Chase, R.L. and Bunce, E.T., 1969. Underthrusting of the eastern margin of the Antilles by the floor of the western North Atlantic Ocean, and the origin of the Barbados Ridge.
J. geophys. Res., 74, 1413-1420.

Christensen, N.I. and Fountain, D.M., 1974. Constitution of the lower continental crust based on experimental studies of seismic velocities in granulites. Bull. geol. Soc. Am. (in press).

Collette, J., Ewing, J., Lagaay, R.A. and Trushan, M., 1969. Sediment distribution in the oceans : the Atlantic between 10° and 19°N. Marine Geol., 7, 279-345.

Dewey, J.W., 1972. Seismicity of western Venezuela. Bull. seism. Soc. Am., 62, 1711-1751.

Dorel, J., Eschenbrenner, S. and Feuillard, M., 1971a. Contribution à l'étude sismique de l'Arc des Petities Antilles. Ann. geophys., 27, 295-302.

Dorel, J., Eschenbrenner, S. and Feuillard, M., 1971b. Vitesses sismiques et anomalies de propagation sous-l'Arc des Petites Antilles. C. R. Acad. Sc. Paris., 273, 302-305.

Eaton, J.F. and Driver, E.S., 1969. Geophysical investigations in the eastern Caribbean Curacao Ridge to Barbados (abstract). Trans. Am. geophys. Un., 50, 208.

Edgar, N.T., Ewing, J.I. and Hennion, J., 1971. Seismic refraction and reflection in the Caribbean Sea. Bull. Am. Ass. Petrol. Geol., 55, 833-870.

Edgar, N.T., Saunders, J.B. et al., 1973. Initial reports of the Deep Sea Drilling Project, 15. Washington (U.S. Government Printing Office), 1137p.

Epp, D., Grim, P.J. and Langseth, M.G. Jr., 1970. Heat flow in the Caribbean and Gulf of Mexico. J. geophys. Res., 75, 5655-5669.

Ergin, K., 1952. Energy ratio of the seismic waves reflected and refracted at a rock-water boundary. Bull. seism. Soc. Am., 42, 349-372.

Ewing, J.I., Edgar, N.T. and Antoine, J.W., 1971a. Structure of the Gulf of Mexico and Caribbean Sea. in, The Sea, ed. Maxwell, A.E., 4, part 2, 321-358, Interscience.

Ewing, J., Ludwig, W.J., Ewing, M. and Eittreim, S.L., 1971b. Structure of the Scotia Sea and Falkland Plateau. J. geophys. Res., 76, 7118-7137.

Ewing, J.I., Officer, C.B., Johnson, H.R. and Edwards, R.S., 1957. Geophysical investigations in the eastern Caribbean - Trinidad Shelf, Tobago Trough, Barbados Ridge and Atlantic Ocean. Bull. geol. Soc. Am., 68, 897-912.

Ewing, M., Crary, A.P. and Rutherford, H.M., 1937. Geophysical investigations in the emerged and submerged Atlantic Coastal Plain : Part I. Bull. geol. Soc. Am., 48, 753-802.

Ewing, M., Woolard, G.P. and Vine, A.C., 1939. Geophysical investigations in the emerged and submerged Atlantic Coastal Plain : Part III. Bull.geol. Soc. Am., 50, 257-296.

Ewing, M., Worzel, J.L., Steenland, N.C. and Press, F., 1950. Geophysical investigations in the emerged and submerged Atlantic Coastal Plain : Part V. Bull. geol. Soc. Am., 61, 877-892.

Fink, L.K. Jr., Harper, C.T., Stipp, J.J. and Nagle, F., 1971. Tectonic significance of La Désirade - possible relict sea-floor crust. Abstracts of 6th Caribbean geol. Conf., Latecomers, 4.

Finlayson, D.M., Cull, J.P., Wiebenga, W.A., Furumoto, A.S. and Webb, J.P., 1972. New Britain - New Ireland crustal seismic refraction investigations 1967 and 1969. Geophys. J. R. astr. Soc., 29, 245-253.

Fox, P.J., Schreiber, E. and Heezen, B.C., 1971. The geology of the Caribbean crust : Tertiary sediments, granitic and basic rocks from the Aves Ridge. Tectonophysics, 12, 89-109.

Frank, F.C., 1968. Curvature of island arcs. Nature, Lond., 220, 363.

Freeland, G.L. and Dietz, R.S., 1971. Plate tectonic evolution of Caribbean - Gulf of Mexico region. Nature, Lond., 232, 20-23.

Fuchs, K. and Landisman, M., 1966. Detailed crustal investigations along a north-south section through the central part of Western Germany. in, The Earth beneath the continents, eds. Steinhart, J. and Smith, T. Geophys. Monogr., 10, 433-452.

Gallovich, E. and Aguilera, L., 1970. Ensayos sismicos de refraccion effectuados en la Isla Aves. La Memoria de la Sociedad de Ciencias Naturales La Salle, 30, Caracas, Venezuela.

Griggs, D.T., 1972. The sinking lithosphere and the focal mechanism of deep earthquakes. in, Nature of the solid Earth, ed. Robinson, E.C., 361.

Gutenburg, B., 1944. Energy ratios of reflected and refracted seismic waves.
Bull. seism. Soc. Am., 34, 85-102.

Hagedoorn, J.G., 1959. The plus-minus method of interpreting seismic refraction sections.
Geophys. Prospect., 7, 158-182.

Hatherton, T. and Dickinson, W.R., 1969. The relationships between andesitic volcanism and seismicity in Indonesia, the Lesser Antilles and other island arcs.
J. geophys. Res., 74, 5301-5310.

Hess, H.H., 1964. Seismic anisotropy of the uppermost mantle under oceans. Nature, Lond., 203, 629-631.

Holcombe, T.L., Vogt, P.R., Matthews, J.E. and Murchison, R.R., 1973. Evidence for sea-floor spreading in the Cayman Trough.
Earth planet. Sci. Lett. (Neth.), 20, 357-371.

Holder, A.P., 1969. A seismic refraction study of the Earth's crust beneath S.W. Britain.
Unpublished Ph.D. thesis, University of Durham.

Holder, A.P. and Bott, M.H.P., 1971. Crustal structure in the vicinity of south-west England.
Geophys. J.R. astr. Soc., 23, 465-489.

Hurley, R.J., 1965. Geological studies of the West Indies.
Canada Geol. Survey Pap., 66-15, 139-150.

Isacks, B., Oliver, J. and Sykes, L.R., 1968. Seismology and the new global tectonics.
J. geophys. Res., 73, 5855-5900.

Johnson, T. and Molnar, P., 1972. Focal mechanisms and plate tectonics of the southwest Pacific.
J. geophys. Res., 77, 5000-5032.

Karig, D.E., 1970. Ridges and basins of the Tonga-Kermadec island arc system.
J. geophys. Res., 75, 239-254.

Karig, D.E., 1971. Origin and development of marginal basins in the western Pacific.
J. geophys. Res., 76, 2542-2561.

Karig, D.E., 1972. Remnant arcs. Bull. geol. Soc. Am., 83, 1057-1068.

Katz, S. and Ewing, M., 1956. Seismic refraction measurements in the Atlantic Ocean. Part VII : Atlantic Ocean basin west of Bermuda.
Bull. geol. Soc. Am., 67, 475-510.

Kearey, P., 1973. Crustal structure of the eastern Caribbean in the region of the Lesser Antilles and the Aves Ridge.
Unpublished Ph.D. thesis, University of Durham.

Kearey, P., 1974. Gravity and seismic reflection investigations into the structure of the Aves Ridge, eastern Caribbean.
Geophys. J.R. astr. Soc., 39, (in press).

Kearey, P., Peter, G. and Westbrook, G.K., 1974. Geophysical maps of the eastern Caribbean. Submitted to
Jl. geol. Soc. Lond.

Khudoley, K.M. and Meyerhoff, A.A., 1971. Palaeogeography and geological history of Greater Antilles.
Mem. geol. Soc. Am., 129, 199p.

Kuno, H., 1968. Origin of andesite and its bearing on the island arc structure.
Bull. volcan., 32, 141-176.

Lattimore, R.K., Weeks, L.A. and Mordock, L.W., 1971. Marine geophysical survey of continental margin north of Paria peninsular, Venezuela.
Bull. Am. Ass. Petrol. Geol., 55, 1719-1729.

Le Pichon, X. and Fox, P.J., 1971. Marginal offsets, fracture zones and the early opening of the North Atlantic.
J. geophys. Res., 76, 6294-6308.

Le Pichon, X. and Hayes, D.E., 1971. Marginal offsets, fracture zones and the early opening of the South Atlantic.
J. geophys. Res., 76, 6283-6293.

Lewis, J.F., 1971. Composition, origin and differentiation of basalt magma in the Lesser Antilles.
Mem. geol. Soc. Am., 130, 159-180.

Long, R.E., 1974. A compact portable seismic recorder.
Geophys. J. R. astr. Soc., 37, 91-98.

MacGillavry, H.J., 1970. Geological history of the Caribbean.
Koninkl. Nederlandsch Akad. Wetensch. Proc., Ser. B., 73, 64-96.

Macintyre, I.G., 1967. Submerged coral reefs, west coast of Barbados, W.I.
Can. J. Earth Sci., 4, 461-474.

Malfait, B.T. and Dinkelman, M.G., 1972. Circum-Caribbean tectonic and igneous activity and the evolution of the Caribbean plate.
Bull. geol. Soc. Am., 83, 251-272.

Maresch, W.V., 1973. Eclogitic-amphibolitic rocks on Isla Margarita, Venezuela. - A preliminary account.
Mem. geol. Soc. Am., 132, 429-437.

Maresch, W.V., 1974. Plate tectonics origin of the Caribbean Mountain system of northern South America : Discussion and proposals.
Bull. geol. Soc. Am., 85, 669-682.

Marlowe, J.I., 1968. Geological reconnaissance of parts of Aves Ridge.
Trans. 5th Caribbean geol. Conf., 50-51.

Martin-Kaye, P.H.A., 1969. A summary of the geology of the Lesser Antilles.
Overseas Geology and Mineral Resources Inst. Geol. Sci., 10 (2), 172-206.

Masson Smith, D.J. and Andrew, F.M., 1965. Gravity and magnetic measurements in the Lesser Antilles. (preliminary report and illustrations).
Overseas Geol. Survey, Lond., 166p.

Matthews, D.J., 1939. Tables of the velocity of sound in pure water and sea water for use in echo sounding and sound ranging.
Admiralty Office, London, 52p.

Mattinson, J.M., Fink, L.K. and Hopson, C.A., 1973. Age and origin of ophiolitic rocks on La Désirade Island, Lesser Antilles island arc.
Yb. Carnegie Instn. Wash., 72, 616-623.

Mereu, R.F., 1966. An iterative method for solving the time-term equations. in, Earth beneath the continents, eds., Steinhart, J.S. and Smith, T.J.,
Geophys. Monogr., 10, 495-497.

Metz, H.E., 1968. Geology of the El Pilar fault zone, state of Sucre, Venezuela.
Trans. 4th Caribbean geol. Conf., 293-299.

Mitchell, A.H. and Reading, H.G., 1971. Evolution of island arcs.
J. Geol., 79, 253-284.

Molnar, P. and Sykes, L.R., 1969. Tectonics of Caribbean and Middle America regions from focal mechanisms and seismicity.
Bull. geol. Soc. Am., 80, 1639-1684.

Molnar, P. and Sykes, L.R., 1971. Plate Tectonics in the Hispaniola area : discussion.
Bull. geol. Soc. Am., 82, 1123-1126.

Monroe, W.H., 1968. The age of the Puerto Rico Trench.
Bull. geol. Soc. Am., 79, 487-493.

Mota, L., 1954. Determination of the dips and depths of geological layers by the seismic refraction method.
Geophysics, 19, 242-254.

Murauchi, S. and Yasui, M., 1968. Geophysical investigations in the seas around Japan.
Kagaku, 38(4). (In Japanese).

Nagle, F., 1971. Rocks from seamounts and escarpments on the Aves Ridge.
Abstracts of 6th Caribbean geol. Conf. - Late arrivals, 3.

Ocola, L.C., 1972. A nonlinear least squares method for seismic refraction mapping.
Geophysics, 37, 260-287.

Officer, C.B., Ewing, J.I., Edwards, R.S. and Johnson, H.R., 1957. Geophysical investigations in the eastern Caribbean : Venezuela Basin, Antilles island arc, and Puerto Rico Trench.
Bull. geol. Soc. Am., 68, 359-378.

Officer, C.B., Ewing, J.I., Hennion, J.F., Harkrider, D.G. and Miller, D.E., 1959. Geophysical investigations in the eastern Caribbean : Summary of 1955 and 1956 cruises.
Physics Chem. Earth, 3, 17-109.

Press, F., 1966. Seismic velocities. Mem. geol. Soc. Am., 97, 195-219.

Raitt, R.W., 1956. Seismic refraction studies of the Pacific ocean basin. Part I : Crustal thickness of the central Equatorial Pacific.
Bull. geol. Soc. Am., 67, 1623-1640.

Raitt, R.W., Shor, G.G. Jr., Morris, G.B. and Kirk, H.K., 1971. Mantle anisotropy in the Pacific Ocean.
Tectonophysics, 12, 173-186.

Ringwood, A.E. and Green, D.H., 1966. Petrological nature of the stable continental crust. in, Earth beneath the continents, eds. Steinhart, J.S. and Smith, T.J.,
Geophys. Monogr., 10, 611-619.

Rod, E., 1956. Strike-slip faults of northern Venezuela.
Bull. Am. Ass. Petrol. Geol., 40, 457-476.

Saunders, J.B., 1968. Field guide to Barbados.
Trans. 4th Caribbean geol. Conf., 443-449.

Scheidegger, A.E. and Willmore, P.L., 1957. The use of a least squares method for the interpretation of data from seismic surveys.
Geophysics, 22, 9-22.

Senn, A., 1940. Paleogene of Barbados and its bearing on the history and structure of the Antillean - Caribbean region.
Bull. Am. Ass. Petrol. Geol., 24, 1548-1610.

Shimshoni, M. and Smith, S.W., 1964. Seismic signal enhancement with three-component detectors.
Geophysics, 29, 664-671.

Shor, G.G. Jr., 1963. Refraction and reflection techniques and procedure. in, The Sea, ed. Hill, M.N., 3, 20-38, Interscience.

Shor, G.G. Jr., 1964. Structure of the Bering Sea and the Aleutian Ridge.
Marine Geol., 1, 213-219.

Shor, G.G. Jr., Kirk, H.K. and Menard, H.W., 1971a. Crustal structure of the Melanesian area.
J. geophys. Res., 76, 2562-2586.

Shor, G.G. Jr., Menard, H.W., Raitt, R.W., 1971b. Structure of the Pacific Basin. in, The Sea, ed. Maxwell, A.E., 4, part 2, 3-28, Interscience.

Sugimura, A. and Uyeda, S., 1973. Island Arcs : Japan and its environs.
Developments in Geotectonics, 3, Elsevier.

Suzuki, Z., 1965. Maine seismic experiment; A study of shear waves.
Bull. seism. Soc. Am., 55, 425-439.

Sykes, L.R. and Ewing, M., 1965. The seismicity of the Caribbean region.
J. geophys. Res., 70, 5065-5074.

Talwani, M., Le Pichon, X. and Ewing, M., 1965. Crustal structure of the mid-ocean ridges (2) : Computed model from gravity and seismic refraction data.
J. geophys. Res., 70, 341-352.

Toksöz, M.N., Minear, J.W. and Julian, B.R., 1971. Temperature field and geophysical effects of a downgoing slab.
J. geophys. Res., 76, 1113-1138.

Tomblin, J.F., 1971. Seismicity and plate tectonics of the eastern Caribbean. Preprint of paper read at :
6th Caribbean geol. Conf., Margarite Is., Venezuela.

Tomblin, J.F., Sigurdsson, H. and Aspinall, W., 1972. Activity at the Soufriere Volcano, St. Vincent, West Indies, in October - November 1971. Nature, Lond., 235, 157-158.

Tschanz, C.M., Marvin, R.F., Cruz, J., Mehnert, H.H. and Cebula, G.T., 1974. Geologic evolution of the Sierra Nevada de Santa Marta, Northeastern Colombia. Bull. geol. Soc. Am., 85, 273-284.

Von Herzen, R.P., Simmons, G. and Folinsbee, A., 1970. Heat flow between the Caribbean Sea and the Mid Atlantic Ridge. J. geophys. Res., 75, 1973-1984.

Walsh, J.B., 1968. Attenuation in partially melted material. J. geophys. Res., 73, 2209-2216.

Walsh, J.B., 1969. New analysis of attenuation in partially melted rocks. J. geophys. Res., 74, 4333-4337.

Westbrook, G.K., 1973. Crust and upper mantle structure in the region of Barbados and the Lesser Antilles. Unpublished Ph.D. thesis, University of Durham.

Westbrook, G.K., Bott, M.H.P. and Peacock, J.H., 1973. The Lesser Antilles subduction zone in the region of Barbados. Nature. Phys. Sci., 244, 18-20.

Weyl, R., 1966. Geologie der Antillen. Gebrüder Borntraeger, Berlin, 410p.

Wiebenga, W.A., 1973. Crustal structure of the New Britain - New Ireland region. in, The Western Pacific : Island Arcs, Marginal Seas, Geochemistry; ed. Coleman, P.J. (University of Western Australia Press), 163-177.

Willmore, P.L. and Bancroft, A.M., 1960. The time-term approach to refraction seismology. Geophys. J.R. astr. Soc., 3, 419-432.

Wills, K.J.A., 1974. The geological history of southern Dominica and plutonic nodules from the Lesser Antilles. Unpublished Ph.D. thesis, University of Durham.

APPENDIX A

L.A.S.P. : 1972 : SHOT DATA

SHOT	SHOT DEPTH(m)	WATER DEPTH(m)	LATITUDE (NORTH)		LONGITUDE (WEST)		SHOT INSTANT (GMT)			
B53	129	4606	12°	57.3'	57°	06.6'	14th	02h	20m	51.76s
B52	127	4557	12	58.0	57	15.4		03	02	49.71
B51	124	4636	12	58.8	57	23.7		03	39	44.75
B50	132	4627	12	58.4	57	32.1		04	15	43.13
B49	129	4259	12	59.2	57	40.9		04	52	46.28
B48	135	3928	12	59.5	57	46.2		05	15	46.64
B47	138	3707	13	00.0	57	50.1		05	36	56.77
B46	124	3570	13	00.5	57	57.0		06	03	42.10
B45	132	3063	13	01.0	58	02.3		06	26	45.27
B44	127	3570	13	01.5	58	08.2		06	52	19.83
B43	118	3016	13	02.1	58	16.2		07	26	38.48
B41	129	2721	13	03.1	58	27.7		08	15	40.04
B40	135	2593	13	03.8	58	35.7		08	51	43.84
B39	124	2083	13	04.7	58	44.8		09	36	41.13
B38	127	1825	13	05.4	58	52.7		10	10	42.27
B37	140	1693	13	06.1	59	01.0		10	44	41.59

APPENDIX A (Continued)

L.A.S.P. : 1972 : SHOT DATA

SHOT	SHOT DEPTH(m)	WATER DEPTH(m)	LATITUDE (NORTH)		LONGITUDE (WEST)		SHOT INSTANT (GMT)			
B36	129	2279	13	06.7	59	10.1	14th	23	42	21.00
B35	138	1037	13	06.9	59	19.2	15th	00	18	47.40
B34	127	148	13	07.8	59	23.7		00	40	48.60
B33	132	170	13	12.4	59	39.7		03	00	57.32
B32	138	898	13	12.9	59	47.0		03	33	49.05
B31	132	1715	13	13.8	59	54.6		04	06	48.14
B30	129	2043	13	15.5	60	02.2		04	41	16.35
B29	143	2339	13	17.2	60	11.0		05	15	53.66
B28	135	2291	13	18.5	60	17.6		05	44	53.71
B27	138	2145	13	20.2	60	26.0		06	20	50.23
B26	121	1957	13	22.0	60	34.2		06	53	46.00
B25	129	1542	13	23.5	60	42.0		07	27	48.86
B24	154	984	13	25.1	60	49.7		08	00	54.92
B23	129	708	13	26.5	60	56.8		08	31	46.97

APPENDIX A (Continued)

L.A.S.P. : 1972 : SHOT DATA

SHOT	SHOT DEPTH(m)	WATER DEPTH(m)	LATITUDE (NORTH)		LONGITUDE (WEST)		SHOT INSTANT (GMT)			
A 1	138	203	14°	22.0'	60°	52.6'	16th	00h	16m	05.21s
A 2	135	967	14	18.4	60	53.5		00	35	46.75
A 3	132	927	14	14.6	60	54.4		00	52	46.15
A 4	135	243	14	11.1	60	55.9		01	10	47.20
A 5	bottom	29	14	07.4	60	55.7		01	34	59.54
A 6	129	529	13	41.1	61	01.1		04	31	48.78
A 7	140	1053	13	37.9	61	02.3		04	48	47.82
A 8	129	457	13	34.2	61	04.1		05	07	12.29
A 9	124	583	13	29.7	61	05.1		05	30	43.23
A10	132	1392	13	26.5	61	05.7		05	47	56.14
A11	135	401	13	21.9	61	06.9		06	14	46.12
A0.7	138	554	15	11.2	61	19.2	16th	22	45	48.16
A0.6	124	1022	15	40.8	61	30.0	17th	01	34	14.68
A0.5	bottom	60	15	48.8	61	33.8		02	16	23.46
A0.4	132	262	15	56.2	61	37.1		03	04	45.24
A0.3	bottom	37	16	23.8	61	47.1		06	02	42.41
A0.2	127	913	16	29.8	61	49.9		06	32	44.21

APPENDIX A (Continued)

L.A.S.P. : 1972 : SHOT DATA

SHOT	SHOT DEPTH(m)	WATER DEPTH(m)	LATITUDE (NORTH)		LONGITUDE (WEST)		SHOT INSTANT (GMT)			
C 1	129	176	15°	32.8'	63°	36.6'	19th	22	40	46.04
C 2	135	552	15	23.6	63	35.6		23	23	47.14
C 3	138	1165	15	14.1	63	34.2	20th	00	05	48.57
C 4	127	1315	15	03.8	63	32.1		00	51	45.43
C 5	129	1465	14	56.2	63	30.2		01	26	44.84
C 6	135	1598	14	46.2	63	28.2		02	10	47.52
C 7	132	1651	14	35.8	63	25.9		02	56	47.41
C 8	124	1587	14	26.9	63	24.1		03	36	43.43
C 9	143	1580	14	19.0	63	22.6		04	11	48.54
C10	124	1469	14	10.1	63	20.8		04	51	42.18
C11	135	1319	14	01.3	63	19.4		05	30	46.32
C12	146	1053	13	51.4	63	16.9		06	13	48.51
C13	127	1019	13	41.3	63	14.7		06	56	42.86
C14	146	333	13	32.7	63	12.5		07	38	48.70
C15	157	927	13	24.7	63	10.6		08	15	48.67
C16	140	1079	13	15.9	63	08.5		08	55	46.94
C18	127	1293	13	03.9	63	05.5		09	51	42.84
C19	135	2836	12	52.4	63	02.7		10	44	47.31

APPENDIX A (Continued)

L.A.S.P. : 1972 : SHOT DATA

SHOT	SHOT DEPTH(m)	WATER DEPTH(m)	LATITUDE (NORTH)		LONGITUDE (WEST)		SHOT INSTANT (GMT)			
A29	138	415	11°	45.5'	62°	03.8'	20th	22h	31m	01.53s
A27	bottom	33	11	52.1	61	56.3		23	23	12.08
A25	,,	27	11	58.3	61	47.2	21st	00	21	53.21
A24	,,	38	12	14.7	61	36.2		02	33	08.98
A23	,,	37	12	18.1	61	33.7		03	05	46.61
A21	,,	37	12	24.8	61	31.1		03	42	10.47
A20	,,	37	12	33.6	61	26.2		04	43	06.48
A18	,,	40	12	40.9	61	22.8		06	03	18.29
A17	,,	42	12	46.2	61	20.0		06	31	40.73
A16	,,	110	12	50.8	61	17.7		06	54	25.77
A14	,,	35	12	58.4	61	14.0		07	40	45.10
A13	154	454	13	05.3	61	12.2		08	20	20.66
B20	138	1957	13	26.9	61	12.0	21st	22	30	52.41
B19	129	2282	13	26.8	61	17.3		22	54	49.24
B18	129	2557	13	27.1	61	22.2		23	17	50.14
B17	127	2813	13	28.0	61	30.4		23	53	49.86
B16	135	2924	13	29.0	61	39.8	22nd	00	29	51.15

APPENDIX A (Continued)

L.A.S.P. : 1972 : SHOT DATA

SHOT	SHOT DEPTH(m)	WATER DEPTH(m)	LATITUDE (NORTH)		LONGITUDE (WEST)		SHOT INSTANT (GMT)			
B15	63	2955	13°	29.8'	61°	46.6'	22nd	00	58	25.34
B14	140	2972	13	30.8	61	57.3		01	44	52.71
B12	140	2981	13	32.1	62	08.4		02	31	54.07
B11	132	2979	13	33.2	62	19.2		03	18	50.00
B10	135	2979	13	33.9	62	27.8		03	54	50.40
B 9	127	2957	13	34.7	62	37.9		04	29	56.54
B 8	138	1915	13	35.5	62	47.0		05	10	49.73
B 7	143	1128	13	37.0	62	54.8		05	44	49.70
B 6	129	1136	13	36.1	63	02.8		06	27	47.64
B 3	129	876	13	35.5	63	22.7		08	02	47.62
B 1	135	1192	13	35.1	63	35.4		08	56	48.71
AO.8	132	2072	15	03.0	61	16.0	23rd	08	15	46.86
AO.9	135	931	14	54.5	61	12.0		08	58	48.24

L.A.S.P. 1972 : STATION DATA

Station Number	Station Name	Latitude (North)	Longitude (West)	Station Height above sea level (m)
001	St Lucia North	14°06.15'	60°56.51'	92
002	St Lucia South	13 42.58	60 56.62	230
003	Carriacou	13 29.42	61 26.93	197
004	Grenada North	12 13.16	61 39.21	121
005	Grenada South	11 59.93	61 45.35	15
006	Barbados Cole Cave	13 10.61	59 34.67	183
007	,, St Phillips	13 08.0	59 29.5	91
008	Aves Island	15 40.57	63 36.61	10
009	Discoverer 1	12 59.9	57 35.0	hydrophone
010	Discoverer 11	13 24.4	60 23.4	hydrophone
011	St Vincent SVT	13 10.08	61 14.70	38
012	St Vincent SVS	13 19.50	61 11.60	792
013	St Vincent SVR	13 19.24	61 10.15	595
014	Guadeloupe DHG	16 18.71	61 47.45	36
015	Guadeloupe MDG	16 10.78	61 46.43	37
016	Guadeloupe OBG	16 01.73	61 40.93	646
017	Guadeloupe LSG	15 52.71	61 34.70	110
018	Dominica PHD	15 33.11	61 27.60	50
019	Dominica LRD	15 24.12	61 24.60	17
020	Dominica GBD	15 14.55	61 20.00	170
021	Martinique GRM	14 52.25	61 10.60	130
022	Martinique OBM	14 44.00	61 09.01	510
023	Martinique FFM	14 37.00	61 04.05	145
024	Martinique DIM	14 29.00	61 01.48	42

APPENDIX A (continued) : UNCORRECTED FIRST ARRIVAL TRAVEL TIMES LINE A : DURHAM AND U.W.I. STATIONS

Shots	STATIONS 1	2	3	4	5	11	12	13
A0.7	18.99	-	-	-	-	-	-	-
A0.8	16.87	24.95	-	-	-	-	-	-
A0.9	13.89	22.38	-	-	-	-	-	-
A1	6.35	14.75	-	-	-	23.49	21.46	21.19
A2	5.48	13.58	32.68	-	-	22.72	-	-
A3	4.30	11.34	-	-	-	21.79	-	20.01
A4	2.47	10.00	30.49	-	-	20.70	-	18.18
A5	0.77	7.95	29.60	-	-	-	-	-
A6	8.50	2.32	22.71	28.21	-	11.53	8.88	8.75
A7	9.80	3.89	21.92	27.76	-	10.89	7.79	7.74
A8	10.63	4.69	20.76	-	-	-	6.63	6.40
A9	-	5.82	19.59	26.08	-	8.04	5.39	5.17
A10	13.67	6.94	19.00	-	-	7.38	4.87	-
A11	14.32	8.35	17.15	23.55	28.53	5.38	2.88	2.60
A13	19.78	13.51	12.97	18.62	22.80	3.33	6.28	6.01
A14	22.20	14.97	10.60	16.35	20.68	4.85	7.76	7.61
A16	-	17.46	8.00	13.74	18.16	7.39	10.37	10.35
A17	-	18.64	6.20	11.96	16.42	8.48	11.38	11.38
A18	-	20.09	4.54	10.29	14.73	10.29	13.40	13.47
A20	-	22.25	2.10	8.13	12.26	12.37	15.54	-
A21	-	-	2.75	5.60	10.10	15.21	-	-
A23	-	-	5.42	2.98	8.03	17.52	-	-
A24	-	-	6.61	1.66	6.93	-	-	-
A25	-	-	12.87	6.33	1.58	-	-	-
A27	-	-	15.68	9.39	5.43	-	-	-
A29	-	-	18.88	12.96	8.71	-	-	-

APPENDIX A (continued) : UNCORRECTED FIRST ARRIVAL TRAVEL TIMES LINE A : FRENCH STATIONS

	STATIONS										
SHOTS	14	15	16	17	18	19	20	21	22	23	24
A0.2	5.23	7.49	10.79	14.09	19.99	22.44	-	-	33.89	-	-
A0.3	2.49	4.99	8.19	11.49	17.69	20.09	-	-	31.39	-	-
A0.4	9.06	6.96	3.91	2.51	9.26	12.06	-	-	23.58	-	28.4
A0.5	11.34	9.14	6.14	2.10	6.80	-	-	-	21.34	-	(25.7)
A0.6	14.52	12.32	9.45	5.84	4.04	6.93	-	-	19.22	-	-
A0.7	-	-	-	-	9.04	5.80	2.29	-	10.49	13.04	15.1
A0.8	26.54	24.34	21.59	18.86	-	10.39	-	6.70	8.92	11.54	13.50
A0.9	27.76	25.96	23.36	20.56	14.36	11.86	-	2.22	4.70	7.36	9.68
A1	37.3	-	-	29.8	24.0	22.0	19.1	11.63	9.29	6.89	4.65
A2	38.8	36.5	33.9	32.1	25.57	23.11	-	12.70	10.65	8.25	6.05
A3	39.5	-	-	32.5	26.8	24.6	21.6	14.37	11.73	9.50	7.15
A4	-	37.4	-	-	-	25.2	22.0	14.5	11.98	9.8	7.5
A5	-	-	-	-	27.5	25.2	22.8	-	12.6	10.5	8.1
A6	-	45.6	-	-	(34.2)	32.7	29.1	-	19.5	-	-
A7	-	-	-	-	(35.1)	34.0	-	-	21.4	-	16.92
A8	-	-	-	-	35.8	34.4	-	-	22.5	-	17.31
A9	-	-	-	-	(36.6)	35.0	-	-	24.0	-	18.37
A10	-	-	-	-	38.2	35.6	-	-	25.11	-	19.76
A11	-	-	-	-	38.9	36.0	-	-	26.38	-	20.68
A13	-	-	-	-	-	-	-	-	30.3	-	-
A14	-	-	-	-	-	-	-	-	32.4	-	-

(values in parentheses are from unreliable 'picks')

APPENDIX A (continued) : UNCORRECTED FIRST ARRIVAL TRAVEL TIMES — LINE B : ALL STATIONS

	STATIONS										
SHOTS	1	2	3	4	6	7	10	11	12	13	22
B7	-	-	29.80	-	-	-	-	-	-	-	34.5
B8	-	-	-	-	-	-	-	-	27.08	-	(32.9)
B9	-	-	27.62	-	-	-	-	25.76	25.90	25.98	32.0
B10	-	-	-	-	-	-	-	24.11	-	-	30.7
B11	-	24.61	-	-	-	-	-	22.05	22.31	22.21	28.7
B12	-	22.53	-	-	-	-	-	-	-	-	27.8
B14	-	19.56	-	-	-	-	-	-	-	-	26.9
B15	-	18.03	22.65	-	-	-	-	-	15.42	15.42	26.4
B16	-	-	23.60	-	-	-	-	14.06	13.56	13.56	25.2
B17	-	14.57	22.33	-	-	-	-	11.78	11.51	11.54	25.2
B18	16.15	12.28	21.75	-	-	-	-	9.64	8.40	8.40	24.0
B19	15.56	10.68	20.60	27.00	-	-	-	8.52	6.48	6.54	24.2
B20	14.53	8.99	19.74	28.05	-	-	-	7.76	5.14	5.07	23.7
B23	-	6.56	19.80	26.68	-	-	14.60	8.43	6.35	6.03	23.1
B24	-	8.03	20.80	27.67	-	-	12.85	10.17	8.77	8.59	25.1
B25	-	10.18	21.73	28.22	-	-	11.22	12.49	11.27	10.87	26.7
B26	-	12.34	23.02	-	-	-	9.05	14.92	13.95	13.49	27.1
B27	-	14.75	24.82	30.84	20.03	-	5.49	17.41	16.62	16.33	29.0
B28	-	17.17	26.48	31.92	18.48	20.78	8.41	20.09	19.39	19.04	30.9
B29	-	18.95	27.49	32.41	-	19.35	11.43	-	-	22.43	31.8
B30	-	20.77	29.00	34.35	15.48	17.61	13.86	-	24.24	24.21	33.7
B31	-	-	30.19	35.25	12.36	14.78	16.33	-	25.79	25.56	34.8
B32	-	23.53	31.65	-	7.43	10.22	19.07	-	27.09	26.96	35.2
B33	-	24.76	-	-	-	-	-	-	-	-	38.7

APPENDIX B

SEISMOMETER CONFIGURATION AT DURHAM SEISMIC STATIONS

(1) Orientation of horizontal seismometers :

Station	Direction to which seismometer handle points NS Seismometer	EW Seismometer	Notes
LASP 1	N 4°W	E 4°S	
LASP 2	N16°E	E16°S	NS lined up with Pt Sable
LASP 3	N	W	Accurate from 14 April
LASP 4	S	W	
LASP 5	N	E	

(2) Order of seismometers on the magnetic tapes :

Station	Record track 1 Seismic I	3 Seismic II	5 Seismic III
LASP 1	NS	V	EW
LASP 2	NS	V	EW
LASP 3	V	EW	NS
LASP 4	NS	EW	V
LASP 5	NS	EW	V

Appendix C

REVERSED-PROFILE METHOD OF INTERPRETATION

(1) Single refractor case

the travel time down-dip is

$$t_{down} = \frac{x.\sin(i_c + \varphi)}{V_o} = \frac{2Z_1 \cos i_c}{V_o}$$

and the travel time up-dip is

$$t_{up} = \frac{x.\sin(i_c - \varphi)}{V_o} = \frac{2Z_2 \cos i_c}{V_o}$$

where φ is the dip angle component in the direction of the profile.

i_c is the critical angle for refraction along the refractor.

V_o is the overburden velocity (assumed constant)

Z_1, Z_2 are the lengths of the perpendiculars to the refractor below the up-dip and down-dip ends of the profile.

The apparent velocities observed are thus :

$$V_1 \text{ down} = V_{o/\sin(i_c + \varphi)} \quad ; \quad V_1 \text{ up} = V_{o/\sin(i_c - \varphi)}$$

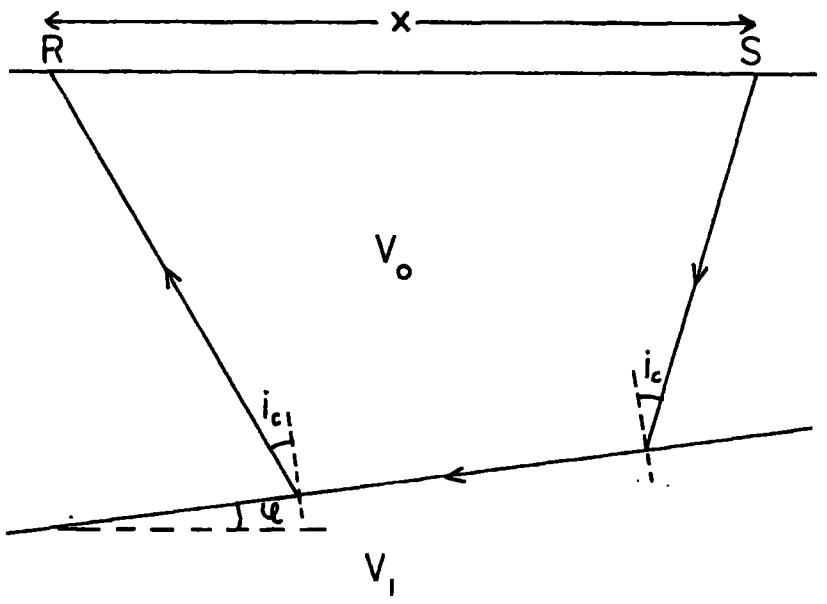

it follows that : $\varphi = \frac{1}{2}\left(\sin^{-1}\frac{V_o}{V_1 down} - \sin^{-1}\frac{V_o}{V_1 up}\right)$

$$i_c = \frac{1}{2}\left(\sin^{-1}\frac{V_o}{V_1 down} - \sin^{-1}\frac{V_o}{V_1 up}\right)$$

$$V_1 = V_o/\sin i_c$$

$$Z_n = \frac{V_o T_{in}}{2\cos i_c} \qquad n = 1,2$$

where T_{i_1}, T_{i_2} are the time intercepts observed at the up-dip and down-dip ends of the profile.

(2) n-refractor case :

A full discussion of the theory is given in Mota (1954). See Fig. C-1 for notation.

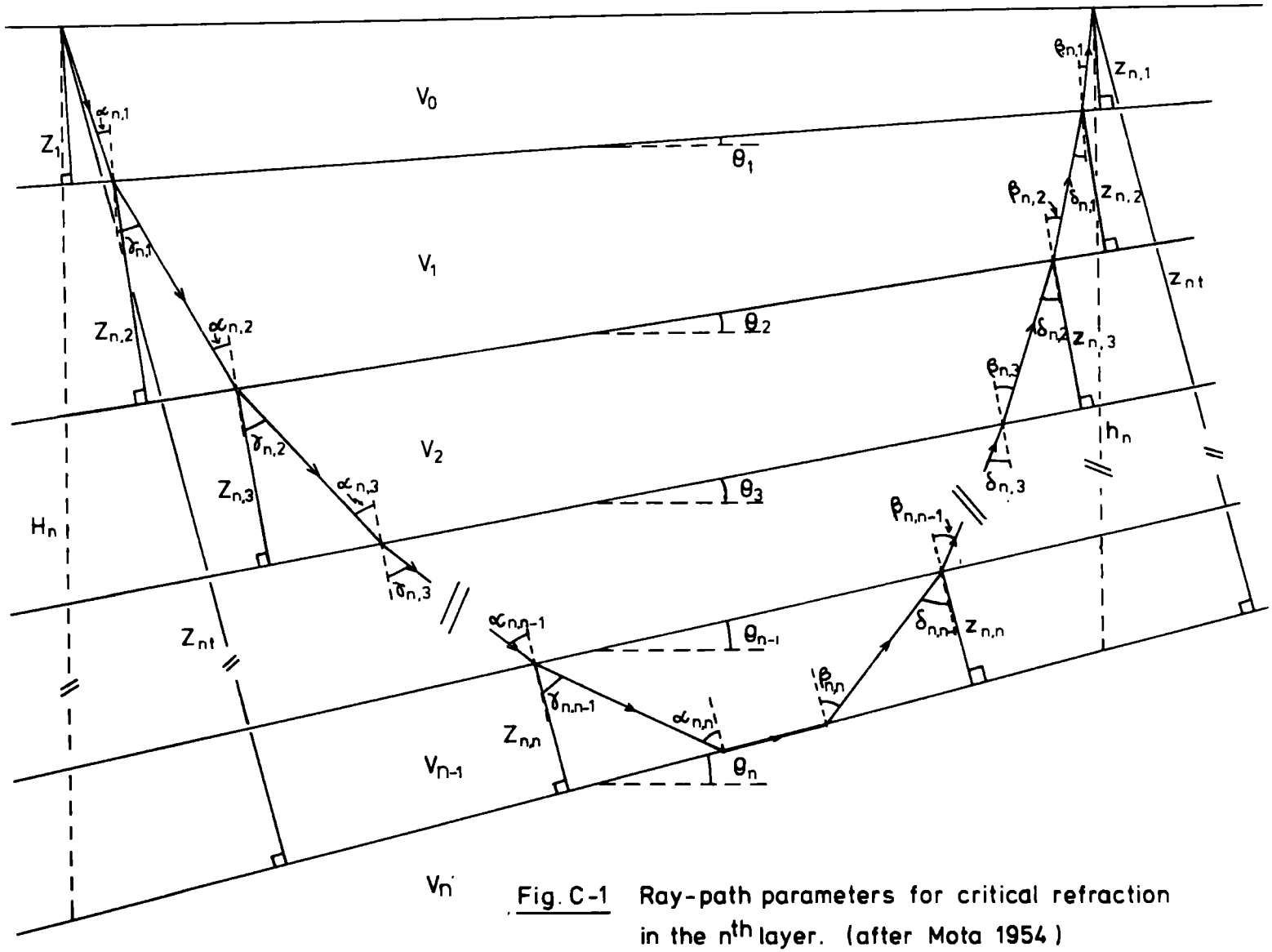

Fig. C-1 Ray-path parameters for critical refraction in the n^{th} layer. (after Mota 1954)

The travel time for a ray critically refracted in the n^{th} refractor is, for x increasing to the right in Fig. C-1.

$$T_{na} = \frac{x}{V_o} .\sin(\beta_{n,1} - \theta_1) + \sum_{L=1}^{n-1} \frac{Zn,L}{V_{L-1}} \frac{\cos(\alpha_{n,L} + \beta_{n,L}) + 1}{\cos \alpha_{n,L}}$$

$$+ \frac{Z_{n,n}}{V_{n-1}} .2.\cos i_n$$

and, for x increasing to the left :

$$T_{nb} = \frac{x}{V_o} .\sin(\alpha_{n,1} + \theta_1) + \sum_{L=1}^{n-1} \frac{z_{n,L}}{V_{L-1}} \frac{\cos(\alpha_{n,L} + \beta_{n,L}) + 1}{\cos \beta_{n,L}}$$

$$+ \frac{z_{n,n}}{V_{n-1}} .2.\cos i_n$$

The following recursive formulae apply :

$$\alpha_{n,m} = \gamma_{n,m-1} - \theta_m + \theta_{m-1}$$

$$\beta_{n,m} = \delta_{n,m-1} + \theta_m - \theta_{m-1} \qquad m = 2,n \qquad (1)$$

$$\theta_n = \frac{\gamma_{n,n-1} - \delta_{n,n-1}}{2} + \theta_{n-1}$$

$$i_n = \frac{\gamma_{n,n-1} + \delta_{n,n-1}}{2} \qquad (2)$$

$$\frac{\sin \alpha_{n,m}}{\sin \gamma_{n,m}} = \frac{\sin \beta_{n,m}}{\sin \delta_{n,m}} = \sin i_m = \frac{V_{m-1}}{V_m} \qquad m = 1,n-1 \qquad (3)$$

$$\sin \alpha_{n,n} = \sin \beta_{n,n} = \sin i_n = \frac{V_{n-1}}{V_n} \quad (\gamma_{n,n} = \delta_{n,n} = \pi/2) \qquad (4)$$

$$V_n = \frac{V_{n-1}}{\sin i_n} \qquad (5)$$

$$Z_{n,n} = \left[T_{na(i)} - \sum_{L=1}^{n-1} \frac{Z_{n,L} \cdot \cos(\alpha_{n,L} + \beta_{n,L})}{\cos \alpha_{n,L}} + 1 \right] x \left[\frac{V_{n-1}}{2 \cos i_n} \right] \quad (6)$$

$$H_n = \frac{Z_{n,t}}{\cos \theta_n} = \frac{1}{\cos \theta_n} \left[\sum_{L=1}^{n-1} \left(\frac{Z_{n,L} \cos(\alpha_{n,L} - \theta_n + \theta_L)}{\cos \alpha_{n,L}} \right) + Z_{n,n} \right] \quad (7)$$

$$z_{n,n} = \left[T_{nb(i)} - \sum_{L=1}^{n-1} \frac{z_{n,L} \cdot \cos(\alpha_{n,L} + \beta_{n,L}) + 1}{V_{L-1} \cdot \cos \beta_{n,L}} \right] x \left[\frac{V_{n-1}}{2 \cos i_n} \right] \quad (8)$$

$$h_n = \frac{z_{n,t}}{\cos \theta_n} = \frac{1}{\cos \theta_n} \left[\sum_{L=1}^{n-1} \left(\frac{z_{n,L} \cos(\beta_{n,L} + \theta_n - \theta_L)}{\cos \beta_{n,L}} \right) + z_{n,n} \right] \quad (9)$$

where $T_{na(i)}$, $T_{nb(i)}$ are the time intercepts observed at either end.

Appendix D

THE MODIFIED 'PLUS-MINUS' METHOD OF INTERPRETATION

A detailed discussion of the method is given in Hagedoorn (1959). Its practical application is outlined here.

Consider two receiving stations A,B at either end of a line of shots of which C is typical (see Figure D-1).

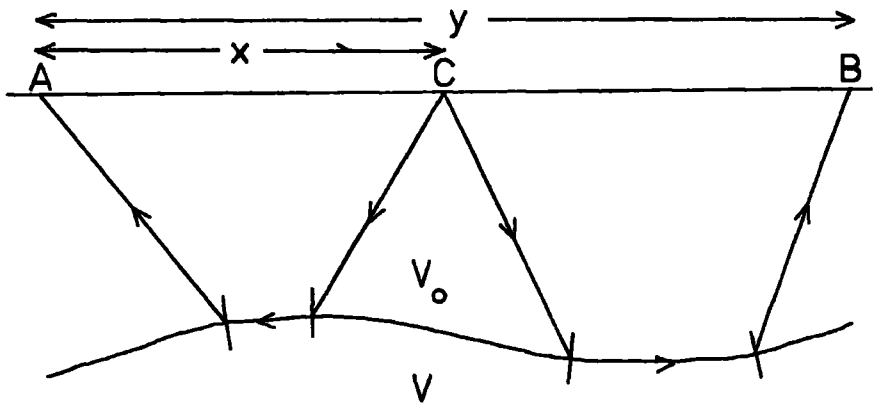

Fig. D-1

The following approximate travel times can be deduced :

travel time from C to A,

$$t_1 = \frac{x}{V} + a + c$$

travel time from C to B,

$$t_2 = \frac{y-x}{V} + b + c$$

travel time from A to B,

$$t_{12} = \frac{y}{V} + a + b$$

a,b,c are delay times below A,B,C.

we can define

'Plus' time, $P = t_1 + t_2 - t_{12}$

$$= \frac{y}{V} + a + b + 2c - \frac{y}{V} - a - b = 2c.$$

'Minus' time, $M = t_2 - t_1$

$$= \frac{y-2x}{V} - a + b$$

The graph of 'minus' time against (y - 2x) is a curve whose tangent at any point represents the reciprocal of the refractor velocity at the position appropriate to the x-value at that point. If V is constant along the profile, then the 'minus' time graph is a straight line with gradient $^1/_V$ and intercept (b-a) on the M axis. The 'minus' times can be used directly to indicate the degree of velocity variation along the refractor.

The true 'plus' time, P, equals twice the delay below the shot site and can be used to find an estimate of the depth to the refractor below the site using the approximate relation,

$$i = P_i \frac{Vo\ Vi}{2\left[Vi^2 - Vo^2 \right]^{\frac{1}{2}}}$$

where, P_i is the 'plus' time at site i

V_i is the refractor velocity below site i.

V_o is the overburden velocity (assumed constant).

However, the true 'plus' time cannot be measured as no shot is fired at the site of either station to give a value for t_{12}. The times $(t_1 + t_2)$ for each shot site will indicate accurate relative variations of depth to the refractor. Also, t_{12} can be estimated from the travel time from the shot closest to the station at the far end of

the line of shots. If the separation of the station from the nearest shot is dx and the refractor in the region below the shot and station has constant velocity V and constant dip θ, then the estimated value of t_{12} is,

$$t_{12} = \text{(measured travel time)} + \frac{dx}{\cos i}\left(\frac{\cos(i-\theta)}{V} - \frac{\sin\theta}{V_o}\right)$$

where $i = \sin^{-1}\left(V_o/V\right)$

the last term approximates to $\frac{dx}{V}$ when θ is small. An iterative procedure can be used to improve the estimated 'plus' time if θ is not small (i.e. $\theta \gtrsim 5^o$).

APPENDIX E

Listings of computer programs

TIMES

DEP2

DEPN

All the programs were written in Fortran IV for use on the NUMAC IBM 360/67 computer.

The theory of the programs is given in Chapter 3.

TIMES : Time-term analysis program (after Mereu, 1966).

DEP2 : Calculates depths from time-terms for two refractors assuming the upper refractor is overlain by a single layer of known velocity.

DEPN : Calculates depths from time-terms for the (N - 1)th and Nth refractors given the velocities of all the layers and the thicknesses of the top (N - 2) layers. DEPN outputs the thicknesses of the (N - 1)th and Nth layers and the total depths to the (N - 1)th and Nth refractors.

Details of the input format for these programs are included in the listings which follow this page.

```
C     ------------- TIMES --------------
C
C     TIME-TERM ANALYSIS PROGRAM
C
C     USES ITERATIVE METHOD OF MEREU (1966)
C
C     Q = DATA SET NO.
C     N = NO. OF SHOT SITES
C     M = NO. OF STATION SITES
C     CPAR = CONVERGENCE PARAMETER
C     ITMAX = MAX. NO. OF ITERATIONS ALLOWED
C     I (=1,N) = SHOT SITE NO.
C     J (=1,M) = STAT. SITE NO.
C     P(I,J) = 1. IF T(I,J) EXISTS AS DATA
C            = 0. IF T(I,J) DOES NT EXIST
C     T(I,J) = TRAVEL TIME FROM ITH SHOT TO JTH STATION
C     X(I,J) = DISTANCE    FROM ITH SHOT TO JTH STATION
C     ------------------------------------
C
      DIMENSION X(100,100),T(100,100),RI(100),TI(100),DI(100),RJ(100),
     1TJ(100),DJ(100),XX(100),YY(100),SUMY(100),SUMX(100),W(100),U(100),
     2SUMW(100),SUMU(100),C(100,100),D(100,100),
     3XLAST(100),WLAST(100),ULAST(100),YLAST(100)
      COMMON P(100,100),RES(100,100),A(100),B(100),N,M
      REAL NUM
   50 READ(5,1)Q,N,M,CPAR,ITMAX
      IF(Q)52,51,52
   52 WRITE(6,2) Q
      DO 11 I=1,N
      DO 12 J=1,M
      P(I,J)=0.0
      T(I,J)=0.0
      X(I,J)=0.0
   12 CONTINUE
   11 CONTINUE
      DO 16 I=1,N
```

```
      READ(5,3)(P(I,J),J=1,M)
   16 CONTINUE
      DO 19 I=1,N
      DO 18 J=1,M
      IF(P(I,J).EQ.0.0) GO TO 66
      READ(5,4)T(I,J),X(I,J)
   66 CONTINUE
   18 CONTINUE
   19 CONTINUE
      DO 21 I=1,N
      RI(I)=0.0
      TI(I)=0.0
      DI(I)=0.0
      DO 22 J=1,M
      RI(I)=RI(I)+P(I,J)
      TI(I)=TI(I)+(P(I,J)*T(I,J))
      DI(I)=DI(I)+(P(I,J)*X(I,J))
   22 CONTINUE
      WRITE(6,70) RI(I),TI(I),DI(I)
   70 FORMAT(1X,3F10.3)
   21 CONTINUE
      DO 23 J=1,M
      RJ(J)=0.0
      TJ(J)=0.0
      DJ(J)=0.0
      DO 24 I=1,N
      RJ(J)=RJ(J)+P(I,J)
      TJ(J)=TJ(J)+(P(I,J)*T(I,J))
      DJ(J)=DJ(J)+(P(I,J)*X(I,J))
   24 CONTINUE
      WRITE(6,70) RJ(J),TJ(J),DJ(J)
   23 CONTINUE
      L=0
      DO 25 J=1,M
      YY(J)=0.0
      W(J)=0.0
```

```
25 CONTINUE
   L=L+1
   IF(L.GT.ITMAX) GO TO 64
   DO 26 I=1,N
   SUMY(I)=0.0
   SUMW(I)=0.0
   IF(L.EQ.1) GO TO 34
   XLAST(I)=XX(I)
   ULAST(I)=U(I)
34 DO 27 J=1,M
   SUMY(I)=SUMY(I)+(P(I,J)*YY(J))
   SUMW(I)=SUMW(I)+(P(I,J)*W(J))
27 CONTINUE
26 CONTINUE
   DO 28 I=1,N
   XX(I)=(TI(I)-SUMY(I))/RI(I)
   U(I)=(-DI(I)-SUMW(I))/RI(I)
28 CONTINUE
   DO 29 J=1,M
   SUMX(J)=0.0
   SUMU(J)=0.0
   IF(L.EQ.1) GO TO 35
   YLAST(J)=YY(J)
   WLAST(J)=W(J)
35 DO 31 I=1,N
   SUMX(J)=SUMX(J)+(P(I,J)*XX(I))
   SUMU(J)=SUMU(J)+(P(I,J)*U(I))
31 CONTINUE
29 CONTINUE
   DO 32 J=1,M
   YY(J)=(TJ(J)-SUMX(J))/RJ(J)
   W(J)=(-DJ(J)-SUMU(J))/RJ(J)
32 CONTINUE
   IF(L.EQ.1)GO TO 25
   DX=ABS(XLAST(N)-XX(N))
   DU=ABS(ULAST(N)-U(N))
```

```
      DY=ABS(YLAST(M)-YY(M))
      DW=ABS(WLAST(M)-W(M))
      IF(DX.LT.CPAR.AND.DY.LT.CPAR.AND.DW.LT.CPAR.AND.DU.LT.CPAR)GOTO 33
      GO TO 25
   64 WRITE(6,8)L,CPAR
      GO TO 100
   33 WRITE(6,5)L,CPAR
      WRITE(6,6)
      DO 67 I=1,N
      WRITE(6,7) I,XX(I),U(I)
   67 CONTINUE
      WRITE(6,14)
      DO 68 J=1,M
      WRITE(6,7) J,YY(J),W(J)
   68 CONTINUE
      NUM=0.0
      DEN=0.0
      DO 41 I=1,N
      DO 42 J=1,M
      IF(P(I,J).EQ.0.) GO TO 42
      C(I,J)=P(I,J)*(XX(I)+YY(J)-T(I,J))
      D(I,J)=P(I,J)*(U(I)+W(J)+X(I,J))
      NUM=NUM+(D(I,J)*D(I,J))
      DEN=DEN+(D(I,J)*C(I,J))
   42 CONTINUE
   41 CONTINUE
      WRITE(6,71) NUM,DEN
C
C     V = COMPUTED LEAST-SQUARES VELOCITY
C
      V=-NUM/DEN
      DO 43 I=1,N
C
C     A(I) = SHOT TIME-TERM
C
      A(I)=XX(I)+(U(I)/V)
```

```
   43 CONTINUE
      DO 44 J=1,M
C
C     B(J) = STAT. TIME-TERM
C
      B(J)=YY(J)+(W(J)/V)
   44 CONTINUE
      WRITE(6,15)
      NUM=0.0
      DEN=0.0
      DO 45 I=1,N
      DO 46 J=1,M
      IF(P(I,J).EQ.0) GO TO 46
C
C     RES(I,J) = TRAVEL TIME RESIDUAL FOR CONNECTION I,J
C
      RES(I,J)=T(I,J)-X(I,J)/V-A(I)-B(J)
      WRITE(6,17) I,J,T(I,J),X(I,J),C(I,J),D(I,J),RES(I,J)
      NUM=NUM+(RES(I,J)**2)*P(I,J)
      DEN=DEN+P(I,J)
   46 CONTINUE
   45 CONTINUE
      DEN=DEN-(N+M+1)
      IF(DEN.LE.0.5)GO TO 47
C
C     SIGMAV = STANDARD DEVIATION ON THE VELOCITY
C
      SIGMAV=SQRT(NUM/DEN)
      WRITE(6,9)
      WRITE(6,10) V,SIGMAV
      GO TO 48
   47 WRITE(6,13) V
   48 CALL ERRORS
  100 CONTINUE
      GO TO 50
   51 CONTINUE
```

```
    1 FORMAT(F3.0,2I3,F6.3,I3)
    2 FORMAT(1X,2HQ=,F3.0)
    3 FORMAT(40F2.0)
    4 FORMAT(2F8.3)
    5 FORMAT(/27H  CONVERGENCE REACHED AFTER,I3,12H  ITERATIONS,10X,
     16HCPAR= ,F6.3)
    6 FORMAT(/5X,'I',7X,'X(I)',7X,'U(I)'/)
    7 FORMAT(3X,I3,2(3X,F8.3))
    8 FORMAT(/32H  CONVERGENCE NOT OBTAINED AFTER,I3,12H  ITERATIONS,10X
     1,6HCPAR= ,F6.3//17HPROGRAM ABANDONED)
    9 FORMAT(//2X,'CALCULATED VELOCITY',5X,'STD.DEV.OF VELOCITY'/)
   10 FORMAT(10X,F6.3,15X,F8.6)
   13 FORMAT(10X,F6.3)
   14 FORMAT(/5X,'I',7X,'Y(I)',7X,'W(I)'/)
   15 FORMAT(//4X,'I',3X,'J',7X,'T(I,J)',3X,'X(I,J)',3X,'C(I,J)',3X,'D(I
     1,J)',1X,'RES(I,J)'/)
   17 FORMAT(1X,2I4,4X,5F9.3)
   71 FORMAT(1X,2F10.3)
      END
C
      SUBROUTINE ERRORS
C     -----------------
C
C     ERROR CALCULATIONS FOLLOWING BERRY & WEST (1966)
C
      COMMON P(100,100),RES(100,100),A(100),B(100),N,M
      REAL NUM
      WRITE(6,101)
      DO 5000 I=1,N
      NUM=0.
      DEN=0.
      DO 6000 J=1,M
      NUM=NUM+(RES(I,J)**2)*P(I,J)
      DEN=DEN+P(I,J)
 6000 CONTINUE
      DEN=DEN-1.
```

```
      IF(DEN.LE.0.5) GO TO 7000
C
C     SIGMA = STANDARD DEVIATION ON A TIME-TERM
C
      SIGMA=SQRT(NUM/DEN)
C
C     SIGMAS = STANDARD ERROR ON A TIME-TERM
C
      SIGMAS=SIGMA/SQRT(DEN+1)
      WRITE(6,102) I,A(I),SIGMA,SIGMAS
      GO TO 5000
 7000 WRITE(6,103) I,A(I)
 5000 CONTINUE
      DO 3000 J=1,M
      NUM=0.
      DEN=0.
      DO 4000 I=1,N
      NUM=NUM+(RES(I,J)**2)*P(I,J)
      DEN=DEN+P(I,J)
 4000 CONTINUE
      DEN=DEN-1.
      IF(DEN.LE.0.5) GO TO 8000
      SIGMA=SQRT(NUM/DEN)
      SIGMAS=SIGMA/SQRT(DEN+1)
      WRITE(6,102) J,B(J),SIGMA,SIGMAS
      GO TO 3000
 8000 WRITE(6,103) J,B(J)
 3000 CONTINUE
  101 FORMAT(//2X,'SHOT/STAT NO.',2X,'TIME TERM',2X,'STD.DEV',2X,'STD.ER
     1ROR'/)
  102 FORMAT(I9,9X,F6.2,4X,F8.5,F10.5)
  103 FORMAT(I9,9X,F6.2)
      END
```

```
C      --------------- DEP2 ---------------
C
C      PROGRAM TO COMPUTE LAYER THICKNESSES FROM TIME-TERMS
C
C      ASSUMES ONE 'AVERAGE-VELOCITY' SEDIMENT LAYER
C      V1 = AVR. WATER VELOCITY;V2 = AVR. SED. VEL.
C      V3 = UPPER CRUSTAL LAYER VELOCITY
C      V4 = LOWER CRUSTAL LAYER / UPPERMOST MANTLE VEL.
C      DV3,DV4 = ERRORS ON V3,V4
C      DZW = RELIABILITY OF WATER DEPTHS
C      N = NO. OF SITES
C      ZW = WATER DEPTH BELOW SITE
C      TTG = UPPER CRUSTAL LAYER TIME-TERM
C      TTN = LOWER CRUSTAL LAYER/MANTLE TIME-TERM
C      DTG,DTN = ERRORS ON TTG,TTN
C      K = SITE CODE NO.
C      ------------------------------------
C
       DIMENSION TTG(50),TTN(50),ZW(50),Z2(50),Z3(50),ZM(50),DZ2(50),
      1 DZ3(50),DTG(50),DZM(50),DTN(50),K(50)
       WRITE(6,4)
   20  READ(5,1) V1,V2,V3,V4,DV3,DV4,DZW
       READ(5,2) N
       WRITE(6,5) V1,V2,V3,V4,DV3,DV4
       WRITE(6,6)
       F13=SQRT((1./V1**2)-(1./V3**2))
       F23=SQRT((1./V2**2)-(1./V3**2))
       F14=SQRT((1./V1**2)-(1./V4**2))
       F24=SQRT((1./V2**2)-(1./V4**2))
       F34=SQRT((1./V3**2)-(1./V4**2))
       DF13=DV3/(V3**3)*F13
       DF23=DV3/(V3**3)*F23
       DF14=DV4/(V4**3)*F14
       DF24=DV4/(V4**3)*F24
       DF34=SQRT((2.*DV3/V3**3)+(2.*DV4/V4**3))/2.*F34
       DO 10 I=1,N
```

```
      READ(5,3) ZW(I),TTG(I),DTG(I),TTN(I),DTN(I),K(I)
C
C     Z2(I) = THICKNESS OF SEDIMENT LAYER BENEATH SITE I
C
      Z2(I)=(TTG(I)-F13*ZW(I))/F23
C
C     Z3(I) = THICKNESS OF UPPER CRUSTAL LAYER BENEATH SITE I
C
      Z3(I)=(TTN(I)-(ZW(I)*F14+Z2(I)*F24))/F34
C
C     ZM(I) = DEPTH TO BASE OF UPPER CRUSTAL LAYER BENEATH SITE I
C
      ZM(I)=ZW(I)+Z2(I)+Z3(I)
      IF(ZW(I).LT.0.005) GO TO 50
C
C     DZ2,DZ3,DZM = ERRORS ON Z2,Z3,ZM
C
      DZ2(I)=Z2(I)*((SQRT((F13*ZW(I)*((DF13/F13)+(DZW/ZW(I))))**2+DTG(I)
     1**2)/(TTG(I)-(F13*ZW(I))))-(DF23/F23))
      DZ3(I)=Z3(I)*((SQRT(DTN(I)**2+(Z2(I)*F24*(DZ2(I)/Z2(I)+DF24/F24))*
     1*2+(ZW(I)*F14*(DZW/ZW(I)+DF14/F14))**2))/(TTN(I)-(ZW(I)*F14+Z2(I)*
     2F24))-DF34/F34)
      DZM(I)=SQRT(DZW**2+DZ2(I)**2+DZ3(I)**2)
      GO TO 60
   50 CONTINUE
      DZ2(I)=Z2(I)*(DTG(I)/TTG(I)-DF23/F23)
      DZ3(I)=Z3(I)*((SQRT(DTN(I)**2+(Z2(I)*F24*(DZ2(I)/Z2(I)+DF24/F24))*
     1*2))/(TTN(I)-(Z2(I)*F24))-DF34/F34)
      DZM(I)=SQRT(DZ2(I)**2+DZ3(I)**2)
   60 CONTINUE
      WRITE(6,7) K(I),TTG(I),DTG(I),TTN(I),DTN(I),ZW(I),Z2(I),DZ2(I),
     1Z3(I),DZ3(I),ZM(I),DZM(I)
   10 CONTINUE
      READ(5,8) L
      IF(L)30,30,20
   30 CONTINUE
```

```
1 FORMAT(7F5.2)
2 FORMAT(I2)
3 FORMAT(F6.3,F5.2,F6.3,F5.2,F6.3,1X,I3)
4 FORMAT('1',10X,'THICKNESSES OF CRUSTAL LAYERS FROM TIME-TERMS'/
 1 10X,45(1H_) )
5 FORMAT(///'VELOCITY MODEL',5X,'V1=',F5.2,2X,'V2=',F5.2,2X,'V3=',F5
 1.2,2X,'V4=',F5.2/40X,'(',F5.2,')',4X,'(',F5.2,')')
6 FORMAT(//'SHOT/STAT NO.',5X,'TTG',4X,'DTG',5X,'TTN',4X,'DTN',5X,'Z
 1W',5X,'Z2',4X,'DZ2',4X,'Z3',4X,'DZ3',4X,'ZM',4X,'DZM')
7 FORMAT(5X,I3,10X,F5.2,2X,F5.3,3X,F5.2,2X,F5.3,2X,F6.3,1X,F5.2,1X,
 1F6.3,1X,F5.2,1X,F6.3,1X,F5.2,1X,F6.3)
8 FORMAT(I1)
  STOP
  END
```

```
C      --------------- DEPN ---------------
C
C      PROGRAM TO COMPUTE LAYER THICKNESSES FROM TIME-TERMS
C
C      UP TO SIX SEDIMENT LAYERS CAN BE INCLUDED
C      M = NO. OF LAYERS
C      L = NO. OF SITES
C      V(I) = VELOCITY IN LAYER I
C      DV1,DV2 = ERROR ON VELOCITIES DETERMINED BY TIME-TERM ANALYSIS
C      K = SITE CODE NO.
C      TTG = TIME-TERM FOR CRIT. REFRACTION IN THE (M-1)TH LAYER
C      TTN = TIME-TERM FOR CRIT. REFRACTION IN THE M TH LAYER
C      DTG,DTN = ERRORS ON TTG,TTN
C      Z(I,J) = THICKNESS OF JTH LAYER BENEATH ITH SHOT
C      -----------------------------------
C
       DIMENSION TTG(50),TTN(50),DTN(50),DTG(50),Z(50,10),K(50),V(10),
      1F(10,10),DF(10,10),SUM1(50),SUM2(50),SUMZ(50),Z1(50),Z2(50),ZQ(50)
      2,ZM(50),DSUM1(50),ESUM1(50),DSUM2(50),FSUM2(50),DZ1(50),DZQ(50),
      3DZ2(50),DZM(50)
       INTEGER Q,P,G
       DZ=0.005
       WRITE(6,4)
   50  READ(5,1)M,L
       IF(M) 55,60,55
   55  CONTINUE
       READ(5,2)(V(I),I=1,M)
       READ(5,3) DV1,DV2
       WRITE(6,6)(V(I),I=1,M)
       WRITE(6,8) DV1,DV2
       WRITE(6,9)
       N=M-2
       P=M-3
       DO 10 I=1,L
       READ(5,5) K(I),TTG(I),DTG(I),TTN(I),DTN(I),(Z(I,J),J=1,P)
   10  CONTINUE
```

```
      Q=M-1
      DO 20 I=1,Q
      DO 30 J=Q,M
      IF(I.EQ.J) GO TO 30
      F(I,J)=SQRT((1./V(I)**2)-(1./V(J)**2))
      IF(J.EQ.Q) GO TO 22
      IF(I.EQ.Q) GO TO 21
      DF(I,J)=DV2/(V(J)**3)*F(I,J)
      GO TO 30
   22 DF(I,J)=DV1/(V(J)**3)*F(I,J)
      GO TO 30
   21 DF(I,J)=SQRT((2.*DV1/V(I)**3)+(2.*DV2/V(J)**3))/2.*F(I,J)
   30 CONTINUE
   20 CONTINUE
      DO 40 I=1,L
      SUM1(I)=0.
      SUM2(I)=0.
      SUMZ(I)=0.
      DSUM1(I)=0.
      DSUM2(I)=0.
      ESUM1(I)=0.
      ESUM2(I)=0.
      DO 41 G=1,P
      IF(Z(I,G).EQ.0.0) GO TO 41
      SUM1(I)=SUM1(I)+Z(I,G)*F(G,Q)
      SUM2(I)=SUM2(I)+Z(I,G)*F(G,M)
      SUMZ(I)=SUMZ(I)+Z(I,G)
      DSUM1(I)=DSUM1(I)+(Z(I,G)*F(G,Q)*(DZ/Z(I,G)+DF(G,Q)/F(G,Q)))**2
      ESUM1(I)=ESUM1(I)+Z(I,G)*F(G,Q)
      DSUM2(I)=DSUM2(I)+(Z(I,G)*F(G,M)*(DZ/Z(I,G)+DF(G,M)/F(G,M)))**2
      ESUM2(I)=ESUM2(I)+Z(I,G)*F(G,M)
   41 CONTINUE
C
C     Z1(I) = THICKNESS OF (M-2)TH LAYER BENEATH ITH SITE
C     ZQ(I) = DEPTH TO BASE OF (M-2)TH LAYER BENEATH ITH SITE
C     Z2(I) = THICKNESS OF (M-1)TH LAYER BENEATH ITH SITE
```

```
C      ZM(I) = DEPTH TO BASE OF (M-1)TH LAYER BENEATH ITH SITE
C
       Z1(I)=(TTG(I)-SUM1(I))/F(N,Q)
       DZ1(I)=Z1(I)*((SQRT(DSUM1(I)+DTG(I)**2)/(TTG(I)-ESUM1(I)))-DF(N,Q)
      1/F(N,Q))
       ZQ(I)=SUMZ(I)+Z1(I)
       DZQ(I)=SQRT(P*(DZ**2)+DZ1(I)**2)
       Z2(I)=(TTN(I)-(SUM2(I)+Z1(I)*F(N,M)))/F(Q,M)
       DZ2(I)=Z2(I)*((SQRT(DSUM2(I)+(Z1(I)*F(N,M)*(DZ1(I)/Z1(I)+DF(N,M)/F
      1(N,M)))**2+DTN(I)**2)/(TTN(I)-(ESUM2(I)+Z1(I)*F(N,M))))-DF(Q,M)/F(
      2Q,M))
       ZM(I)=ZQ(I)+Z2(I)
       DZM(I)=SQRT(P*(DZ**2)+DZ1(I)**2+DZ2(I)**2)
C
C      DZ1,DZQ,DZ2,DZM = ERRORS ON Z1,ZQ,Z2,ZM
C
       WRITE(6,7) K(I),TTG(I),DTG(I),TTN(I),DTN(I),Z1(I),DZ1(I),ZQ(I),
      1DZQ(I),Z2(I),DZ2(I),ZM(I),DZM(I),(Z(I,J),J=1,P)
   40 CONTINUE
       GO TO 50
    1 FORMAT(2I2)
    2 FORMAT(10F8.2)
    3 FORMAT(2F8.2)
    4 FORMAT('1',10X,'THICKNESS OF CRUSTAL LAYERS FROM TIME-TERMS'/10X,
      145(1H_))
    5 FORMAT(I3,F5.2,F6.3,F5.2,F6.3,9F6.2)
    6 FORMAT(///'VELOCITY MODEL',5X,10F6.2)
    7 FORMAT(3X,I3,4X,17F6.2)
    8 FORMAT(20X,2F6.2//)
    9 FORMAT(/'SITE NO.',3X,'TTG   DTG   TTN   DTN   Z1    DZ1   ZQ    '
      1'DZQ   Z2    DZ2   ZM    DZM    UPPER LAYER THICKNESSES'/)
   60 CONTINUE
       STOP
       END
```